Distribution Agreement

In presenting this thesis or dissertation as a partial fulfillment of the requirements for an advanced degree from Emory University, I hereby grant to Emory University and its agents the non-exclusive license to archive, make accessible, and display my thesis or dissertation in whole or in part in all forms of media, now or hereafter known, including display on the world wide web. I understand that I may select some access restrictions as part of the online submission of this thesis or dissertation. I retain all ownership rights to the copyright of the thesis or dissertation. I also retain the right to use in future works (such as articles or books) all or part of this thesis or dissertation.

Signature:

Maizie Margaret Lee Date

Development of New Diaryl Diazo Compounds and the Study of their application in C-H Functionalization Chemistry

By

Maizie Margaret Lee

Doctor of Philosophy

Chemistry

Huw M. L. Davies, Ph.D.

Advisor

Dennis C. Liotta, Ph.D.

Committee Member

William Wuest, Ph.D.

Committee Member

Accepted:

Kimberly Jacob Arriola, Ph.D.

Dean of the James T. Laney School of Graduate Studies

Date

Development of New Diaryl Diazo Compounds and the Study of their application in C-H Functionalization Chemistry

By

Maizie Margaret Lee

B.S., California State University, Fresno, 2018

Advisor: Huw M. L. Davies, Ph.D.

An abstract of

A dissertation submitted to the Faculty of the

James T. Laney School of Graduate Studies of Emory University

in partial fulfillment of the requirements for the degree of

Doctor of Philosophy

in Chemistry

2023

Abstract

Development of New Diaryl Diazo Compounds and the Study of their application in C-H Functionalization Chemistry

By Maizie Margaret Lee

This dissertation is divided into four chapters discussing the work conducted throughout my tenure in the Davies group.

Chapter One is an overview of dirhodium catalyst development over the past decade, and the impact this has had on C-H Functionalization strategies. A review Dirhodium catalysts and their applications is discussed.

Chapter Two focuses on the background of diazo compounds and their reactivity. Previous work on donor/donor systems in discussed and examples of diaryl diazo carbenes including their applications in natural product synthesis are disclosed. Based on these precedence, new diaryl diazo compounds were synthesized and a systematic study comparing their reactivity to that of donor/acceptor carbenes is described. The key findings of this chapter are that diaryl diazo compounds exhibit similar electronics of a push/pull donor/acceptor system; and compounds with sterically bulky *ortho* substituents can behave with high diastereo- and enatio- control.

Chapter Three leverages the findings of chapter two regarding the reactivity of diaryl diazo compounds to generate triarylmethanes with high levels of asymmetric induction. The C–H insertion of 1,4 cyclohexadiene then oxidation lead to a variety of triarylmethane compounds. This work demonstrates the first examples of an asymmetric intermolecular C–H insertion with diaryl diazo compounds, and provides more evidence for diaryl diazo compounds being in an extended class of donor/acceptor carbenes.

Chapter Four investigates the strategies used to generate diazo compounds. In collaboration with the Stahl group at University of Wisconsin, Madison a catalytic aerobic oxidation of hydrazones to diazo compounds is disclosed. This method is amendable to flow conditions, making it an attractive method for industry. Follow up studies use heterogenous M-N-C catalyst to achieve the in tandem oxidation of hydrazones to diazo compounds then C–H functionalization.

Development of New Diaryl Diazo Compounds and the Study of their application in C-H Functionalization Chemistry

By

Maizie Margaret Lee
B.S., California State University, Fresno, 2018

Advisor: Huw M. L. Davies, Ph.D.

A dissertation submitted to the Faculty of the
James T. Laney School of Graduate Studies of Emory University
in partial fulfillment of the requirements for the degree of
Doctor of Philosophy
in Chemistry
2023

Acknowledgements

The past five years have been some of the most challenging and rewarding experiences in my life. I am grateful to the people in my life who have helped me navigate my early twenties and graduate school and wish to thank them for making me the person I am today.

I would like to start by thanking my advisor, Huw M. L. Davies. Huw has encouraged me to grow as a chemist and has been a great support over my graduate career. My chemistry did not always work but Huw made time to work through problems and pushed me to understand the reaction systems. All of my achievements would not have been possible without his support and guidance.

I would like to thank my committee members Dennis Liotta, William(Bill) Wuest, and former committee member Nathan Jui. During my annual committee evaluations, they provided helpful feedback and guidance. I would like to thank Bill for especially encouraging me to pursue engagement in EBCC and AWIS. Bill also advocated for me and offered his support during less-than-ideal times, and for that I am thankful. I would like to thank Dennis for agreeing to join as a committee member during my third year and for giving me sound career advice. Nate was on my committee for my first three years before moving to industry and taught me so much. His passion for science was evident and he taught one of my favorite classes, advanced synthesis, at Emory.

I would like to give my sincerest thanks to my undergraduate advisor Dr. Qiao-Hong Chen, without her support and mentorship I would not have been a successful scientist. She taught me how to think strategically, and has always encouraged me to set and achieve my goals. She believed in me and became a role model. In her lab, I had many mentors and friends including Xiang(Jimmy) Li, Bao Vue, Ziran Jian, and Pravien Rajaram. Jimmy had the patience to teach me all of the synthetic organic techniques and always has the silliest metaphors. I am thankful for all

I have learned from them and wish them the best as they are pursuing their own graduate studies at different universities.

Emory Chemistry has staff that are very kind and helpful. I would like to specifically thank Steve Krebs for managing stockroom and chemical orders, Dr. Shaoxiong Wu and Dr. Bing Wang for all the NMR-related studies, Dr. John Bacsa for X-ray crystallography, Dr. Fred Strobel for HRMS, and Suzan Brown for keeping all Davies group things in order. Without them, this doctorial work would not have been possible.

Through the CCHF I have met some amazing chemists and got the opportunity to be on multiple collaborations. I would like to thank Dan Morton, Rio Febrian, and Rachael Hall for organizing all events, and their support in my future career goals. I wish to thank my collaborators in Shannon Stahl's lab Jack Twilton and Melissa Hall, they have taught me so much about oxidation chemistry. In addition, Melissa was a great host when I traveled to Madison to work on our M-N-C project together.

In the Davies group, I have had many mentors and great friends who made my time at Emory more bright. Firstly, I wish to thank previous members of the group who provides guidance when I was a young student in the lab. Dr. Zachary Garlets, Dr. Zhi Ren, Dr. Wenbin Liu Dr. Bowen Zhang. Dr. Ben Wertz, Dr. Janakiram Vita, and Dr. Robert Kubiak, you have given me many helpful suggestions at group meetings, and Dr. Zhi Ren taught me a lot through our collaboration on diaryl diazo compounds. I am fortunate to have had the opportunity to learn from specific members of the Davies lab who have become great friends: Dr. Jiantao(JT) Fu, Dr. Aaron Bosse, Dr. Bo Wei, Dr. Yannick Boni, and Dr. Jack Sharland. I am a better scientist and person because of you all. JT, you have always been humble about your work and during my time at Merck, you were a delight to be around. Aaron, thank you for showing me that mental health

matters more than grad school and for always sticking up for me in the lab. Thank you for being a great rock climbing pal and for jamming cool music in the lab, I miss working in the same bay and lab isn't the same. Bo, I don't think I can put into words how much I admire you, you are an exceptional scientist and are one of the kindest people I know. She has made me laugh in lab so many times and made our collaborations together so fun; I wish we could work together all the time just to hear you saying "Woah… so nice". She became the best gym buddy with Yannick. Yannick, you are the most determined person I have met at Emory and I strive to have that type of dedication. We discussed the current literature on the Emory shuttle and somehow survived Atlanta's potholes. You've helped me grow as a scientist and we are growing as future commune owners. Thank you for providing additional feedback on my thesis and helping me with my job search! Jack, we started in the same cohort and I am happy to have had you by my side throughout grad school, we've grown so much in the past five years and finally made it to the finish line! Sharing an office with you we'd always have something to chat about and your impressions of Huw deserve an award.

Current members of the Davies lab, Jasper Luo, Kristen Shimabukuro, Yasir Naeem, William Tracy, Terrence-Than Nguyen, Josh Sailer, Brockton Keen, Ziyi Chen, Dr. Christian Bettencourt, and Dr. Feng Zhai it was a pleasure working in the same lab as you and I am thankful for all the support. I am especially thankful to Dr. Feng Zhai for helping set up our glovebox and for providing very helpful edits to my dissertation. As he is starting his independent career at Emory, students who get the opportunity to work with him will be in great hands. I had the opportunity to do a co-op for six months and wish to thank my mentors during that time. Mycha Uehling, Michael Wleklinski, Dipa Kalyani taught me so much about high-throughput experimentation and went out of their way to make my experiences great.

At Emory, I have made great friends from my cohort and greater community and would like to especially thank Cecie Hendy and Alyssa Johnson for surviving the first two years of grad school with me. We were not in the same lab but studied together for classes and spent much-needed quality time together outside of grad school and I am grateful to call you my friends. People always joke that grad students can't survive without caffeine, and Ingrid Wilt, Andrew Mahoney, and I couldn't agree more. Our daily walks to get free Panera coffee made me so happy and got me into work every day. The coffee was subpar but your friendship made it all worth it. Ingrid, I look up to you in so many ways. Thank you for introducing me to the joys of breakfast club and buddy. I look forward to many more adventures in our future.

Outside of Emory, I have an amazing support system within the Atlanta community. I would like to thank them for giving me the support and friendship that allowed me to make it through graduate school. Biking pals became rock climbing pals and so much more. Danielle Cicka, Abby Crombie, and Ramey Cook completed a century ride with me, and managed to make it the most fun experience. Climbing brought me one of my dearest friends Rachael Stabbert. 6 am morning climbs and breakfast clubs help fortify our friendship, and I can confidently say you're stuck with me for life. You've shown me true kindness in some challenging times and have always been someone I can count on and admire. Thank you for allowing me in your life buddy. I joined the Atlanta Snack Club with Ingrid and Danielle during the pandemic and was led around the most obscure parts of Atlanta via a queue sheet. Alley runs, quad camp, and secret Saturdays have made me love Atlanta and the community it can foster. I would like to thank Kyle and Hilary for running such a rad non-profit. I have made great running friends Rachel Exelbirt and Nigel Dawson who have given me so much support, especially during the months of writing this dissertation. Lastly, I would like to thank my Rankin Street roomies Grace Wood, Minite Pardoe, and Amellia

Armstrong. You all made our home so lively and fun, I loved our sushi nights and walks to lingering shade on the beltline.

My friends back in California, although not in person still provide great friendship over the years. Miranda and Marissa Imamura have known me since middle school and have continued to be some of the funniest people I know. No matter how much time has passed since seeing them, I know I can count on them. Codi Bedrosian taught me coworkers can and should be friends and that shifts go by way more quickly when you're giggling. I'd like to think that mentality got me through grad school and allowed me to make the best lab friends I have today. I appreciate all the facetimes over the years, and you getting a job just so you can come visit me in Atlanta multiple times a year.

Lastly, I wish to thank my family. My mom has done an amazing job raising me and my siblings and is so caring. She has always made an effort to understand and support me throughout my graduate schooling. My sisters, Kenzie and Madi thank you for always believing in me. I am especially thankful to Kenzie for inviting me to all holiday events at her home, and for giving me the privilege of being an aunt. My girl Emma Grace is such a light and it's been a joy watching her grow. I am also thankful to my brother Sawyer, for always being old-reliable, whenever I was able to come home he'd act like no time had passed.

Table of Contents

List of Tables, Figures and Schemes

Chapter One. Dirhodium Carbene Chemistry and Diazo Compounds

Chapter One. Dirhodium Carbene Chemistry and Diazo Compounds

1.1 Introduction

There has been significant effort in the scientific community to develop novel methods to access carbon-carbon(C–C) and carbon-halogen(C–X) bonds for the synthesis of materials, pharmaceutical drugs, and agricultural agents.[1-4] Expanding the synthetic toolbox for C–C and C–X bond manipulations allow for compounds to be made efficiently and have seen significant advancements in the past century.[5-7] Due to the prevalence of C–H bonds in organic molecules, C–H functionalization has emerged as a promising tool to generate complex molecules.[8-12] One of the main challenges with C–H functionalization is associated with selectivity due to the vast amount of hydrogen atoms in most organic compounds. C–H bonds can differ sterically (primary, secondary, tertiary, allylic, vinyl, equatorial, or axial) or they can be differentiated based on proximity to other functional groups, known as directing groups albeit selectivity can still be challenging in such cases.[13] Early examples relied on intramolecular reactions or varying reactivity profiles of the substrates.[14, 15] Radical reactions, which have gained popularity due to the advancement of photoredox protocols, can achieve selective C–H functionalization by selectively activating one substrate or using sterically encumbered hydrogen abstraction agents.[16-18] Most notably, transition metals offer unique reactivity toward activated and unactivated C–H bonds through metal carbene complexes.[19-21]

The term carbene was adopted to describe divalent carbon species which can be classified as free carbenes or stabilized metal carbene complexes; more recently N-heterocyclic carbenes(NHCs) have shown unique ability in catalysis that will not be covered in this chapter.[22] Transition metal carbenes have a wide range of reactivity based on the substituents on the carbene and the interaction with the transition metal. This interaction allows for metal carbenes to have the

potential for more selective reactivity compared to that of the highly reactive free carbene.[23, 24] Transition metal carbenes harness the highly reactive carbene species but have the stabilization of the metal-bound complex allowing for a highly selective transformation. This chapter will focus on the development of rhodium carbene complexes and their uses in the advancement of C–H functionalization chemistry.

1.2 Metal Carbene Complexes

Metal carbene complexes are versatile reagents that are controlled by both the metal and the substituents.[25, 26] Diazo compounds are one of the most common precursors and form the metal carbene through the elimination of nitrogen (Scheme 1a).[27] Diazo compounds can be made with a variety of electronic properties, with substituents bearing electron-donating or electron-withdrawing groups, which have a great effect on the reactivity and stability of the subsequent metal carbene.[13, 28] Phenyliodonium ylides can form metal carbenes through PhIO or $PhI(OAc)_2$ in the presence of an acidic methylene substrate (Scheme 1b).[29] Müller developed an enantioselective cyclopropanation of terminal alkenes using malonate and PhIO to generate the ylide *in situ*. Similarly, sulfonium and sulfoxonium ylides can form metal carbene complexes which can be formed without the need for electron-withdrawing substituents at the ylide center (Scheme 1c).[30, 31] Trost first discovered sulfur ylides could decompose to carbene intermediates in 1966.[32] Since then, sulfonium ylides have been utilized in a variety of transformations including work on metal or carbene-free transformations by leveraging the nucleophilicity of the sulfoxonium ylides.[31, 33] Lastly, 1,2,3-triazoles upon heating can ring-open through a Dimroth rearrangement to unveil a latent diazo which can then form a metal carbene in situ (Scheme 1d).[34] Triazoles are attractive carbene precursors because they have the ability to introduce heteroatom (O or N) groups and have proven to be successful in many C–H functionalization reactions.[35]

1a.) Diazo Compounds

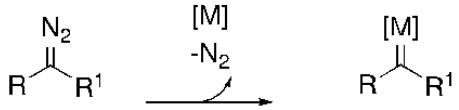

1b.) Phenyliodonium Ylides

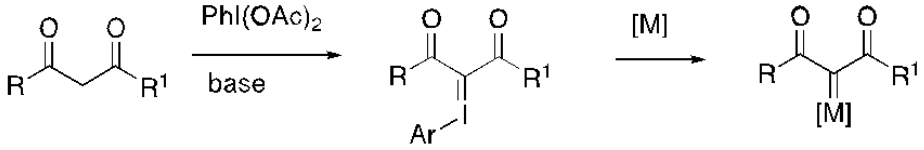

1c.) Sulfonium or Sulfoxonium Ylides

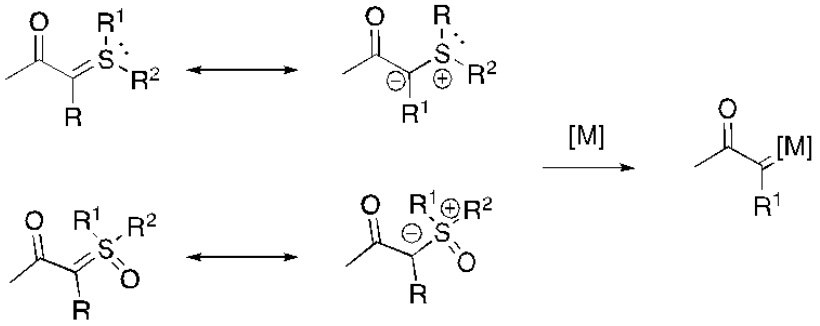

1d.) 1,2,3-triazoles

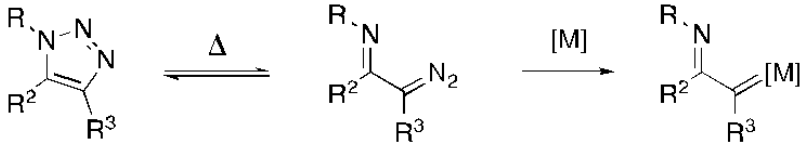

Scheme 1. Access to Metal Carbene Complexes

Metal carbenes can be formed in a variety of ways and can have an array of reactivity, which can be grouped into five main categories: acceptor/acceptor, acceptor only, donor/acceptor, donor only, and donor/donor. (Figure 1). The term "acceptor" refers to the ability of substituents to be electron-withdrawing and increases the metal carbene electrophilicity and reactivity. The term "donor" refers to the substituent's ability to be an electron-donor which helps stabilize the metal carbene through resonance.

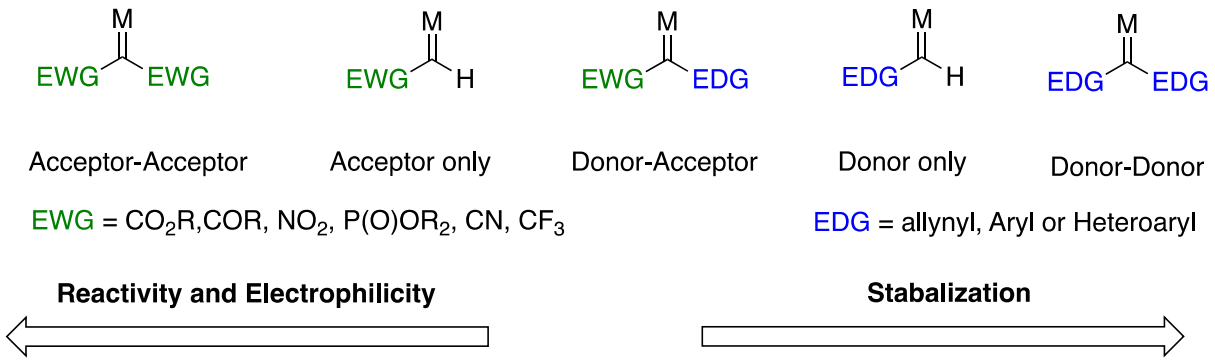

Figure 1. Classification of Metal Carbenes

Acceptor only and acceptor/acceptor carbenes are highly electrophilic and can functionalize unactivated C–H bonds.[36] Due to their reactivity, site-selectivity, and enantioselectivity of intermolecular C–H insertion reactions are limited.[37] Conversely, donor/donor type carbenes are thought to offer more stabilization to the metal carbene, and not be reactive with unactivated C–H bonds.[38] These compounds have remained underexplored due to their umpolung reactivity, nucleophilic diazo reacting with electrophilic carbene, but recently have shown great synthetic promise in intra- and inter- molecular C–H functionalization reactions.[39] Further discussion of the application toward selective C–H insertion of donor/donor carbenes will be given in Chapter Two. In the middle, Donor/acceptor carbenes have emerged as a unique class of carbenes due to their attenuated reactivity; bearing an electron-rich and electron-poor substituent they can achieve highly selective transformations.[26]

1.3 Dirhodium Catalysts for Highly Selective C-H Functionalization Reactions

Dirhodium tetracarboxylates and tetracarboxamidates have proven to be the most effective catalysts for the asymmetric carbene–mediated C–H functionalization reactions.[40] Dirhodium catalysts are stable to heat and moisture, and can be handled under ambient conditions, and reactivity and selectivity can be tuned based on the surrounding ligands.[37] The dirhodium complex forms a paddlewheel structure with four ligands and both axial sites are open (Figure 2).

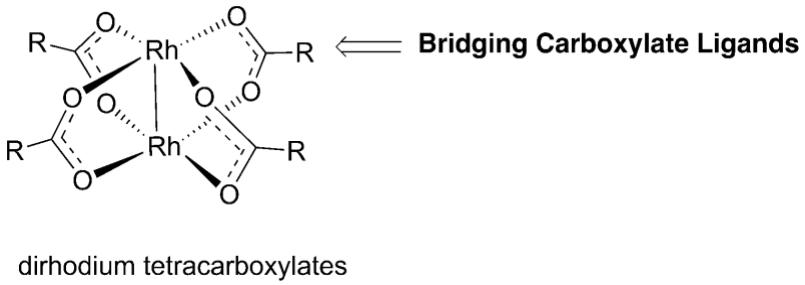

Figure 2. Dirhodium Paddlewheel Complex

One of the first catalysts was dirhodium tetraacetate, $Rh_2(OAc)_4$, which can readily form the desired rhodium carbene, and perform a variety of C–H functionalization reactions in an asymmetric fashion.[41] To achieve an asymmetric transformation chiral ligands must be used, one of the first examples was the cyclopropanation of styrene by Brunner, although minimal enantioselectivity was achieved.[42] Later, Hashimoto developed phthalimido amino acid-based ligands that were effective with acceptor/acceptor carbenes in C–H insertion reactions.[37] The most notable catalysts were derived from *tert*-leucine, such as Rh_2(*S*-PTTL)$_4$ (**3**). Rh_2(*S*-PTTL)$_4$, is able to catalyze the C-H insertion of **α**-diazo ester **1** containing a tethered phenyl group to give product **2** in high yield and 92% ee. [43] Müller later developed a related phthalimido-based catalyst Rh_2(*S*-NTTL)$_4$.[44] This catalyst has been found to be an effective catalyst for reactions involving N-sulfonyltriazoles.[34]

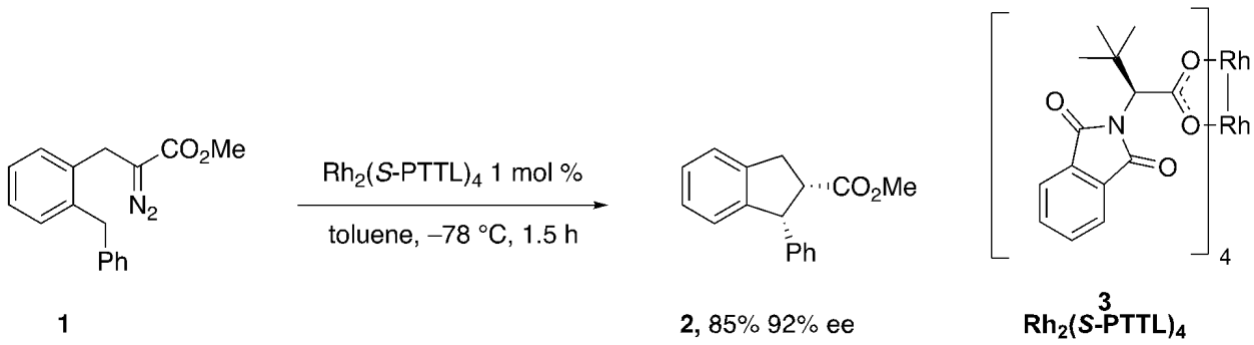

1 **2**, 85% 92% ee **3** Rh_2(*S*-PTTL)$_4$

Scheme 1. Intramolecular C-H Insertion with Rh_2(*S*-PTTL)$_4$

Proline-based catalysts were able to achieve high degrees of selectivity for intramolecular C–H insertions and were later optimized by the Davies group for intermolecular cyclopropanation.[45] Rh_2(*S*-DOSP)$_4$ is a tetra(N-arylsulfonylprolinate catalyst that is soluble in hydrocarbon solvents and performs well in a variety of intermolecular C–H insertion reactions.[46] Since its initial synthesis, Rh_2(*S*-DOSP)$_4$ has been utilized with donor/acceptor carbenes to perform many highly selective transformations.[26] Many studies have been conducted to understand the orientation of the ligands and it is proposed the catalyst is D_2 symmetric with the arylsulfonyl groups existing in an up–down–up–down arrangement (Figure 3).

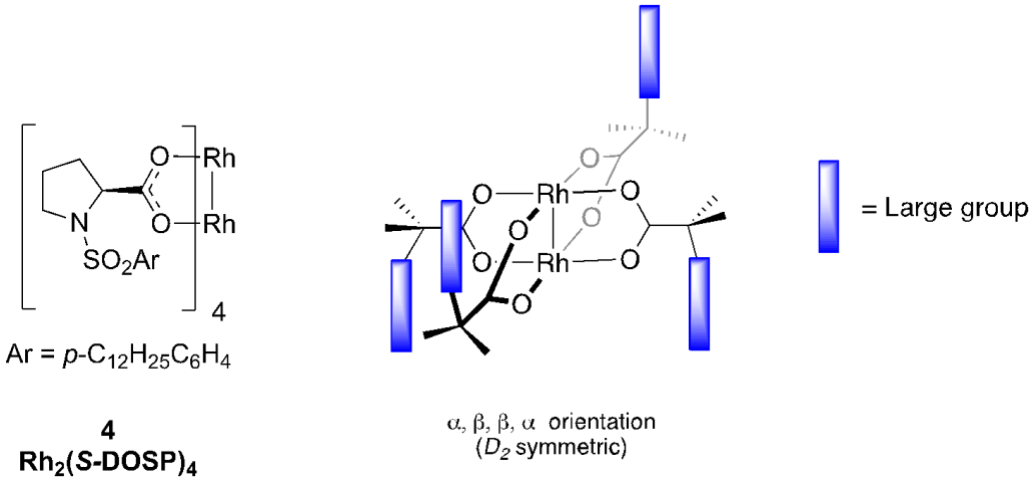

Figure 3. Rh_2(*S*-DOSP)$_4$ Proposed Symmetry

In addition to understanding the symmetry of the ligands around the dirhodium core, the mechanism of the C–H functionalization reaction has been studied (Scheme 2). In the presence of dirhodium complex I, the diazo compound forms the zwitterion intermediate III, which extrudes nitrogen to form the metal bound carbene IV. In the presence of a C–H bond, the rhodium carbene does a C–H insertion and hydride abstraction in step V, to afford the final product VI.[26] Computational studies and X-ray characterization of the carbene intermediates help support this mechanism.[25, 47]

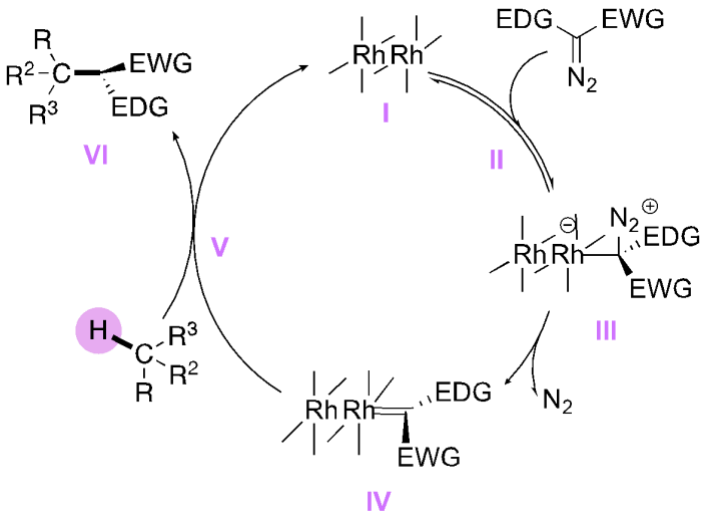

Scheme 2. General Mechanism for Rh(II) catalyzed C-H Insertion Reaction

1.4 Next Generations of Chiral Rhodium Catalysts

The initial success of C–H functionalization made a dramatic impact on the field, but much work was needed to achieve highly selective C–H insertions. C–H bonds, as mentioned earlier can vary in their electronic and steric properties which can be exploited to achieve a highly specific transformation (Figure 4).

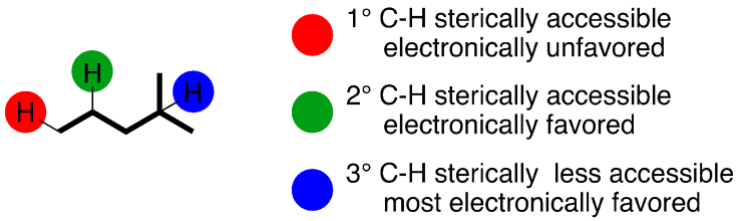

Figure 4. C–H Bond Reactivity Trend

The Davies lab sought to make a variety of chiral dirhodium catalysts that are selective for a specific C–H bond. The second generation of catalysts included bulkier phthalimido based Rh_2(*S*-PTAD)$_4$ and Rh_2(*S*-TCPTAD)$_4$ (Figure 5).[48]

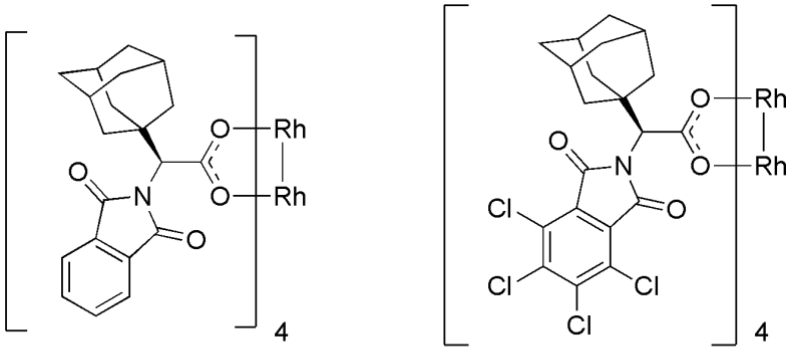

5
Rh_2(*S*-PTAD)$_4$

6
Rh_2(*S*-TCPTAD)$_4$

Figure 5. Second Generation Phthalimido Based Catalysts

Rh_2(*S*-PTAD)$_4$ worked well with methylester diazoacetates and generated benzodihydrofuran compounds in high yield and selectivity compared to Rh_2(*S*-DOSP)$_4$ and Rh_2(*S*-PTTL)$_4$ (Scheme 3).[48] Both Rh_2(*S*-PTAD)$_4$ and Rh_2(*S*-PTTL)$_4$ were able to form product **8** as one major diastereomer, but Rh_2(*S*-PTAD)$_4$ gave a significant increase to the asymmetric induction with 87% ee. Rh_2(*S*-PTAD)$_4$ has since been used to generate highly selective benzohydrofuran and benzodihydrofurans through the intramolecular C–H insertions of donor/donor carbenes; discussed in greater detail in chapter two.[39] Rh_2(*S*-TCPTAD)$_4$ was later found to functionalize tertiary C–H bonds, which are electronically favored but least sterically accessible.[49]

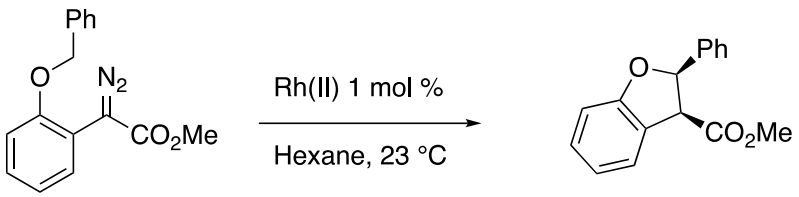

7 **8**

Entry	Catalyst	yield (%)	d.r.	ee (%)
1	Rh_2(*S*-DOSP)$_4$	60	1.5:1	38
2	Rh_2(*S*-PTTL)$_4$	78	>30:1	70
3	Rh_2(*S*-PTAD)$_4$	83	>30:1	87

Scheme 3. Intramolecular C–H insertion with Methylester Diazoacetate

The third generation of chiral catalysts featured a triphenyl cyclopropane ligand and have varying substituents around the aryl rings (Figure 6). Rh_2(*S*-TPCP)$_4$, is the least sterically bulky catalyst, followed by Rh_2(*S*-p-BrTPCP)$_4$ and Rh_2(*S*-p-PhTPCP)$_4$. These catalysts were developed in the hope of being able to differentiate C–H bonds in a highly selective manner.

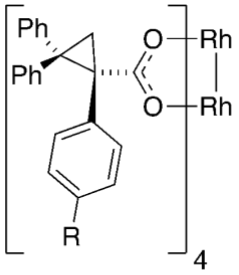

R= Br Rh_2(S-p-Br-TPCP)$_4$ (**9**)
R= Ph Rh_2(S-p-Ph-TPCP)$_4$ (**10**)

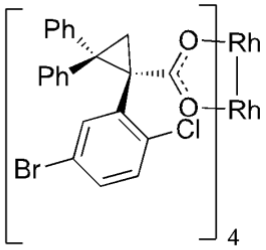

Rh_2(*S*-2-Cl-5-BrTPCP)$_4$ (**11**)

Figure 6. Third Generation Triarylcyclopropane Catalysts

Rh_2(*S*-2-Cl-5-BrTPCP)$_4$ contains an *o*-Cl substituent on one of the phenyl rings that allow for selective C–H insertion to a terminal 2° C–H bonds even in the presence of electronically activated

benzylic C–H (Scheme 6).[50] This site selectivity is thought to be due to the *o*-Cl substituent making the catalyst C_4 symmetric, while other catalysts in the TPCP family adopt D_2 or C_2 symmetry.

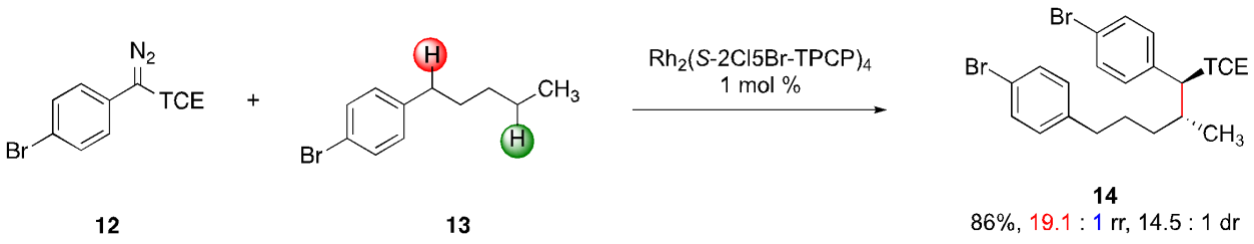

Scheme 6. Rh_2(*S*-2-Cl-5-BrTPCP)$_4$ Selectivity

More recently the Davies lab has begun exploring more variants around the phthalimido-based catalysts, and in 2018 developed Rh_2(*S*-TPPTTL)$_4$ (**15**), which has an extended C_4 symmetric bowl structure. This catalyst is able to desymmetrize cyclohexane **16** and give very high levels of asymmetric induction (Figure 7).[51] Inspired by this, more bulky catalysts have been synthesized and have shown promise for highly selective transformations.[52] The extended catalysts, **17**, contain functional groups around the aromatic rings. These catalysts were able to achieve similar selectivity profiles to Rh_2(*S*-TPPTTL)$_4$ in the desymmetrization of cyclohexane and display exceptional reactivity in some cases, such as the C–H insertion of ethyltolune even outperforming the parent catalyst.

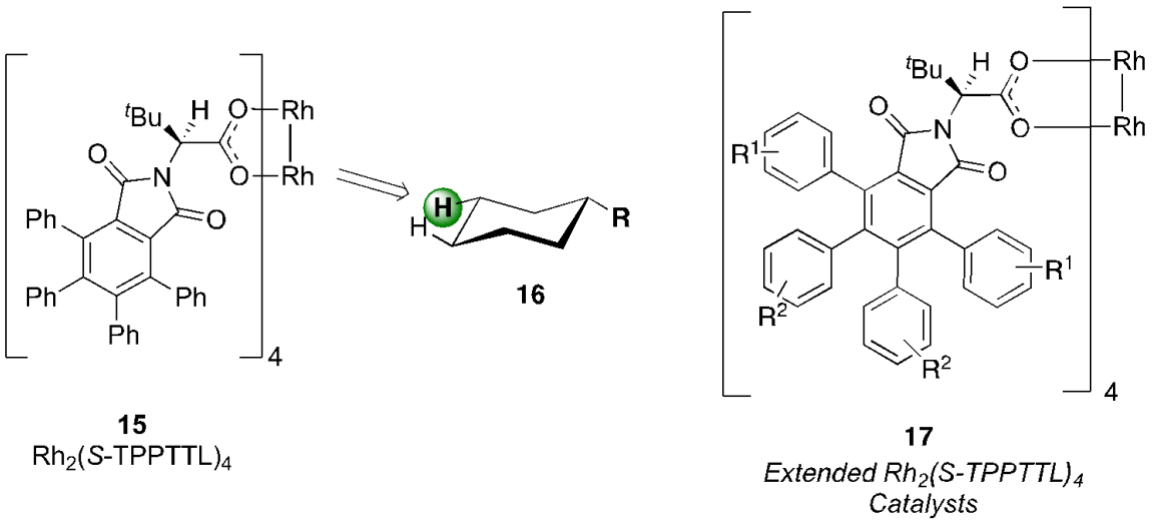

Figure 7. C_4 Symmetric Bowl Shaped Catalysts

1.5 Select Examples of C-H Functionalization using Donor/Acceptor Diazo Compounds

C–H functionalization has emerged as an effective tool to generate compounds with high degrees of site-selectivity, regio- and enantio- control. The Davies lab in particular has made several chiral dirhodium catalysts capable of differentiating C–H bonds based on their steric and electronic profile.[13] These transformations have been used in a variety of transformations toward natural products and pharmaceutical agents, with select examples shown below. Venlafaxine is an antidepressant and has a C–H disconnection that can be easily accessed using dirhodium chemistry. The C–H insertion of silyl-protected methylamine **19** of phenyldiazoacetate **18** by Rh_2(*S*-DOSP)$_4$ affords the **β**-amino ester **20** in moderate yield and excellent selectivity, 97% ee (Scheme 7).[53] The material can be converted to the final desired product in two steps and can be made as either isomer, making this an attractive -alternative to the established synthesis.

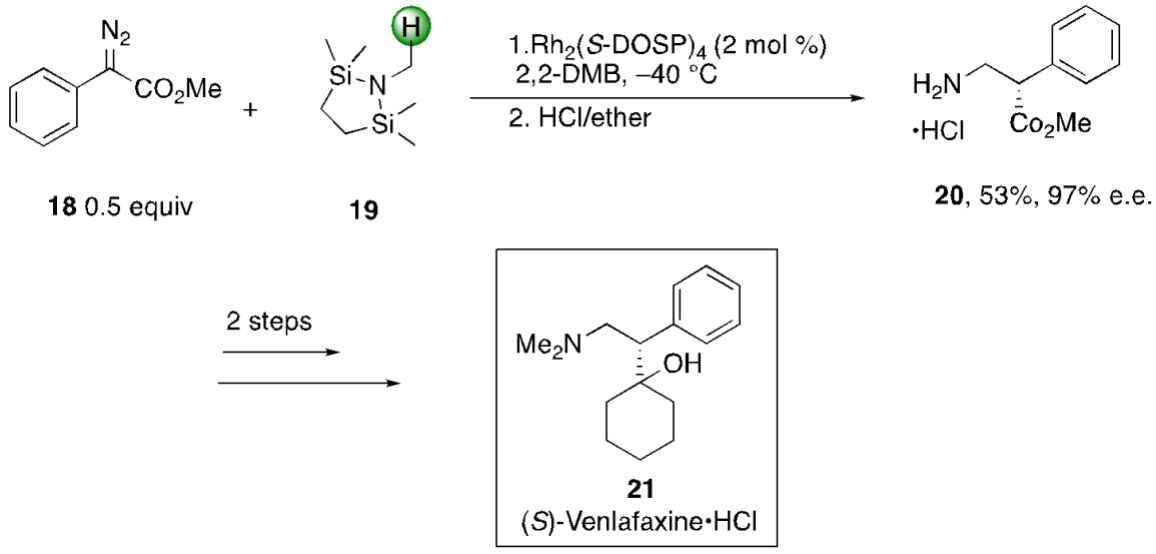

Scheme 7. Synthesis of Venlafaxine using C-H insertion

In 2021 in collaboration with the Sorensen lab, the Davies lab leveraged C–H functionalization to construct (–)-aflatoxin B_2.[54] The C–H insertion of (*E*)-2-hexene, **23**, into the primary allylic C–H bond over the more electron-rich secondary allylic site could be achieved using 0.5 mol % Rh_2(*R*-p-PhTPCP)$_4$. The reaction proceeded with 11:1 regioselectivity favoring the desired primary insertion in excellent yield and high asymmetric induction, 98:2 er. In subsequent steps the authors employed the Yu group's method for palladium-catalyzed directed acetoxylation, which could be cyclized to the key intermediate **25**.[55] This work highlights the use of dirhodium catalysts for site-selective C–H functionalization toward the synthesis of natural products.

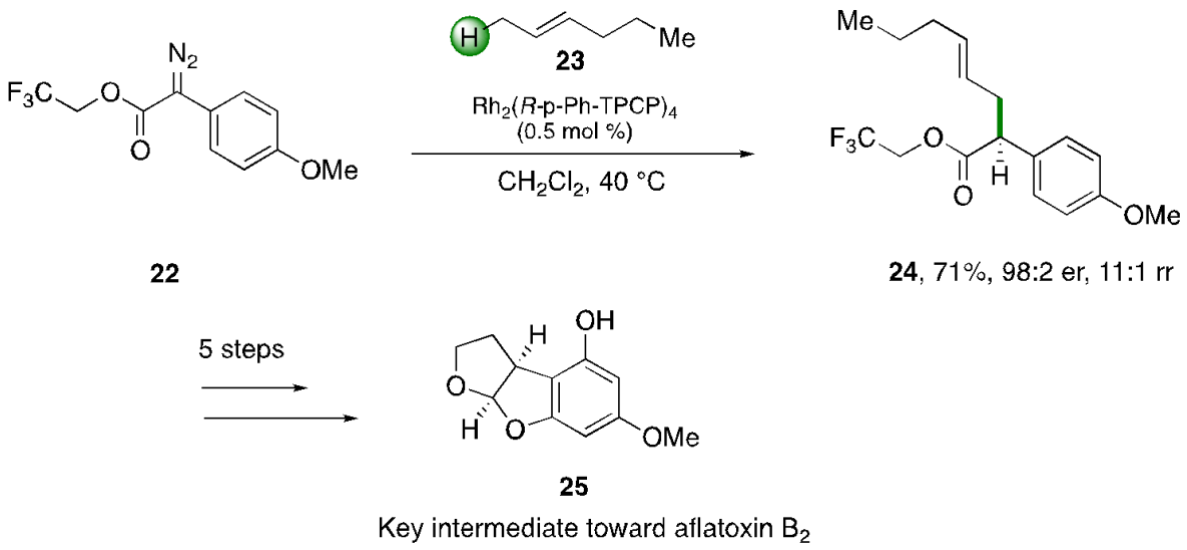

Scheme 8. C-H Insertion Strategy Toward the Synthesis of Aflatoxin B_2

1.6 Bedaquiline Synthesis and Donor/Donor Hypothesis

The Center for Selective C–H Functionalization (CCHF) hosts molecule of the month meetings, wherein a known natural product or pharmaceutical drug is presented and participants come up with creative retrosynthetic strategies involving C–H functionalization. The semester I joined the lab, the chosen molecule was Bedaquiline. Bedaquiline was approved by the FDA in 2012 for the treatment of multidrug-resistant tuberculosis.[56] Bedaquiline is a diarylquinoline that was first synthesized by Johnson & Johnson(Scheme 9).[57] It was synthesized via a highly convergent method, and the team was able to synthesize over 200 diarylquinolines in this manner. Quinoline derivative **26** was reacted with the naphthyl substrate **27** using LDA which formed the racemate of bedaquiline, **28**. Unfortunately, the original synthesis did not construct the core in an asymmetric fashion, and the enantiopure material needed to be isolated by chiral chromatography.

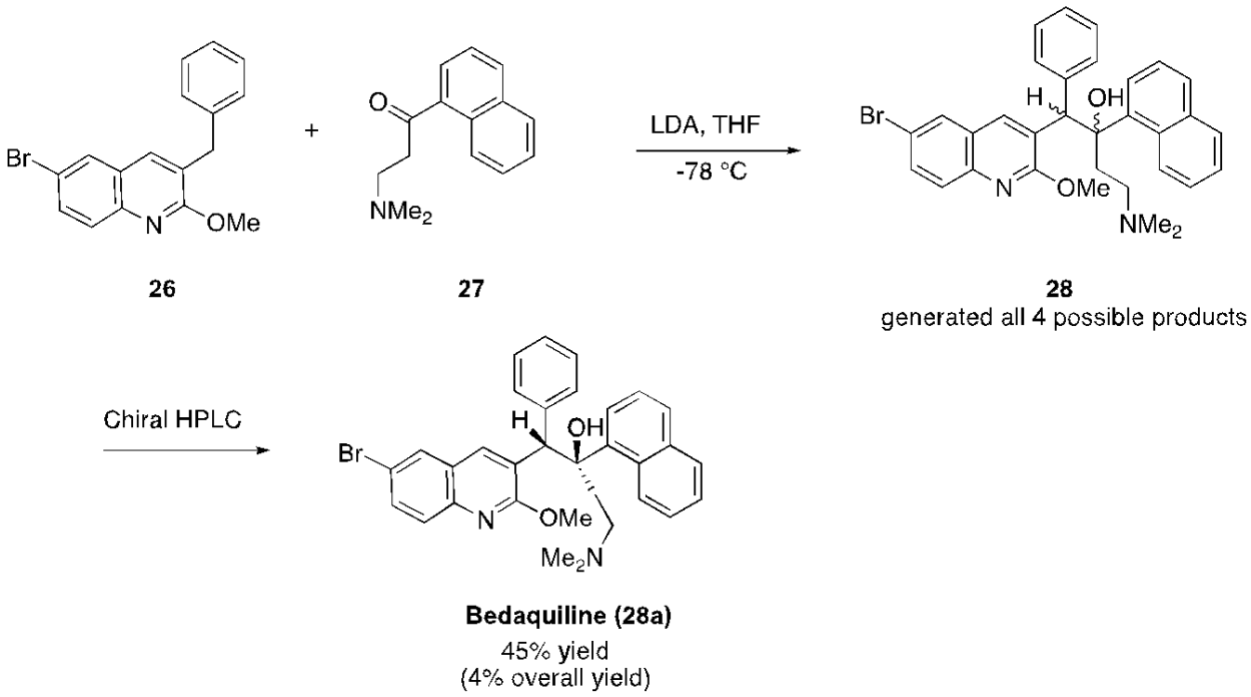

Scheme 9. First Synthetic Route of Bedaquiline

Eric Sorensen, a member of the CCHF, thought it would be advantageous to make the key disconnection of Bedaquiline a C–H Insertion using a diaryl diazo compound (Scheme 10). The proposed disconnection unveiled some interesting questions about the potential limits of the current C–H functionalization chemistry performed in the Davies lab. First, diaryl diazo compounds were thought to be donor/donor diazo compounds and unreactive with C–H bonds, except in the case of intramolecular C–H bonds. The proposed C–H insertion site would be activated, but also sterically crowded making it an interesting substrate to test for selectivity using the known dirhodium catalysts in the Davies Lab.

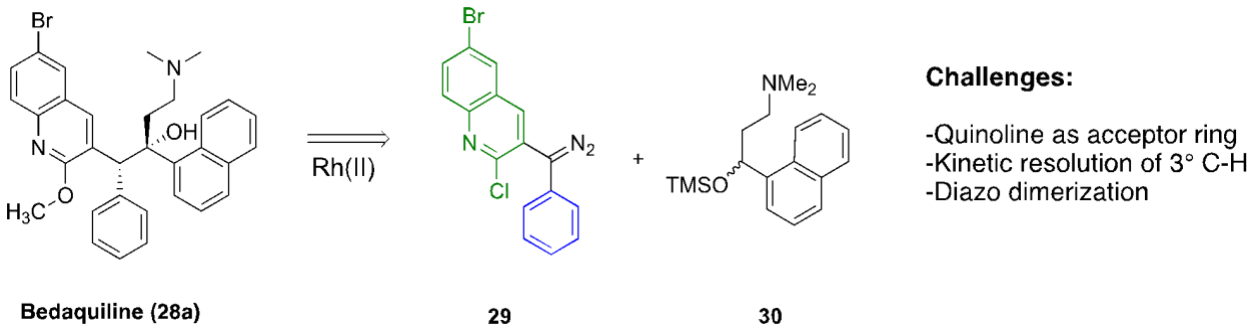

Scheme 10. Proposed Retrosynthesis of Bedaquiline using Donor/Donor Diazo Compound

1.7 Conclusions

C–H Functionalization has made significant impacts on the ways C–C and C–X bonds can be formed in a selective way. The Davies group in particular, has made significant advancements to asymmetric C–H functionalization through the use of donor/acceptor carbenes and the development of dirhodium tetracarboxylate catalysts. Although the donor/acceptor has been the most successful carbene precursor, ideas out of CCHF have pushed the Davies group to think of other candidates that may be successful, like a diaryl donor/donor type system. This idea, although at the time seemed far-fetched, spun out into the projects outlined in this thesis. Chapter two aims to understand the reactivity of diaryl diazo compounds and demonstrates that with some functional group manipulation diaryl diazo compounds can behave similarly to donor/acceptor type diazo compounds. Chapter three moves to C–H insertion reactions and application in the synthesis of triarylmethanes. Lastly, chapter four describes an alternate method to generate these diazo compounds, making them more suitable for flow applications. The ultimate goal of the outlined work in this thesis is to expand the toolbox of chemical reactivity allowing other researchers to make compounds, especially pharmaceutical-relevant compounds, in a more efficient and robust manner.

1.8 References

1. Kibayashi, C., Development of new synthetic methods and its application to total synthesis of nitrogen-containing bioactive natural products. *Chemical & Pharmaceutical Bulletin* **2005,** *53* (11), 1375-1386.
2. Nagai, T., New drug development by innovative drug administration - "change" in pharmaceutical field. *Yakugaku Zasshi-Journal of the Pharmaceutical Society of Japan* **1997,** *117* (10-11), 963-971.
3. Tokuyama, H., Development of new synthetic methods and their application to synthesis of useful compounds. *Yakugaku Zasshi-Journal of the Pharmaceutical Society of Japan* **2003,** *123* (12), 1007-1021.
4. Node, M., Development of new methods in asymmetric reactions and their applications. *Yakugaku Zasshi-Journal of the Pharmaceutical Society of Japan* **2002,** *122* (1), 71-88.
5. De Abreu, M.; Belmont, P.; Brachet, E., Synergistic Photoredox/Transition-Metal Catalysis for Carbon-Carbon Bond Formation Reactions. *Eur. J. Org. Chem.* **2020,** *2020* (10), 1327-1378.
6. Mondal, A.; Mukhopadhyay, C., Construction of Carbon-Carbon and Carbon-Heteroatom Bonds: Enabled by Visible Light. *Current Organic Chemistry* **2020,** *24* (1), 44-73.
7. Bi, X. F.; Zhang, Q. C.; Gu, Z. H., Transition-Metal-Catalyzed Carbon-Carbon Bond Activation in Asymmetric Synthesis. *Chinese Journal of Chemistry* **2021,** *39* (5), 1397-1412.
8. Ackermann, L.; Vicente, R.; Kapdi, A. R., Transition-Metal-Catalyzed Direct Arylation of (Hetero)Arenes by C-H Bond Cleavage. *Angew. Chem.-Int. Edit.* **2009,** *48* (52), 9792-9826.
9. Baudoin, O., Transition metal-catalyzed arylation of unactivated C(sp(3))-H bonds. *Chem. Soc. Rev.* **2011,** *40* (10), 4902-4911.
10. Sinha, S. K.; Guin, S.; Maiti, S.; Biswas, J. P.; Porey, S.; Maiti, D., Toolbox for Distal C-H Bond Functionalizations in Organic Molecules. *Chem. Rev.* **2022,** *122* (6), 5682-5841.
11. Singh, P.; Chouhan, K. K.; Mukherjee, A., Ruthenium Catalyzed Intramolecular C-X (X=C, N, O, S) Bond Formation via C-H Functionalization: An Overview. *Chem.-Asian J.* **2021,** *16* (17), 2392-2412.
12. Abedinifar, F.; Mahdavi, M.; Asadi, M.; Hamedifar, H.; Ansari, S.; Larijani, B., Recent Opportunities and Challenges in Selective C-H Functionalization of Methyl Azaarenes: A Highlight from 2010 to 2020 Studies. *Current Organic Synthesis* **2021,** *18* (8), 761-789.
13. Davies, H. M. L.; Morton, D., Guiding principles for site selective and stereoselective intermolecular C-H functionalization by donor/acceptor rhodium carbenes. *Chem. Soc. Rev.* **2011,** *40* (4), 1857-1869.
14. Adams, J.; Spero, D. M., Rhodium (Ii) Catalyzed-Reactions of Diazo-Carbonyl Compounds. *Tetrahedron* **1991,** *47* (10-11), 1765-1808.
15. Fischer, R. H.; Baumann, M.; Kobrich, G., Intramolecular C-H insertion in alkylidene carbenoids for cyclopentene derivatives. *Tetrahedron Lett.* **1974,** (13), 1207-1208.
16. Holmberg-Douglas, N.; Nicewicz, D. A., Photoredox-Catalyzed C-H Functionalization Reactions. *Chem. Rev.* **2022,** *122* (2), 1925-2016.
17. Qin, Q. X.; Jiang, H.; Hu, Z. T.; Ren, D.; Yu, S. Y., Functionalization of C-H Bonds by Photoredox Catalysis. *Chemical Record* **2017,** *17* (8), 754-774.
18. Monika; Selvakumar, S., Recent Developments in Direct C-H Functionalization of Quinoxalin-2(1H)-ones via Radical Addition Processes. *Synthesis* **2019,** *51* (22), 4113-4136.

19. Bertrand, G., Special issue: Carbene chemistry - Preface. *Journal of Organometallic Chemistry* **2005,** *690* (24-25), 5397-5397.
20. Doyle, M. P.;Duffy, R.; Ratnikov, M.; Zhou, L., Catalytic Carbene Insertion into C-H Bonds. *Chem. Rev.* **2010,** *110* (2), 704-724.
21. Davies, H. M. L.; Manning, J. R., Catalytic C-H functionalization by metal carbenoid and nitrenoid insertion. *Nature* **2008,** *451* (7177), 417-424.
22. Padwa, A.; Krumpe, K. E., Application Of Intramolecular Carbenoid Reactions In Organic-Synthesis. *Tetrahedron* **1992,** *48* (26), 5385-5453.
23. Frenking, G.;Solà, M.; Vyboishchikov, S. F., Chemical bonding in transition metal carbene complexes. *Journal of Organometallic Chemistry* **2005,** *690* (24-25), 6178-6204.
24. Ren, Z.; Sunderland, T. L.; Tortoreto, C.; Yang, T.; Berry, J. F.; Musaev, D. G.; Davies, H. M. L., Comparison of Reactivity and Enantioselectivity between Chiral Bimetallic Catalysts: Bismuth Rhodium- and Dirhodium-Catalyzed Carbene Chemistry. *ACS Catal.* **2018,** *8* (11), 10676-10682.
25. Werle, C.;Goddard, R.; Philipps, P.; Fares, C.; Furstner, A., Structures of Reactive Donor/Acceptor and Donor/Donor Rhodium Carbenes in the Solid State and Their Implications for Catalysis. *J. Am. Chem. Soc.* **2016,** *138* (11), 3797-3805.
26. Davies, H. M. L., Finding Opportunities from Surprises and Failures. Development of Rhodium-Stabilized Donor/Acceptor Carbenes and Their Application to Catalyst-Controlled C-H Functionalization. *J. Org. Chem.* **2019,** *84* (20), 12722-12745.
27. Ford, A.; Miel, H.; Ring, A.; Slattery, C. N.; Maguire, A. R.; McKervey, M. A., Modern Organic Synthesis with alpha-Diazocarbonyl Compounds. *Chem. Rev.* **2015,** *115* (18), 9981-10080.
28. Xiao, Q.;Zhang, Y.; Wang, J. B., Diazo Compounds and N-Tosylhydrazones: Novel Cross-Coupling Partners in Transition-Metal-Catalyzed Reactions. *Accounts Chem. Res.* **2013,** *46* (2), 236-247.
29. Muller, P., Asymmetric transfer of carbenes with phenyliodonium ylides. *Accounts Chem. Res.* **2004,** *37* (4), 243-251.
30. Corey, E. J.; Chaykovsky, M., Dimethylsulfoxonium Methylide. *J. Am. Chem. Soc.* **1962,** *84* (5), 867-868.
31. Caiuby, C. A. D.; Furniel, L. G.; Burtoloso, A. C. B., Asymmetric transformations from sulfoxonium ylides. *Chem Sci* **2022,** *13* (5), 1192-1209.
32. Trost, B. M., Decomposition of Sulfur Ylides. Evidence for Carbene Intermediates. *J. Am. Chem. Soc.* **1966,** *88* (7), 1587-1588.
33. Kaiser, D.; Klose, I.;Oost, R.; Neuhaus, J.; Maulide, N., Bond-Forming and -Breaking Reactions at Sulfur(IV): Sulfoxides, Sulfonium Salts, Sulfur Ylides, and Sulfinate Salts. *Chem Rev* **2019,** *119* (14), 8701-8780.
34. Davies, H. M. L.; Alford, J. S., Reactions of metallocarbenes derived from N-sulfonyl-1,2,3-triazoles. *Chem. Soc. Rev.* **2014,** *43* (15), 5151-5162.
35. Chuprakov, S.; Kwok, S. W.; Zhang, L.; Lercher, L.; Fokin, V. V., Rhodium-Catalyzed Enantioselective Cyclopropanation of Olefins with N-Sulfonyl 1,2,3-Triazoles. *J. Am. Chem. Soc.* **2009,** *131* (50), 18034-+.
36. Doyle, M. P., Catalytic Methods For Metal Carbene Transformations. *Chem. Rev.* **1986,** *86* (5), 919-939.

37. Hashimoto, S.;Watanabe, N.; Sato, T.; Shiro, M.; Ikegami, S., Enhancement Of Enantioselectivity In Intramolecular C-H Insertion Reactions Of Alpha-Diazo Beta-Keto-Esters Catalyzed By Chiral Dirhodium(Ii) Carboxylates. *Tetrahedron Lett.* **1993,** *34* (32), 5109-5112.
38. Zhu, D.; Chen, L. F.; Fan, H. L.; Yao, Q. L.; Zhu, S. F., Recent progress on donor and donor-donor carbenes. *Chem. Soc. Rev.* **2020,** *49* (3), 908-950.
39. Lamb, K. N.; Squitieri, R. A.; Chintala, S. R.; Kwong, A. J.; Balmond, E. I.; Soldi, C.; Dmitrenko, O.; Reis, M. C.; Chung, R.; Addison, J. B.; Fettinger, J. C.; Hein, J. E.; Tantillo, D. J.; Fox, J. M.; Shaw, J. T., Synthesis of Benzodihydrofurans by Asymmetric C-H Insertion Reactions of Donor/Donor Rhodium Carbenes. *Chem.-Eur. J.* **2017,** *23* (49), 11843-11855.
40. Doyle, M. P., Perspective on dirhodium carboxamidates as catalysts. *J. Org. Chem.* **2006,** *71* (25), 9253-9260.
41. Wee, A. G. H.;Liu, B. S.; Zhang, L., Dirhodium Tetraacetate Catalyzed Carbon-Hydrogen Insertion Reaction In N-Substituted Alpha-Carbomethoxy-Alpha-Diazoacetanilides And Structural Analogs - Substituent And Conformational Effects. *J. Org. Chem.* **1992,** *57* (16), 4404-4414.
42. Brunner, H.;Kluschanzoff, H.; Wutz, K., ENANTIOSELECTIVE CATALYSIS .47. RHODIUM(II)-CARBOXYLATE COMPLEXES AND THEIR USE IN THE ENANTIOSELECTIVE CYCLOPROPANATION. *Bulletin Des Societes Chimiques Belges* **1989,** *98* (1), 63-72.
43. Hashimoto, S.;Watanabe, N.; Anada, M.; Ikegami, S., Site- and enantiocontrol in intramolecular C-H insertion reactions of alpha-diazo carbonyl compounds catalyzed by dirhodium(II) carboxylates. *Journal of Synthetic Organic Chemistry Japan* **1996,** *54* (11), 988-999.
44. Muller, P.; Allenbach, Y.; Robert, E., Rhodium(II)-catalyzed olefin cyclopropanation with the phenyliodonium ylide derived from Meldrum's acid. *Tetrahedron-Asymmetry* **2003,** *14* (7), 779-785.
45. Davies, H. M. L.; Bruzinski, P. R.; Lake, D. H.; Kong, N.; Fall, M. J., Asymmetric cyclopropanations by rhodium(II) N-(arylsulfonyl)prolinate catalyzed decomposition of vinyldiazomethanes in the presence of alkenes. Practical enantioselective synthesis of the four stereoisomers of 2-phenylcyclopropan-1-amino acid. *J. Am. Chem. Soc.* **1996,** *118* (29), 6897-6907.
46. Davies, H. M. L.; Grazini, M. V. A.; Aouad, E., Asymmetric intramolecular C-H insertions of aryldiazoacetates. *Org. Lett.* **2001,** *3* (10), 1475-1477.
47. Kornecki, K. P.;Briones, J. F.; Boyarskikh, V.; Fullilove, F.; Autschbach, J.; Schrote, K. E.; Lancaster, K. M.; Davies, H. M. L.; Berry, J. F., Direct Spectroscopic Characterization of a Transitory Dirhodium Donor-Acceptor Carbene Complex. *Science* **2013,** *342* (6156), 351-354.
48. Reddy, R. P.;Lee, G. H.; Davies, H. M. L., Dirhodium tetracarboxylate derived from adamantylglycine as a chiral catalyst for carbenoid reactions. *Org. Lett.* **2006,** *8* (16), 3437-3440.
49. Davies, H. M. L.; Liao, K. B., Dirhodium tetracarboxylates as catalysts for selective intermolecular C-H functionalization. *Nat. Rev. Chem.* **2019,** *3* (6), 347-360.
50. Liu, W. B.; Ren, Z.; Bosse, A. T.; Liao, K. B.; Goldstein, E. L.; Bacsa, J.; Musaev, D. G.; Stoltz, B. M.; Davies, H. M. L., Catalyst-Controlled Selective Functionalization of Unactivated C-H Bonds in the Presence of Electronically Activated C-H Bonds. *J. Am. Chem. Soc.* **2018,** *140* (38), 12247-12255.
51. Fu, J. T.; Ren, Z.; Bacsa, J.; Musaev, D. G.; Davies, H. M. L., Desymmetrization of cyclohexanes by site- and stereoselective C-H functionalization. *Nature* **2018,** *564* (7736), 395-+.

52. Garlets, Z. J.; Boni, Y. T.; Sharland, J. C.; Kirby, R. P.; Fu, J. T.; Bacsa, J.; Davies, H. M. L., Design, Synthesis, and Evaluation of Extended C4-Symmetric Dirhodium Tetracarboxylate Catalysts. *ACS Catal.* **2022,** *12* (17), 10841-10848.
53. Davies, H. M. L.; Ni, A. W., Enantioselective synthesis of beta-amino esters and its application to the synthesis of the enantiomers of the antidepressant Venlafaxine. *Chem. Commun.* **2006,** (29), 3110-3112.
54. Falcone, N. A.; Bosse, A. T.; Park, H.; Yu, J. Q.; Davies, H. M. L.; Sorensen, E. J., A C-H Functionalization Strategy Enables an Enantioselective Formal Synthesis of (-)-Aflatoxin B-2. *Org. Lett.* **2021,** *23* (24), 9393-9397.
55. Li, G.;Wan, L.; Zhang, G. F.; Leow, D.; Spangler, J.; Yu, J. Q., Pd(II)-Catalyzed C-H Functionalizations Directed by Distal Weakly Coordinating Functional Groups. *J. Am. Chem. Soc.* **2015,** *137* (13), 4391-4397.
56. Belard, S.; Heuvelings, C. C.; Janssen, S.; Grobusch, M. P., Bedaquiline for the treatment of drug-resistant tuberculosis. *Expert Review of Anti-Infective Therapy* **2015,** *13* (5), 535-553.
57. Andries, K.; Verhasselt, P.; Guillemont, J.; Göhlmann, H. W. H.; Neefs, J.-M.; Winkler, H.; Van Gestel, J.; Timmerman, P.; Zhu, M.; Lee, E.; Williams, P.; de Chaffoy, D.; Huitric, E.; Hoffner, S.; Cambau, E.; Truffot-Pernot, C.; Lounis, N.; Jarlier, V., A Diarylquinoline Drug Active on the ATP Synthase of Mycobacterium tuberculosis. *Science* **2005,** *307* (5707), 223-227.

Chapter 2. Study and Evaluation of Diaryl Diazo Compounds as Pseudo Donor/Acceptor Carbene Compounds

The work discussed in this chapter has been published in the journal ACS Catalysis.[1] *Adapted with permission* from *ACS Catal*. **2020,** 10, 6240-6247. *Copyright 2020 American Chemical Society.*

2.1 Background and Previous Work on Diaryl Diazo Compounds

Metal carbenes are important reactive intermediates that have been demonstrated to generate highly selective C–H functionalization products. As discussed in the previous chapter, Davies has classified these metal carbenes into five main categories based on the varying substituents.[2] Extensive work has been done on donor/acceptor metal carbenes which feature an electron-withdrawing group and an electron-donating group. Donor/donor type carbenes are those lacking an electron-withdrawing substituent and most commonly have two aromatic rings. Until recently, these carbene compounds remained underexplored due to their lack of reactivity toward C–H bonds.[3, 4] In addition, one of the major known undesired products of these compounds are homo-dimerization products. This occurs when the highly nucleophilic diazo compound reacts with the highly electrophilic metal carbene shown in Figure 1.

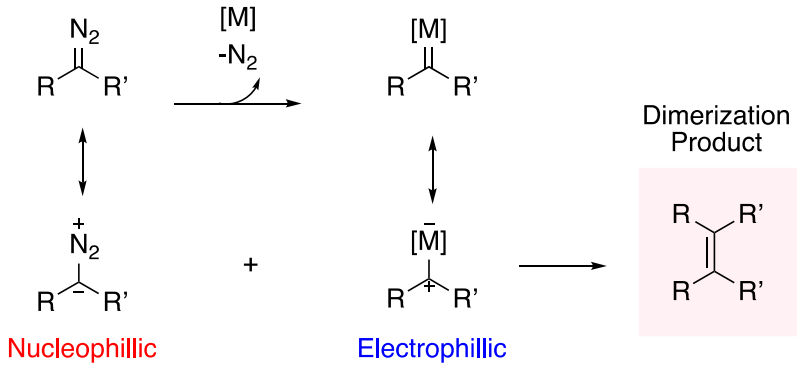

Figure 1. Umpolung Reactivity of Donor/Donor Diazo Compounds

In order to overcome this limitation most reactions explored were intramolecular reactions to decrease dimerization as the major byproduct.[5] A promising method to generate these carbene compounds is through the oxidation of hydrazones to the diazo compound, which can lose nitrogen to form a carbene.[6] Alternative precursors to donor/donor type carbenes, including propargyl esters and ethers, enynones, cycloheptatrienes, cyclopropenes, and allenes, have been shown to be useful and avoid the evolution of nitrogen, but are out of the scope of this chapter.[7-16]

Thermal and photo-decompositions of diazo compounds form free donor carbene intermediates, lead to uncontrolled reactions with many byproducts.[17-19] Transition metal-catalyzed diazo decomposition enables controlling the carbene reactivity for productive C–H insertion, X–H insertion, ylide formation, and cross coupling reactions.[20-23]

In 2001, Che and co-workers reported a reaction with diphenyldiazomethane with osmium porphyrin to form cyclic alkenes.[24] In a subsequent publication, they demonstrated that iron porphyrin **1** could react with activated C–H bonds such as cyclohexene and cumene shown in Scheme 1.[25] 3-(Diphenylmethyl)cyclohexene, **2**, was furnished in a 24% yield at an elevated temperature. The cumene insertion product **3** was produced at 59% yield. Interestingly, the authors noted that, in the presence of ethylbenzene, no C–H insertion product was detected at elevated temperatures and longer reaction times, and only the dimerization product was produced. Ethylbenzene is less substituted than cumene but still α to an activating benzene group, this example shows the limitations of a less reactive diaryl donor/donor carbene system.

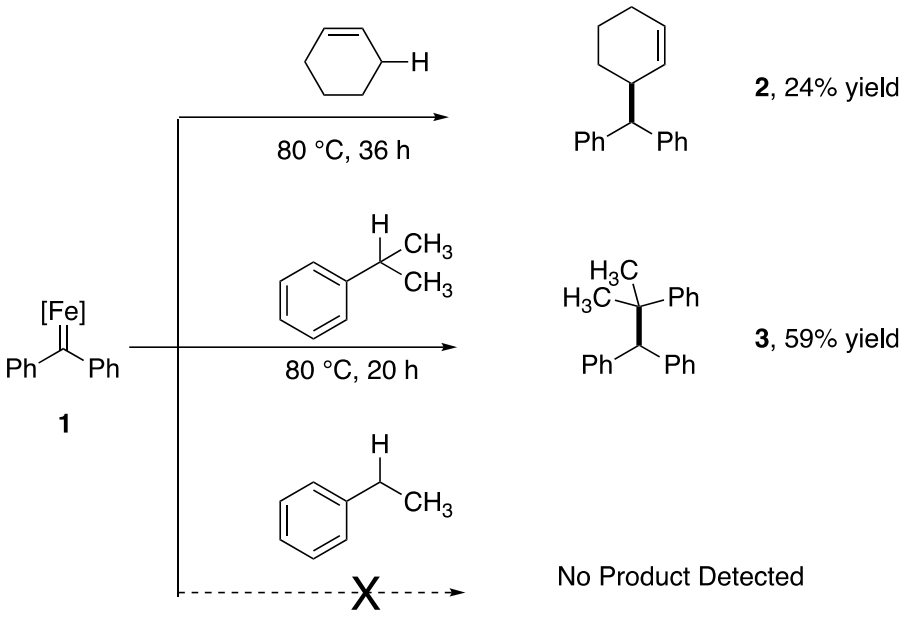

Scheme 1. Iron Porphyrin C–H Insertion Reactions

Although there are other transition metals capable of promoting the decomposition of diazo compounds to the corresponding metal carbene, rhodium(II) complexes, as discussed in Chapter 1 have been shown to be the most efficient. Aggarwal and co-workers reported the synthesis of non-racemic epoxides from carbonyls with phenyl carbene compounds in the presence of homochiral sulfide and 1 mol% $Rh_2(OAc)_4$.[26]

In 2014, the Shaw lab began exploring asymmetric intramolecular C–H insertion reactions using diaryl systems.[27] They found it effective in their work to utilize the diaryl hydrazone precursor and oxidize to the diazo compound *in situ,* followed by the desired C–H insertion. This work enabled the synthesis of substituted benzodihydrofurans, indanes, benzodihydrothiophenes, and indolines shown in Scheme 2.[28, 29] This method offers a rapid generation substituted five-membered rings with a high degree of diastereo- and enantiocontrol. In addition, the optimal catalyst for this system was found to be Rh_2(*S*-PTAD)$_4$, which was previously shown to be the most effective catalyst for the intramolecular C–H insertion to generate benzodihydrofurans with the donor/acceptor methylester diazoacetate.[30]

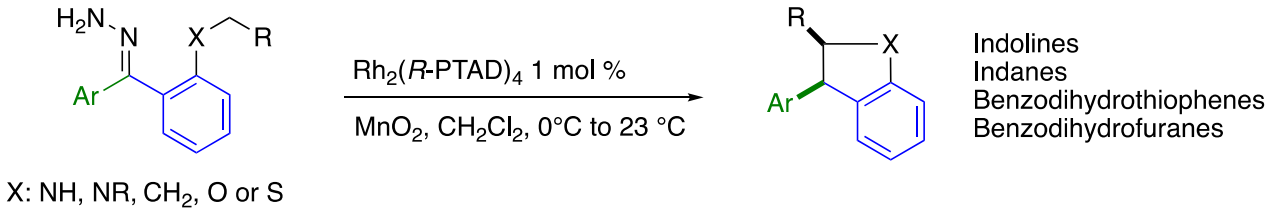

Scheme 2. Intramolecular C–H Insertion of Diaryl Diazo Compounds

These ring systems are prevalent in many medicinally relevant compounds and natural products. The Shaw lab saw a key disconnection leading back to the key diaryl moiety and was able to synthesize E-δ-viniferin **6**, shown in Scheme 3.[27] E-δ-Viniferin is a resveratrol dimer isolated from grapes in response to fungal infection and is a member of the oligoresveratrol natural products. This work represents the first reported enantioselective synthesis of a member of the oligoresveratrol, and the key step was the conversion of ketone **4** to the hydrazone and subsequent diazo *in situ* generation and C–H insertion to form the highly selective benzodihydrofuran **5** in 95:5 d.r. and 93:7 e.r. The Shaw lab has since published strategies toward the total syntheses of other natural products.[31, 32] These works showcase substituted diaryl compounds are capable of achieving high degrees of selectivity for intramolecular C–H insertion, but intermolecular reactions, specifically C–H insertion reactions were generally unexplored.

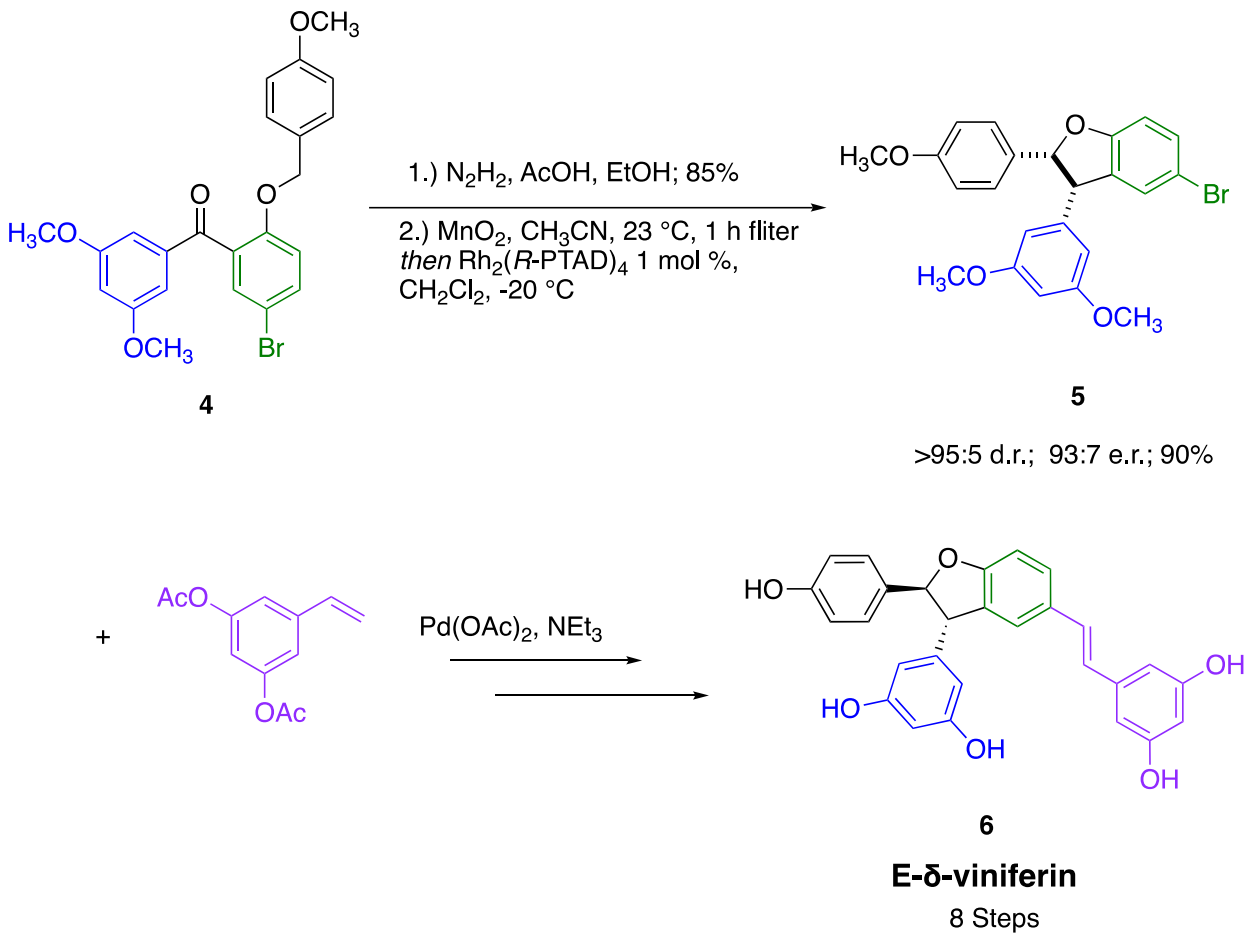

Scheme 3. Synthesis of E-δ-viniferin using Intramolecular C–H Insertion of Diaryl Diazo Compound as the Key Step

One of the first examples of a dirhodium donor/donor carbene system was a study done by Fürstner and co-workers investigating the metal-carbene intermediate in the crystal state for mechanistic investigations. At –20° C, they were able to crystalize a diaryl carbene/rhodium complex CH_2Cl_2. The bond orienations of the diaryl carbene to the rhodium in the crystal structure is shown in the partial structure **7**. This carbene, due to the presence of both electron-rich and electron-poor aryls in it, demonstrates a push/pull system analogous to that of a donor/acceptor carbene.The *p*-(dimethylamino)phenyl ring shown in blue is coplanar with the Rh−carbene bond and stabilizes the carbene center. In contrast, the electron-deficient p-(trifluoromethyl)phenyl ring

is orthogonal to carbene and does not provide stabilization. The NMR data of this complex in solution suggests that the major form is resonance structure **7a**, as the quinoid species.

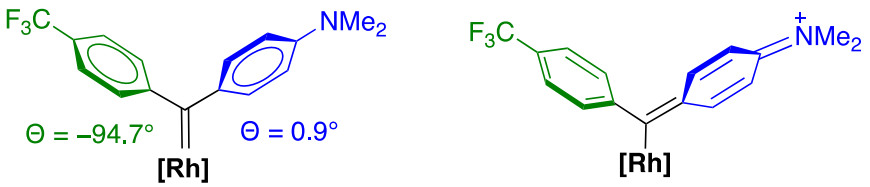

7 **7a**

Figure 2. Dirhodium Complex in the Solid State Characterized by Fürstner

While Fürstner's study mainly focused on structural characterization, one example showcased the reactivity of diaryl diazo compound **8** in the presence of 1 mol % $Rh_2(esp)_2$ to cyclopropanate an electron-rich *p*-(methoxy)styrene, shown in Scheme 4. The cyclopropane product **10** was afforded in 59% yield, however, the stereochemistry was not reported. This example utilized $Rh_2(esp)_2$ an achiral catalyst and sets up the framework to further investigate these diaryl compounds for their potential in enantioselective processes. Furthermore, it was noted that the reaction was able to form cyclopropane **10** in a diastereoselective manner, but the product epimerized during attempted purification by chromatography.[33] Fürstner found the cyclopropane generated epimerized during chromatography, presumably because the *N*,*N*-dimethylamino group is too strong as a donor group and would favor a cyclopropane ring-opening/ring-closing reaction via zwitterionic intermediates.

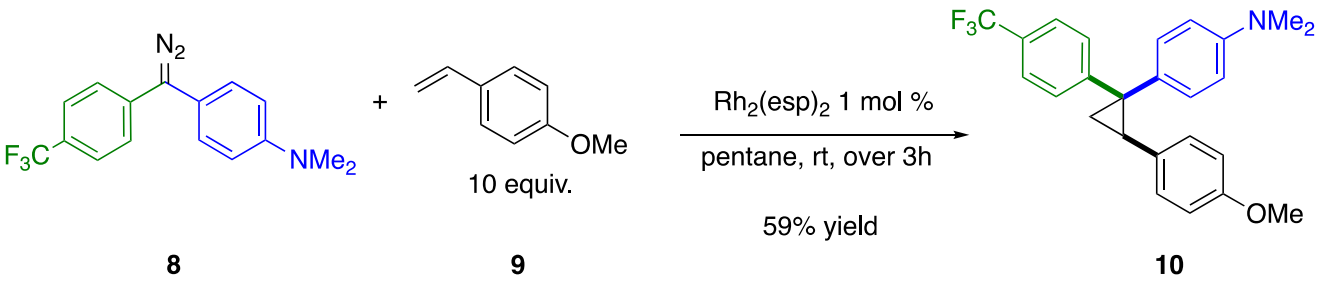

Scheme 4. Cyclopropanation of *p*-(Methoxy)styrene

2.2 Diaryl Diazo Compounds as Pseudo Donor/Acceptors

To understand this system further, in collaboration with Dr. Zhi Ren, we computationally and experimentally studied the cyclopropanation of styrene with varying steric and electronic moieties in a diaryl carbene system. In this chapter, all computational work and calculations were performed by Dr. Ren, and all experimental work in the lab was carried out by the author. The structures of the (tetraacetate)dirhodium carbene intermediates and the following cyclopropanation transition states were calculated and conducted at the B3LYP level of density functional theory[34-36] with the D3BJ dispersion corrections[37] using Gaussian09 program, the 6-31(d,p) basis set for the main-group elements, and the LANL2DZ basis sets and associated Hay−Wadt effective core potentials for rhodium atoms.[38, 39]

Based on Fürstner's work, we became interested in the possibility of diaryl diazo compounds behaving more similarly to donor/acceptor compounds. Donor/acceptor carbenes achieve high degrees of selectivity because the ester group remains orthogonal to the rhodium carbene and the electron-rich aryl ring remains in the plane stabilizing the rhodium carbene, shown in Figure 3. The cyclopropanation of styrene **12** by the donor/acceptor carbene **11** is a highly diastereoselective process. The donor group lies virtually in the same plane as the rhodium−carbene bond, whereas the acceptor group is orthogonal, shown in compound **11**. This arrangement influences the approach of the styrene, **12**, during the cyclopropanation: the π−π

interaction between the aryl group of styrene and the donor group of the carbene drives the diastereoselectivity of the reaction. The preferential approach of the styrene over the electron-rich phenyl ring is depicted in the transition state **13.** Figure 3a omits the ligands on the rhodium metal, but in the presence of chiral ligands, the process can be highly enantioselective. Based on the understanding of the bulkiness of a diphenyl system, we propose that in order to mitigate the steric clash of the two hydrogen molecules, one ring must tilt out of the plane, shown in compound **16.**

The premise is that both aryl groups would not be able to align in the same plane as the rhodium carbene at the same time, and one of the rings will be tilted out of the plane and will only weakly interact with the empty π orbital of the carbene: i.e., will act as an acceptor group. If the substituents on the rings are not equal and behave sterically and electronically different, there is a possibility of achieving a diastereoselective process similar to that of the donor/acceptor system. In Figure 3c, if one aryl ring is always tilted out of the plane, then the styrene would prefer to approach on the same side the phenyl in plane with the rhodium, shown in blue. This would lead to a highly diastereoselective cyclopropanation product **18**. One of the rings will be tilted out of the plane and will only weakly interact with the empty π–orbital of carbene, i.e., it will act as an acceptor group. This feature of the diarylcarbene should be even more pronounced if one of the aryl groups had an electron-withdrawing substituent and the other had an electron-donating substituent.

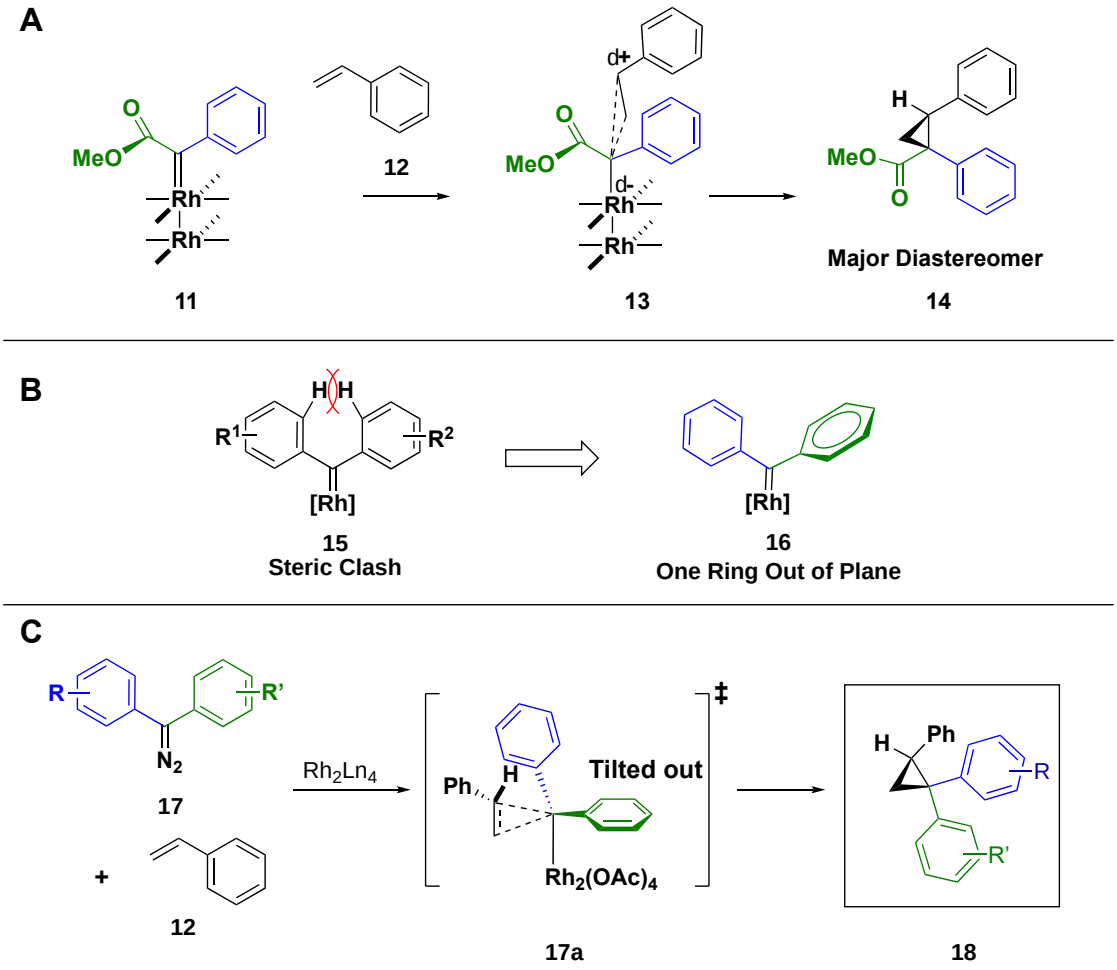

Figure 3. Diaryl System as Donor/Acceptor Carbene

To understand the effect of the electronics on the system, we first looked at the lowest occupied molecular orbital (LUMO) of rhodium bound carbenes complexes **19–22**. Complex **19** is a well-studied methyl phenyldiazoacetate donor/acceptor system. The LUMO shows considerable delocalization into the aryl ring and very little into the ester which is a consequence of stronger interaction of the ring's occupied π orbital with the carbene's empty π orbital. In the case of the diphenyl complex **20,** the delocalization occurs equally into both rings, suggesting that the carbene will be stabilized but would not have the distinctive features of a donor/acceptor carbene. However, when the two rings are differentiated in the case of **21** and **22** the delocalization occurs mainly into the more electron-donating ring with very little electron density in the sterically

constrained or electron-deficient ring. For **21**, with an electron-rich *para* methoxy group and a bulky *ortho* chloro substituent, the only delocalization occurs into the methoxy ring. For **22**, without the electron-rich methoxy, we still see preferential delocalization into the phenyl ring when a *para* nitro group and *ortho* chloro subsistent is present on the other rings. These LUMO diagrams suggest that it would be reasonable to expect these carbenes to exhibit a reactivity profile similar to what is observed with a classic donor/acceptor carbene.

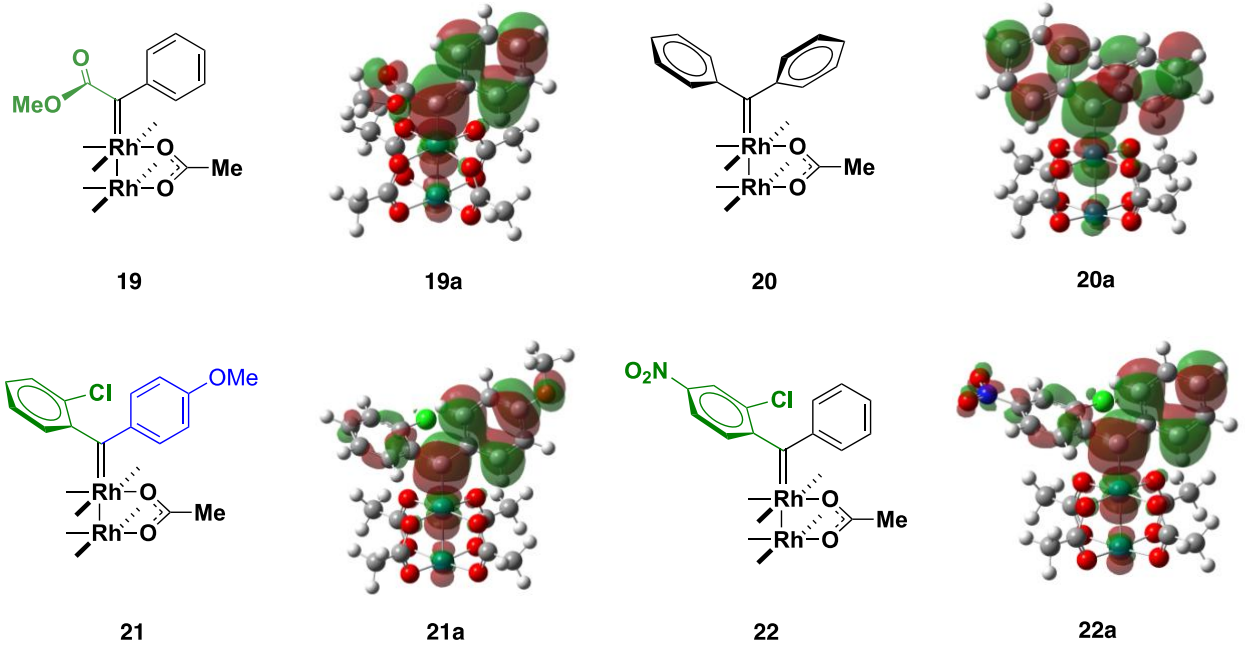

Figure 4. LUMO Diagram of Donor/Acceptor and Diaryl Carbene Complexes

2.3 Experimental Studies

Diaryl diazo compounds have been previously disclosed in the literature but most are generated *in situ* and used immediately in the reaction and therefore were previously not fully characterized.[29, 40] One of the most common ways to prepare phenyldiazoacetate diazo compound is through the use of mild diazo transfer reagents such as *p*-ABSA in the presence of DBU as a base.[41] This method is not feasible for a diaryl system due to their weak acidity with diphenylmethane having a pK_a of 32 in DMSO; they require harsh bases such as *n*-BuLi at –78 °C

or $NaNH_2$ in liquid ammonia to deprotonate.[42, 43] Instead, hydrazone oxidation to the diazo is the most common protocol.[44] Although diphenyldiazomethane is a known compound with literature reported syntheses, the reported oxidation conditions proved to be initially challenging.[45] After failed attempts using the classic MnO_2 oxidation, other routes were explored, shown in Scheme 5. At the time, Dr. Wenbin Liu was working on developing a system using copper(II) acetate and oxygen as oxidant to convert hydrazones to diazo compounds in collaboration with the Stahl Lab at the University of Wisconsin, Madison. While this method yielded the desired diaryl diazo compound **24**, it was low yielding due to favored decomposition to the dimer and ketone. This was attributed to the use of silica, which is slightly acidic, even after treated with triethylamine, causing nitrogen evolution that leads to diazo dimerization and other undesired pathways. However, this system was further optimized and is discussed in detail in Chapter Four.

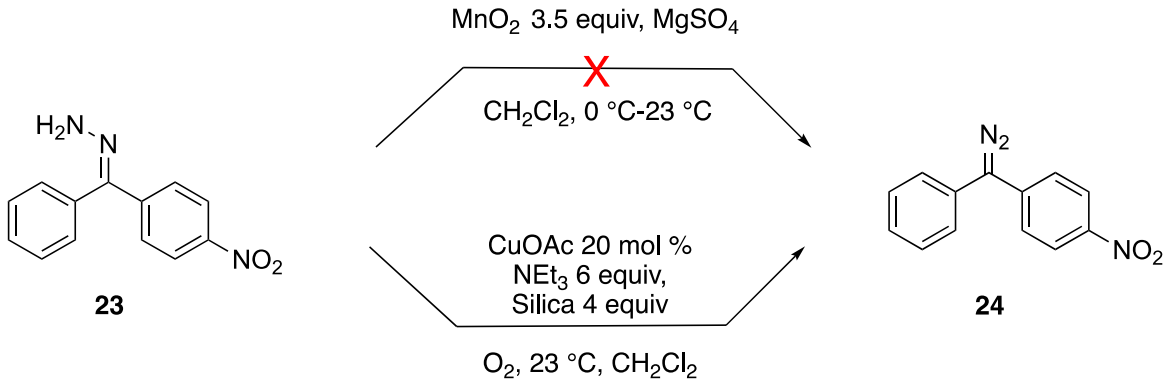

Scheme 5. Initial Oxidation Attempts Toward Diaryl Diazo Compounds

An alternative oxidation method was reported by Moody utilizing potassium *N*-iodo *p*-toluenesulfonamide (TsNIK) as an effective oxidant.[46] This method proved to be quite robust and provided a variety of diaryl diazo compounds **27–32** in high yields, shown in Scheme 6. The diazo compounds are stable when stored under an inert atmosphere at 4 °C for up to a month, yet long-term storage led to decomposition products that were detected by NMR analysis.

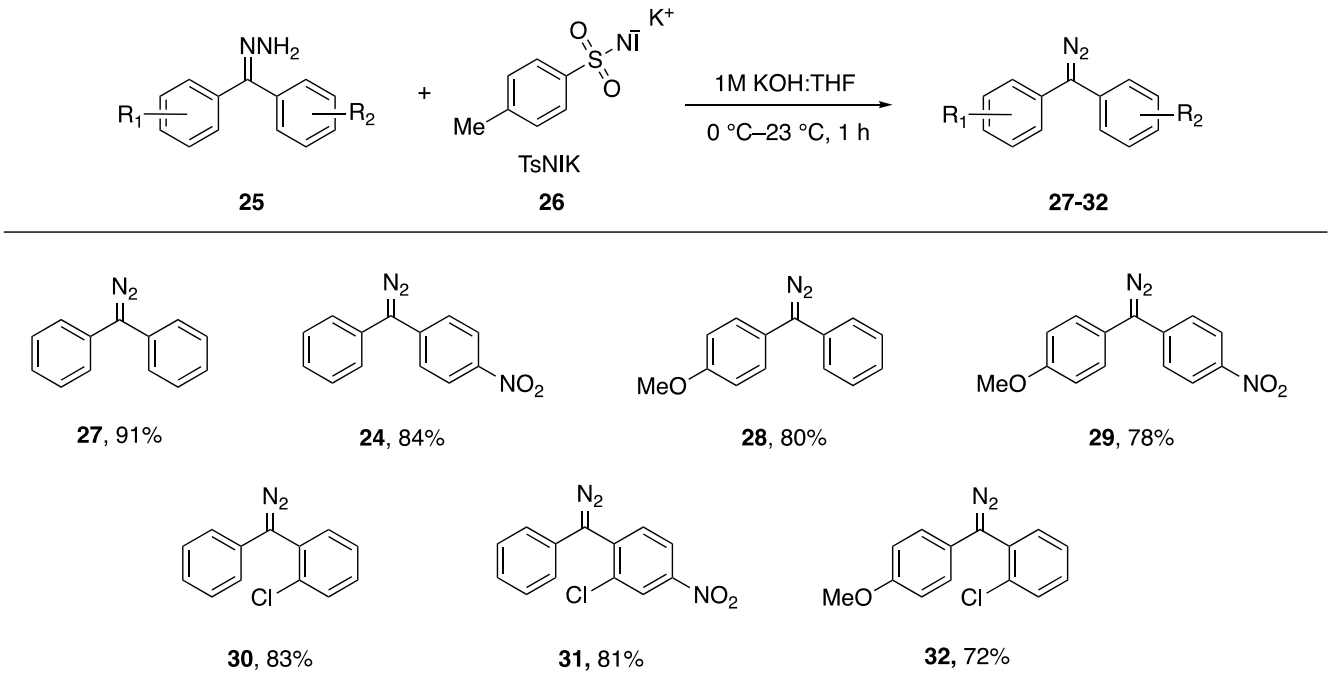

Reaction conditions: The desired hydrazone(3 mmol) was dissolved in 8 mL THF and TsNIK reagent (1.1 equiv, 3.3 mmol)was added, the mixture was stirred under air and placed in an ice bath. 1 M KOH(2 mL) was added dropwise over 5 mins. The reaction was allowed to continue at rt until all hydrazone was consumed based on TLC analysis.

Scheme 6. Hydrazone Oxidation to Diazo Compound using TsNIK Reagent

With the diazo compounds in hand, we first explored the possibility of asymmetric cyclopropanation reaction using chiral dirhodium catalyst. The reaction of **27** with styrene to form cyclopropane **33** proceeded in relatively low yield unless a large excess of styrene (10 equiv) was used as a trapping agent. A major side product was the azine **34**, which is a known side product of diarylcarbene reactions.[29, 47] This suggests that the carbene does not react very quickly with the styrene, allowing time for the carbene to react with additional diaryldiazomethane, which is added slowly via inverse addition. To increase the yield of the reaction, attempts were made to decrease the rate of addition up to 3 h instead of 1 h, but the diazo compound began crystallizing over the course of the addition and the syringe system provided a source of unreliability due to leaking. The Rh_2(*S*-DOSP)$_4$ catalyst gave relatively low levels of enantioselectivity, but this was expected

because Rh_2(*S*-DOSP)$_4$ tends to only give high enantioselectivity with donor/acceptor carbenes in which the acceptor group is a methyl ester and in hydrocarbon solvents.[48] In contrast, both Rh_2(*S*-NTTL)$_4$ and Rh_2(*S*-PTAD)$_4$ generated **33** with very high enantioselectivity. Remarkably, this result suggested that the aryl rings were differentially tilted and the two faces of the carbene were differentiated leading to a highly selective product.

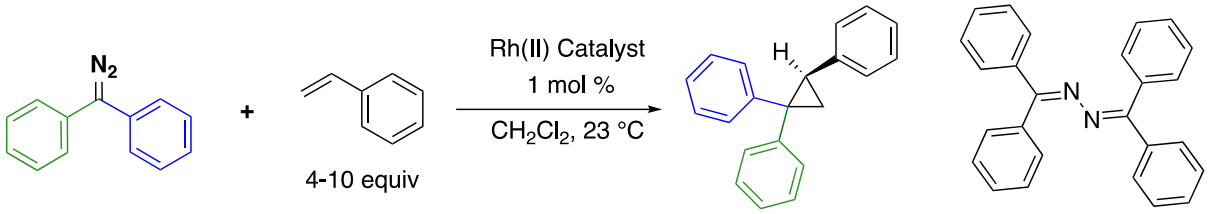

27 **12** **33** **34**

Entry	catalyst	styrene equiv.	yield, %	ee, %[a]
1	$Rh_2(OAc)_4$	4	21	–
2	Rh_2(S-DOSP)$_4$	4	23	18
3	Rh_2(S-NTTL)$_4$	4	36	93
4	Rh_2(S-PTAD)$_4$	4	36	92
5	Rh_2(S—NTTL)$_4$	10	86	93
6	**Rh_2(S-PTAD)$_4$**	**10**	**88**	**92**

Reaction conditions: 0.20 mmol diazo was inversely added to a solution of $Rh_2(Ln)_4$ and 4 or 10 equiv of styrene substrate in 1 mL CH_2Cl_2 over 1h. [a] ee (%) was determined using chiral HPLC analysis.

Scheme 7. Catalyst Screening of the Cyclopropanation of Diphenyldiazomethane

To investigate the diastereoselectivity of the diaryl diazo system *p*-nitro diazo compound **24** was studied in the cyclopropanation of styrene to generate the cyclopropanation product **35.** A series of dirhodium catalysts were tested and shown in Table 1. The d.r. for Rh_2(*S*-DOSP)$_4$ was 12:1 favoring the approach of styrene on the same side as the unsubstituted phenyl ring. The enantioselectivity of Rh_2(*S*-DOSP)$_4$ was low, but this again was an expected result due to the

solvent. Entries 3, 4 and 6 are phthalimido-based catalysts; the unsubstituted Rh_2(*S*-PTAD)$_4$ gave the highest asymmetric induction of 92%. Naphthalimido-based catalyst Rh_2(*S*-NTTL)$_4$ developed by Müller[22] gave an impressive 97% ee, but the diastereoselectivity of the reaction was just slightly above 1:1. Two triarylcyclopropane catalysts were tested, entries 7 and 8, where the diastereoselectivity of the reaction was enhanced to 8:1 with Rh_2(*S*-*p*-Ph-TPCP)$_4$.

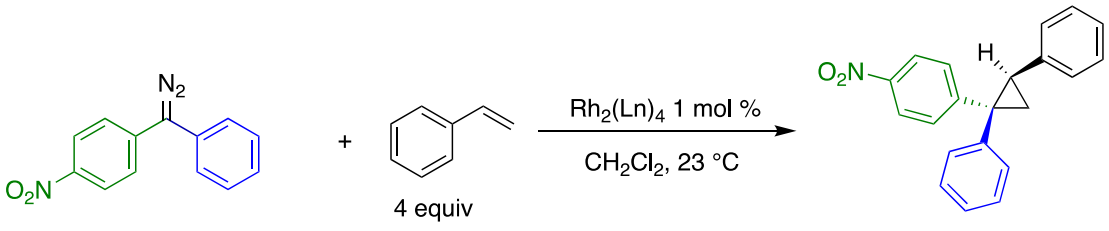

Entry	Catalyst	yield,%	d.r.[a]	ee,%[b] (major, minor)
1	$Rh_2(OAc)_4$	43	6:1	n.a.
2	Rh_2(*S*-DOSP)$_4$	62	12:1	18, 19
3	**Rh_2(*S*-PTAD)$_4$**	**90**	**2:1**	**92, 67**
4	Rh_2(*S*-TCPTAD)$_4$	31	1.5:1	81, 71
5	**Rh_2(*S*-NTTL)$_4$**	**82**	**1.2:1**	**97, 89**
6	Rh_2(*S*-TPPTTL)$_4$	61	7:1	62, 15
7	Rh_2(*S*-p-PhTPCP)$_4$	31	8:1	37, 58
8	Rh_2(*S*-p-BrTPCP)$_4$	41	3:1	41, 33

Reaction conditions: 0.20 mmol diazo was inversely added to a solution of $Rh_2(Ln)_4$ and 4 equiv of styrene substrate in 1 mL CH_2Cl_2 over 1h. [a] d.r. ratios were determined by crude NMR analysis. [b] ee (%) was determined by chiral HPLC analysis.

Table 1. Catalyst Screening of Cyclopropanation of Styrene with *p*-Nitro Diazo Compound

As seen with the other bulkier catalysts the enantioselectivity remained less than 50% ee.

To understand if the enantioselectivity was greatly affected by the choice of solvent in the

reaction system, two other solvents that were able to solubilize the diazo compound were screened shown in Table 2. Both toluene and trifluorotoluene were able to form the desired cyclopropanation product **35** in high yield, 93 and 87%, respectively. In both cases the diastereoselectivity of the reaction was slightly improved to 2:1 and 3:1. The enantioselectivity of the reaction was slightly less than with CH_2Cl_2 as the solvent. Based on these results, and our hypothesis that the diastereoselectivity of this system could be controlled based on the substituents on the aryl rings CH_2Cl_2 was chosen as the optimal solvent.

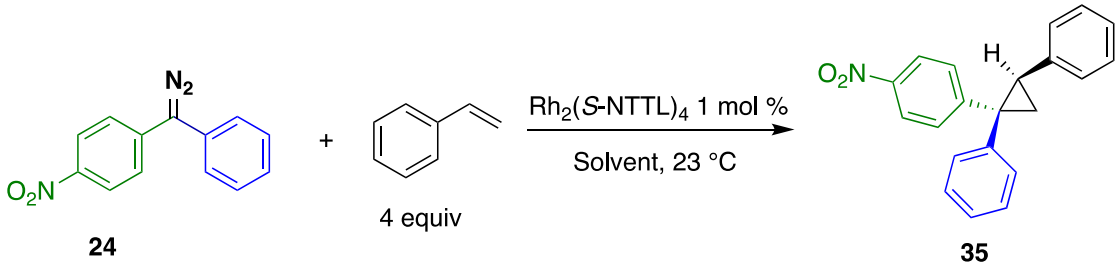

Entry	Solvent	yield,%	d.r.[a]	ee,%[b] (major, minor)
1	**Dichloromethane**	**82**	**1.2:1**	**97, 89**
2	Toluene	93	3:1	94, 60
3	Trifluorotoluene	87	2:1	96, 33

Reaction conditions: 0.20 mmol diazo was inversely added to a solution of $Rh_2(Ln)_4$ and 4 or 10 equiv of styrene substrate in 1 mL CH_2Cl_2 over 1h. [a] d.r. ratios were determined by crude NMR analysis. [b] ee (%) was determined by chiral HPLC analysis.

Table 2. Solvent Screen- Cyclopropanation of Styrene with *p*-Nitro Diazo Compound

To this end, incorporation of an electron-donating *p*-methoxy group led to the formation of cyclopropane **36** with 20:1 d.r. and excellent enantioselectivity with Rh_2(*S*-PTAD)$_4$. With Rh_2(*S*-NTTL)$_4$, the d.r. was slightly less at 8:1, but the ee was maintained at 98%. The yield for **36** was around 60% as the more donor like characteristics allowed for more undesired dimerization

byproducts to form, thus lowering the yield. To determine the absolute stereoconfiguration, an X-ray crystal structure of **36** was obtained. When the diaryldiazomethane most closely resembles the characteristics of a donor/acceptor compound, bearing one electron-rich and one electron-poor ring, as in **37**, the reaction is high yielding and highly selective. The Rh_2(*S*-PTAD)$_4$ catalyzed reaction generated **37** in 88% yield, 50:1 d.r., and 92% ee.

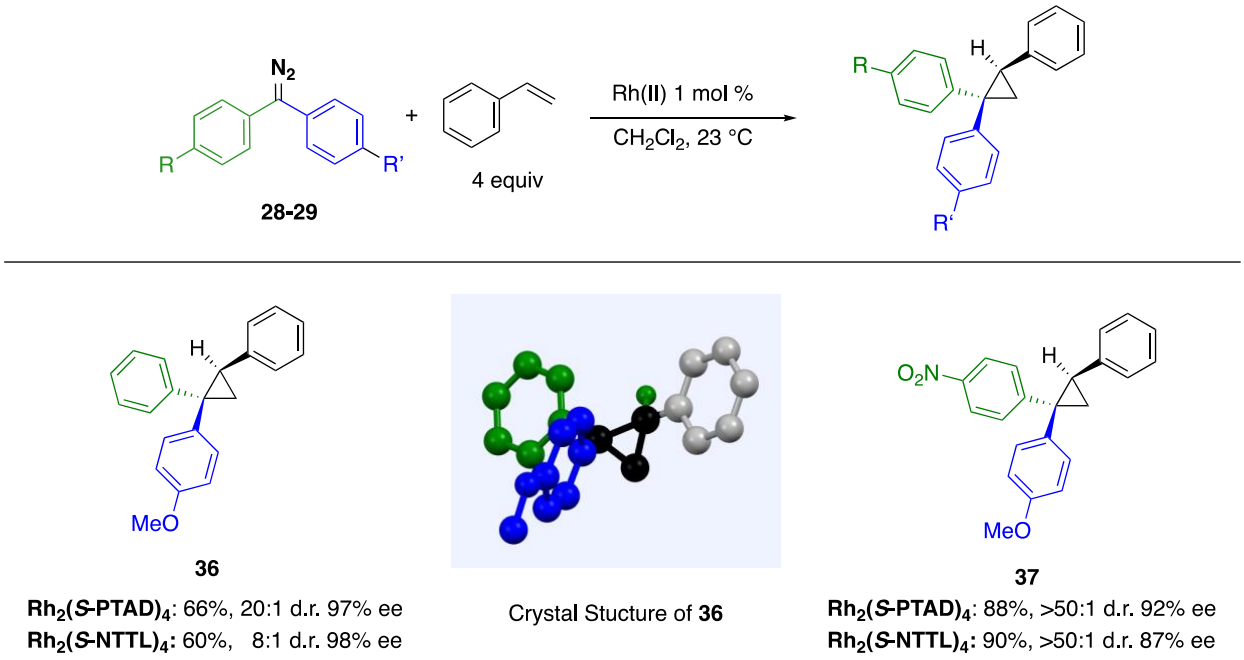

Reaction conditions: 0.20 mmol diazo was inversely added to a solution of $Rh_2(Ln)_4$ and 4 equiv of styrene substrate in 1 mL CH_2Cl_2 over 1h. d.r. ratios were determined by crude NMR analysis. ee (%) was determined by chiral HPLC analysis.

Scheme 8. Cyclopropanation of Electronically Different Diaryldiazo Compounds

Next, we explored the steric effects of a bulky *ortho*-chloro substituent on the diazo. The bulkiness of the chlorine should increase the tilt of the substituted aryl ring, which would then lead to more a diastereoselective cyclopropanation event. Indeed, as seen in Scheme 9, for all diazo compounds baring an *o*-Cl substituent, the diastereoselectivity is >50:1. Due to the decreased stability of the diazo compound, 10 equiv of styrene was used to increase the yield. When only an *o*-Cl substituent was used, **38**, the enantioselectivity was between 82 and 85% yield. However,

when an electron-withdrawing *p*-nitro group was added (**39**), the enantioselectivity dropped significantly. This result varies from incorporating the nitro group merely, where the enantioselectivity was >90% for most catalysts. Although this result was initially intriguing and perplexing, further optimization on this substrate was not explored at the time. The addition of *p*-methoxy to the other aryl ring (**40**) proceeded with high enantioselectivity of 93% catalyzed by Rh_2(*S*-PTAD)$_4$ and 92% catalyzed by Rh_2(*S*-NTTL)$_4$. The yield was slightly diminished with this diazo compound, presumably because the carbene is not sufficiently electrophilic leading to greater formation of a dimerization byproduct.

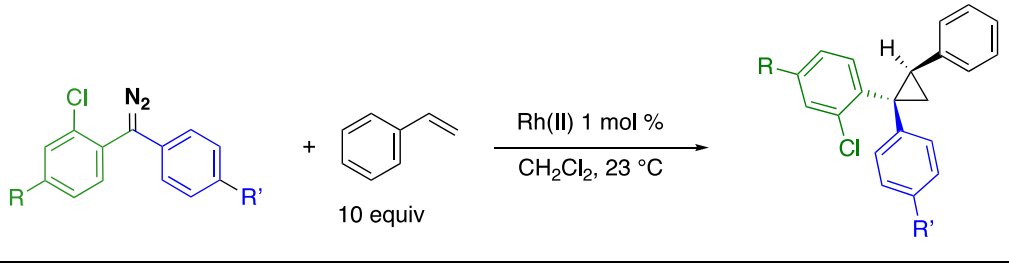

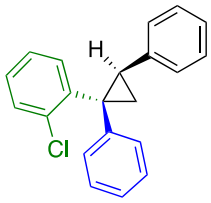

38

Rh_2(*S*-PTAD)$_4$: 91%, 50:1 d.r. 85% ee
Rh_2(*S*-NTTL)$_4$: 72%, 50:1 d.r. 82% ee

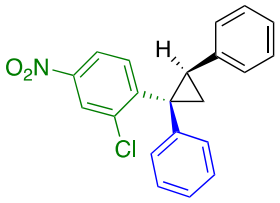

39

Rh_2(*S*-PTAD)$_4$: 89%, 50:1 d.r. 22% ee
Rh_2(*S*-NTTL)$_4$: 88%, 50:1 d.r. 57% ee

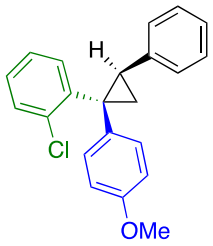

40

Rh_2(*S*-PTAD)$_4$: 56%, 50:1 d.r. 93% ee
Rh_2(*S*-NTTL)$_4$: 34%, 50:1 d.r. 92% ee

Reaction conditions: 0.20 mmol diazo was inversely added to a solution of $Rh_2(Ln)_4$ and 10 equiv of styrene in 1 mL CH_2Cl_2 over 1h. d.r. ratios were determined by crude NMR analysis. ee (%) was determined by chiral HPLC analysis.

Scheme 9. Cyclopropanation of Sterically Different Diaryldiazo Compounds

2.4 Computational studies

The cyclopropanation of styrene with these substituted diaryl diazo compounds was then studied computationally, Dr. Ren performed all of the calculations discussed herein. The

transition states for the cyclopropanation of diazo compounds **24** and **28–32** are described in Scheme 10. The calculations were conducted for the approach of the styrene occurring over the electron-rich or the electron-deficient aryl ring, leading to four possible transition states **TS1**–**TS4**. The most stable of the transition states, **TS1**, has the styrene approaching over the electron-rich ring, shown in blue, which is most similar to the donor group in a donor/acceptor system. The energy differences between the calculated transition states gives a prediction for the diastereoselectivity of each given compound. In the case of compound **35**, the smallest free energy difference is 1.7 kcal mol^{-1}, which leads to a predicted diastereomeric ratio of **35** to **35'** of 16:1 d.r. This value is slightly higher than the experimentally observed value of 6:1, however, overall rationalized the observed selectivity. The most notable energy differences are **37**, **39**, and **40** are around 3 kcal mol^{-1}, which predicts the cyclopropanation to proceed with >50:1 d.r. These values agree with the experimentally observed values. **TS1** is the preferred lowest energy transition state and has the electron-rich ring closer in plane to the rhodium, tilted 17–22° out of plane whereas the electron-deficient ring is tilted 41–57°. There was a significant increase in the tilt changing from the rhodium carbene complex to the transition state of the cyclopropanation. This tilting is similar to the behavior of that of a donor/acceptor carbene transition state and the calculated results show a similar high degree of selectivity. These calculations were performed with $Rh_2(OAc)_4$, an achiral catalyst, to minimize complexity, however, if a chiral catalyst was used which is capable of distinguishing the approach from the front face versus the back face of the rhodium carbene, then the cyclopropanation would occur with high values of both enantio- and diastereoselectivity.

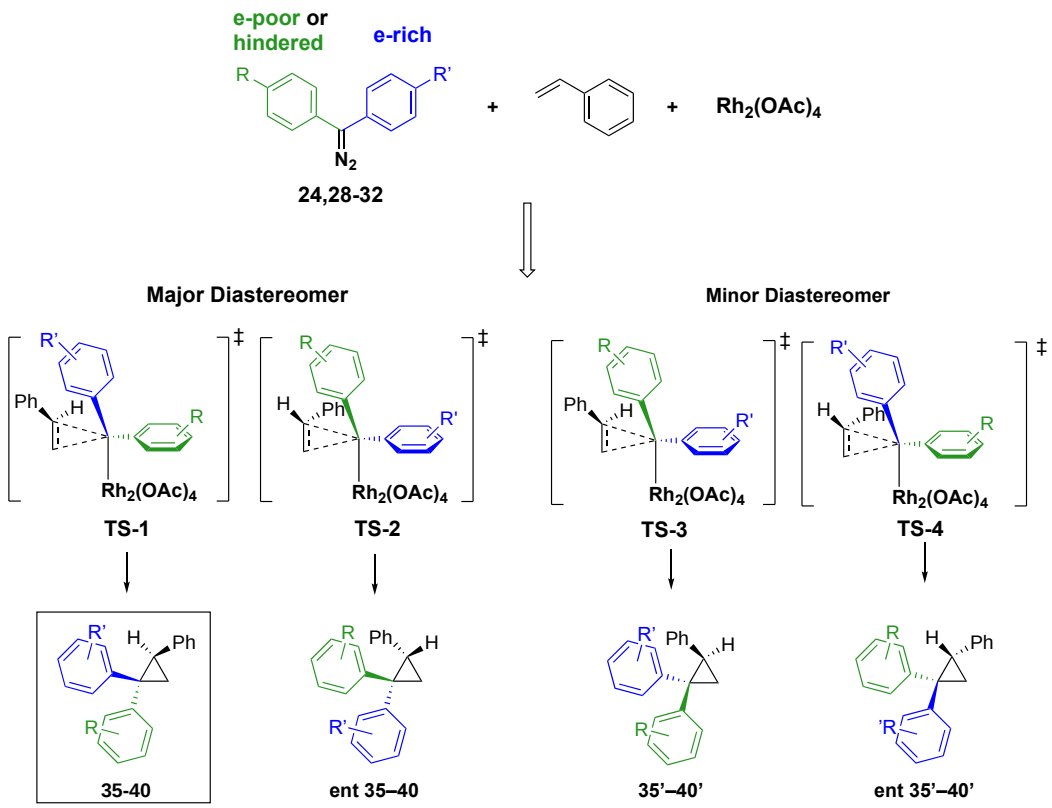

	Substituents R	R'	TS-1	TS-2	TS-3	TS-4	Energy Difference and Calculated d.r.[b]		The Lowest TS[c,d] Torsion Angle Aryl Ring/Aryl Ring (°)
			(kcal mol^{-1})[a]						
35	4-NO_2	H	0.0/0.0	5.9/4.7	1.7/1.7	3.7/1.9	1.7/1.7	16:1	48.2 (2.6) / 17.3 (-13.9)
36	H	4-OMe	0.0/0.0	5.1/3.8	2.0/1.8	4.7/3.7	2.0/1.8	19:1	41.9 (0.9) / 21.2 (-7.4)
37	4-NO_2	4-OMe	0.0/0.0	7.5/6.0	4.1/4.0	4.8/3.6	4.8/3.6	>50:1	46.0 (-3.2) / 20.0 (-5.2)
38	2-Cl	H	0.0/0.0	6.2/6.4	2.6/2.0	5.2/4.7	2.6/2.0	30:1	53.7 (-6.1) / 20.0 (-3.8)
39	2-Cl, 4-NO_2	H	0.0/0.0	9.3/8.0	4.8/3.2	5.0/3.4	4.8/3.2	>50:1	56.9 (-24.8) / 18.4 (9.8)
40	2-Cl	4-OMe	0.0/0.0	6.8/5.4	3.7/2.8	5.9/4.6	3.7/2.8	>50:1	51.5 (-25.5) / 21.8 (15.1)

[a] The relative enthalpy and Gibbs free energies are shown as ΔH/ΔG. [b] The diastereomeric ratio is calculated on the basis of the Gibbs free energies (calculated at 25 °C and 1 atm). [c]The distortion angle of the electron-poor or hindered aryl ring is presented in orange, and that of the electron- rich aryl ring is presented in blue. [d]Deviation from its carbene is shown in parentheses. [e]The styrene is shown approaching from the front face of the carbene.

Scheme 10. Computational Analysis of the Transition States for Cyclopropanation of Styrene with Diaryldiazo Compounds

2.5 Kinetic studies *via* ReactIR

Diazo compounds have a distinct IR stretch around 2050 cm^{-1}, which can be studied to measure the decomposition rate of the diazo compound in the presence of a rhodium catalyst. We

were interested in comparing the relative rates of the diaryl diazo compounds to the well-studied donor/acceptor diazo compounds using ReactIR. The low yields in certain systems were proposed to be due to the slow rate of reaction of the diarylcarbenes with the styrene compared to the reactions of donor/acceptor carbenes. In order to probe this idea further ReactIR studies were performed to determine the reactivity of the different diazo compounds. It has been previously reported that aryl diazoacetates can perform at low catalyst loading (0.0025 mol %). However, when diaryl diazo compounds were subjected to lower catalyst loading, little to no diazo decomposition was observed, which indicates no formation of a rhodium carbene. The reaction was then tried at lab scale (1 mol %) to compare which catalyst performed at a faster rate between the two best performing cyclopropanation results. These results, shown in Figure 5, revealed that the diazo consumption is approximately 3x faster when using Rh_2(*S*-PTAD)$_4$ compared to Rh_2(*S*-NTTL)$_4$. Previous studies conducted by Dr. Bo Wei demonstrated that at 1 mol % the donor/acceptor diazo, trichloroethyl (*p*-bromophenyl)diazoacetate reacts too fast to generate data points at 5 s intervals and all diazo is consumed in under 30 s. To obtain data of the decomposition of this diazo the cyclopropanation needed to be carried out with a catalyst loading of 0.0025 mol %.[49] The reactions with diaryldiazomethane were conducted with 1 mol % of catalyst, due to little to no diazo decomposition at lower loading and at 0.0025 mol % no decomposition was observed. Based on these results we can conclude the diaryl diazo compound reacts at a rate that is at least 400 times slower than the trichloroethyl (*p*-bromophenyl)diazoacetate. The less reactive nature helps to explain why the dimerization observed in our reactions because if the diazo compound is not quickly decomposed into rhodium carbene, the remaining diazo can compete with styrene to form azine dimer instead of the desired cyclopropanation product.

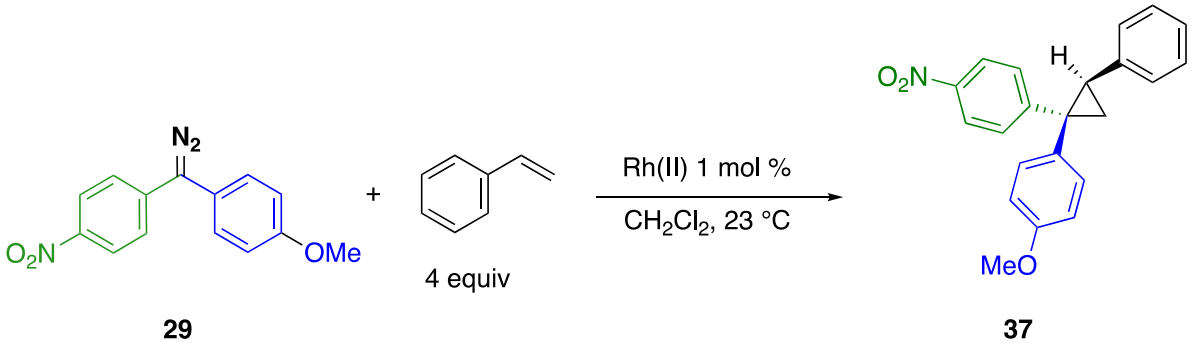

29 **37**

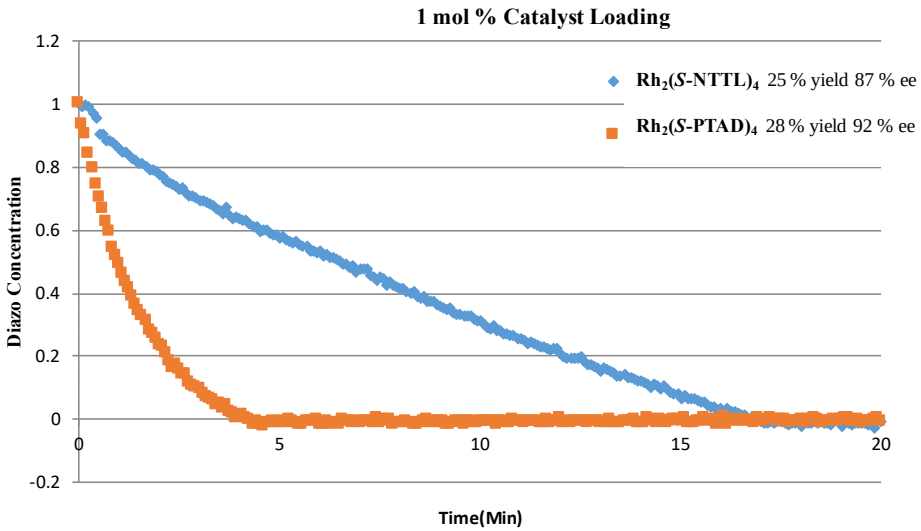

Reaction Conditions: Reaction rates of various catalysts in the cyclopropanation reaction with 0.1 M concentration of diazo compound **29** and 1 mol % catalyst loading. The catalyst was added in one portion to the reaction mixture, and the rate of disappearance of the signal for the diazo group was followed by ReactIR.

Figure 5. ReactIR Graph of the Decomposition of Diazo 29 with Rh_2(*S*-NTTL)$_4$ and Rh_2(*S*-PTAD)$_4$

2.6 Conclusion

The experimental and computational studies discussed showcase that diaryl diazo carbenes have many similar characteristics to that of donor/acceptor carbenes. This work demonstrates an expansion of the type of reactivity possible for a diaryl system by utilizing steric and electronic effects of substituents on the diaryl carbene system. The cyclopropanation of styrene is highly diastereoselective, achieving over 50:1 d.r. when an *ortho* substituent was used or one electron-rich and one electron-poor aryl ring, which is a distinct feature of donor/acceptor carbenes. When

chiral catalysts Rh_2(*S*-PTAD)$_4$ and Rh_2(*S*-NTTL)$_4$ are used the reactions are also highly enantioselective. These studies set the foundation to the concept that diaryldiazomethanes can have an unexpected range of reactivity toward intermolecular reactions because they behave more like donor/acceptor carbenes rather than donor/ donor carbenes. The work discussed in this chapter has been published in the journal *ACS Catalysis*.[1] Figures and analysis from this paper have been incorporated into this chapter.

2.7 Experimental Data

2.7.1 General Considerations

Substrates and reagents were purchased from the following suppliers and used without further purification: Sigma-Aldrich, Alfa-Aesar, Oakwood Chemical America, and Fisher Scientific.

All solvents were purified and dried by a Glass Contour Solvent System, and stored over 4 Å molecular sieves 24 hours before use. All reactions were carried out in flamed-dried glassware under Nitrogen unless otherwise stated. ^{1}H NMR spectra were recorded at 600 MHz on Bruker-600 spectrometer, Varian INOVA 500 MHz or Varian 400 MHz. ^{13}C NMR spectra were recorded at 150 MHz on Bruker-600. NMR spectra samples were prepared using deuterated chloroform($CDCl_3$) with residual solvent serving as internal standard 7.26 ppm for ^{1}H and 77.16 ppm for ^{13}C; or with Deuterated chloroform 0.03% TMS with residual TMS serving at internal standard (0.00 ppm). Abbreviations for signal multiplicity are as follows: s= singlet, d= doublet, t= triplet, m= multiplet, dd= doublet of doublets dt= doublet of triplets. Coupling constants(J-values) were calculated directly from spectra. IR spectra were collected on a Nicolet Is10 FT-IR spectrometer. *In situ* IR reaction monitoring experiments were carried out with a Mettler Toledo ReactIR 45m instrument equipped with a 9.5 mm x 12'' AgX 1.5 m SiComp probe. Mass spectra were taken on a Thermo Finnigan LTQ-FTMS spectrometer with APCI or NSI. Thin layer chromatographic analysis (TLC) was performed on aluminum-sheet silica gel plates, and visualized with UV light. Melting point were measured in open capillary tubes with a Mel-Temp apparatus and recorded as a range. Racemic standards for enantiomeric determination were generated with reactions with $Rh_2(OAc)_4$ or from Rh_2((*R*) and (*S*)-DOSP)$_4$ which was generated by dissolving equimolar mixture of R and S catalyst in a minimal amount of benzene and

lyophilizing. High performance liquid chromatography analysis (HPLC) was performed on Agilent 1100 Technologies HPLC instrument.

Caution: Diazo compounds are high energy compounds and should be handled with caution. Although we have had no difficulties with working with these compounds, it is advisable to carry out reactions on small scale behind a blast shield. Hydrazine hydrate is highly toxic compound and needs to be handled using the established safety protocols. In addition, Diaryl Diazo compounds are known to be unstable and must be handled with caution and stored in a -20 °C freezer to avoid decomposition over time.

2.7.2 General Procedure for Diazo Compounds

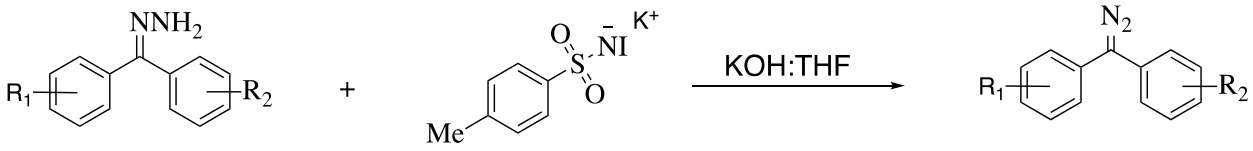

Procedure adopted from literature.[50] A 50 mL dried round bottom flask was charged with hydrazone (1.1 mmol) and THF (4 mL) followed by tsNIK(1.2 mmol) prepared by following the literature procedure.[4] The potassium hydroxide in 1 M solution (1 mL) was slowly added to the flask. The reaction was monitored by TLC, with disappearance of all starting hydrazone derivatives by 1.5 h. The reaction was poured into 5 mL potassium hydroxide in 1 M solution and extracted with diethyl ether (2 x 30 mL). The organic layers were combined then washed with brine (2 x 30 mL) and dried over $MgSO_4$. After removal of the solvent, the desired diazo compound was obtained. If necessary diazo was purified using an alumina column under gradient 0 to 5 % diethyl ether in hexanes. Product was stored under Argon at -20 °C.

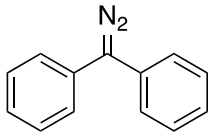

27

(Diazomethylene)dibenzene (27)

Prepared using general procedure, benzophenone hydrazone (216 mg, 1.10 mmol) was used to afford the titled diazo compound (190 mg, 91 % yield). ^{1}H NMR (500 MHz, $CDCl_3$) δ 7.42 – 7.38 (m, 2H), 7.31 (d, J=7.3 Hz 2H), 7.20 (t, *J* = 7.3 Hz, 1H). This is a known compound in the literature.[50]

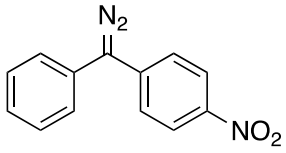

24

1-(Diazo(phenyl)methyl)-4-nitrobenzene (24)

Prepared using general procedure, ((4-nitrophenyl)(phenyl)methylene)hydrazone (270 mg, 1.10 mmol) was used to afford the titled diazo compound (194 mg,84 % yield). ^{1}H NMR (600 MHz, $CDCl_3$) δ 7.78 (d, *J* = 8.99 Hz, 2H), 7.07 – 7.00 (m, 2H), 6.95 (t, *J* = 7.46 Hz, 1H), 6.88 (dd, *J* = 8.32, 1.25 Hz, 2H), 6.52 (d, *J* = 8.97 Hz, 2H). This is a known compound in the literature.[51]

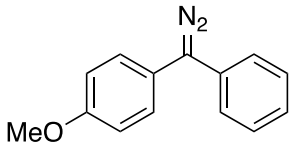

28

1-(Diazo(phenyl)methyl)-4-methoxybenzene (28)

Prepared using general procedure, 4-methoxyphenyl)(phenyl)methylene)hydrazone (250 mg, 1.10 mmol) was used to afford the titled diazo compound (198 mg, 80% yield). ^{1}H NMR (500 MHz,

$CDCl_3$) δ 7.38 – 7.33 (m, 2H), 7.28 (d, *J* = 8.97 Hz, 2H), 7.25 – 7.18 (m, 2H), 7.17 – 7.11 (m, 1H), 6.98 (d, *J* = 9.01 Hz, 2H), 3.84 (s, 3H). This compound is known in the literature.[51]

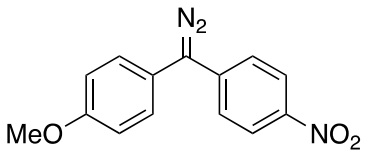

29

1-(Diazo(4-methoxyphenyl)methyl)-4-nitrobenzene (29)

Prepared using general procedure, ((4-methoxyphenyl)(4-nitrophenyl)methylene)hydrazone (300 mg, 1.1 mmol) was used to afford the titled diazo compound (231 mg, 78% yield). ^{1}H NMR (600 MHz, $CDCl_3$) δ 7.94 (d, *J* = 8.99 Hz, 2H), 6.96 (d, *J* = 8.76 Hz, 2H), 6.80 (d, *J* = 8.76 Hz, 2H), 6.64 (d, *J* = 8.96 Hz, 2H), 3.37 (s, 3H). ^{13}C NMR (126 MHz, $CDCl_3$) δ 159.55, 143.90, 139.77, 129.56, 124.59, 122.20, 118.47, 115.21, 55.45, the signal due to CN_2 was not observed. IR (in $CDCl_3$) 2836, 2035, 1585, 1505, 1319, 1248, 1105, 850, 830, 748, 690. HRMS (+p NSI) calculated for $C_{14}H_{12}O_3N$ $[M+H-N_2]^+$ 242.0822 found 242.0810. Melting point: 93-94 °C.

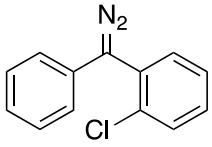

30

1-Chloro-2-(diazo(phenyl)methyl)benzene (30)

Prepared using general procedure, ((2-chlorophenyl)(phenyl)methylene)hydrazone (250 mg, 1.1 mmol) was used to afford the titled diazo compound (213 mg, 83% yield). This compound is unstable and was immediately subject to the cyclopropanation reaction and was not stable enough to obtain a pure ^{13}C NMR. ^{1}H NMR (400 MHz, $CDCl_3$) δ 7.52 – 7.46 (m, 2H), 7.36 – 7.29 (m, 4H), 7.12 – 7.07 (m, 1H), 7.03 – 6.99 (m, 2H). This is a known compound in the iterature.[52]

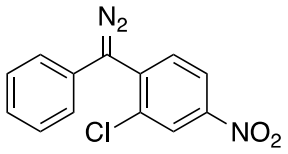

31

2-Chloro-1-(diazo(phenyl)methyl)-4-nitrobenzene (31)

Prepared using general procedure, (2-chloro-4-nitrophenyl)(phenyl)methylene)hydrazone (303 mg, 1.10 mmol) was used to afford the titled diazo compound (250 mg, 81% yield). ^{1}H NMR (600 MHz, $CDCl_3$) δ 8.35 (d, *J* = 2.4 Hz, 1H), 8.10 (dd, *J* = 8.7, 2.4 Hz, 1H), 7.53 (d, *J* = 8.8 Hz, 1H), 7.40 (dd, *J* = 8.4, 7.5 Hz, 2H), 7.25 – 7.20 (m, 1H), 7.16 – 7.13 (m, 2H). ^{13}C NMR (150 MHz, $CDCl_3$) δ 146.41, 135.79, 132.96, 129.69, 129.44, 128.87, 126.45, 126.28, 124.43, 122.02, the signal due to CN_2 was not observed. IR (in $CDCl_3$) 3099, 2053, 1674, 1520, 1344, 1280, 878, 765, 744, 696. HRMS (+p NSI) calculated for $C_{13}H_9ClNO_2$ $[M+H-N_2]^+$ 246.0327 found 246.03148. Melting point: 72-74 °C.

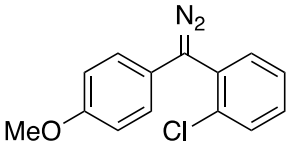

32

1-Chloro-2-(diazo(4-methoxyphenyl)methyl)benzene (32)

Prepared using general procedure, ((2-chlorophenyl)(4-methoxyphenyl)methylene)hydrazone (287 mg,1.10 mmol) was used to afford the titled diazo compound (216 mg,72% yield). The desired diazo was sensitive to acid and light, and was not stable enough to obtain a pure ^{13}C NMR. Diazo compound was prepared, concentrated in vacuum in the dark and immediately subject to the cyclopropanation reaction. ^{1}H NMR (500 MHz, $CDCl_3$) δ 7.47 (dd, *J* = 7.9, 1.5 Hz, 1H), 7.41 (dd,

J = 7.5, 2.0 Hz, 1H), 7.31 – 7.23 (m, 2H), 6.97 – 6.89 (m, 4H), 3.80 (s, 3H). The product is sensitive to acid and was unstable in chloroform and other deuterated solvents.

2.7.3 General procedure for cyclopropanation:

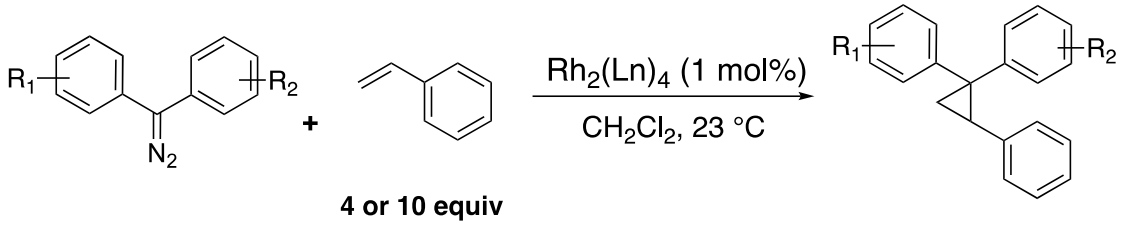

To a flame-dried the desired dirhodium catalyst $Rh_2(OAc)_4$ (0.88 mg, 1 mol %) added by stock (1.0 mL of 0.002 M in CH_2Cl_2 or Rh_2(*S*-NTTL)$_4$ (2.90 mg, 1 mol %) or Rh_2(*S*-PTAD)$_4$ (3.12 mg, 1 mol %) was added, and the reaction vial was purged with argon three times and dissolved in CH_2Cl_2 (1.0 mL) and was charged with styrene. The corresponding diazo compound (0.2 mmol) was weighed in a 20 mL vial and dissolved in dry degassed DCM (4.0 mL). The diazo compound solution was then added to the reaction vial dropwise over 1 h at room temperature (23 °C) *via* a syringe pump. Reaction was stopped after 14 h and concentrated under vacuum for crude ^{1}H NMR to determine the diasteromeric ratio. The product was purified *via* flash column chromatography (a mixture of diastereomers and enantiomers) with a gradient of 0 to 25 % diethyl ether in hexanes.

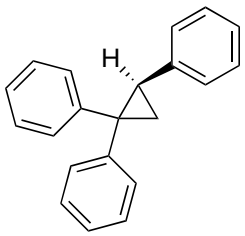

(*R*)-cyclopropane-1,1,2-triyltribenzene (33)

Prepared using general procedure, styrene (0.23 mL, 2.0 mmol, 10 equiv) with diazo compound **27** (39 mg, 0.50 mmol) using dirhodium catalyst (1 mol %) with a reaction time of 14 h. Flash

chromatography (gradient 0 to 10 % diethyl ether/hexanes) to afford the titled product **33**. ^{1}H NMR (600 MHz, $CDCl_3$) δ 7.27 (tdd, *J* = 10.0, 7.3, 1.8 Hz, 4H), 7.16 (td, *J* = 7.0, 1.9 Hz, 1H), 7.12 – 7.02 (m, 8H), 6.87 – 6.84 (m, 2H), 2.85 (ddd, *J* = 8.6, 6.5, 1.7 Hz, 1H), 1.99 – 1.96 (m, 1H), 1.80 (ddd, *J* = 9.4, 5.3, 1.7 Hz, 1H).^{13}C NMR (150 MHz, $CDCl_3$) δ 147.00, 140.20, 138.69, 131.16, 128.33, 127.92, 127.90, 127.62, 127.41, 126.21, 125.89, 125.57, 39.31, 32.37, 20.86. This is a known compound in literature[53]

With $Rh_2(OAc)_4$: obtained **33**, 12 mg in 21 % yield.

With Rh_2(*S*-PTAD)$_4$: obtained **33**, 48 mg, 88 % yield, 92 % ee.

With Rh_2(*S*-NTTL)$_4$: obtained **33**, 47 mg, 86 % yield, 93 % ee.

HPLC: (4900 column, hexane, 1 mL min^{-1} 0.5 mg mL^{-1} 30 min, UV 230 nm) retention times of 15. 4 min (minor) and 18.6 min (major) 92 % ee with Rh_2(*S*-PTAD)$_4$ and of 16.60 min (minor) and 19.7 min (major) 93 % ee with Rh_2(*S*-NTTL)$_4$.

$[\alpha]^{20}_D$ +133.8 ° (c = 0.58, $CHCl_3$) for 92 % ee.

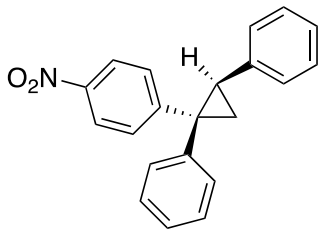

35

((1*S*,2*R*)-1-(4-nitrophenyl)cyclopropane-1,2-diyl)dibenzene (35)

Prepared using general procedure, styrene (0.09 mL, 0.80 mmol, 4 equiv) with diazo compound **24** (48 mg, 0.50 mmol) using dirhodium catalyst (1 mol %) with a reaction time of 14 h. Flash chromatography (gradient 0 to 15% diethyl ether/hexanes) afforded the titled product **35**. ^{1}H NMR (600 MHz, $CDCl_3$) δ 8.13 – 8.09 (m, 2H), 7.36 – 7.32 (m, 2H), 7.25 – 7.01 (m, 8H), 6.86 – 6.83

(m, 2H), 2.89 (dd, *J* = 9.1, 6.8 Hz, 1H), 2.13 (dd, *J* = 6.8, 5.7 Hz, 1H), 1.90 (dd, *J* = 9.1, 5.7 Hz, 1H). ^{13}C NMR (150 MHz, $CDCl_3$) δ 154.54, 145.93, 138.38, 137.49, 131.48, 128.31, 127.90, 127.81, 127.55, 127.00, 126.13, 123.63, 39.02, 34.08, 22.07. This is a known compound in the literature.[53]

With $Rh_2(OAc)_4$: obtained **35**, 27 mg, 43% yield.

With Rh_2(*S*-PTAD)$_4$: obtained **35**, 57 mg, 90% yield, 2:1 d.r. 97% ee.

With Rh_2(*S*-NTTL)$_4$: obtained **35**, 52 mg 82% yield, 1.2:1 d.r. 87% ee.

With Rh_2(*S*-DOSP)$_4$: obtained **35**, 39 mg, 62% yield, 12:1 d.r. 18% ee.

HPLC (ADH column, hexane, 1.0 mL min^{-1} 0.5 mg mL^{-1} 30 min, UV 230 nm) retention times of 12.65 min (major) and 14.12 min (minor) 92% ee with Rh_2(*S*-PTAD)$_4$, 12.70 min (major) and 14.17 min (minor) 97% ee with Rh_2(*S*-NTTL)$_4$, and of 14.20 min (major) and 12.69 min (minor) 20% ee with Rh_2(*S*-DOSP)$_4$. The diastereomer was also visible with retention times of 14.12 min (major) and 15.61 min (minor) 68% ee with Rh_2(*S*-PTAD)$_4$ and 14.2 min (major) and 15.64 min (minor) 87% ee with Rh_2(*S*-NTTL)$_4$, and of 12.69 min (major) and 13.56 min (minor) 20% ee with Rh_2(*S*-DOSP)$_4$.

$[\alpha]^{20}_D$ +154.1° (c = 1.00, $CHCl_3$) for 92% ee.

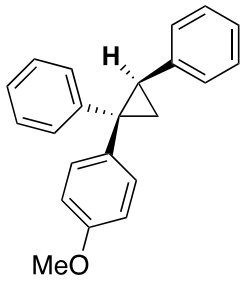

36

((1*R*,2*R*)-1-(4-methoxyphenyl)cyclopropane-1,2-diyl)dibenzene (36)

Prepared using general procedure, styrene (0.09 mL, 0.80 mmol, 4 equiv) with diazo compound **28** (45 mg, 0.50 mmol) using dirhodium catalyst (1 mol %) with a reaction time of 14 h. Flash chromatography (gradient 0 to 15 % diethyl ether/hexanes) afforded the titled product **11c**.^{1}H NMR (400 MHz, , $CDCl_3$) δ 7.35 – 7.22 (m, 4H), 7.14 (d, *J* = 14.77 Hz, 1H), 7.14 – 7.03 (m, 3H), 7.01 (d, *J* = 8.73 Hz, 2H), 6.92 – 6.80 (m, 2H), 6.66 (d, *J* = 8.73 Hz, 2H), 3.71 (s, 3H), 2.81 (dd, *J* = 9.00, 6.58 Hz, 1H), 1.93 (dd, *J* = 6.61, 5.31 Hz, 1H), 1.80 (dd, *J* = 8.99, 5.31 Hz, 1H). This is a known compound in the literature.[54]

With $Rh_2(OAc)_4$: obtained **36**,23 mg, 39% yield)

With Rh_2(*S*-PTAD)$_4$: obtained **36**, 40 mg, 66% yield, 20:1 d.r., 97% ee.

With Rh_2(*S*-NTTL)$_4$: obtained **36**, 36 mg 60% yield, 8:1 d.r., 98% ee.

With Rh_2(*S*-DOSP)$_4$: obtained **36**, 21 mg, 36% yield, 10:1 dr, 21% ee.

HPLC (ADH column, hexane, 1.5 mL min^{-1} 0.5 mg mL^{-1} 30 min, UV 230 nm) retention times of 4.6 min (minor) and 5.3 min (major) 97 % ee with Rh_2(*S*-PTAD)$_4$, 4.6 min (minor) and 5.3 min (major) 98 % ee with Rh_2(*S*-NTTL)$_4$ and of 4.6 min (minor) 5.3 min (major) 21 % ee with Rh_2(*S*-DOSP)$_4$.

$[\alpha]^{20}_D$ +99.0 ° (c = 0.25, $CHCl_3$) for 97% ee.

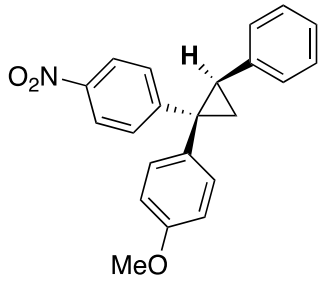

37

1-methoxy-4-((1*R*,2*R*)-1-(4-nitrophenyl)-2-phenylcyclopropyl)benzene (37)

Prepared using general procedure, styrene (0.09mL, 0.90 mmol, 4 equiv) with diazo compound **29** (54 mg, 0.50 mmol) using dirhodium catalyst (1 mol%) with a reaction time of 14 h. Flash chromatography (gradient 0 to 15 % diethyl ether/hexanes) afforded the titled product **37**. ^{1}H NMR (600 MHz, $CDCl_3$) δ 8.10 (d, *J* = 8.90 Hz, 2H), 7.30 (d, *J* = 8.96 Hz, 2H), 7.14 – 7.07 (m, 3H), 6.96 (d, *J* = 8.80 Hz, 2H), 6.89 – 6.80 (m, 2H), 6.70 (d, *J* = 8.77 Hz, 2H), 3.73 (s, 3H), 2.85 (dd, *J* = 9.1, 6.8 Hz, 1H), 2.08 (dd, *J* = 6.9, 5.6 Hz, 1H), 1.89 (dd, *J* = 9.1, 5.7 Hz, 1H). ^{13}C NMR (150 MHz, $CDCl_3$) δ 158.44, 155.01, 145.83, 137.64, 132.56, 130.37, 127.92, 127.82, 127.31, 126.08, 123.60, 113.73, 55.15,38.28,34.37,22.50. IR(in $CDCl_3$) 3004, 2932, 2835, 2360,1593,1510,1343,1245,1031,860, 757,697. HRMS (+p APCl) calculated for $C_{22}H_{20}O_3N$ $[M+H]^+$ 346.1438 found 346.1431.

With $Rh_2(OAc)_4$: obtained **37**, 50 mg, 73% yield.

With Rh_2(*S*-PTAD)$_4$: obtained **37**, 60 mg, 88% yield, >50:1 d.r., 92% ee.

With Rh_2(*S*-NTTL)$_4$: obtained **37**, 62 mg 90% yield, >50:1 d.r. ,87% ee.

HPLC (ADH column, hexane, 1.0 mL min^{-1} 0.5 mg mL^{-1} 60 min, UV 320 nm) retention times of 26.9 min (minor) and 32.8 min (major) 92 % ee with Rh_2(*S*-PTAD)$_4$ and of 27.13 min (minor) and 33.74 min (major) 87% ee with Rh_2(*S*-NTTL)$_4$.

$[\alpha]^{20}_D$ +213.3 ° (c = 1.00, $CHCl_3$) for 92% ee.

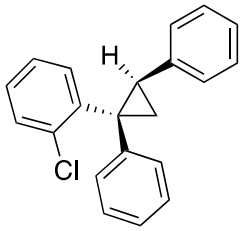

38

((1*S*,2*R*)-1-(2-chlorophenyl)cyclopropane-1,2-diyl)dibenzene (38)

Prepared using general procedure, styrene (0.23mL, 2.0 mmol, 10 equiv) with diazo compound **30** (46 mg, 0.50 mmol) using dirhodium catalyst (1 mol %) with a reaction time of 14 h. Flash chromatography (gradient 0 to 5% diethyl ether/hexanes) afforded the titled product **11e.** ^{1}H NMR (400 MHz, $CDCl_3$) δ 7.74 (dd, *J* = 7.6, 1.7 Hz, 1H), 7.32 (dd, *J* = 7.9, 1.4 Hz, 2H), 7.22 – 6.96 (m, 11H), 2.89 (dd, *J* = 9.2, 6.6 Hz, 1H), 2.11 (dd, *J* = 6.6, 5.6 Hz, 1H), 1.72 (dd, *J* = 9.2, 5.6 Hz, 1H). ^{13}C NMR (100 MHz, $CDCl_3$) δ 143.93, 139.22, 138.27, 135.43, 132.28, 130.21, 130.11, 128.29, 128.02, 127.67, 127.62, 126.93, 126.09, 125.75, 38.20, 31.45, 19.65. This is a known compound in literature.[40]

With $Rh_2(OAc)_4$: obtained **38**, 24 mg, 39% yield.

With Rh_2(*S*-PTAD)$_4$: obtained **38**, 55 mg, 91% yield, >50:1 d.r., 85% ee.

With Rh_2(*S*-NTTL)$_4$: obtained **38**, 44 mg 72% yield, , >50:1 d.r., 82% ee.

HPLC (ADH column, hexane, 1.0 mL min^{-1} 0.5 mg mL^{-1} 30 min, UV 230 nm) retention times of 4.72 min (minor) and 5.00 min (major) 85 % ee with Rh_2(*S*-PTAD)$_4$ and of 4.72 min (minor) and 5.02 min (major) 82% ee with Rh_2(*S*-NTTL)$_4$.

$[\alpha]^{20}_{D}$ +141.4 ° (c = 0.90, $CHCl_3$) for 85% ee.

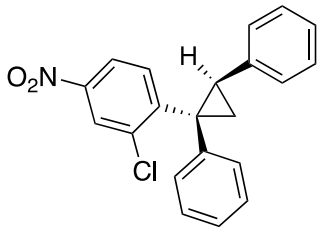

39

((1*S*,2*R*)-1-(2-chloro-4-nitrophenyl)cyclopropane-1,2-diyl)dibenzene (39)

Prepared using general procedure, styrene (0.23mL, 2.0 mmol, 10 equiv) with diazo compound **31** (55 mg, 0.50 mmol) using dirhodium catalyst (1 mol%) with a reaction time of 14 h. Flash chromatography (gradient 0 to 15% diethyl ether/hexanes) afforded the titled product **39** ^{1}H NMR

(600 MHz, $CDCl_3$) δ 8.22 (d, *J* = 2.3 Hz, 1H), 8.14 (dd, *J* = 8.5, 2.4 Hz, 1H), 7.91 (d, *J* = 8.5 Hz, 1H), 7.18 – 7.16 (m, 2H), 7.14 – 7.11 (m, 2H), 7.10 – 7.03 (m, 4H), 6.99 – 6.95 (m, 2H), 2.90 (dd, *J* = 9.3, 6.7 Hz, 1H), 2.20 (dd, *J* = 6.7, 5.9 Hz, 1H), 1.74 (dd, *J* = 9.3, 5.9 Hz, 1H). ^{13}C NMR (150 MHz, $CDCl_3$) δ 150.96, 146.96, 137.53, 137.21, 136.48, 132.82, 130.28, 128.17, 127.96, 127.83, 126.78, 126.16, 125.45, 121.97, 38.07, 31.46, 19.59. IR(in $CDCl_3$) 3027, 1519,1347, 1121,892, 775, 740,720, 697.HRMS (+p APCI) calculated for $C_{21}H_{16}ClNO_2$ $[M+H]^+$ 350.0943 found 350.09369.

With $Rh_2(OAc)_4$: obtained **39**, 32 mg, 46% yield)

With Rh_2(*S*-PTAD)$_4$: obtained **39**, 64 mg, 91% yield, >50:1 d.r., 20% ee.

With Rh_2(*S*-NTTL)$_4$: obtained **39,** 50 mg 72% yield, >50:1 d.r., 57% ee.

HPLC (ODH column, hexane, 1.5 mL min^{-1} 0.5 mg mL^{-1} 60 min, UV 280 nm) retention times of 21.04 min (major) and 31.17 min (minor) 20% ee with Rh_2(*S*-PTAD)$_4$ and of 20.81 min (major) and 31.10 min (minor) 57% ee with Rh_2(*S*-NTTL)$_4$.

$[\alpha]^{20}_D$ +107.5 ° (c = 0.52, $CHCl_3$) for 57% ee.

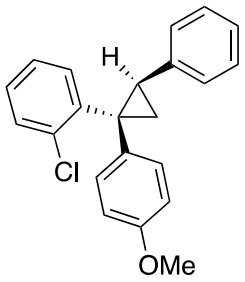

40

1-chloro-2-((1*S*,2*R*)-1-(4-methoxyphenyl)-2-phenylcyclopropyl)benzene (40)

Prepared using general procedure, styrene (0.23mL, 2.0 mmol, 4 equiv) with diazo compound **32** (52 mg, 0.50 mmol) using dirhodium catalyst (1 mol %) with a reaction time of 14 h. Flash chromatography (gradient 0 to 15% diethyl ether/hexanes) afforded the titled product **40**. ^1H NMR (600 MHz, $CDCl_3$) δ 7.70 (dd, *J* = 7.7, 1.7 Hz, 1H), 7.31 (dd, *J* = 7.9, 1.3 Hz, 1H), 7.26 (dd, *J* =

15.0, 1.3 Hz, 1H), 7.16 – 7.10 (m, 5H), 7.08 – 7.05 (m, 1H), 7.00 – 6.97 (m, 2H), 6.60 (d, *J* = 8.85 Hz, 2H), 3.66 (s, 3H), 2.83 (dd, *J* = 9.1, 6.6 Hz, 1H), 2.02 (dd, *J* = 6.6, 5.5 Hz, 1H), 1.71 (dd, *J* = 9.1, 5.6 Hz, 1H). ^{13}C NMR 150 MHz, $CDCl_3$) δ 157.77, 144.27, 138.48, 135.22, 132.09, 131.43, 131.33, 130.09, 128.22, 127.87, 127.67, 126.92, 125.65, 113.06, 37.65, 31.23, 19.88. IR (in $CDCl_3$) 3003, 2834, 1608, 1510, 1470, 1244, 1176, 1032, 907, 734, 695, 614. HRMS (+p NSI) calculated for $C_{22}H_{19}ClONa$ $[M+Na]^+$ 357.1016 found 357.1015.

With $Rh_2(OAc)_4$: obtained **40**, 18 mg, 27% yield

With Rh_2(*S*-PTAD)$_4$: obtained **40**, 37 mg, 56% yield, , >50:1 d.r., 93% ee.

With Rh_2(*S*-NTTL)$_4$: obtained **40**, 23 mg 34% yield, , >50:1 d.r., 92% ee.

HPLC (ADH column, hexane, 1.0 mL min^{-1} 0.5 mg mL^{-1} 30 min, UV 230 nm) retention times6 min (minor) and 8.51 min (major) 93 % ee with Rh_2(*S*-PTAD)$_4$ and of 7.16 min (minor) and 8.50 min (major) 92% ee with Rh_2(*S*-NTTL)$_4$.

$[\alpha]^{20}_D$ +73.8 ° (c = 0.58, $CHCl_3$) for 93% ee.

React IR- Set Up

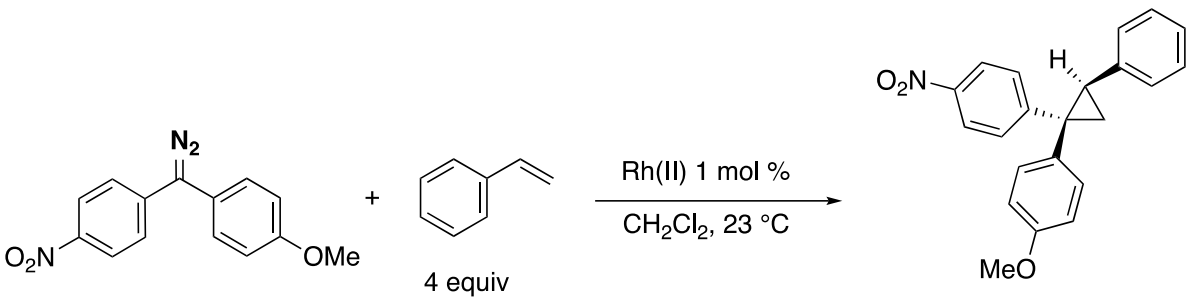

29 **37**

The ReactIR instrument was filled with liquid nitrogen and allowed to equilibrate while the reaction flask was being set-up. An oven-dried 100 mL 3-neck round-bottom flask was fitted with a rubber septum (left neck, 14/20), ReactIR probe (center neck, 24/40 to 19/25 adapter, 19/25 neck), and argon inlet (right neck, 14/20). The flask was cooled to room temperature under

vacuum, then backfilled with argon and placed in an oil bath, with the temperature of the stir plate set to the desired temperature and stir rate on 700 rpm. Once the reaction flask was at the desired temperature, the background and water vapor spectrum were taken via the ReactIR instrument. 12 mL CH_2Cl_2 through the rubber septum. The data collection was started on the ReactIR^{TM} software, and the solvent was allowed to stir for 15 min. After a reference spectrum of the solvent was taken, styrene (pre-purified by passing through a pipette column 0.26 mL, 4 equiv) was added using a plastic syringe. The reaction mixture was allowed to stir while the diazo compound **29** (150 mg, 0.56 mmol**)** was weighed out. A reference spectrum of styrene was taken after subtracting out the solvent spectrum, and then the diazo compound (solid) was added by removing and quickly replacing the rubber septum. A reference spectrum of the diazo compound was taken after subtracting out the reference spectrum of styrene, and the reaction mixture was allowed to stir for 15 min. 1 mL of the catalyst stock solution (1 mol % Rh) was added to the reaction mixture and allowed to stir until the complete consumption of the diazo compound by tracking the disappearance of the $C{=}N_2$ stretch frequencies (around 2048 cm^{-1}). Upon reaction completion the solvent was removed in vacuo. The crude residue was purified based on Rf by flash column chromatography. Pure product fractions were combined, and solvent was evaporated to calculate yield. Product was characterized by chiral-HPLC. Varian Prostar to analyze enantioselectivity.

The data was extracted directly from the software as a text-file and copied into Microsoft Excel®. The first time point in the diazo decomposition curve was set as "00:00:00" (HH:MM:SS) by subtracting the relative time at that point from itself, and all subsequent time points were set by subtracting the relative time of the beginning of the data set from the relative time extracted. To normalize the absorbance, the absorbance of the first point in the data set was set as "1.0 M" (actual concentration of diazo compound is 0.10 M), which was obtained from dividing the absorbance of

the first point by itself, and all subsequent absorbances were divided by the absorbance of the first point. In doing so, it is possible to get the relative concentration of diazo compound over the course of the reaction and monitor the time of its decomposition.

2.7.4 Crude NMR for d.r. determination

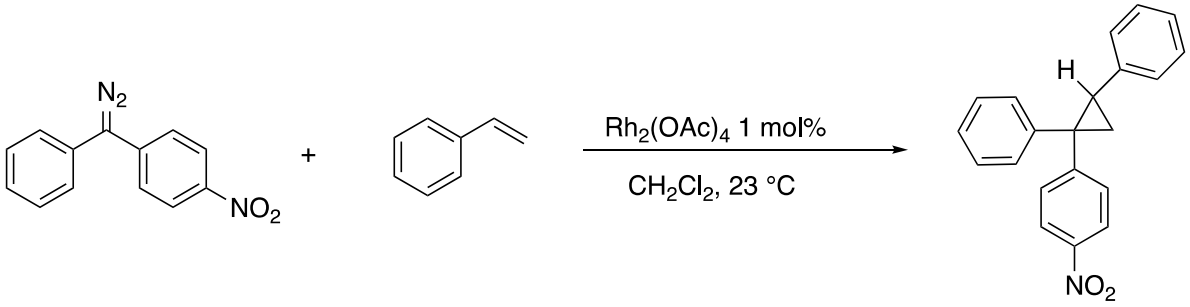

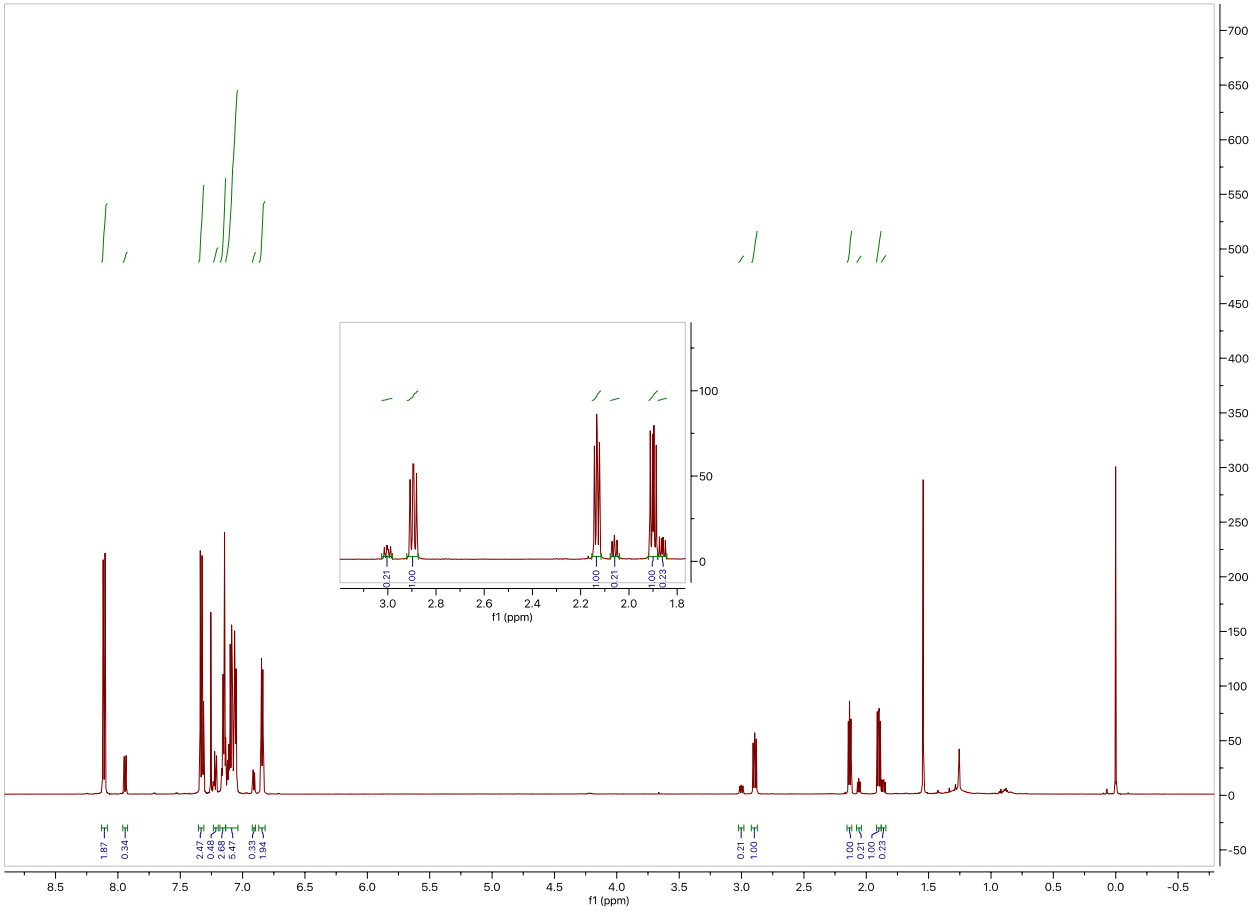

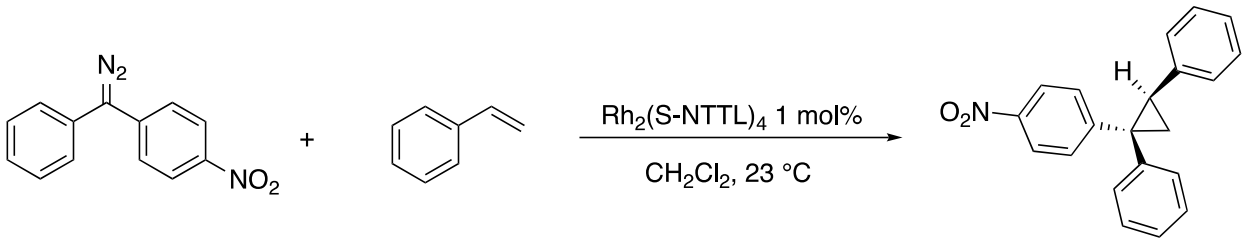
N2
NO2
+
Rh2(S-NTTL)4 1 mol%
CH2Cl2, 23 °C
O2N
H

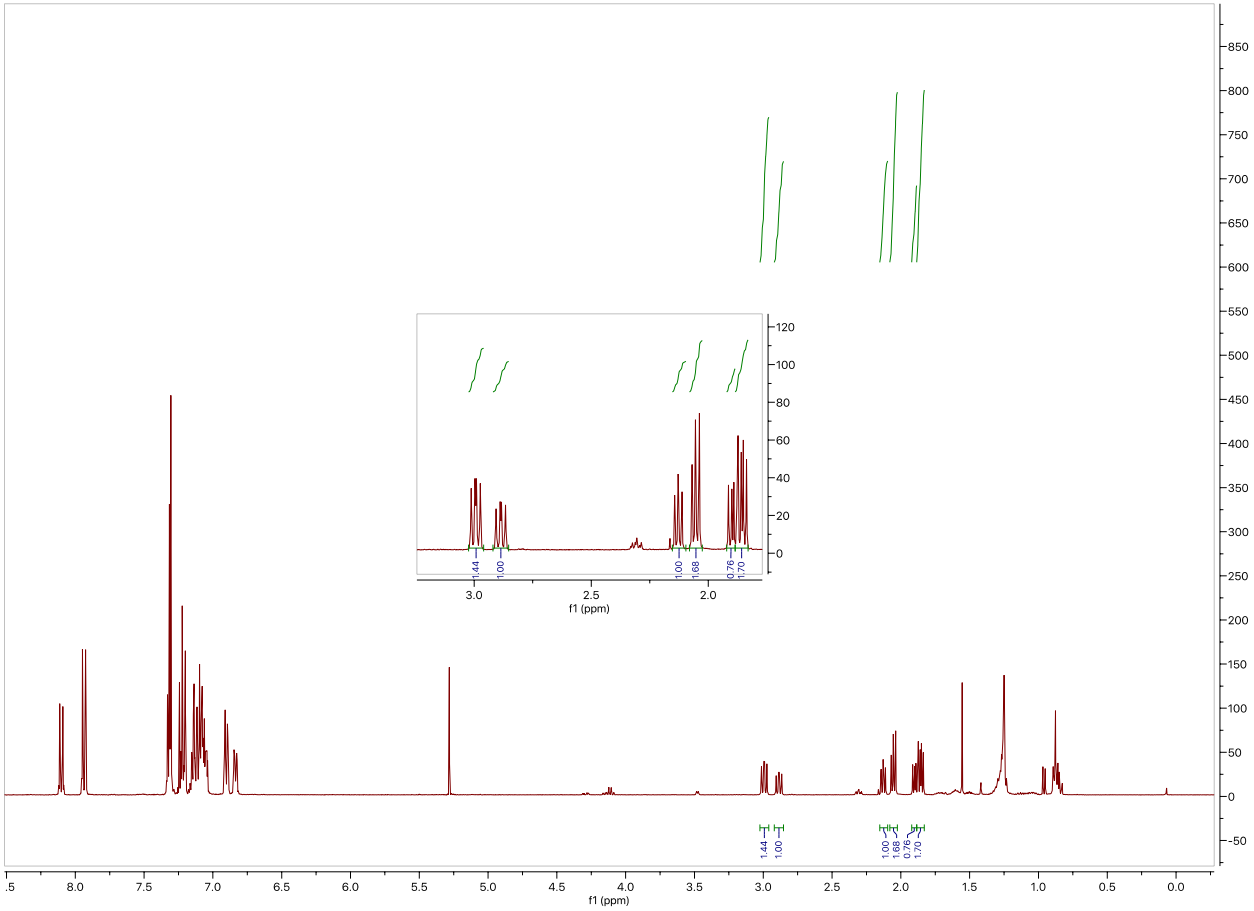
f1 (ppm)
1.44
1.00
1.00
1.68
0.76
1.70

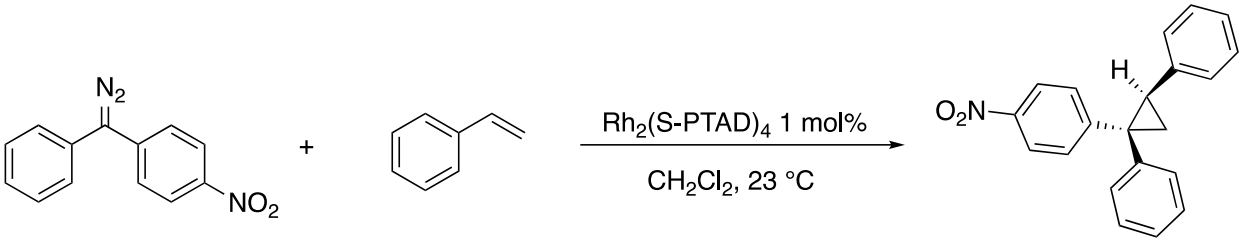
N2
NO2
+
Rh2(S-PTAD)4 1 mol%
CH2Cl2, 23 °C
O2N
H

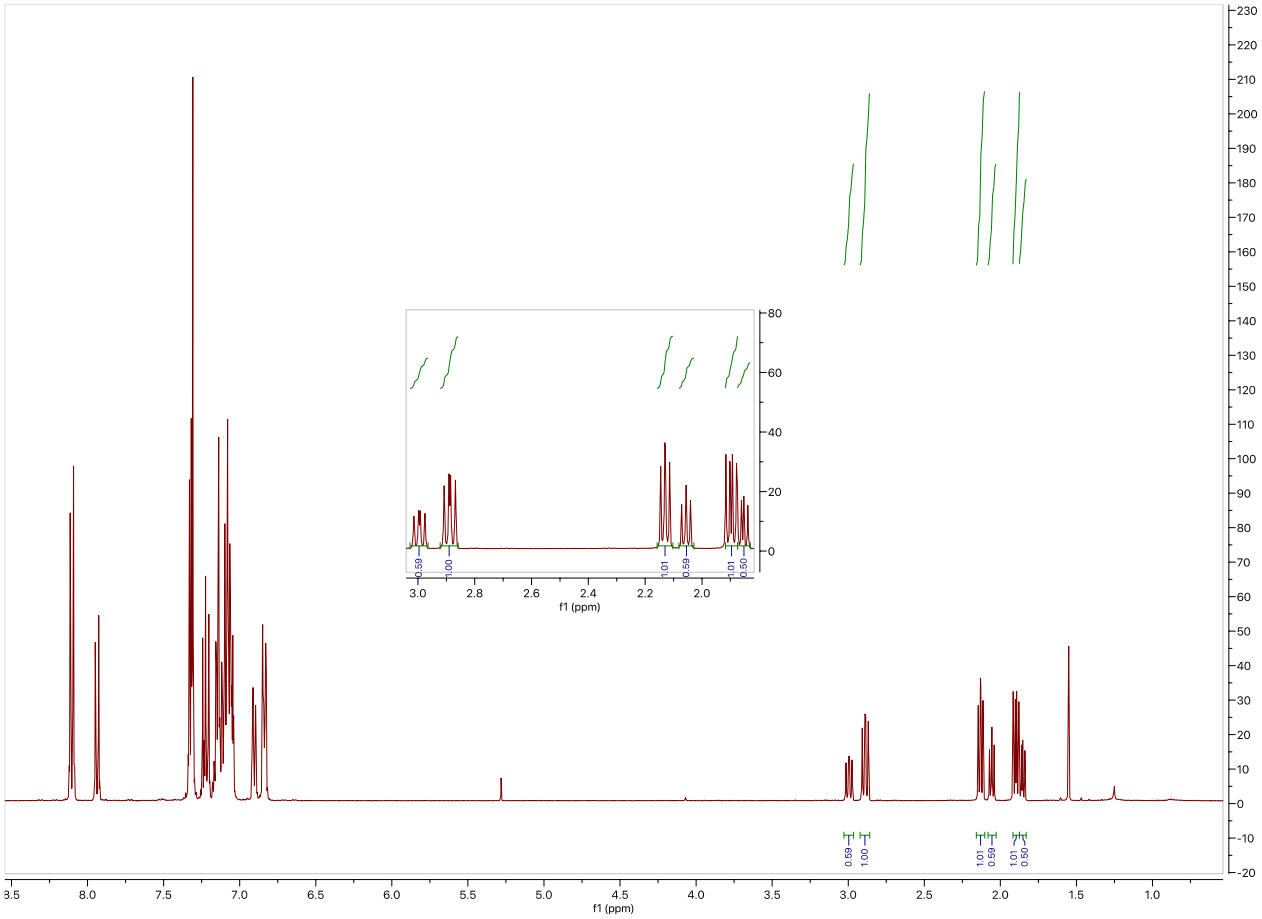
f1 (ppm)
0.59
1.00
1.01
0.59
1.01
0.50

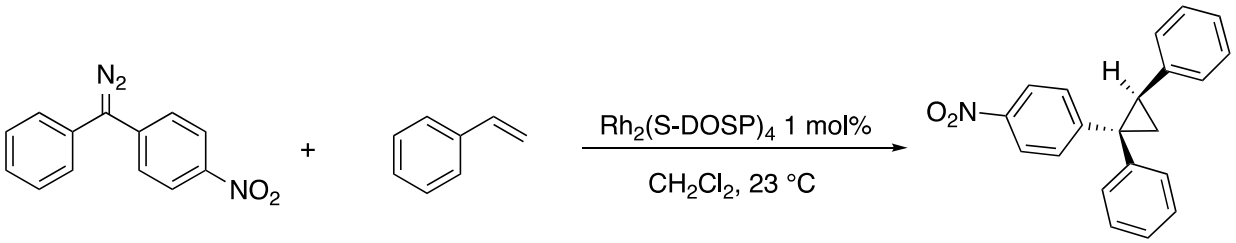
N2
NO2
+
Rh2(S-DOSP)4 1 mol%
CH2Cl2, 23 °C
O2N
H

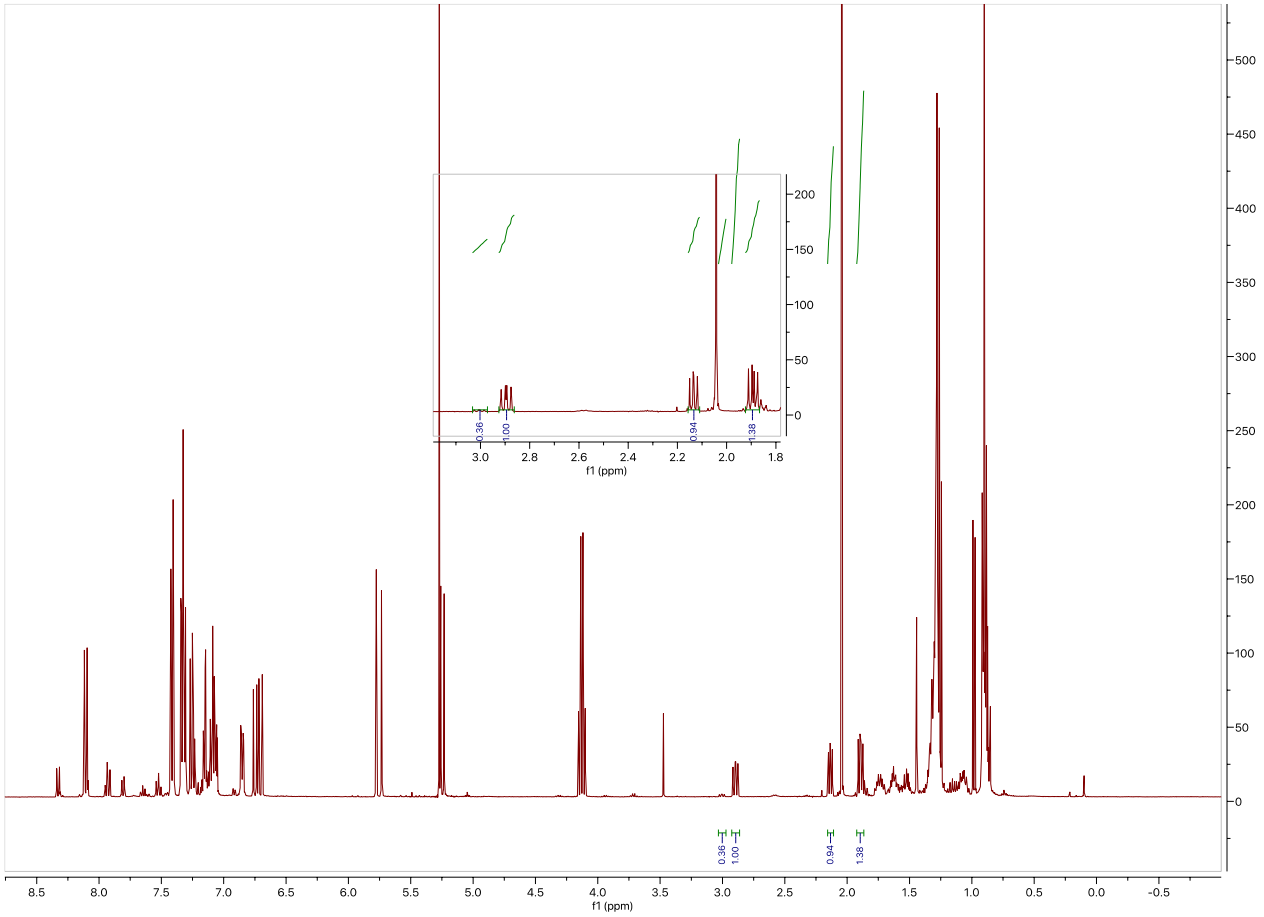
f1 (ppm)
0.36
1.00
0.94
1.38

Stacked Spectrum

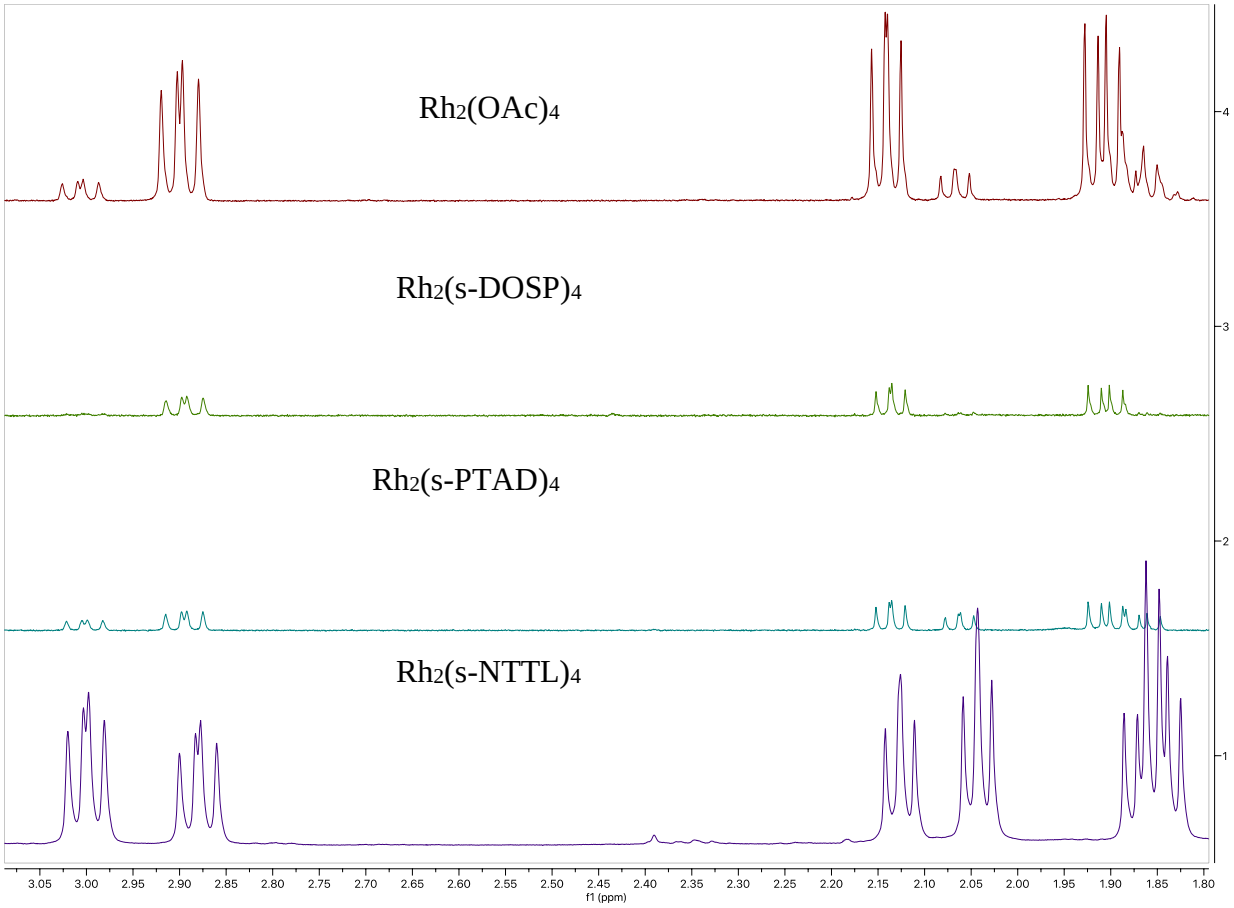

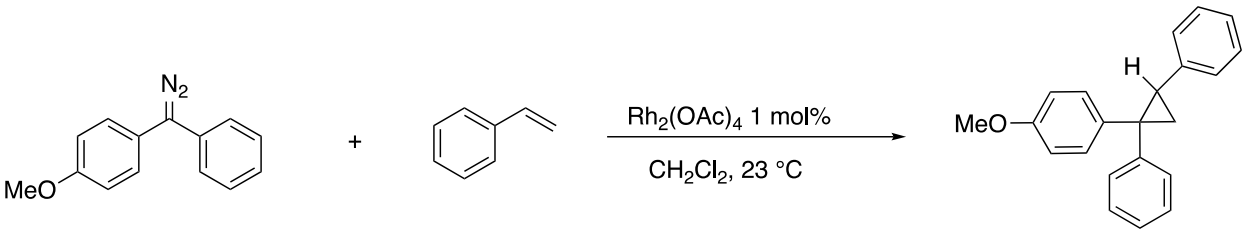
N2
MeO
+
Rh2(OAc)4 1 mol%
CH2Cl2, 23 °C
H
MeO

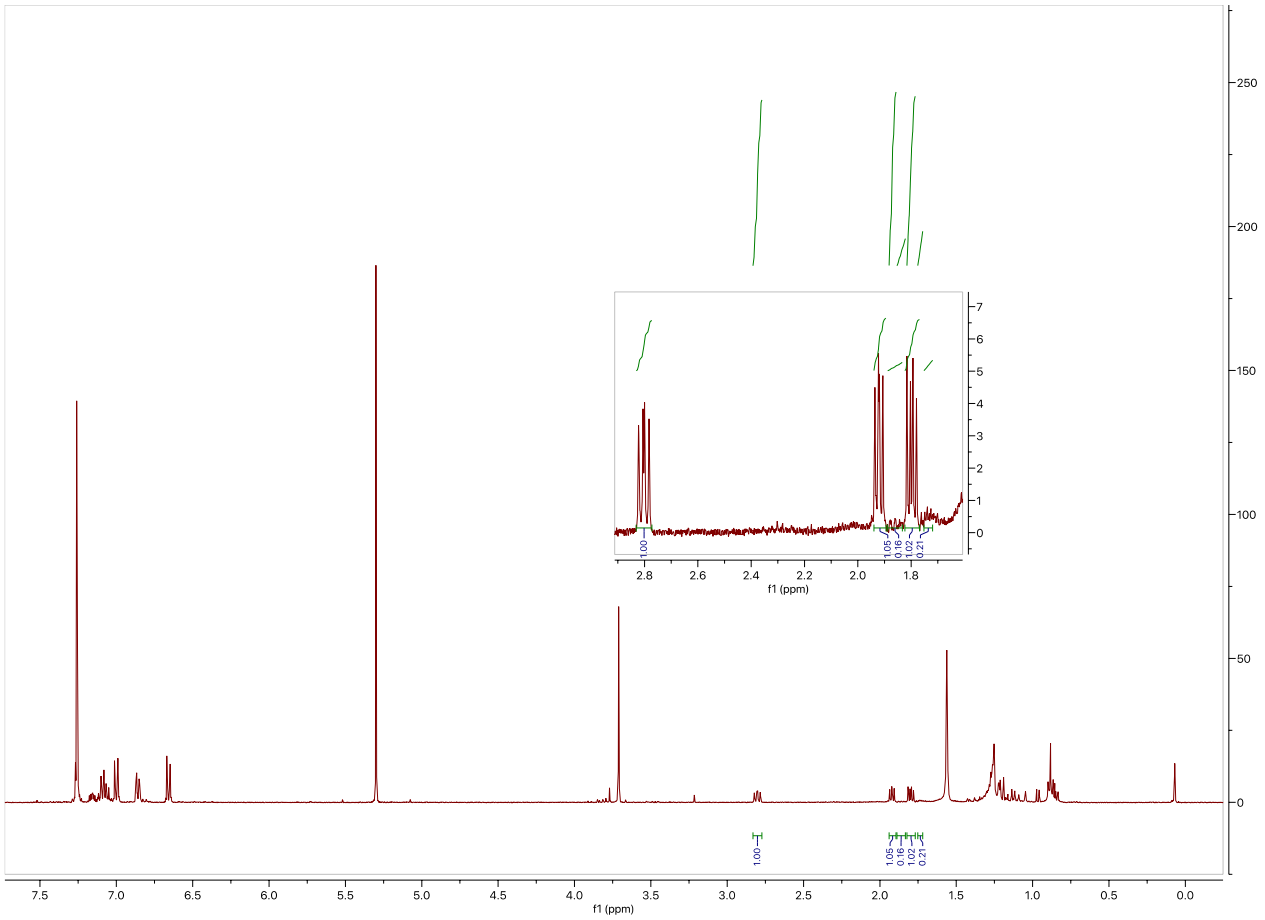
f1 (ppm)
1.00
1.05
0.16
1.02
0.21

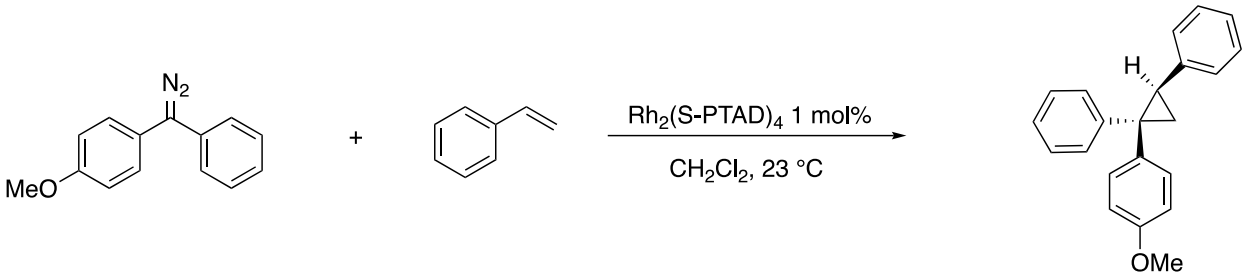
N2
MeO
+
Rh2(S-PTAD)4 1 mol%
CH2Cl2, 23 °C
H
OMe

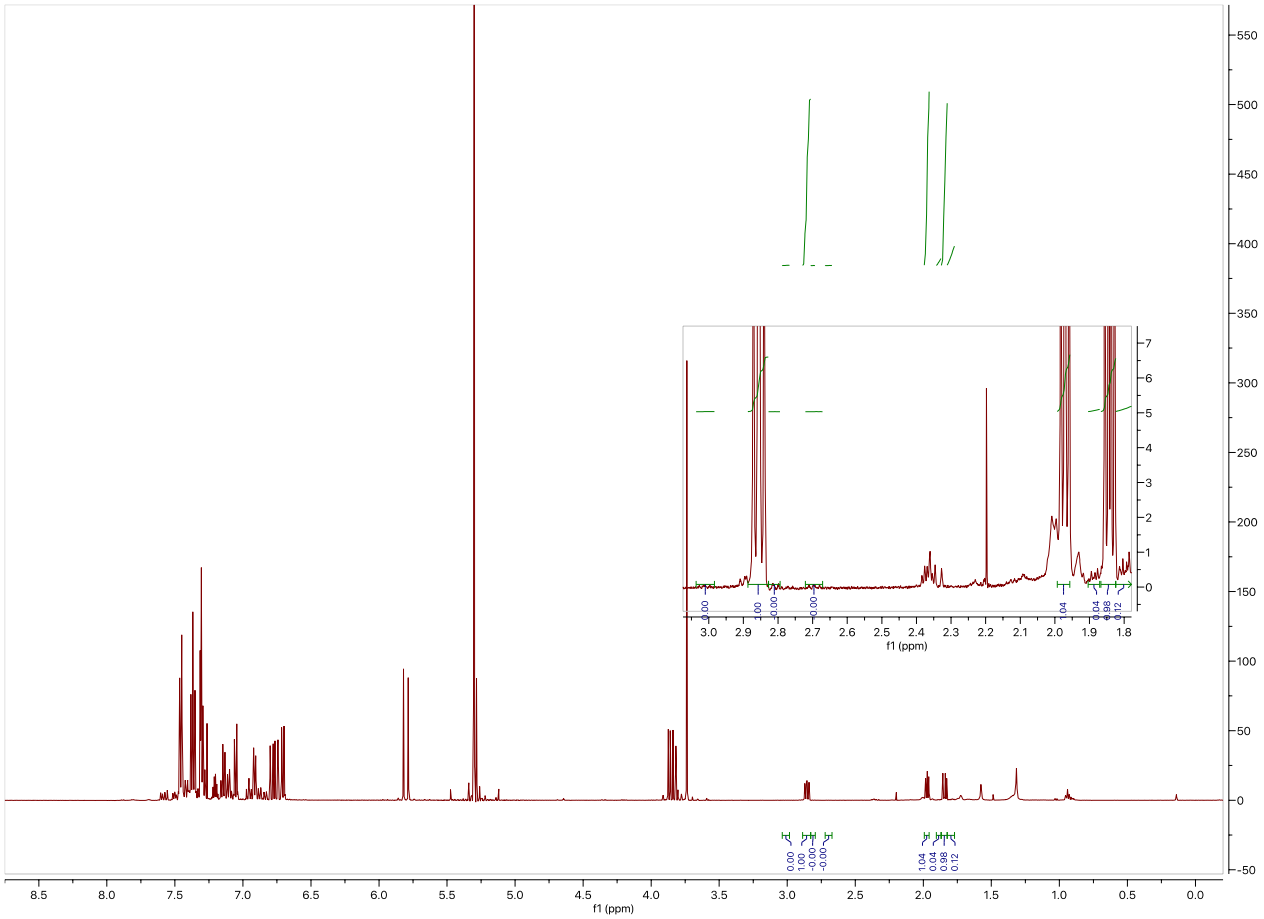
f1 (ppm)
0.00
1.00
0.00
0.00
1.04
0.04
0.98
0.12

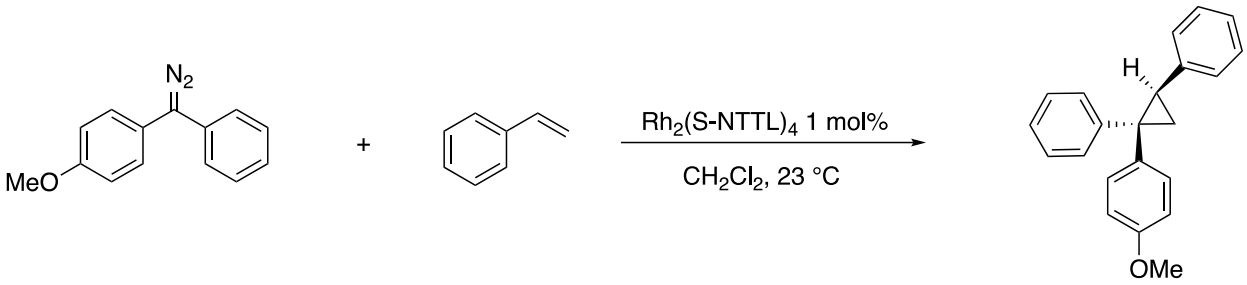
N2
MeO
+
Rh2(S-NTTL)4 1 mol%
CH2Cl2, 23 °C
H
OMe

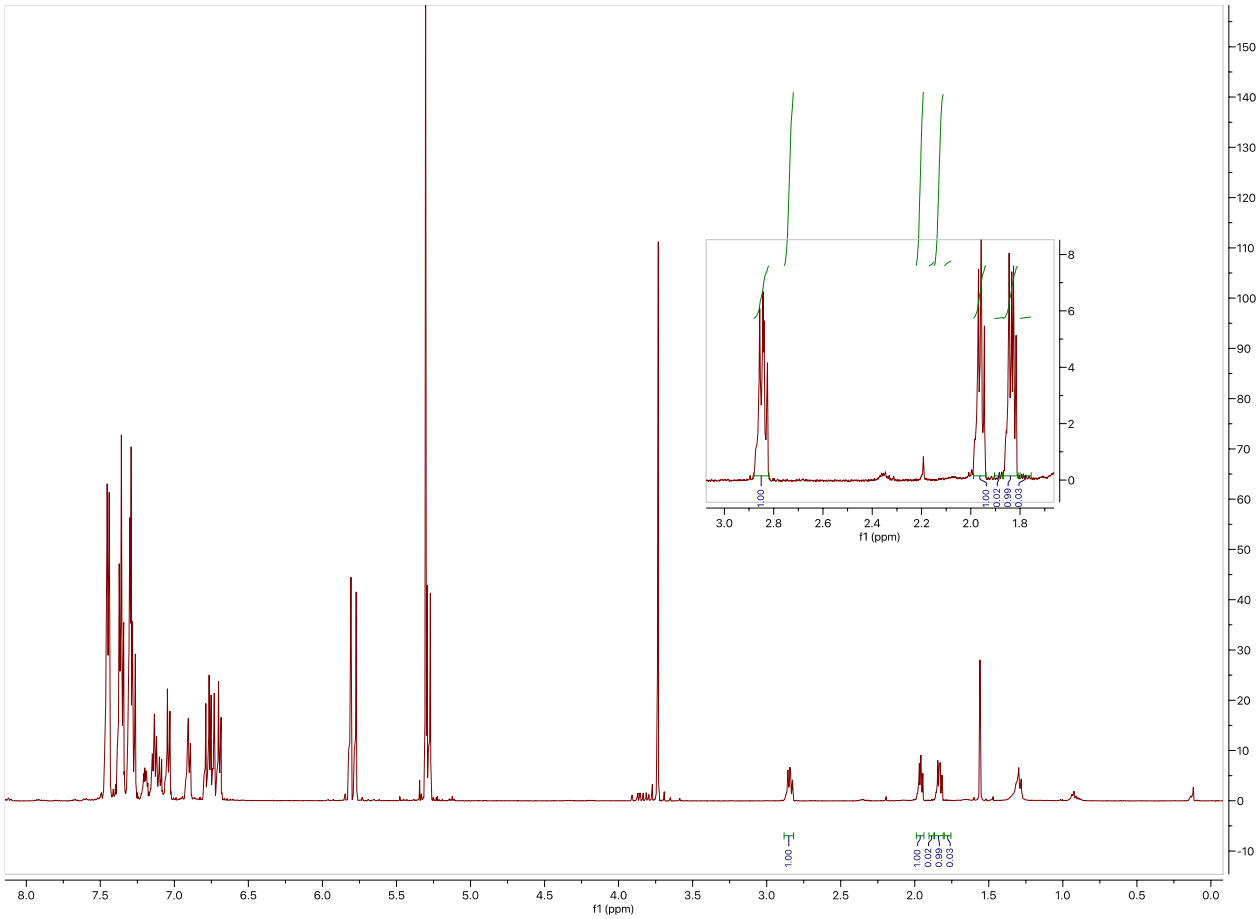
f1 (ppm)
1.00
1.00
0.02
0.99
0.03

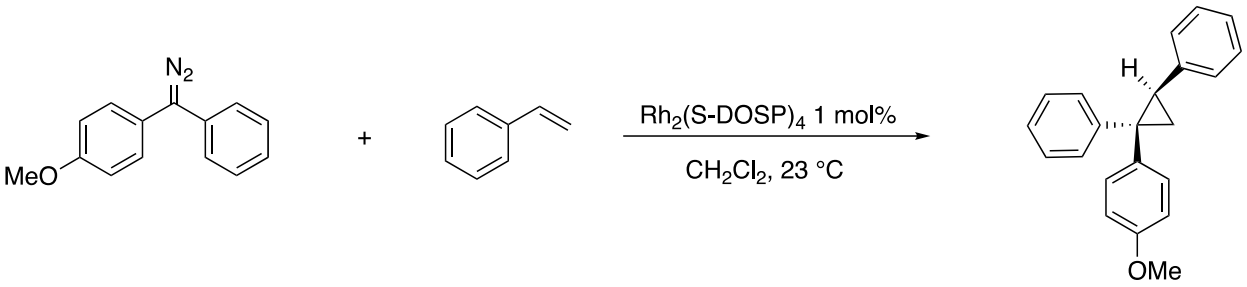
N2
MeO
+
Rh2(S-DOSP)4 1 mol%
CH2Cl2, 23 °C
H
OMe

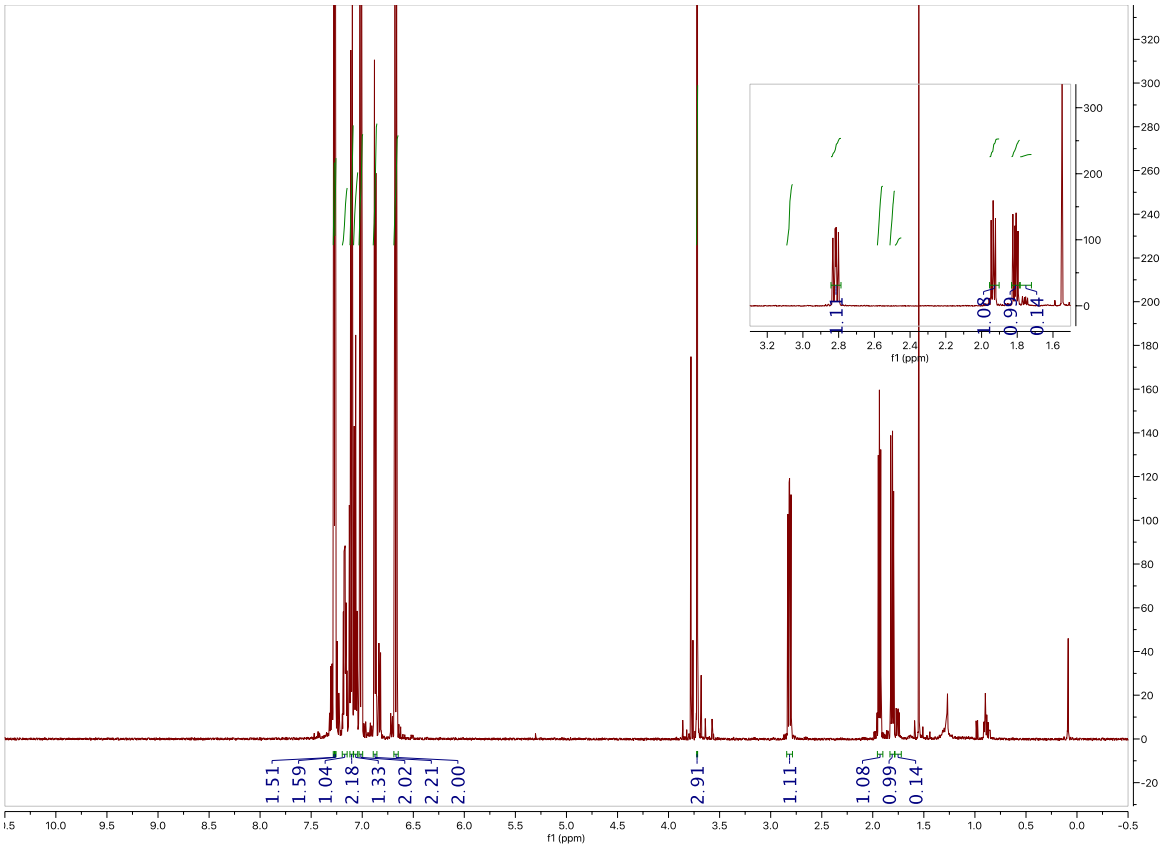
1.51
1.59
1.04
2.18
1.33
2.02
2.21
2.00
2.91
1.11
1.08
0.99
0.14
f1 (ppm)

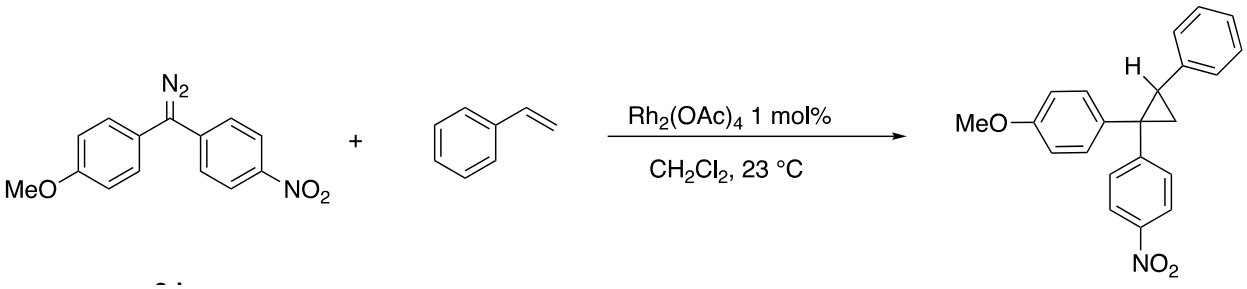
N2
MeO
NO2
+
Rh2(OAc)4 1 mol%
CH2Cl2, 23 °C
H
MeO
NO2

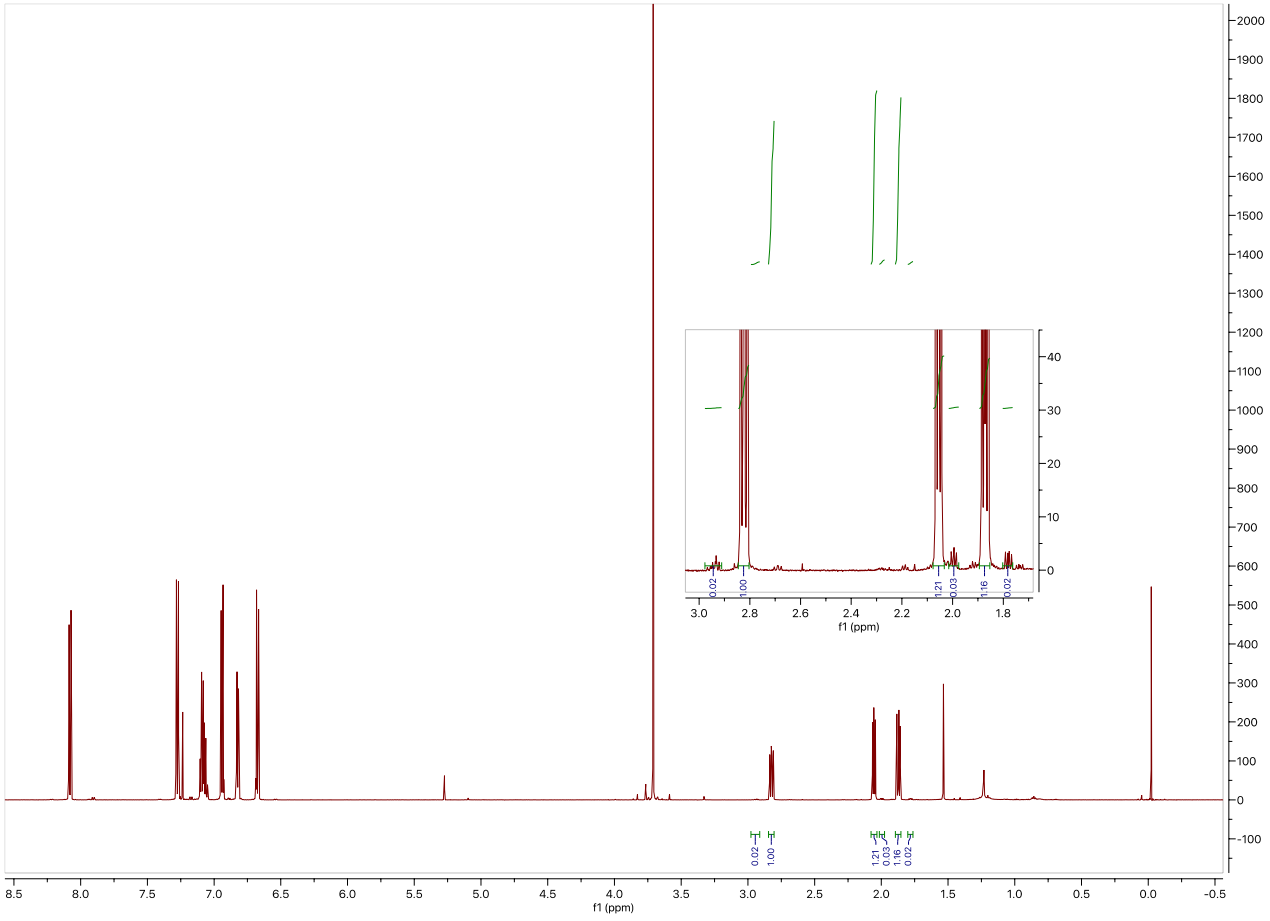
f1 (ppm)
0.02
1.00
1.21
0.03
1.16
0.02

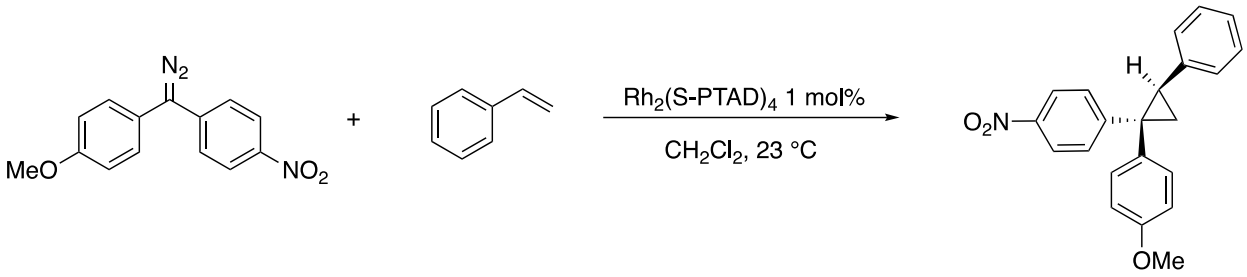
N2
MeO
NO2
+
Rh2(S-PTAD)4 1 mol%
CH2Cl2, 23 °C
H
O2N
OMe

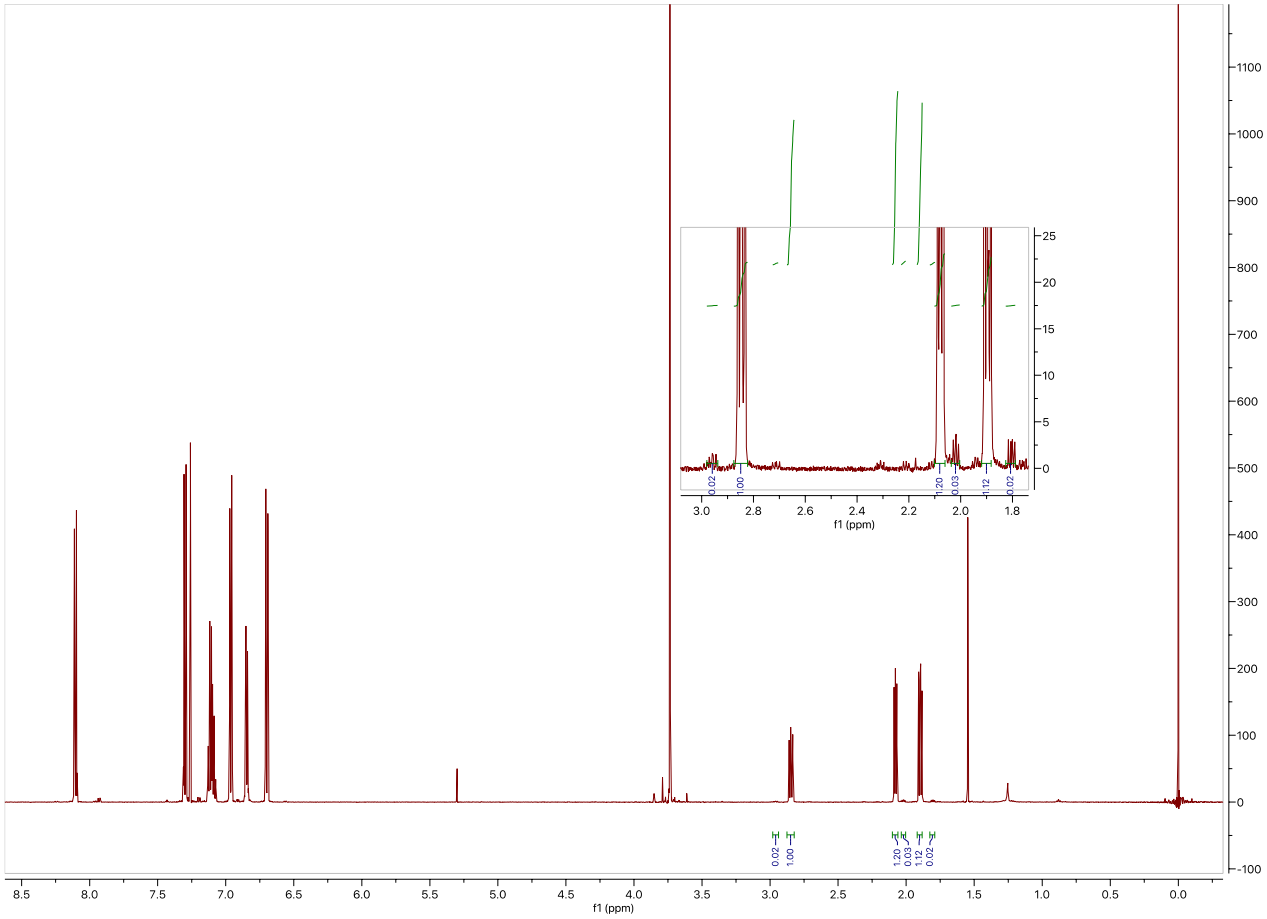
f1 (ppm)
0.02
1.00
1.20
0.03
1.12
0.02

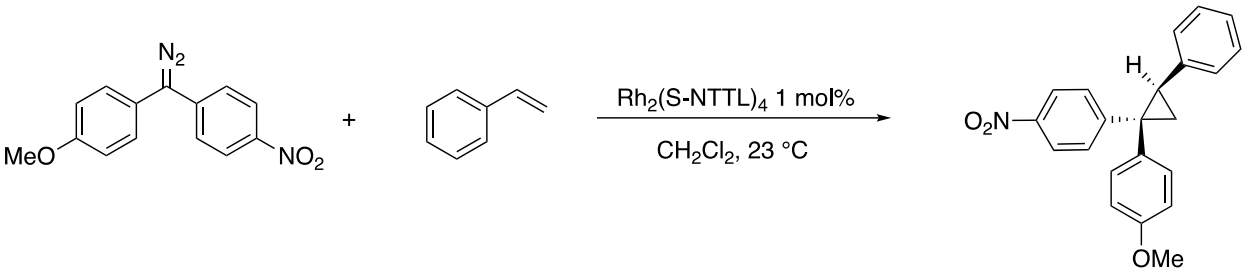
N2
MeO
NO2
+
Rh2(S-NTTL)4 1 mol%
CH2Cl2, 23 °C
H
O2N
OMe

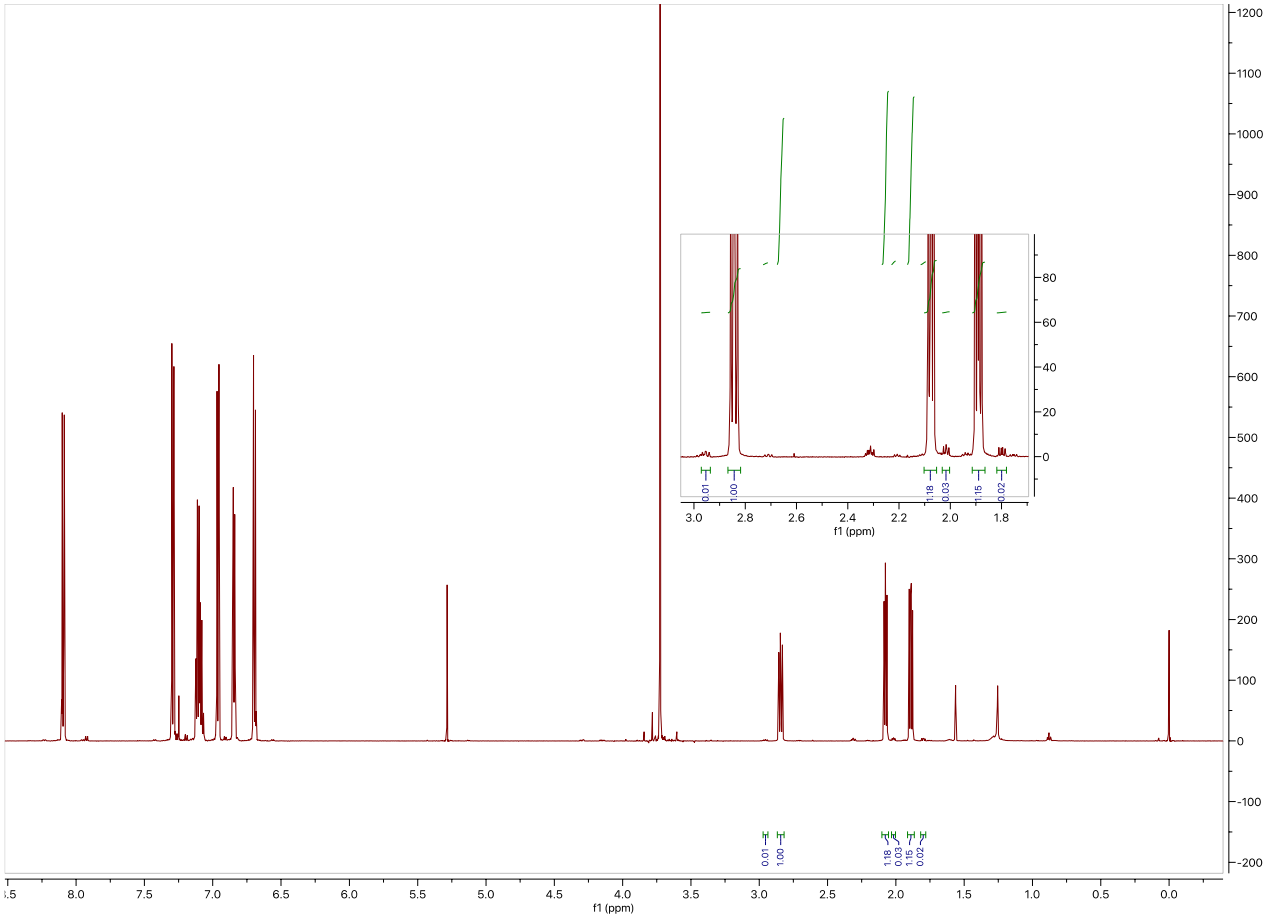
f1 (ppm)
0.01
1.00
1.18
0.03
1.15
0.02

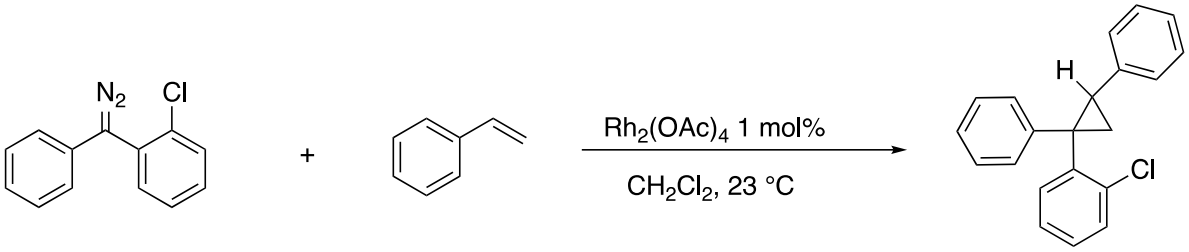
N2
Cl
+
Rh2(OAc)4 1 mol%
CH2Cl2, 23 °C
H
Cl

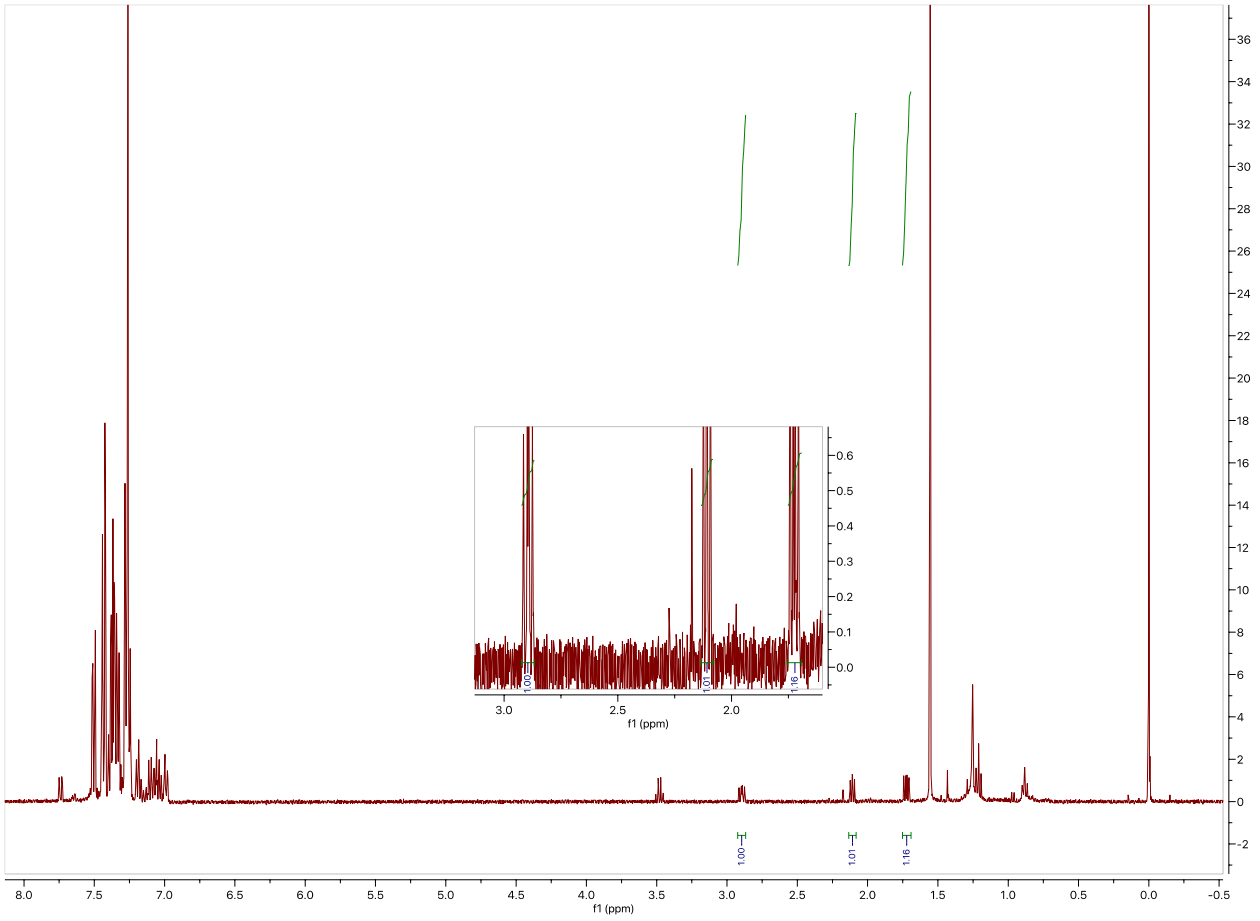
f1 (ppm)
1.00
1.01
1.16

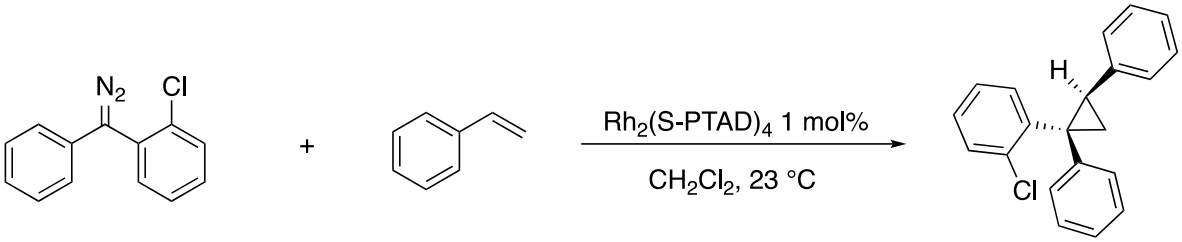
N2
Cl
+
Rh2(S-PTAD)4 1 mol%
CH2Cl2, 23 °C
H
Cl

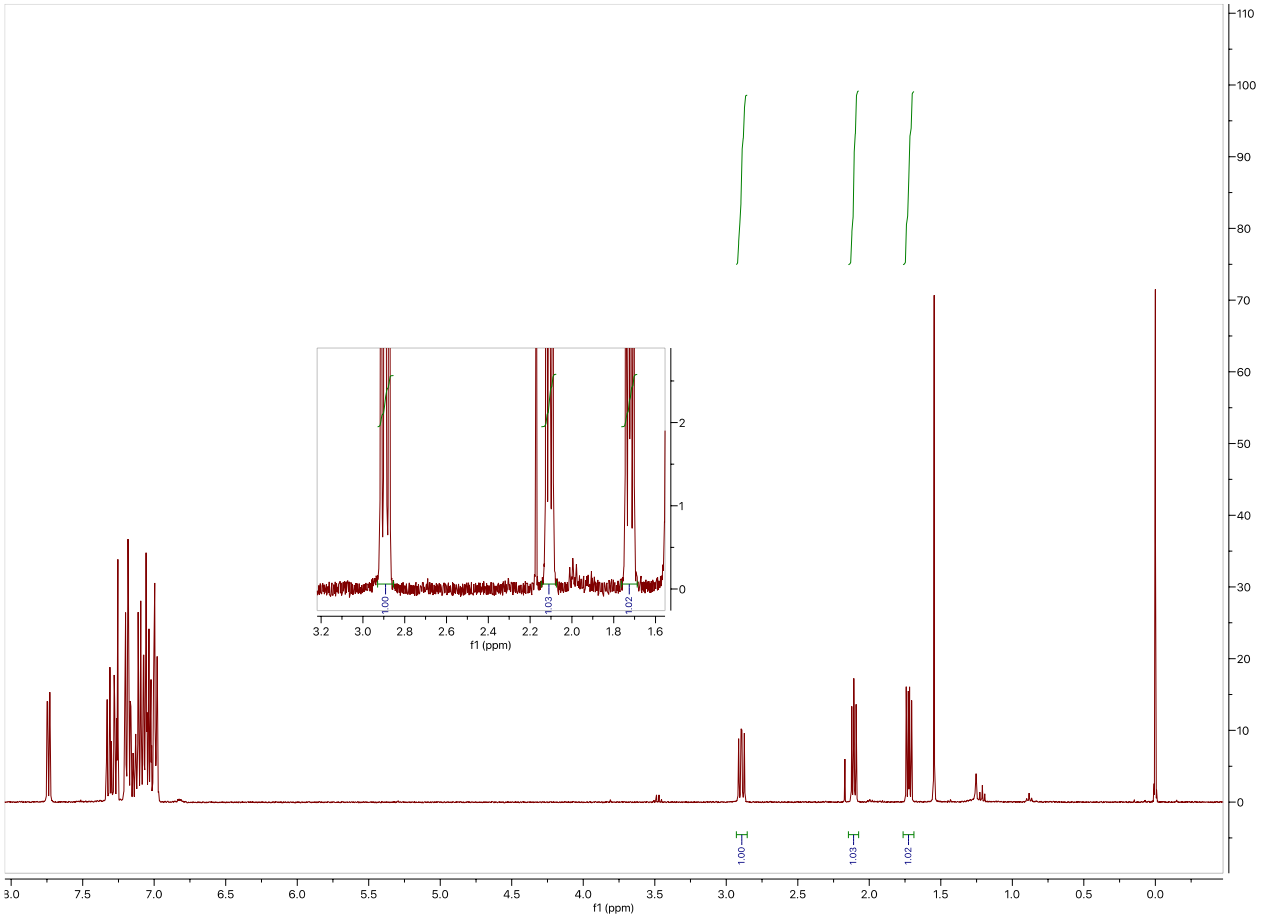
f1 (ppm)
1.00
1.03
1.02

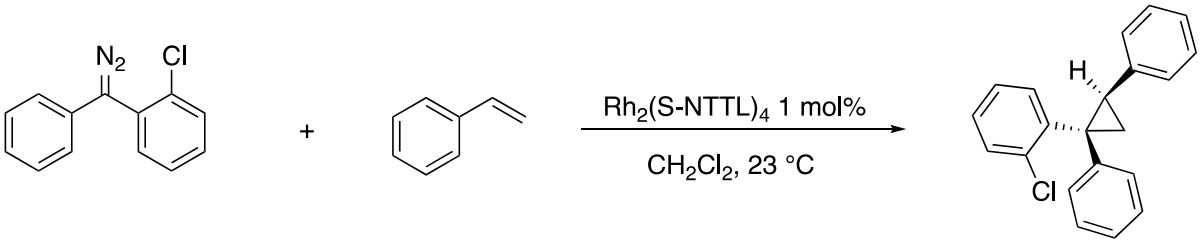
N2
Cl
+
Rh2(S-NTTL)4 1 mol%
CH2Cl2, 23 °C
H
Cl

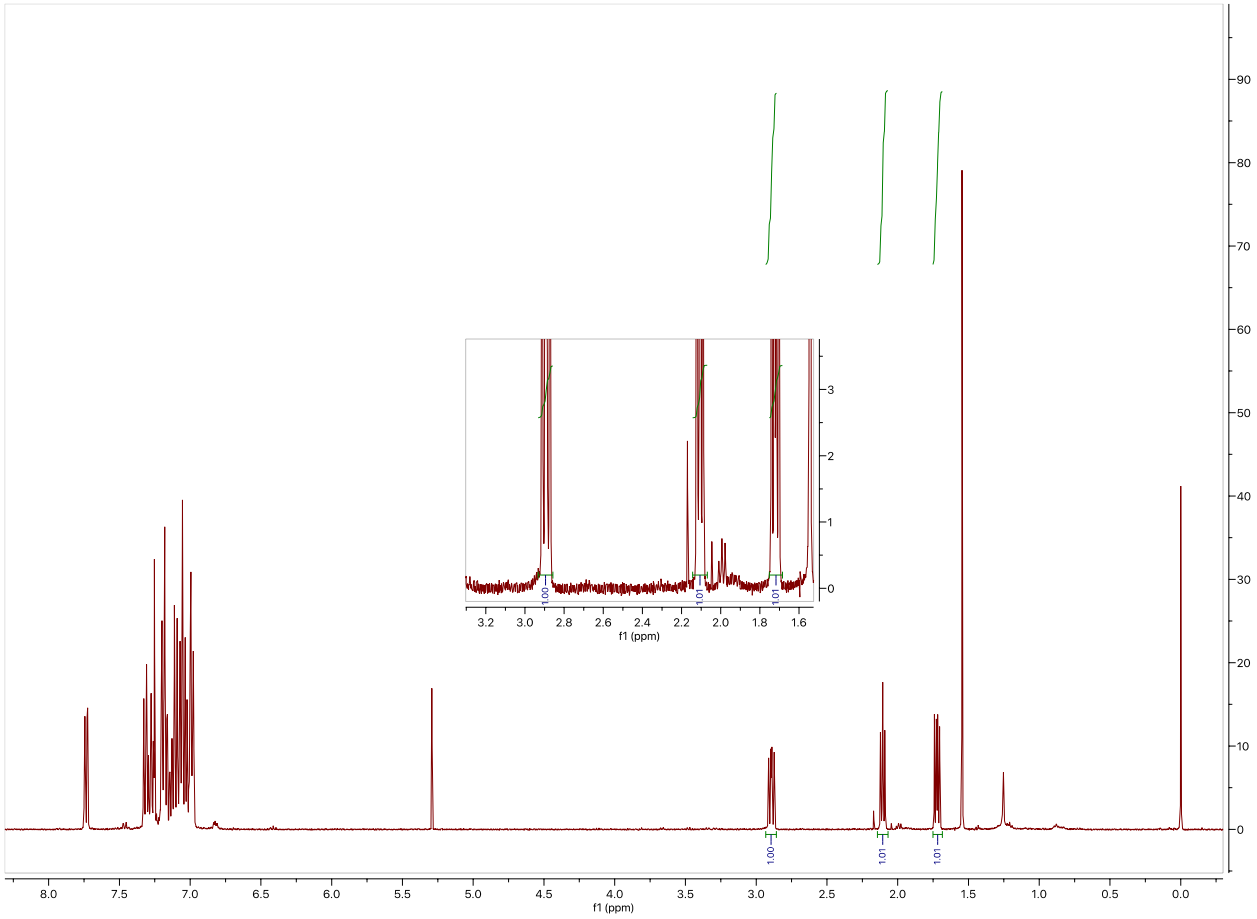
f1 (ppm)
1.00
1.01
1.01

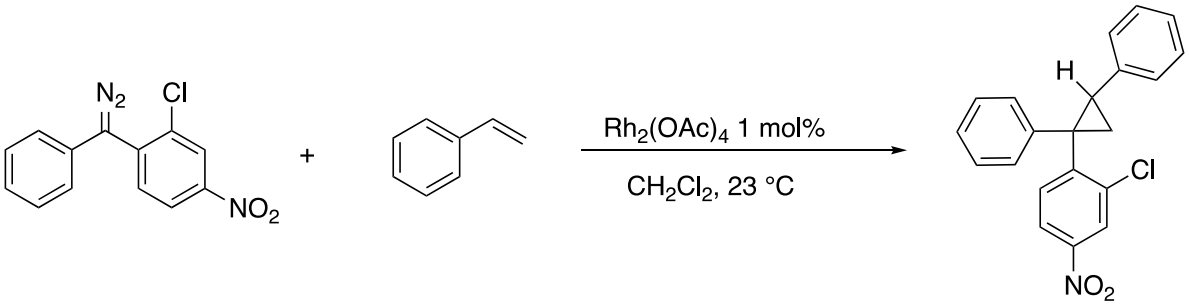
N2
Cl
NO2
+
Rh2(OAc)4 1 mol%
CH2Cl2, 23 °C
H
Cl
NO2

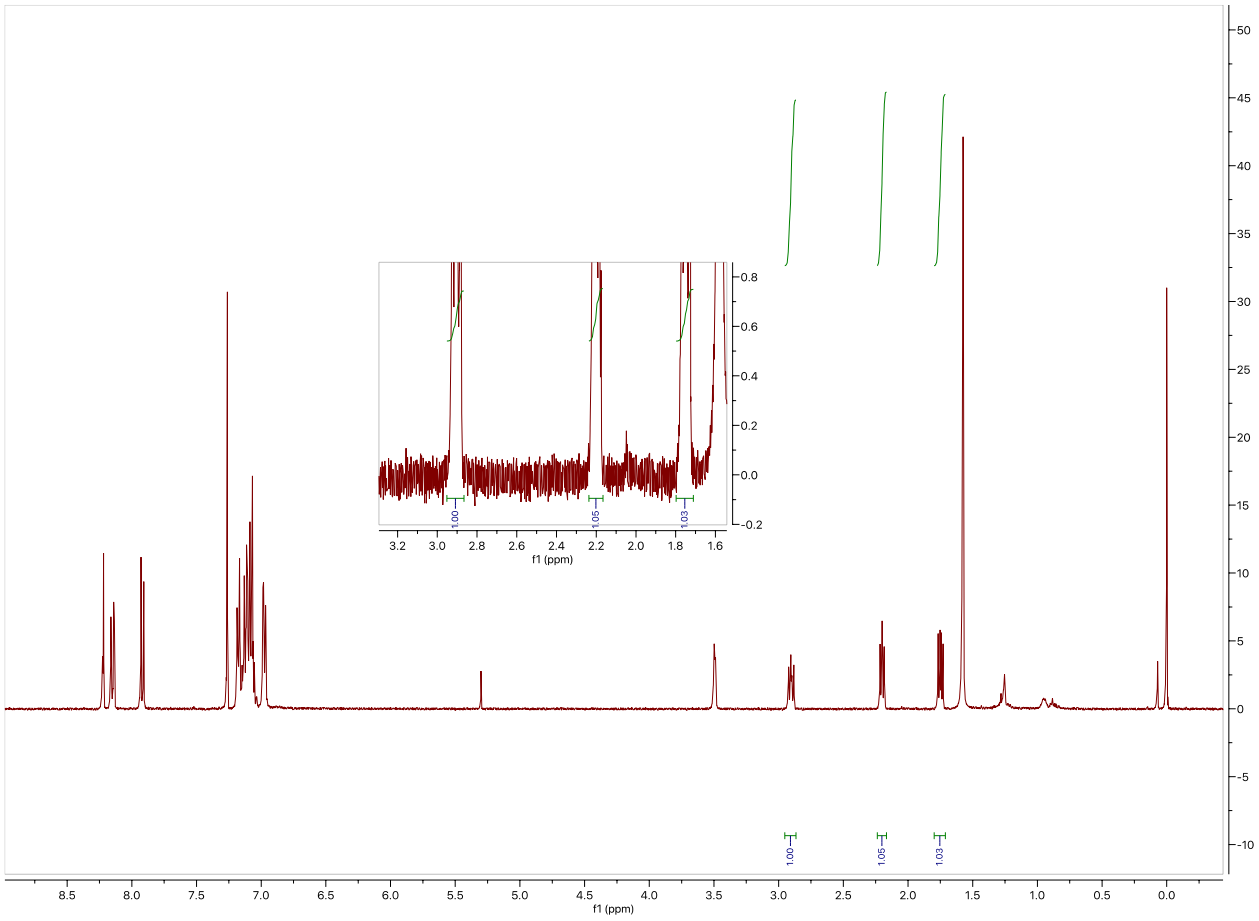
f1 (ppm)
1.00
1.05
1.03

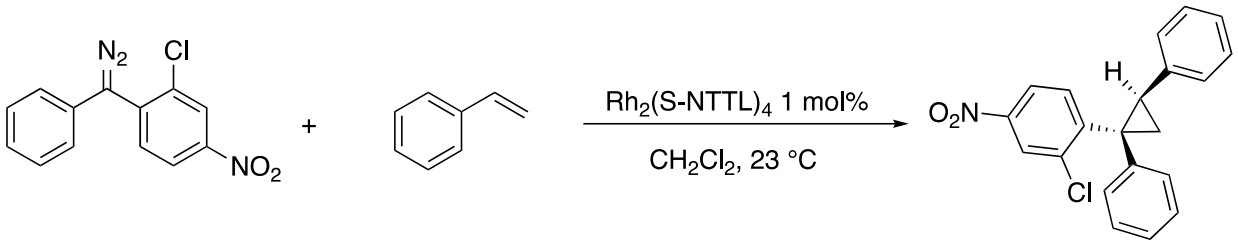
N2
Cl
NO2
+
Rh2(S-NTTL)4 1 mol%
CH2Cl2, 23 °C
O2N
H
Cl

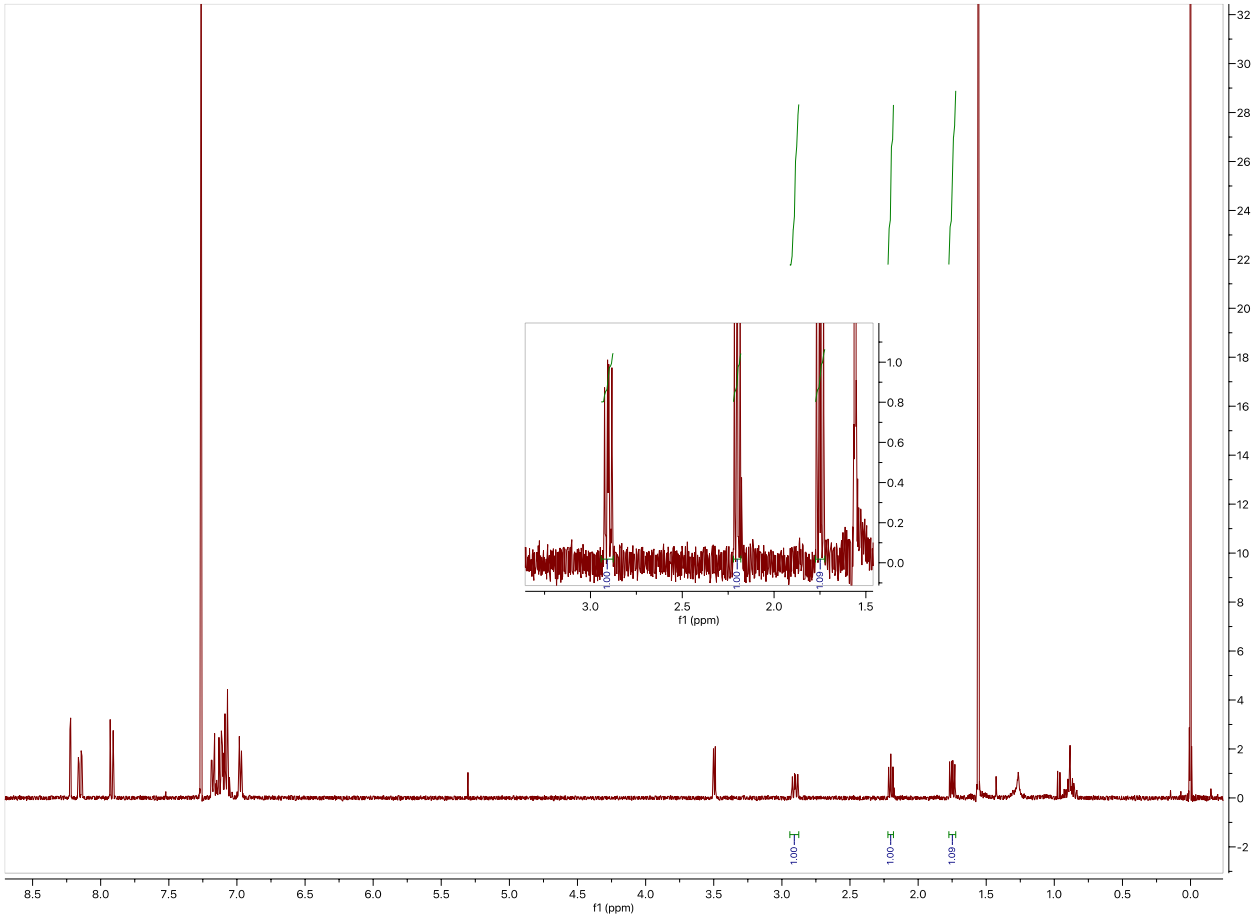
f1 (ppm)
1.00
1.00
1.09

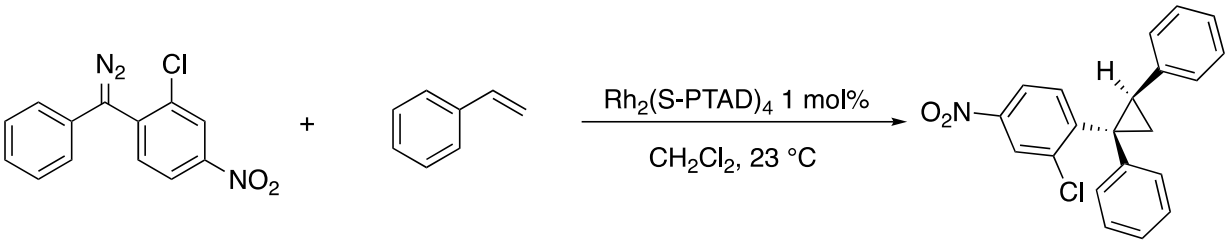
N2
Cl
NO2
+
Rh2(S-PTAD)4 1 mol%
CH2Cl2, 23 °C
O2N
H
Cl

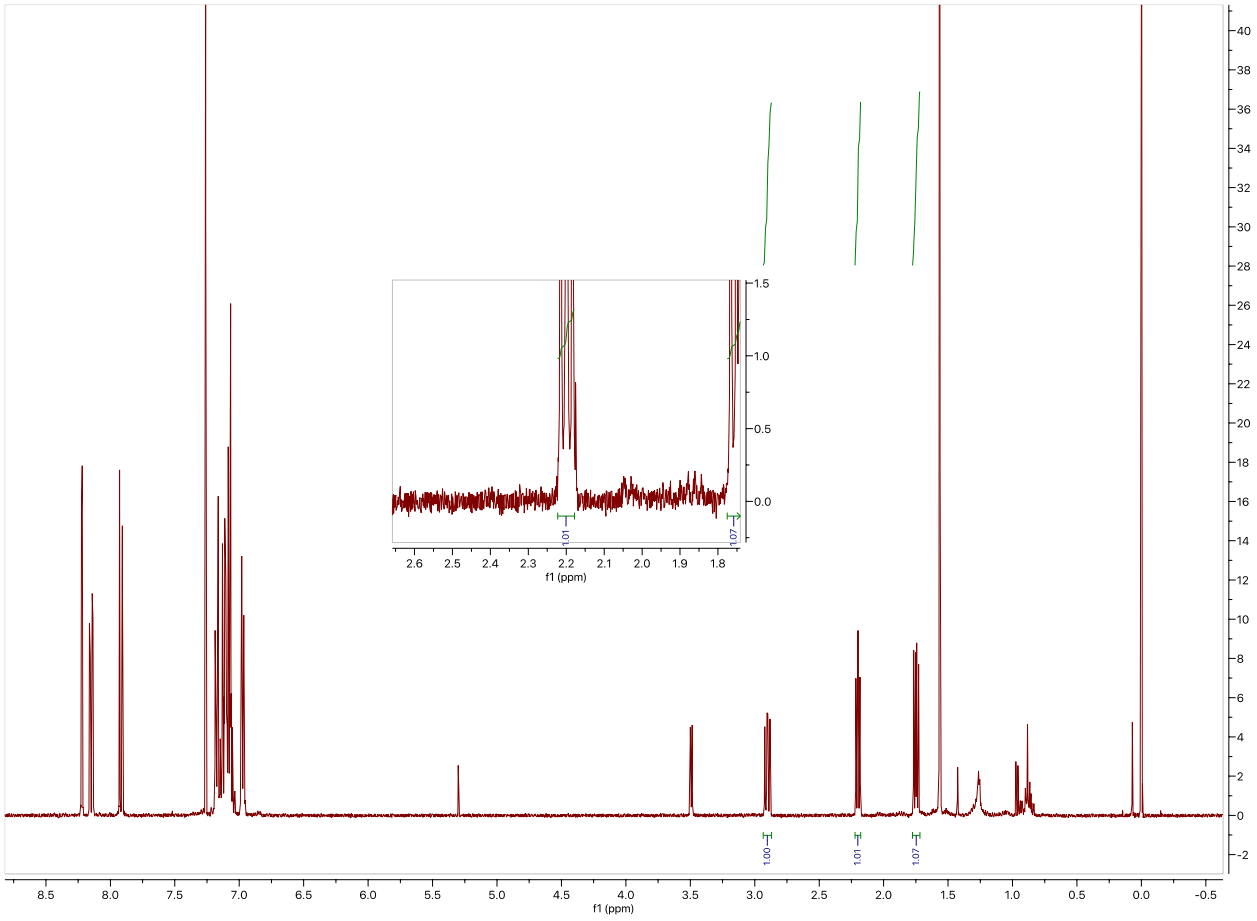
f1 (ppm)
1.00
1.01
1.07

2.7.5 ^{1}H and ^{13}C NMR

Compound **29** ^{1}H and ^{13}C

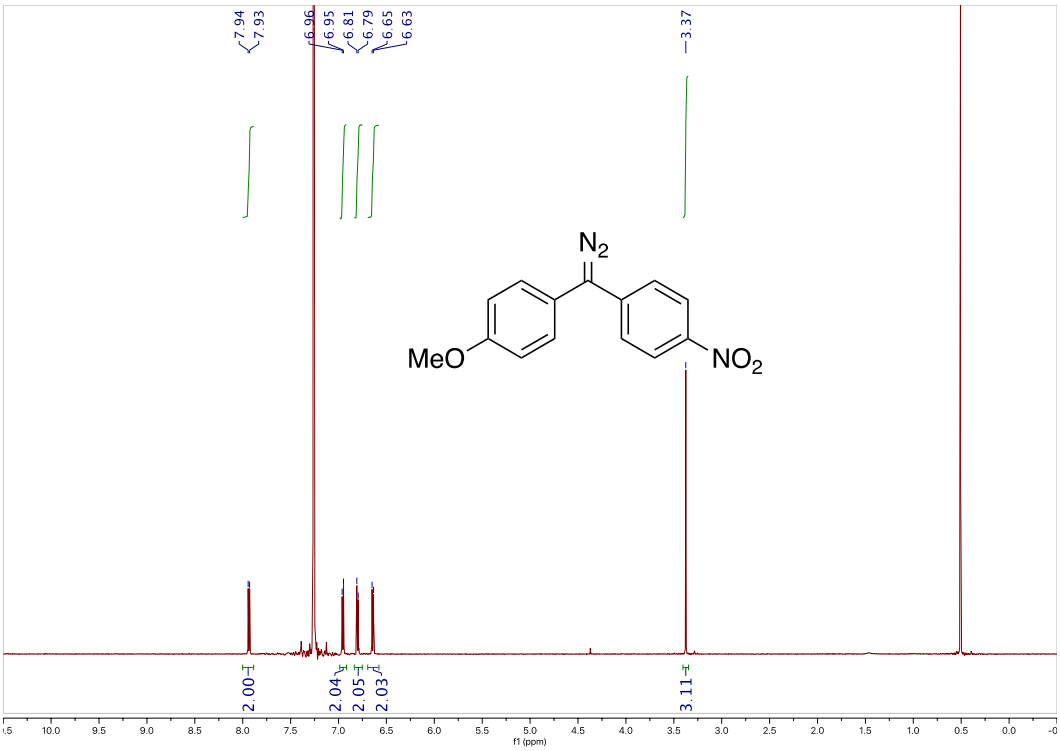

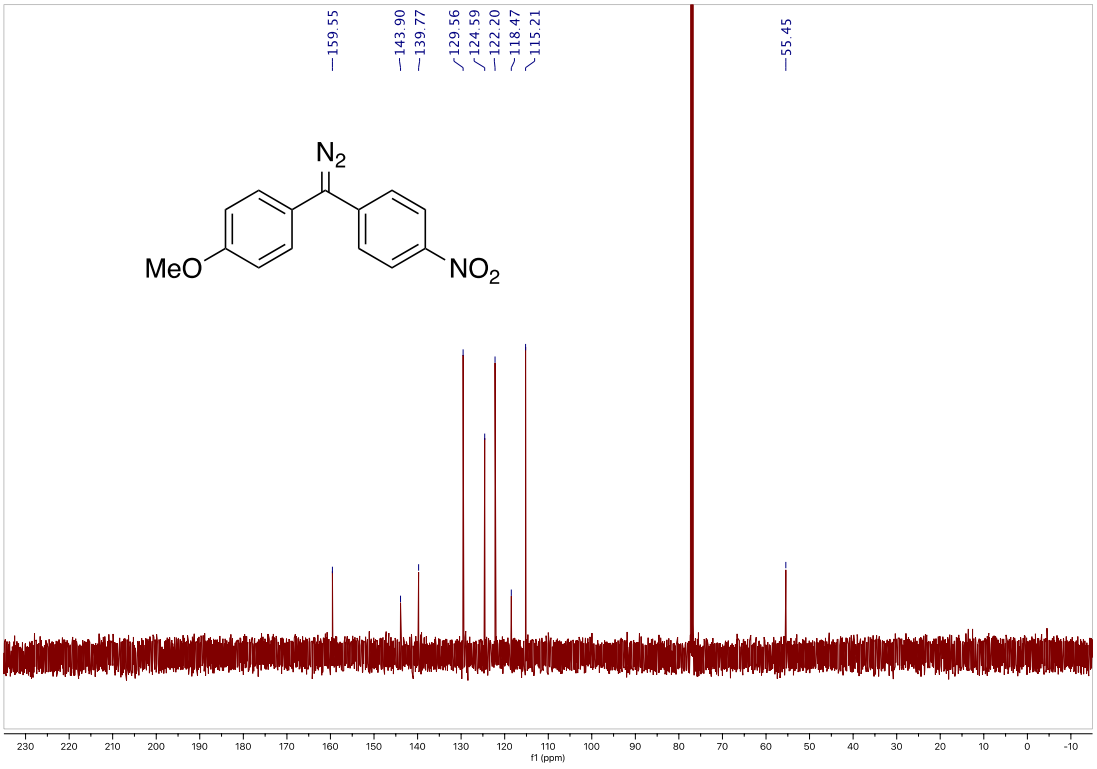

Compound **30** ^{1}H

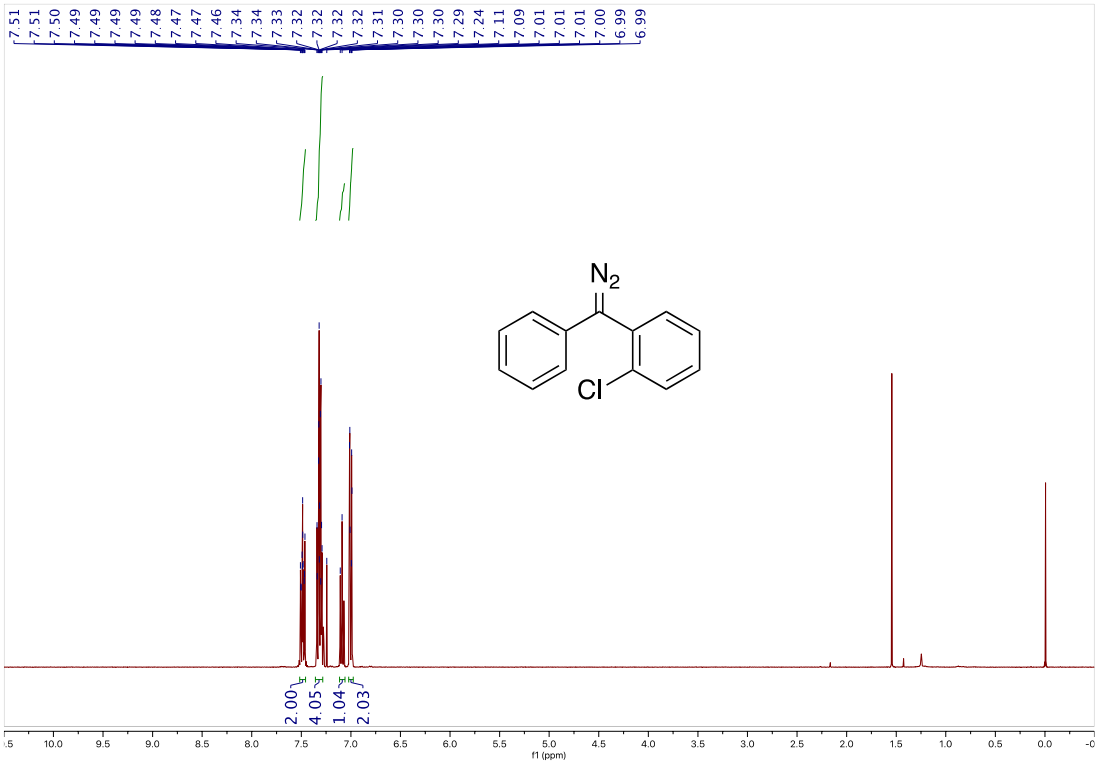

Compound **31** ^{1}H and ^{13}C

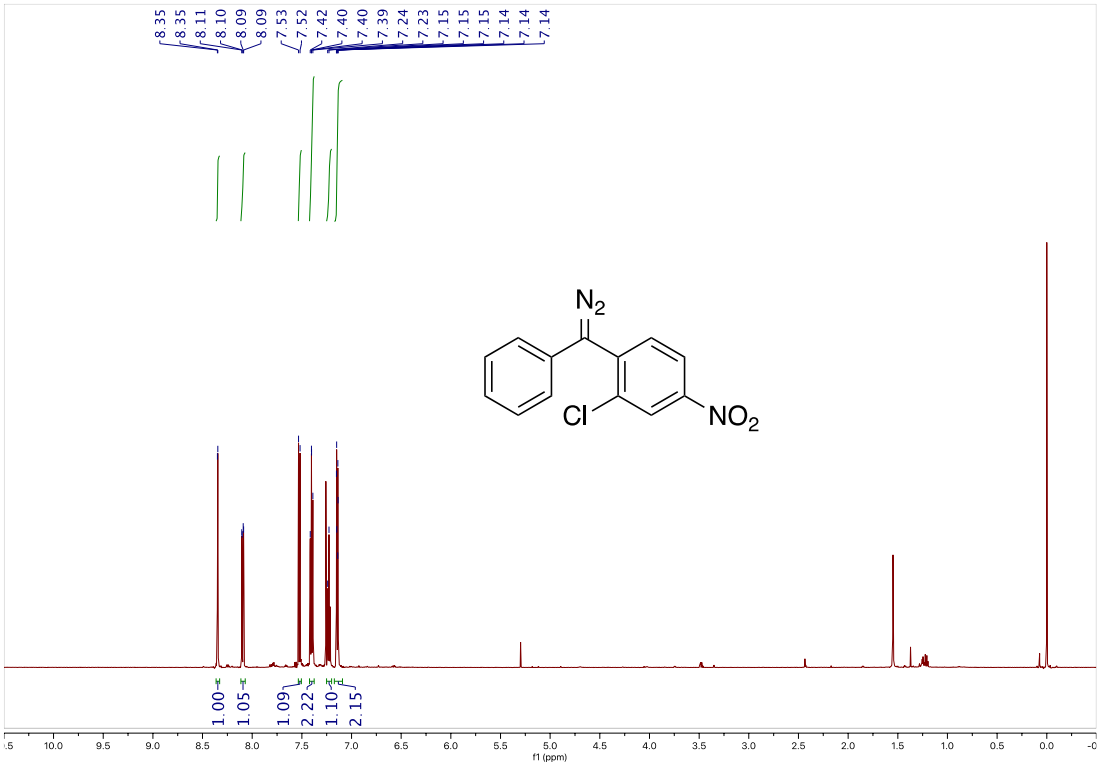

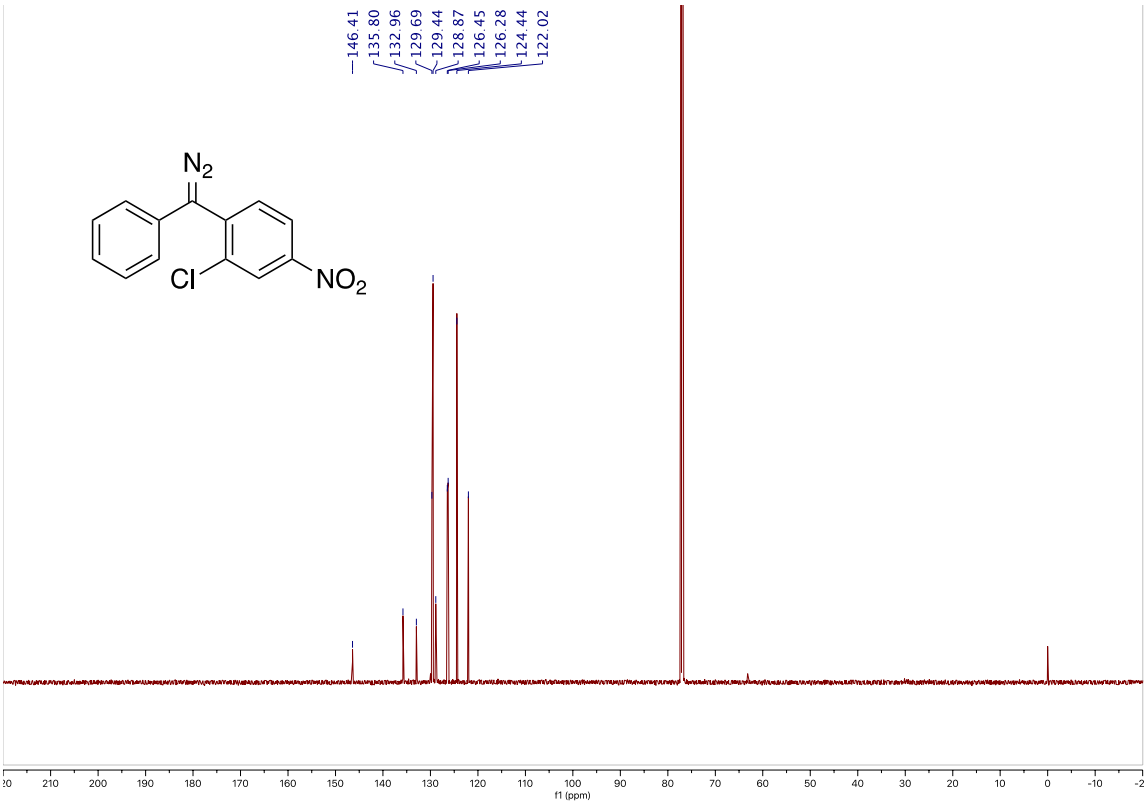

Compound **32** ^{1}H

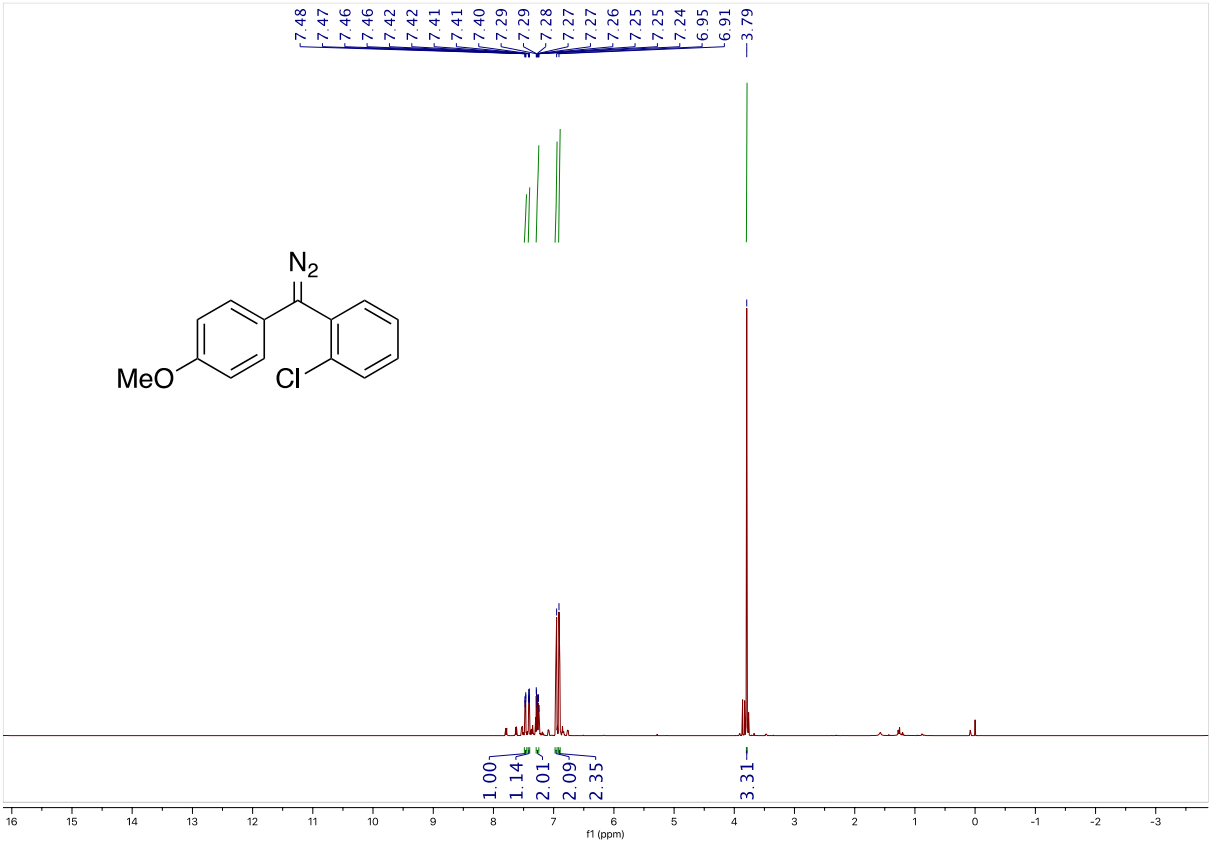

Compound **35** ^{1}H and ^{13}C

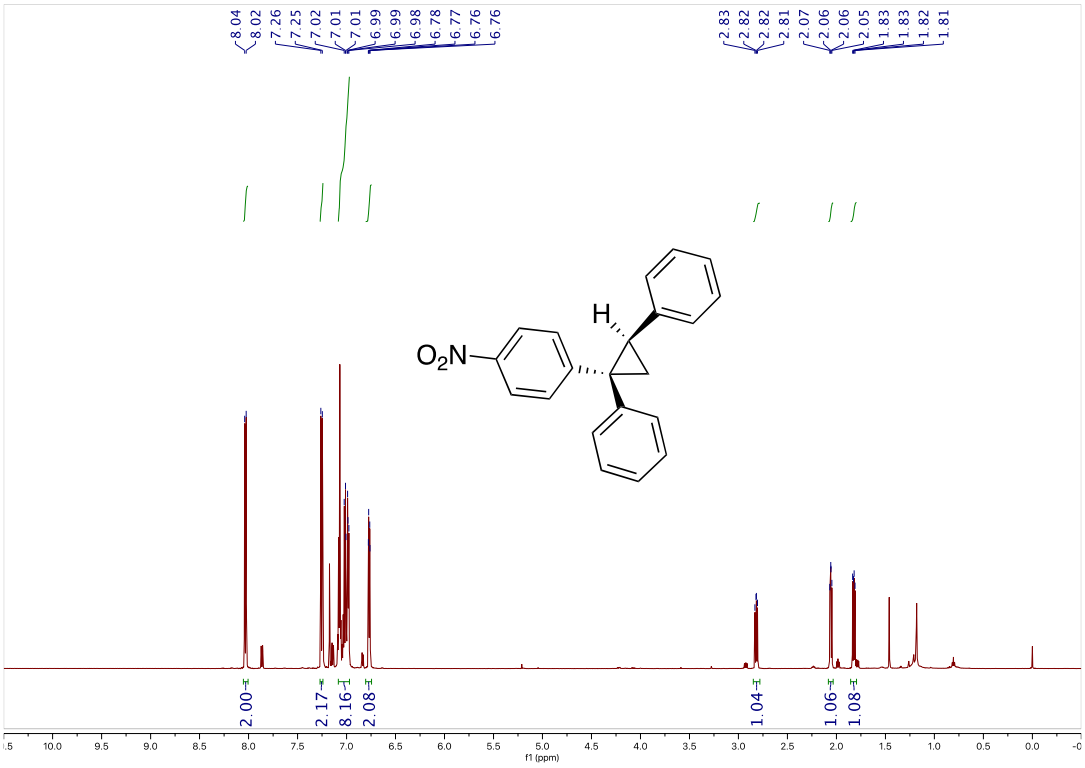

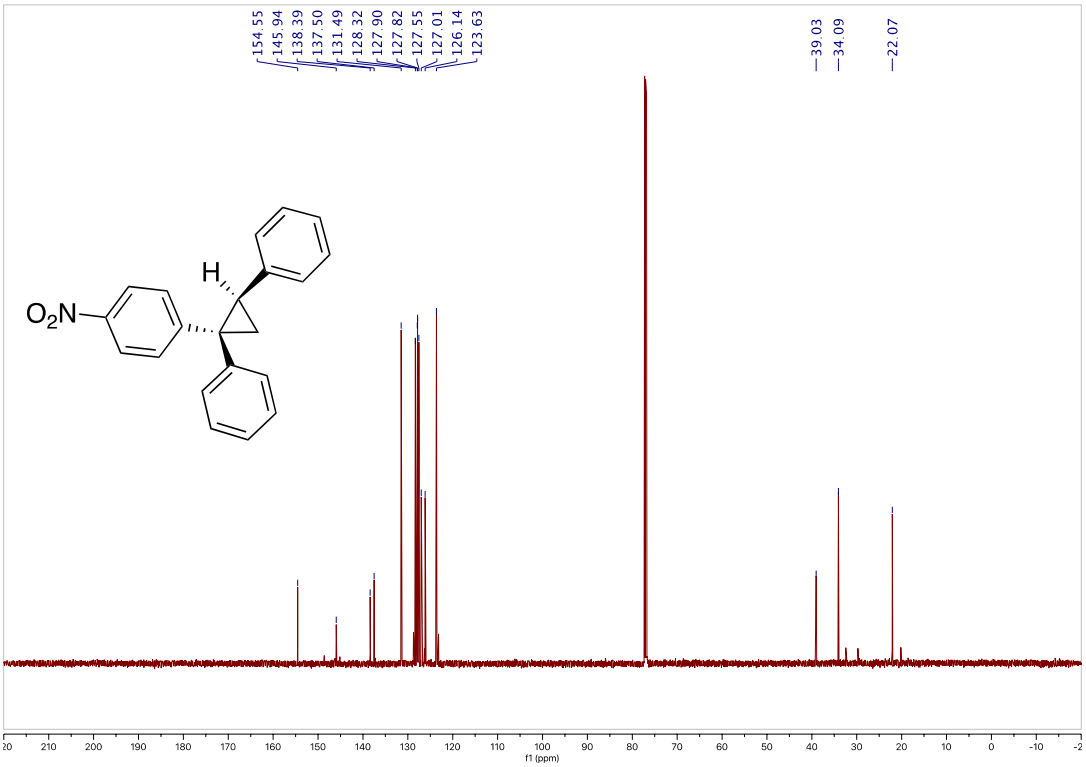

Compound **36** ^{1}H and ^{13}C

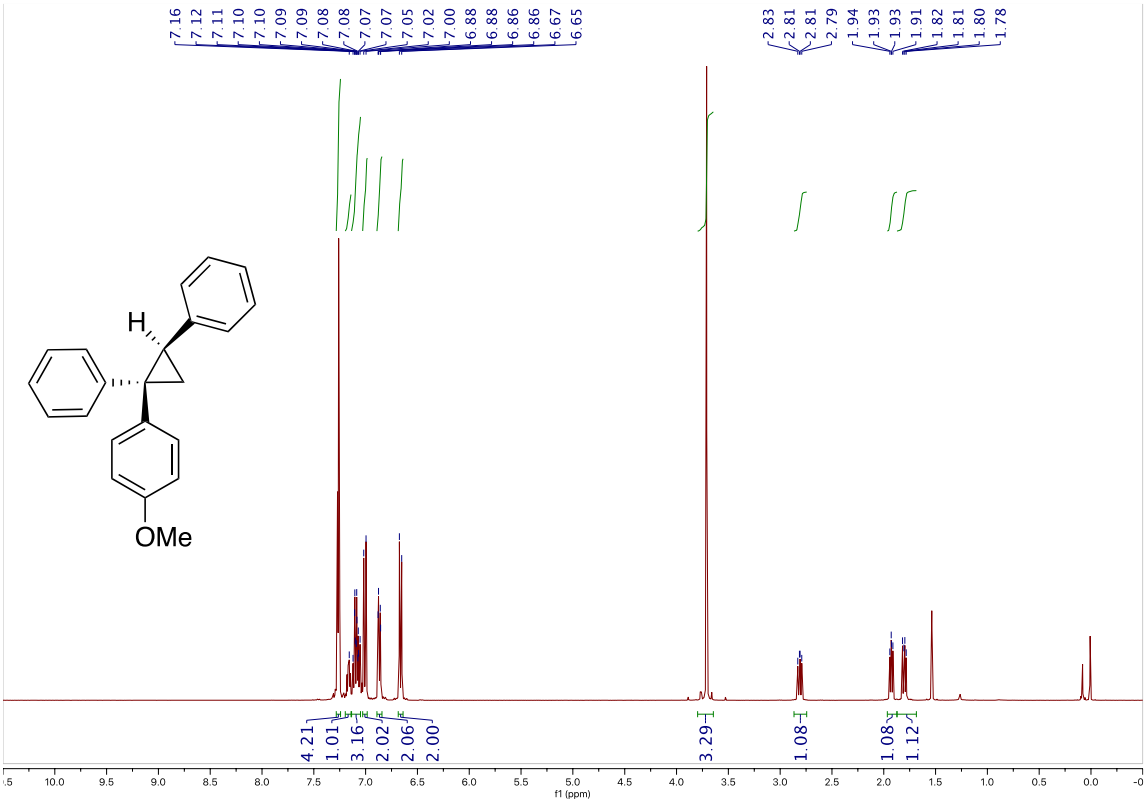

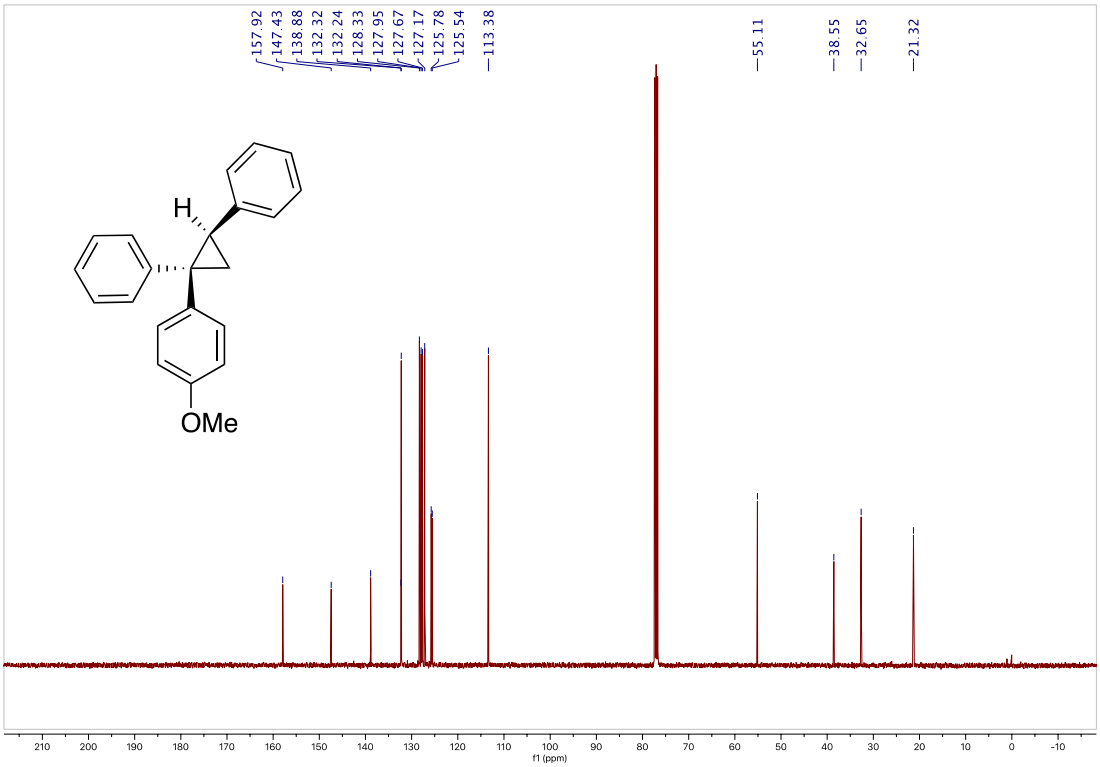

Compound **37** ^{1}H and ^{13}C

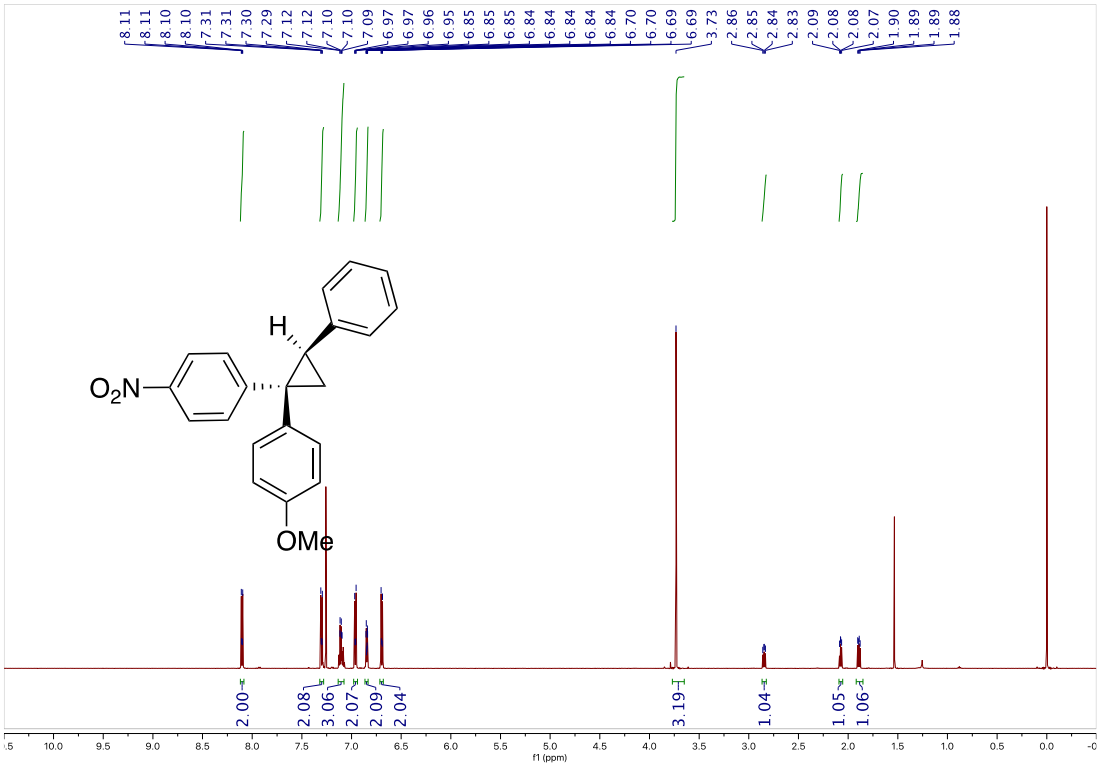

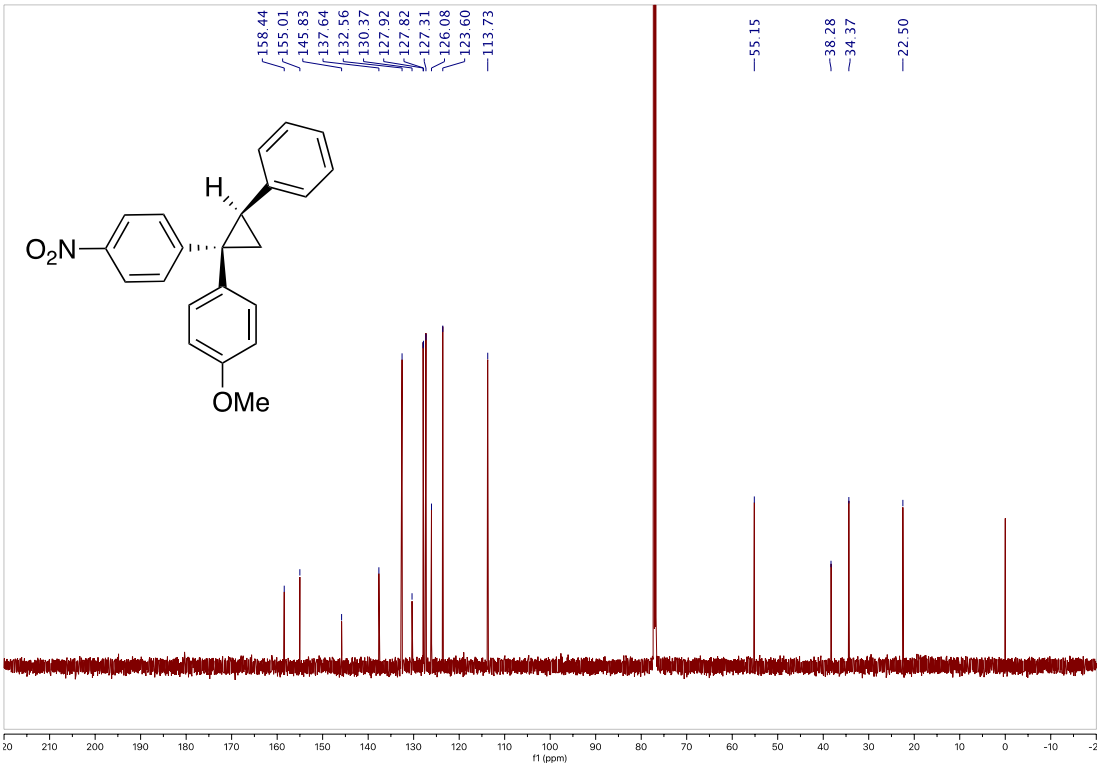

Compound **38** ^{1}H and ^{13}C

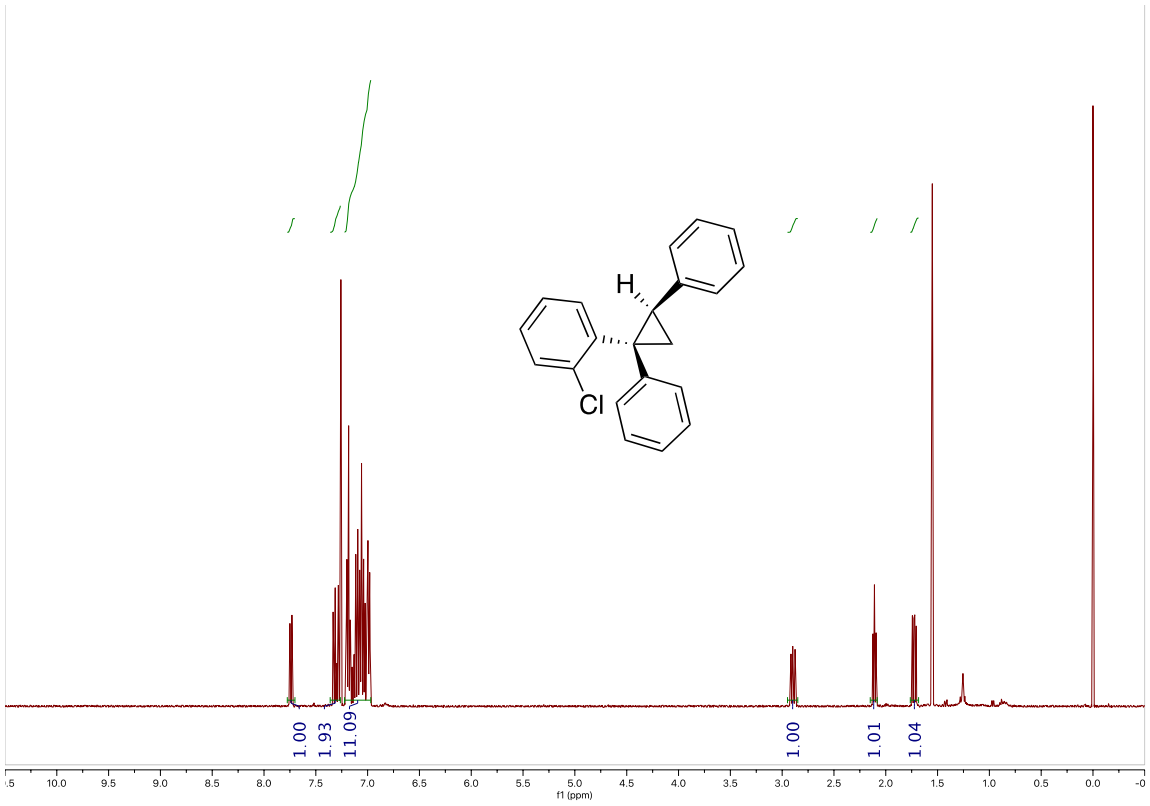

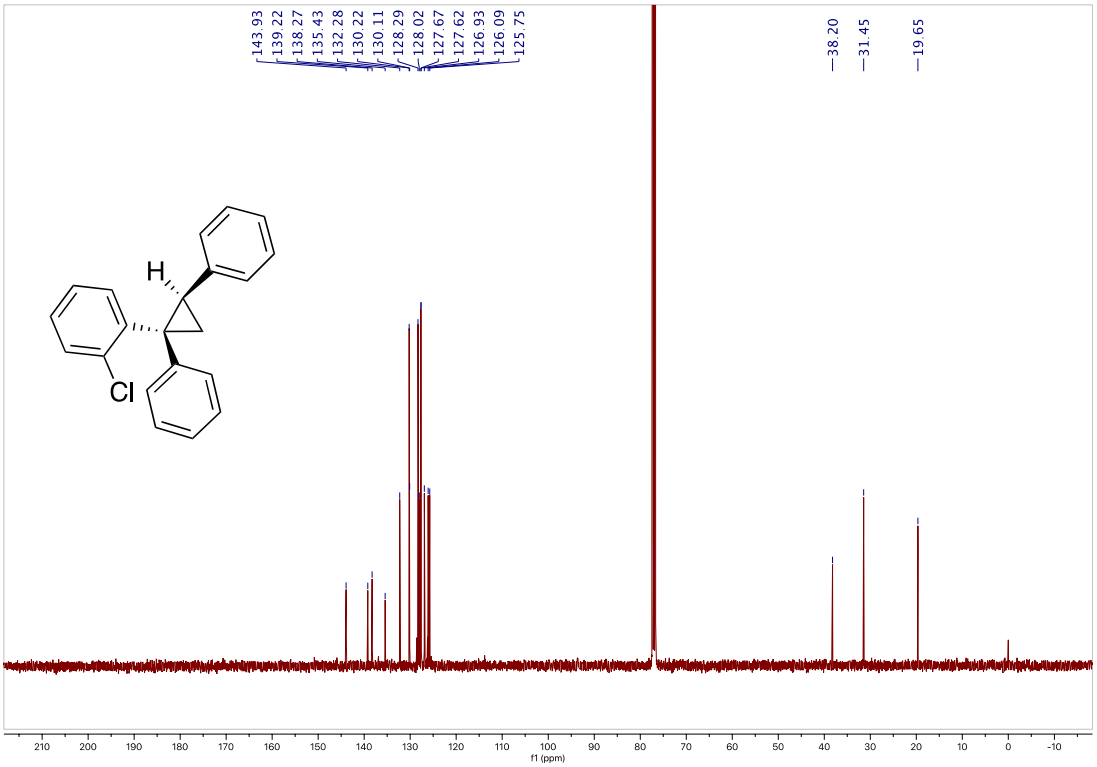

Compound **39** ^{1}H and ^{13}C

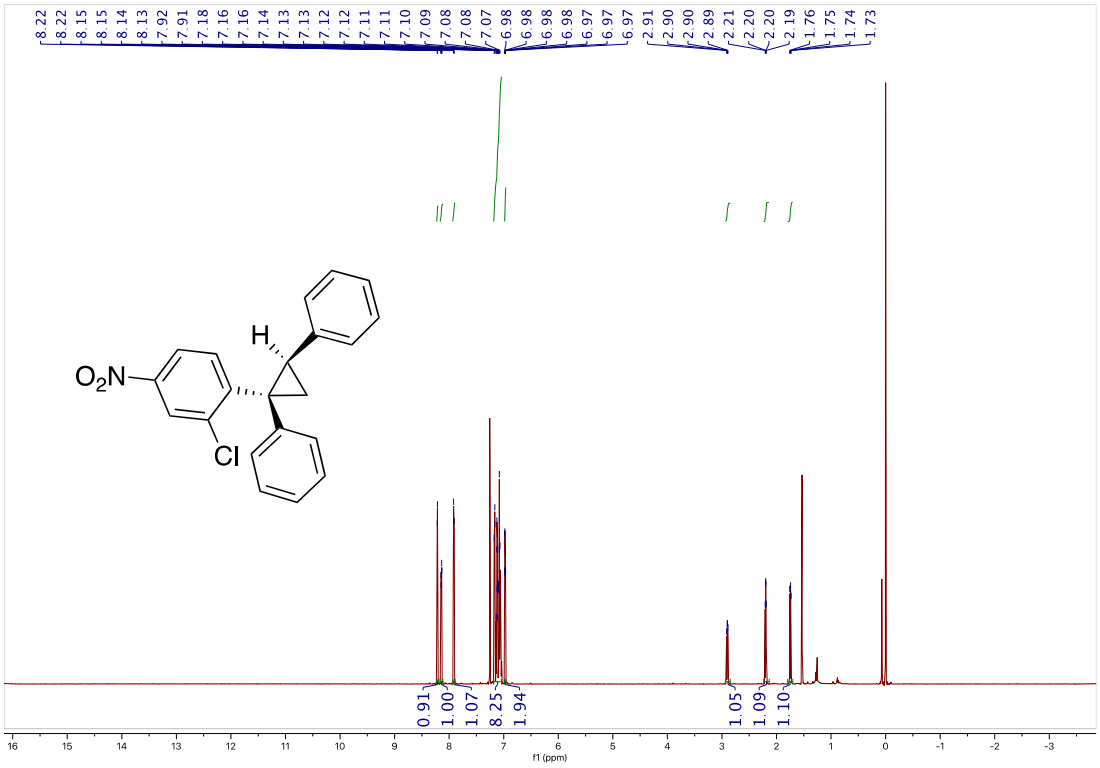

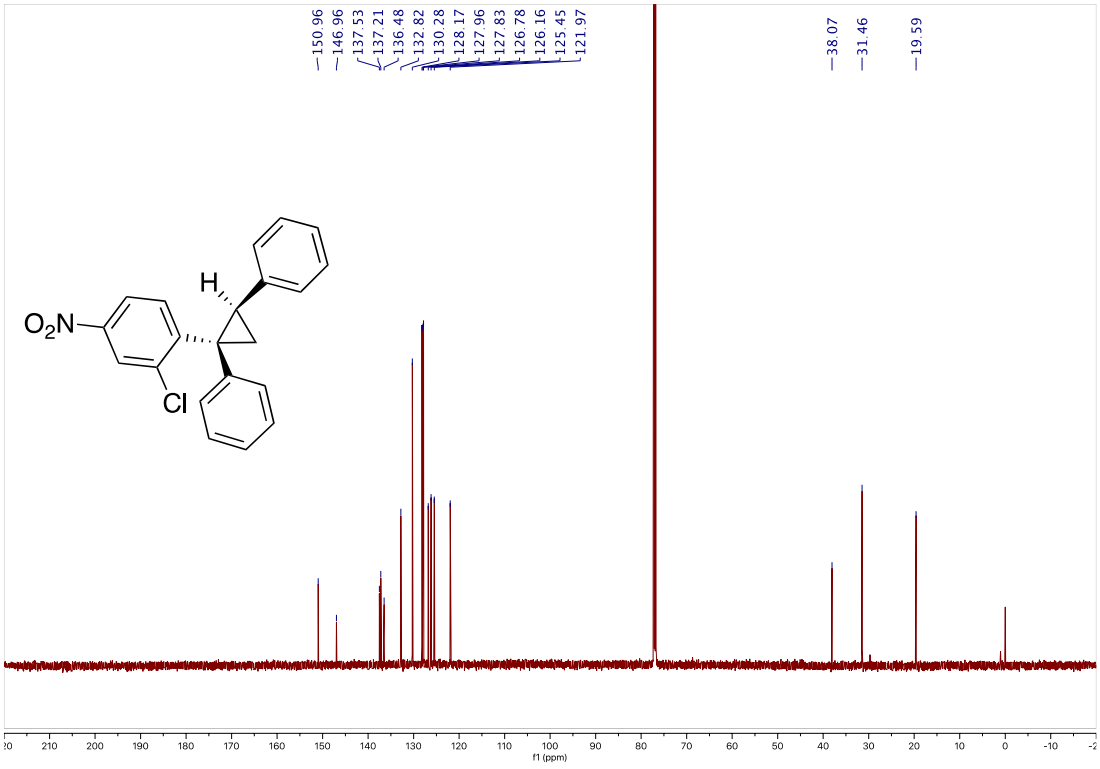

Compound **40** ^{1}H and ^{13}C

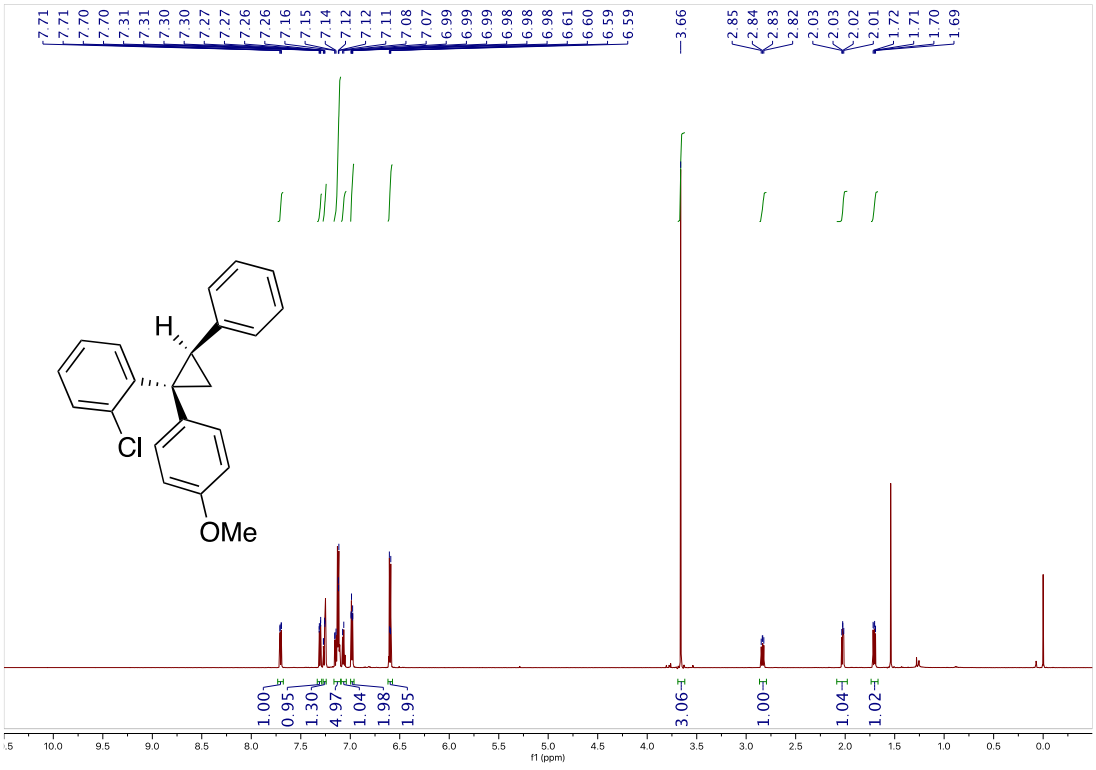
7.71
7.71
7.70
7.70
7.31
7.31
7.30
7.30
7.27
7.27
7.26
7.26
7.16
7.15
7.14
7.12
7.12
7.11
7.08
7.07
6.99
6.99
6.98
6.98
6.98
6.61
6.60
6.59
6.59
3.66
2.85
2.84
2.83
2.82
2.03
2.03
2.02
2.01
1.72
1.71
1.70
1.69
H
Cl
OMe
1.00
0.95
1.30
4.97
1.04
1.98
1.95
3.06
1.00
1.04
1.02
f1 (ppm)

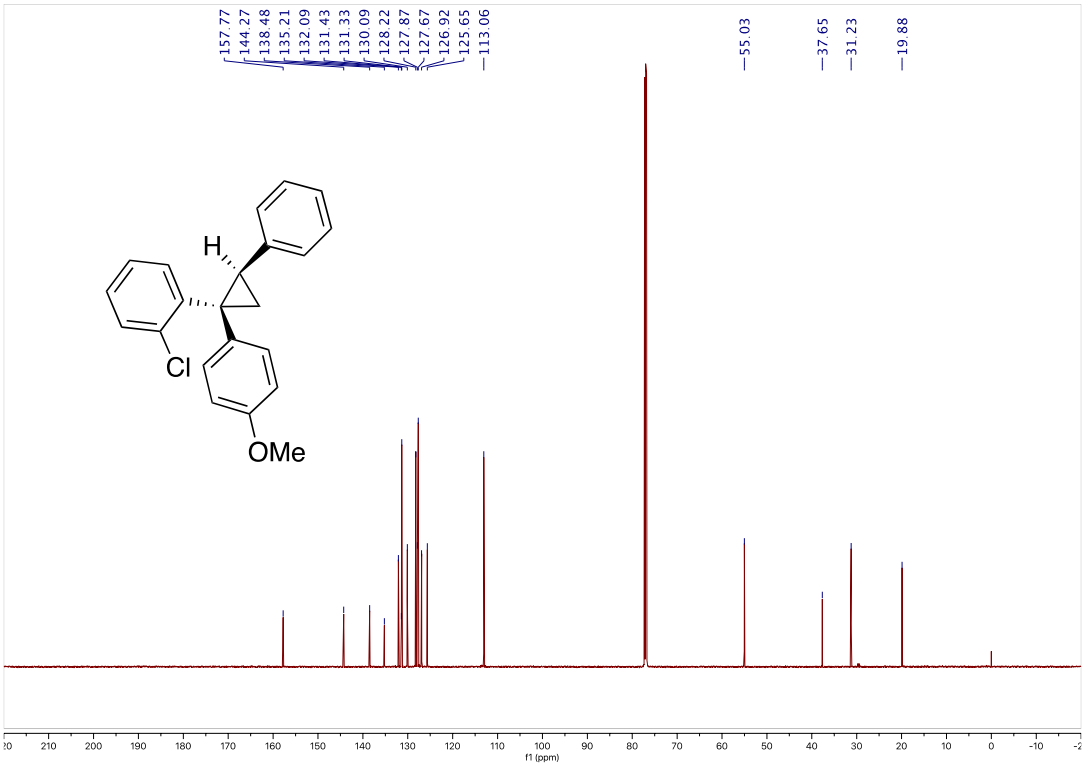
157.77
144.27
138.48
135.21
132.09
131.43
131.33
130.09
128.22
127.87
127.67
126.92
125.65
113.06
55.03
37.65
31.23
19.88
H
Cl
OMe
f1 (ppm)

2.8 HLPC Spectra for Enatnioselective Determination

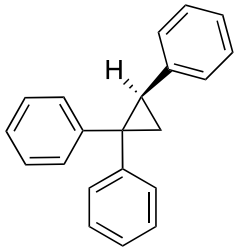

Compound 33 Racemic Trace:

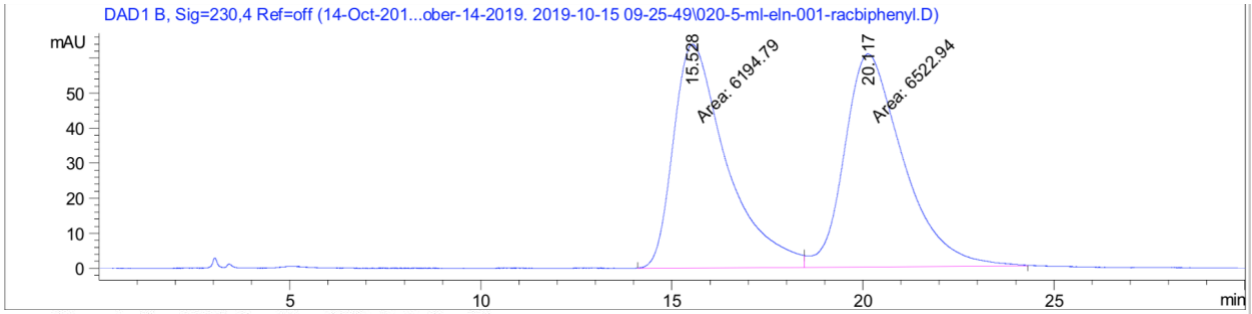

Signal 2: DAD1 B, Sig=230,4 Ref=off

Peak #	RetTime [min]	Type	Width [min]	Area [mAU*s]	Height [mAU]	Area %
1	15.528	MF	1.6156	6194.78613	63.90763	48.7098
2	20.117	FM	1.7875	6522.94336	60.81913	51.2902
Totals :				1.27177e4	124.72676	

Compound 33 Trace with Rh_2(*S*-PTAD)$_4$:

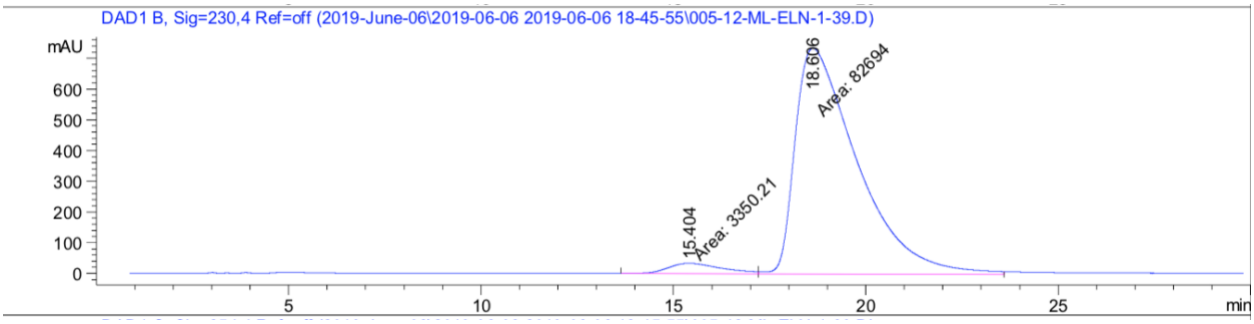

Signal 2: DAD1 B, Sig=230,4 Ref=off

Peak #	RetTime [min]	Type	Width [min]	Area [mAU*s]	Height [mAU]	Area %
1	15.404	MF	1.6434	3350.20605	33.97601	3.8936
2	18.606	FM	1.8737	8.26940e4	735.56940	96.1064
Totals :				8.60442e4	769.54541	

Compound 33 Trace with Rh_2(*S*-NTTL)$_4$:

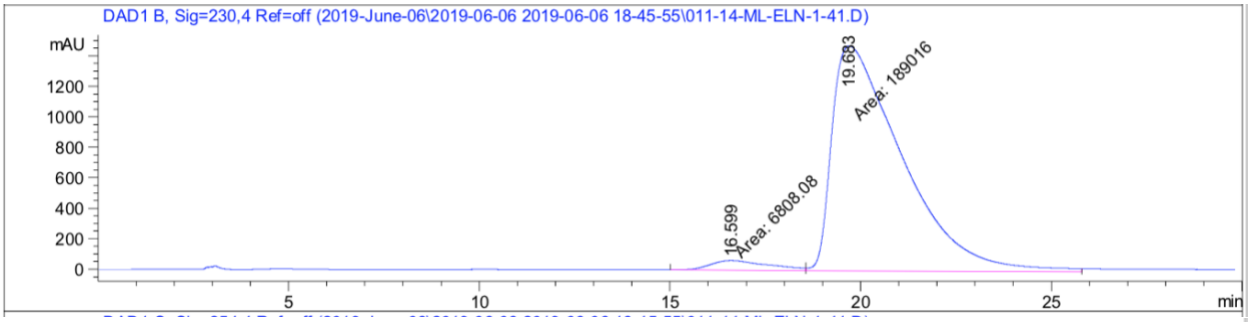

Signal 2: DAD1 B, Sig=230,4 Ref=off

Peak #	RetTime [min]	Type	Width [min]	Area [mAU*s]	Height [mAU]	Area %
1	16.599	MF	1.7812	6808.08057	63.70425	3.4766
2	19.683	FM	2.1348	1.89016e5	1475.68250	96.5234
Totals :				1.95824e5	1539.38674	

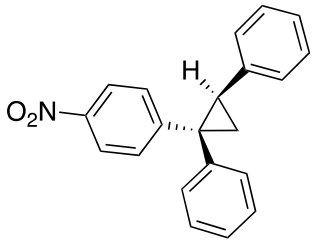

Compound 35 Racemic Trace:

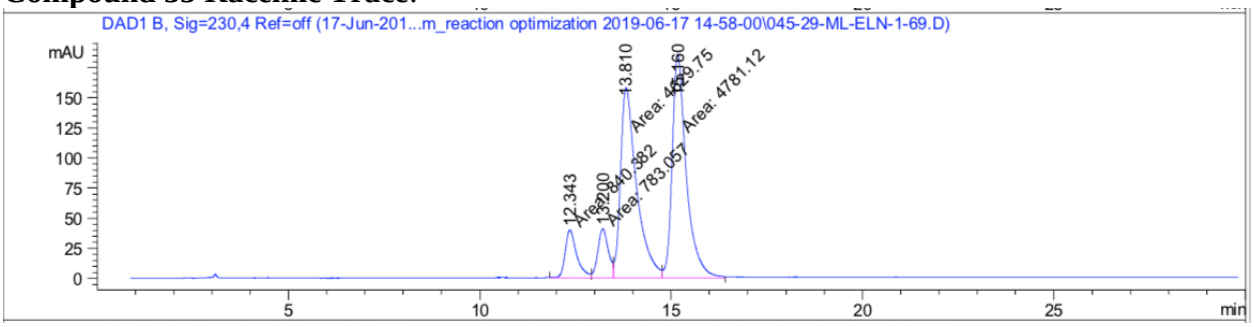

Signal 2: DAD1 B, Sig=230,4 Ref=off

Peak #	RetTime [min]	Type	Width [min]	Area [mAU*s]	Height [mAU]	Area %
1	12.343	MF	0.3525	840.38214	39.73832	7.6161
2	13.200	MF	0.3202	783.05688	40.76136	7.0966
3	13.810	MF	0.4890	4629.74609	157.79266	41.9578
4	15.160	FM	0.4287	4781.11523	185.89740	43.3296
Totals :				1.10343e4	424.18975	

Compound 35 Trace with Rh_2(*S*-NTTL)$_4$:

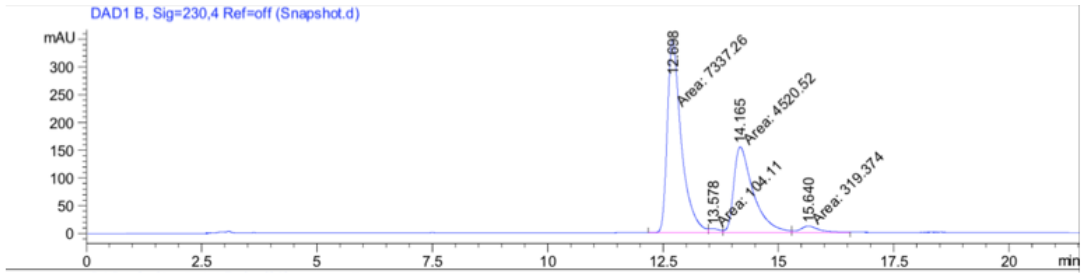

Signal 2: DAD1 B, Sig=230,4 Ref=off

Peak #	RetTime [min]	Type	Width [min]	Area [mAU*s]	Height [mAU]	Area %
1	12.698	MF	0.3510	7337.25732	348.34833	59.7435
2	13.578	MF	0.2654	104.11029	6.53808	0.8477
3	14.165	MF	0.4891	4520.51709	154.05446	36.8083
4	15.640	FM	0.4610	319.37375	11.54610	2.6005
Totals :				1.22813e4	520.48697	

Compound 35 Trace with Rh_2(*S*-PTAD)$_4$:

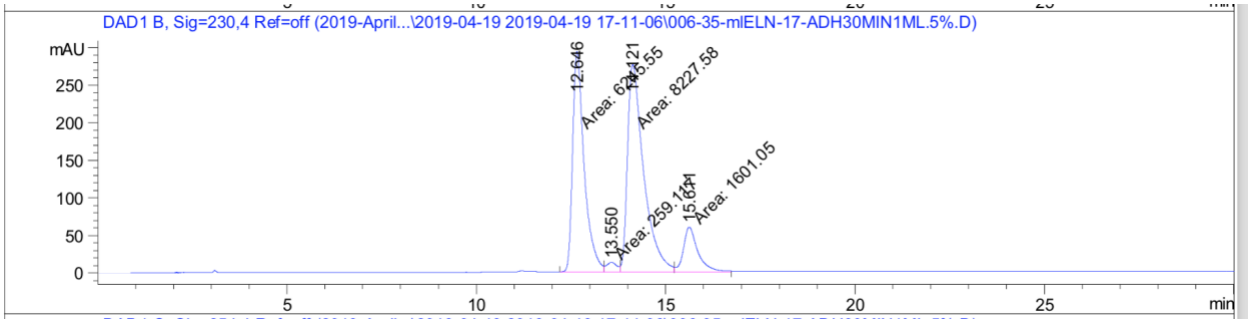

Peak #	RetTime [min]	Type	Width [min]	Area [mAU*s]	Height [mAU]	Area %
1	12.646	MF	0.3549	6245.55225	293.26422	38.2382
2	13.550	MF	0.3376	259.11688	12.79360	1.5864
3	14.121	MF	0.4968	8227.58008	276.01035	50.3730
4	15.611	FM	0.4466	1601.05176	59.75366	9.8024
Totals :				1.63333e4	641.82182	

Compound 35 Trace with Rh_2(*S*-DOSP)$_4$:

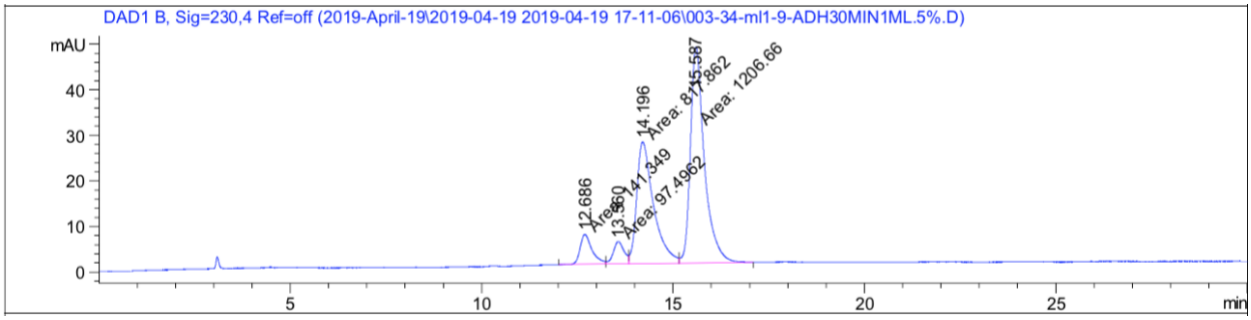

Signal 2: DAD1 B, Sig=230,4 Ref=off

Peak #	RetTime [min]	Type	Width [min]	Area [mAU*s]	Height [mAU]	Area %
1	12.686	MF	0.3578	141.34885	6.58496	6.2451
2	13.560	MF	0.3323	97.49619	4.88990	4.3076
3	14.196	MF	0.5095	817.86188	26.75207	36.1348
4	15.587	FM	0.4244	1206.65723	47.38936	53.3126
Totals :				2263.36414	85.61630	

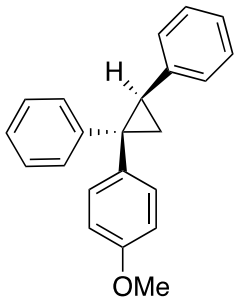

Compound 36 Racemic Trace:

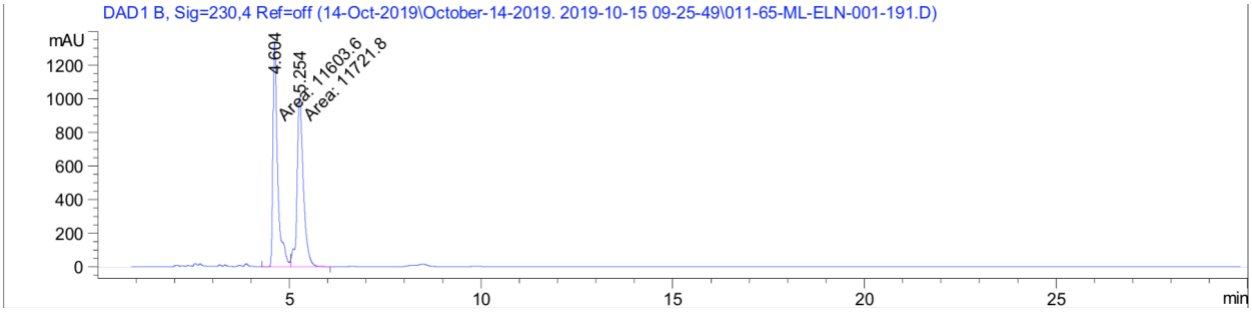

Signal 2: DAD1 B, Sig=230,4 Ref=off

Peak #	RetTime [min]	Type	Width [min]	Area [mAU*s]	Height [mAU]	Area %
1	4.604	MF	0.1449	1.16036e4	1334.61938	49.7466
2	5.254	FM	0.1944	1.17218e4	1005.07471	50.2534
Totals :				2.33254e4	2339.69409	

Compound 36 Trace with Rh_2(*S*-PTAD)$_4$:

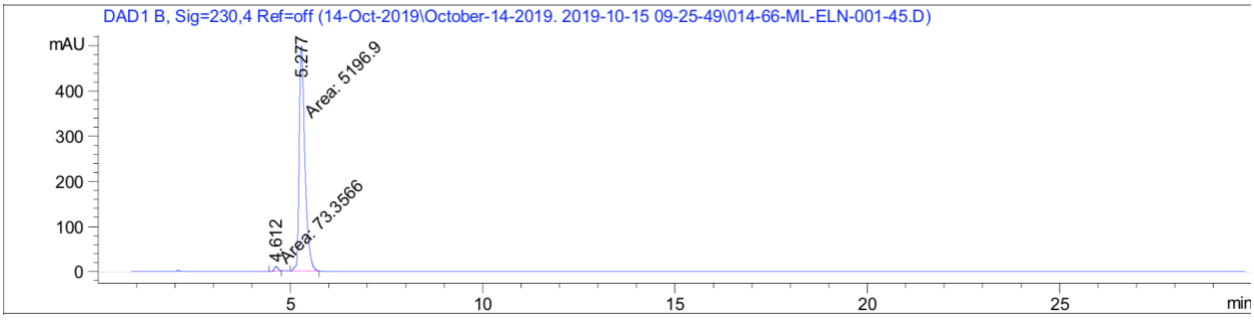

Signal 2: DAD1 B, Sig=230,4 Ref=off

Peak #	RetTime [min]	Type	Width [min]	Area [mAU*s]	Height [mAU]	Area %
1	4.612	MM	0.1117	73.35658	10.94165	1.3919
2	5.277	MM	0.1738	5196.89990	498.45493	98.6081
Totals :				5270.25648	509.39657	

Compound 36 Trace with Rh_2(*S*-NTTL)$_4$:

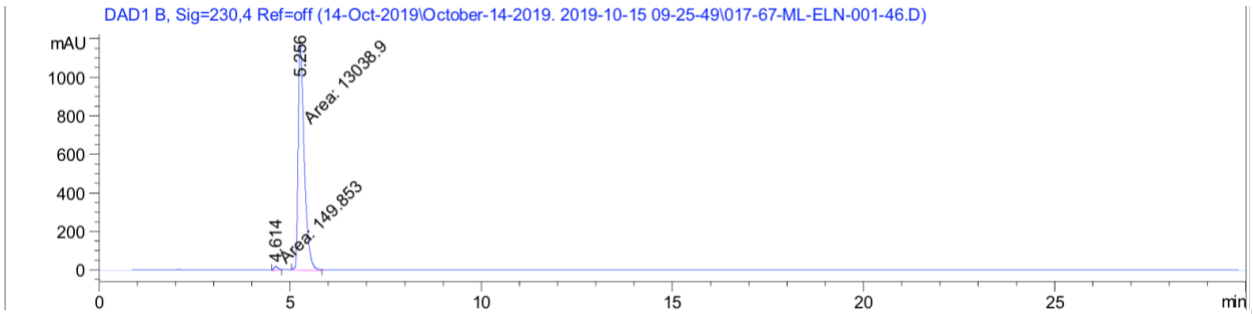

Signal 2: DAD1 B, Sig=230,4 Ref=off

Peak #	RetTime [min]	Type	Width [min]	Area [mAU*s]	Height [mAU]	Area %
1	4.614	MM	0.1286	149.85320	19.42839	1.1362
2	5.256	MM	0.1863	1.30389e4	1166.32764	98.8638
Totals :				1.31887e4	1185.75603	

Compound 36 Trace with Rh_2(*S*-DOSP)$_4$:

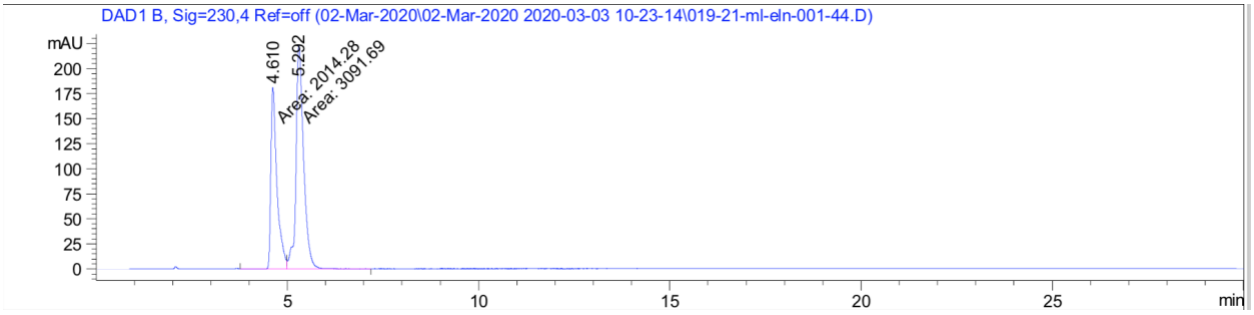

Signal 2: DAD1 B, Sig=230,4 Ref=off

Peak #	RetTime [min]	Type	Width [min]	Area [mAU*s]	Height [mAU]	Area %
1	4.610	MF	0.1855	2014.27637	180.93236	39.4495
2	5.292	FM	0.2308	3091.69092	223.28300	60.5505
Totals :				5105.96729	404.21536	

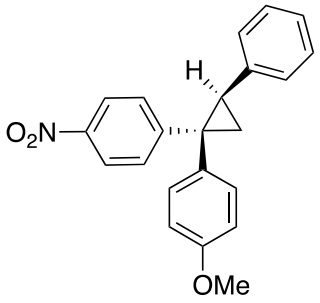

Compound 37 Racemic Trace:

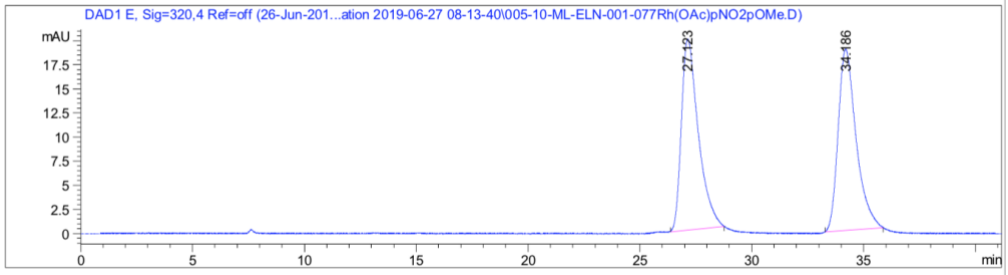

Signal 5: DAD1 E, Sig=320,4 Ref=off

Peak #	RetTime [min]	Type	Width [min]	Area [mAU*s]	Height [mAU]	Area %
1	27.123	BV R	0.6166	1043.66797	19.81052	49.8348
2	34.186	BB	0.6524	1050.58643	18.82965	50.1652
Totals :				2094.25439	38.64016	

Compound 37 Trace with Rh_2(*S*-PTAD)$_4$:

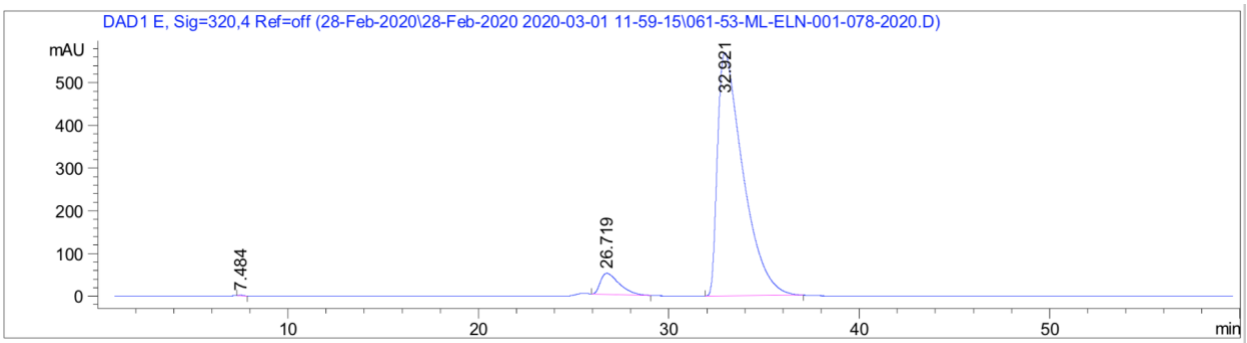

Signal 5: DAD1 E, Sig=320,4 Ref=off

Peak #	RetTime [min]	Type	Width [min]	Area [mAU*s]	Height [mAU]	Area %
1	7.484	BV R	0.1669	24.85926	1.76439	0.0440
2	26.719	VB R	0.8024	3372.18970	49.27880	5.9751
3	32.921	VV R	1.0883	5.30400e4	569.88092	93.9808
Totals :				5.64371e4	620.92411	

Compound 37 Trace with Rh_2(*S*-NTTL)$_4$:

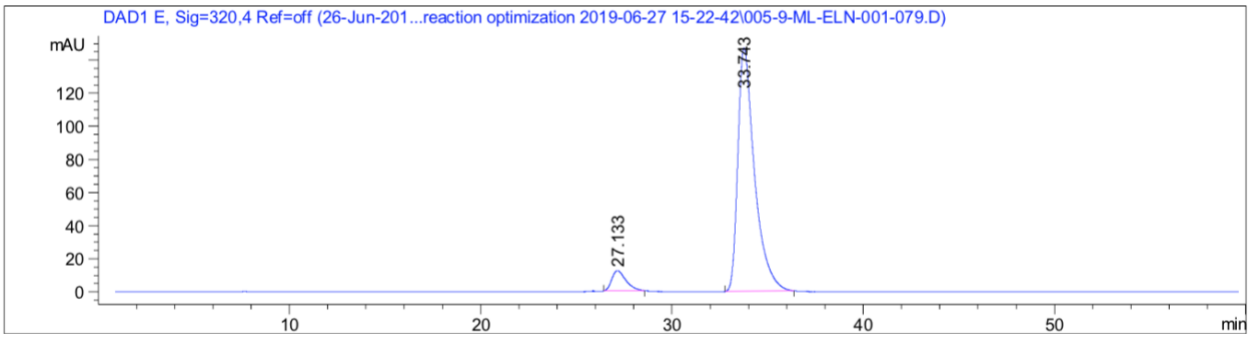

Signal 5: DAD1 E, Sig=320,4 Ref=off

Peak #	RetTime [min]	Type	Width [min]	Area [mAU*s]	Height [mAU]	Area %
1	27.133	BB	0.6037	627.57709	12.19864	6.5758
2	33.743	BB	0.7109	8916.10840	147.05443	93.4242
Totals :				9543.68549	159.25307	

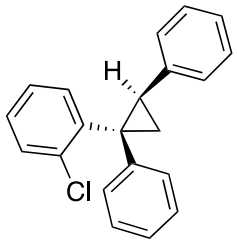

Compound 38 Racemic Trace:

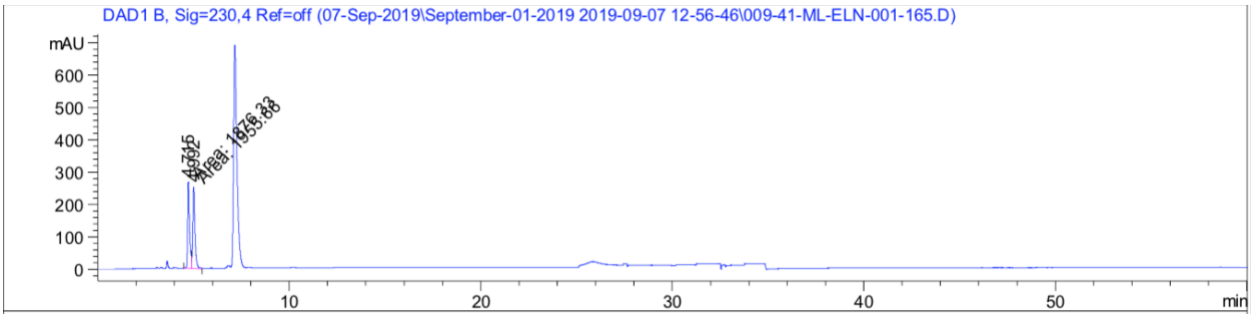

Signal 2: DAD1 B, Sig=230,4 Ref=off

Peak #	RetTime [min]	Type	Width [min]	Area [mAU*s]	Height [mAU]	Area %
1	4.715	MF	0.1170	1876.33179	267.18594	48.9649
2	4.992	FM	0.1291	1955.66211	252.39343	51.0351
Totals :				3831.99390	519.57938	

Compound 38 Trace with Rh_2(*S*-PTAD)$_4$:

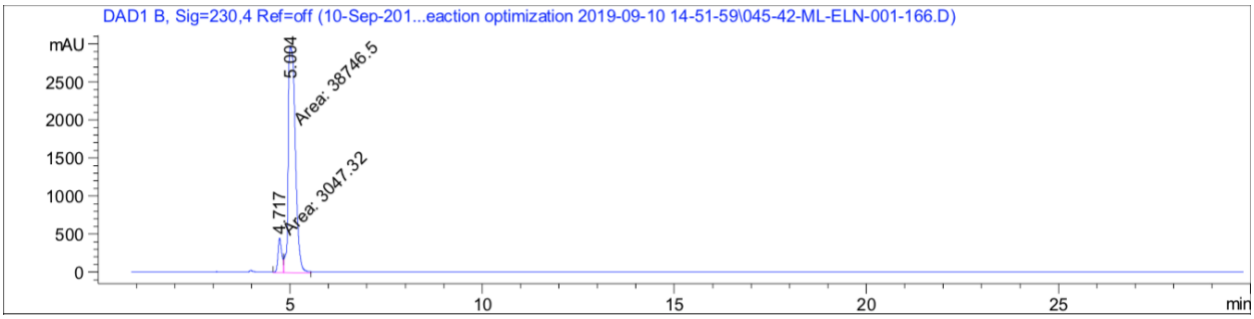

Signal 2: DAD1 B, Sig=230,4 Ref=off

Peak #	RetTime [min]	Type	Width [min]	Area [mAU*s]	Height [mAU]	Area %
1	4.717	MF	0.1131	3047.31519	448.89621	7.2913
2	5.004	FM	0.2170	3.87465e4	2975.54028	92.7087
Totals :				4.17938e4	3424.43649	

Compound 38 Trace with Rh_2(*S*-NTTL)$_4$:

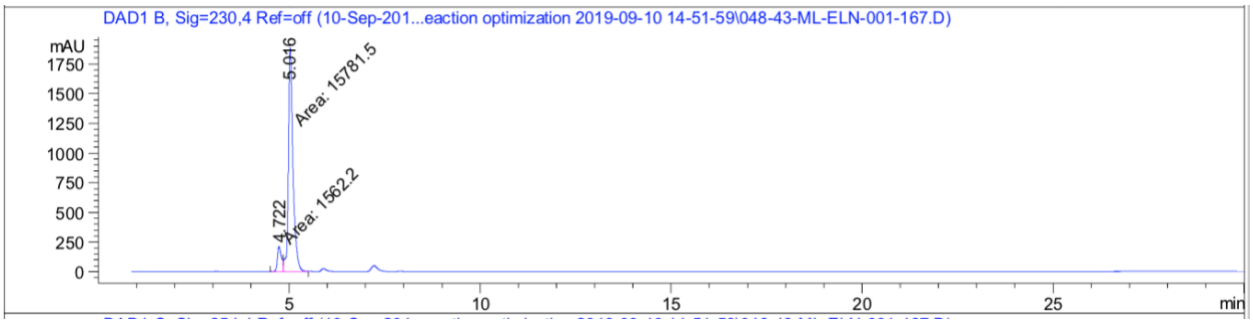

Signal 2: DAD1 B, Sig=230,4 Ref=off

Peak #	RetTime [min]	Type	Width [min]	Area [mAU*s]	Height [mAU]	Area %
1	4.722	MF	0.1229	1562.20068	211.80057	9.0073
2	5.016	FM	0.1395	1.57815e4	1885.17371	90.9927
Totals :				1.73437e4	2096.97427	

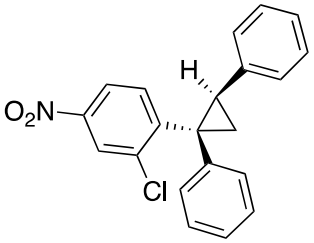

Compound 39 Racemic Trace:

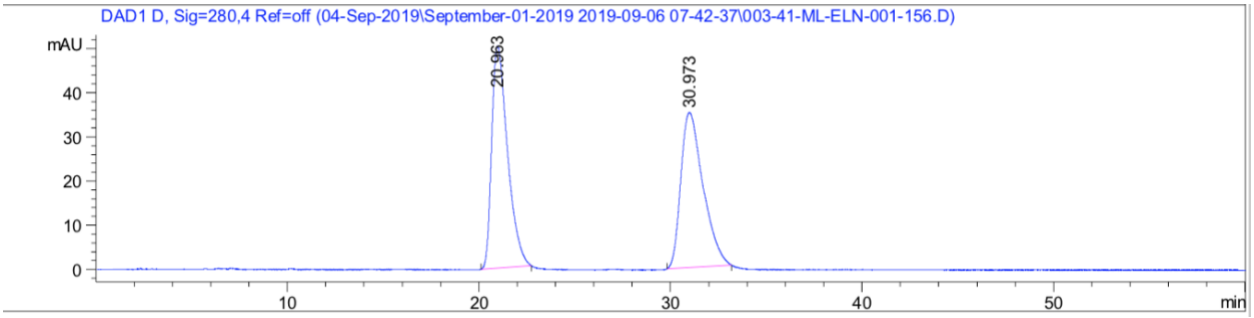

Signal 4: DAD1 D, Sig=280,4 Ref=off

Peak #	RetTime [min]	Type	Width [min]	Area [mAU*s]	Height [mAU]	Area %
1	20.963	BB	0.6757	2891.30493	50.29194	50.6111
2	30.973	BB	0.9418	2821.48755	35.06502	49.3889
Totals :				5712.79248	85.35696	

Compound 39 Trace with Rh_2(*S*-PTAD)$_4$:

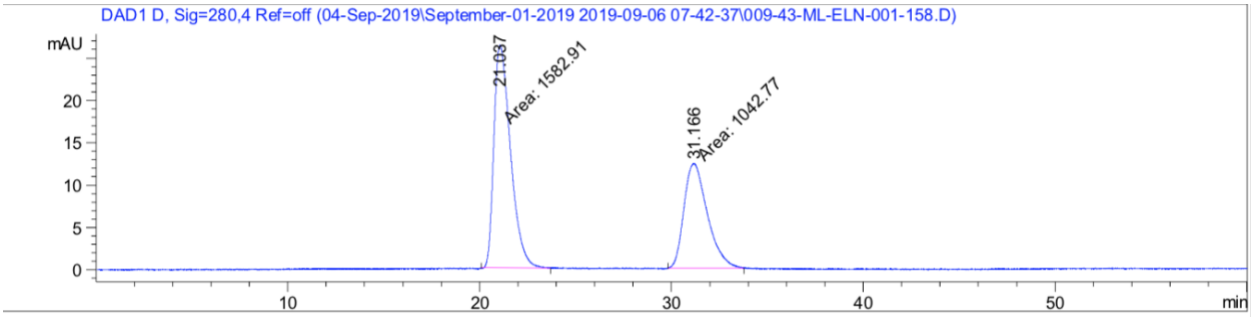

Signal 4: DAD1 D, Sig=280,4 Ref=off

Peak #	RetTime [min]	Type	Width [min]	Area [mAU*s]	Height [mAU]	Area %
1	21.037	MM	1.0029	1582.91003	26.30664	60.2858
2	31.166	MM	1.4096	1042.76563	12.32957	39.7142
Totals :				2625.67566	38.63621	

Compound 39 Trace with Rh_2(*S*-NTTL)$_4$:

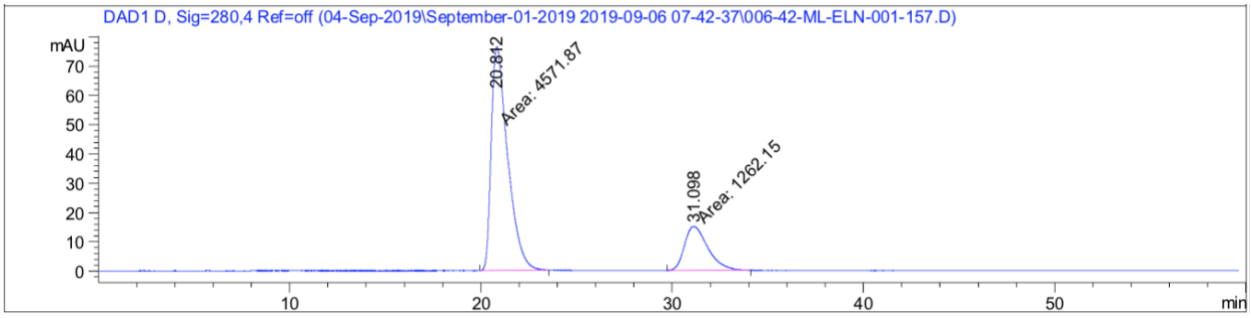

Signal 4: DAD1 D, Sig=280,4 Ref=off

Peak #	RetTime [min]	Type	Width [min]	Area [mAU*s]	Height [mAU]	Area %
1	20.812	MM	0.9968	4571.86865	76.44129	78.3657
2	31.098	MM	1.4080	1262.14636	14.94048	21.6343
Totals :				5834.01501	91.38177	

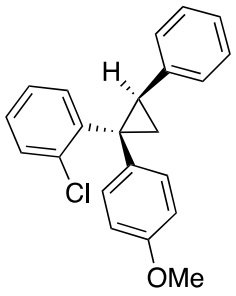

Compound 40 Racemic Trace:

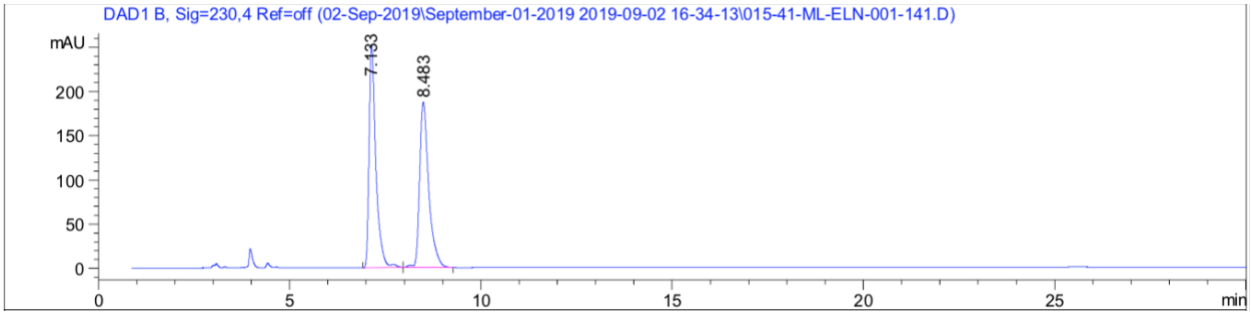

Signal 2: DAD1 B, Sig=230,4 Ref=off

Peak #	RetTime [min]	Type	Width [min]	Area [mAU*s]	Height [mAU]	Area %
1	7.133	BV R	0.1797	3100.63843	252.68707	50.0674
2	8.483	VB R	0.2428	3092.28613	186.84401	49.9326
Totals :				6192.92456	439.53108	

Compound 40 Trace with Rh_2(*S*-PTAD)$_4$:

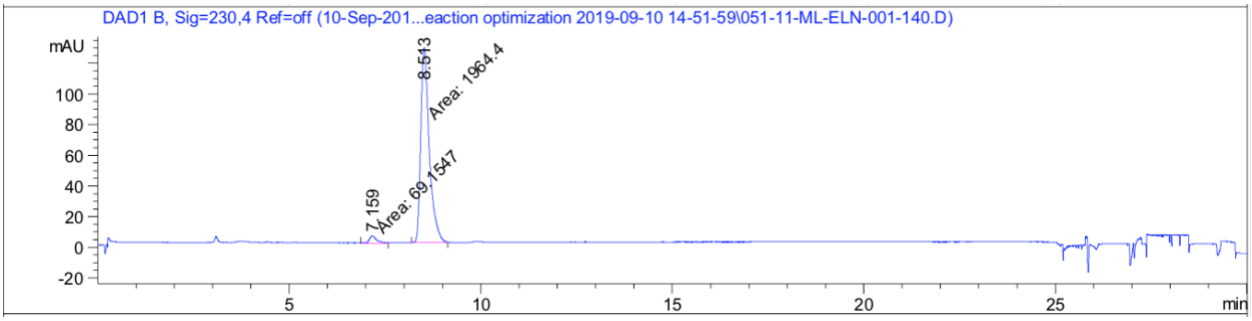

Signal 2: DAD1 B, Sig=230,4 Ref=off

Peak #	RetTime [min]	Type	Width [min]	Area [mAU*s]	Height [mAU]	Area %
1	7.159	MM	0.2355	69.15466	4.89337	3.4007
2	8.513	MM	0.2581	1964.40234	126.85229	96.5993
Totals :				2033.55701	131.74566	

Compound 40 Trace with Rh_2(*S*-NTTL)$_4$:

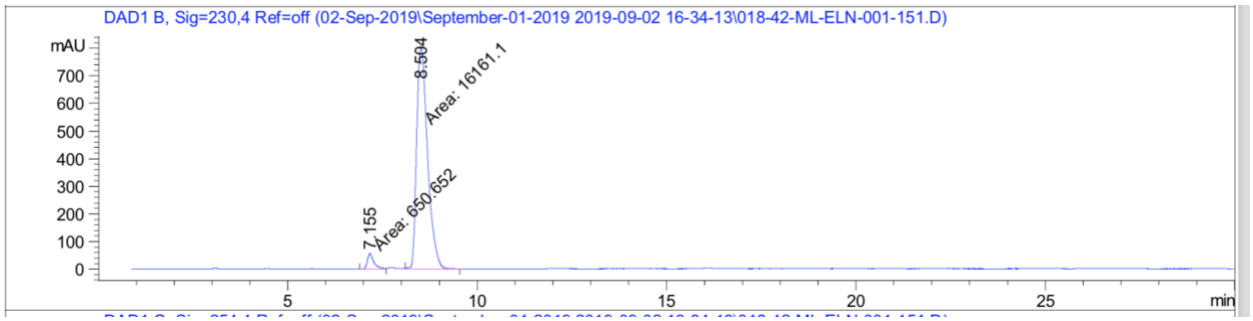

Signal 2: DAD1 B, Sig=230,4 Ref=off

Peak #	RetTime [min]	Type	Width [min]	Area [mAU*s]	Height [mAU]	Area %
1	7.155	MM	0.1949	645.79358	55.21113	3.9143
2	8.504	MM	0.3302	1.58525e4	800.06903	96.0857
Totals :				1.64983e4	855.28016	

2.8 X-Ray Crystal Structure

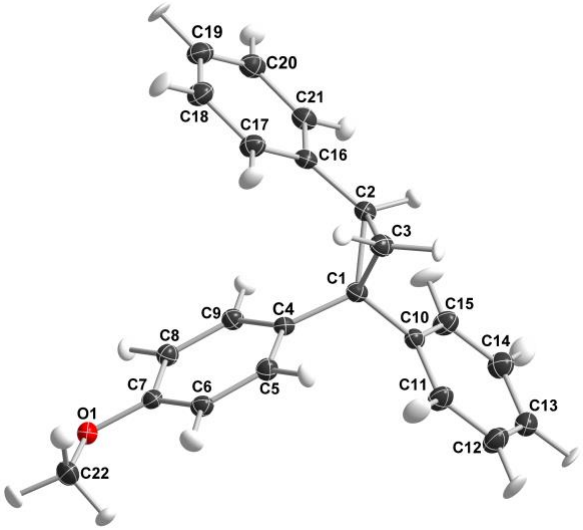

Crystal Data and Experimental

Experimental. Single colorless prism crystals of MeOphenylcyclopropanedibenzene (36) were chosen from the sample as supplied. A suitable crystal with dimensions 0.45×0.28×0.17 mm3 was selected and mounted on a loop on a XtaLAB Synergy-S diffractometer. The crystal was kept at a constant T = 100(1) K during data collection. The structure was solved with the ShelXT solution program using dual methods and by using Olex2 as the graphical interface.[55] The model was refined with olex2.refine 1.3-alpha (Bourhis et al., 2015) using full matrix least squares minimisation on F2.

Crystal Data. C22H20O, Mr = 300.403, monoclinic, P21 (No. 4), a = 11.20707(10) Å, b = 5.82419(4) Å, c = 12.84587(11) Å, □ = 104.9956(9)°, □ = □ = 90°, V = 809.923(12) Å3, T = 100.3(6) K, Z = 2, Z' = 1, □(Cu K□) = 0.567 mm-1, 24510 reflections measured, 3230 unique (Rint = 0.0396) which were used in all calculations. The final wR2 was 0.0554 (all data) and R1 was 0.0214. A colourless prism-shaped crystal with dimensions 0.45 × 0.28 × 0.17 mm^3 was mounted on a loop. Data were collected using a XtaLAB Synergy, Dualflex, HyPix diffractometer equipped with an Oxford Cryosystems low-temperature device operating at *T* = 100.3(6) K.

Data were measured using □ scans using Cu K□ radiation. The diffraction pattern was indexed and the total number of runs and images was based on the strategy calculation from the program CrysAlisPro 1.171.40.68a (Rigaku OD, 2019). The maximum resolution that was achieved was □ = 76.99° (0.79 Å). The unit cell was refined using CrysAlisPro 1.171.40.68a (Rigaku OD, 2019) on 20958 reflections, 86% of the observed reflections.

Data reduction, scaling and absorption corrections were performed using CrysAlisPro 1.171.40.68a (Rigaku OD, 2019). The final completeness is 99.81 % out to 76.99° in □. A numerical absorption correction based on Gaussian integration over a multifaceted crystal model was performed using CrysAlisPro 1.171.40.68a (Rigaku Oxford Diffraction, 2019). An empirical absorption correction using spherical harmonics, implemented in SCALE3 ABSPACK scaling algorithm was also applied. The absorption coefficient □ of this material is 0.567 mm^{-1} at this wavelength (□ = 1.54184Å) and the minimum and maximum transmissions are 0.420 and 1.000.

The structure was solved and the space group $P2_1$ (# 4) determined by the ShelXT structure solution program using dual methods and refined by full matrix least squares minimisation on F^2 using version of olex2.refine 1.3-alpha.[56] All non-hydrogen atoms were refined anisotropically. Hydrogen atom positions were calculated geometrically and refined using the riding model.

_refine_special_details: Refinement using NoSpherA2, an implementation of NOn-SPHERical Atom-form-factors in Olex2.[57] NoSpherA2 makes use of tailor-made aspherical atomic form factors calculatedon-the-fly from a Hirshfeld-partitioned electron density (ED) - not fromspherical-atom form factors.The ED is calculated from a gaussian basis set single determinant SCFwavefunction - either Hartree-Fock or B3LYP - for a fragment of the crystal embedded inan electrostatic crystal field.The following options were used: SOFTWARE: Tonto METHOD: rks

BASIS SET: def2-SVP CHARGE: 0 Multiplicity: 1 Date: 2020-01-21_17-15-31 Cluster Radius: 0

There is a single molecule in the asymmetric unit, which is represented by the reported sum formula. In other words: Z is 2 and Z' is 1.

The Flack parameter was refined to -0.0(2). Determination of absolute structure using Bayesian statistics on Bijvoet differences using the Olex2 results in 0.08(6). Note: The Flack parameter is used to determine chirality of the crystal studied, the value should be near 0, a value of 1 means that the stereochemistry is wrong and the model should be inverted. A value of 0.5 means that the crystal consists of a racemic mixture of the two enantiomers.

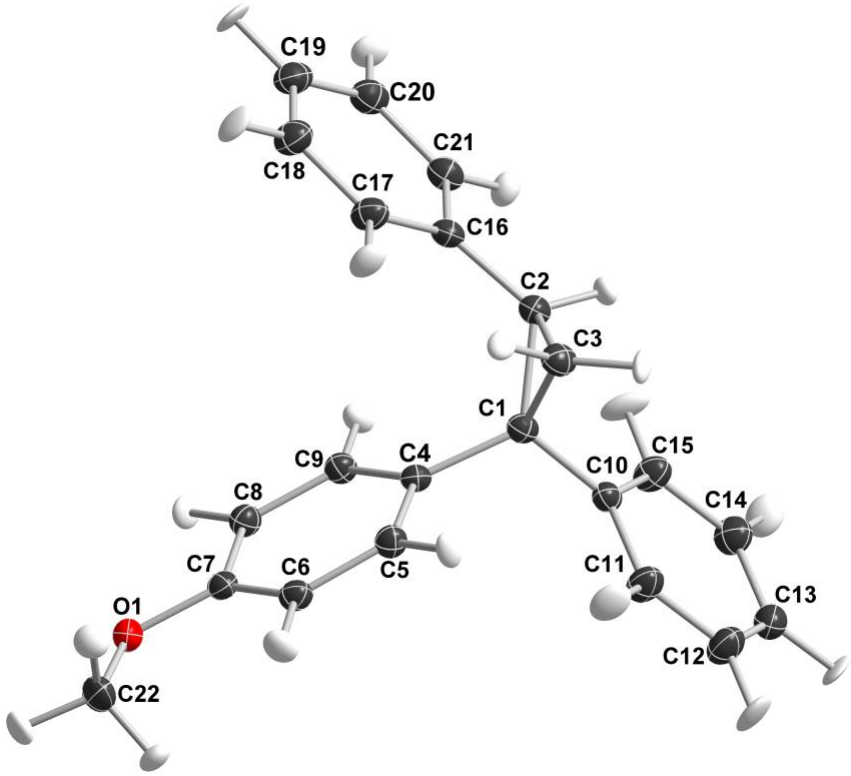

Figure: Thermal ellipsoid plot of the molecular structure.

2.9 References

1. Lee, M.; Ren, Z.; Musaev, D. G.; Davies, H. M. L., Rhodium-Stabilized Diarylcarbenes Behaving as Donor/Acceptor Carbenes. *ACS Catalysis* **2020,** *10* (11), 6240-6247.
2. Davies, H. M. L.; Beckwith, R. E. J., Catalytic enantioselective C-H activation by means of metal-carbenoid-induced C-H insertion. *Chem. Rev.* **2003,** *103* (8), 2861-2903.
3. Bertrand, G., Special issue: Carbene chemistry - Preface. *Journal of Organometallic Chemistry* **2005,** *690* (24-25), 5397-5397.
4. Werle, T.; Schäffler, L.; Maas, G., Dinuclear ruthenium(I) complexes of the type [Ru2(CO)4L2] with carboxylate or 2-pyridonate ligands: Evaluation as catalysts for olefin cyclopropanation with diazoacetates. *Journal of Organometallic Chemistry* **2005,** *690* (24-25), 5562-5569.
5. Soldi, C.; Lamb, K. N.; Squitieri, R. A.; Gonzalez-Lopez, M.; Di Maso, M. J.; Shaw, J. T., Enantioselective Intramolecular C-H Insertion Reactions of Donor Donor Metal Carbenoids. *J. Am. Chem. Soc.* **2014,** *136* (43), 15142-15145.
6. Fulton, J. R.; Aggarwal, V. K.; de Vicente, J., The use of tosylhydrazone salts as a safe alternative for handling diazo compounds and their applications in organic synthesis. *Eur. J. Org. Chem.* **2005,** *2005* (8), 1479-1492.
7. Wang, S. L. B.; Goldberg, D. R.; Liu, X.; Su, J.; Zheng, Q.-H.; Liptak, V.; Wulff, W. D., The first synthesis of cyclopropanone acetals from the reaction of Fischer carbene complexes with ketene acetals. *Journal of Organometallic Chemistry* **2005,** *690* (24-25), 6101-6110.
8. Zhang, L. M.; Sun, J. W.; Kozmin, S. A., Gold and platinum catalysis of enyne cycloisomerization. *Adv. Synth. Catal.* **2006,** *348* (16-17), 2271-2296.
9. Echavarren, A. M.; Nevado, C., Non-stabilized transition metal carbenes as intermediates in intramolecular reactions of alkynes with alkenes. *Chem. Soc. Rev.* **2004,** *33* (7), 431-436.
10. Chuprakov, S.; Gevorgyan, V., Regiodivergent metal-catalyzed rearrangement of 3-iminocyclopropenes into N-fused heterocycles. *Org. Lett.* **2007,** *9* (22), 4463-4466.
11. Kamikawa, K.; Shimizu, Y.; Matsuzaka, H.; Uemura, M., Stereoselective [3+2+2] cycloaddition utilizing optically active binuclear Fischer carbene complexes with alkynes. *Journal of Organometallic Chemistry* **2005,** *690* (24-25), 5922-5928.
12. Gassman, P. G.; Johnson, T. H., Chemistry Of Bent Bonds .49. Retrocarbene Additions - Dissection Of Alkyl-Substituted Cyclopropanes Under Metathesis Conditions. *J. Am. Chem. Soc.* **1976,** *98* (19), 6057-6058.
13. Gonzalez, M. J.; Lopez, L. A.; Vicente, R., Zinc-Catalyzed Cyclopropenation of Alkynes via 2-Furylcarbenoids. *Org. Lett.* **2014,** *16* (21), 5780-5783.
14. Nigam, M.; Platz, M. S.; Showalter, B. M.; Toscano, J. P.; Johnson, R.; Abbot, S. C.; Kirchhoff, M. M., Generation and study of benzylchlorocarbene from a phenanthrene precursor. *J. Am. Chem. Soc.* **1998,** *120* (32), 8055-8059.
15. Iwasawa, N.; Shido, M.; Kusama, H., Generation and reaction of metal-containing carbonyl ylides: Tandem 3+2 -cycloaddition-carbene insertion leading to novel polycyclic compounds. *J. Am. Chem. Soc.* **2001,** *123* (24), 5814-5815.
16. Archambeau, A.; Miege, F.; Meyer, C.; Cossy, J., Intramolecular Cyclopropanation and C-H Insertion Reactions with Metal Carbenoids Generated from Cyclopropenes. *Accounts Chem. Res.* **2015,** *48* (4), 1021-1031.

17. Regitz, M.; Maas, G., *Diazo Compounds: Properties and Synthesis*. Elsevier Science: 1986.
18. Maas, G., New Syntheses of Diazo Compounds. *Angewandte Chemie International Edition* **2009,** *48* (44), 8186-8195.
19. Nozoe, T.; Asao, T.; Yasunami, M.; Wakui, H.; Suzuki, T.; Ando, M., Formation And Structure Of 2-Diazo-2,4-Azulenequinone Derivatives. *J. Org. Chem.* **1995,** *60* (18), 5919-5924.
20. Demonceau, A.; Noels, A. F.; Hubert, A. J.; Teyssie, P., Transition-Metal-Catalyzed Reactions Of Diazoesters - Insertion Into C-H Bonds Of Paraffins By Carbenoids. *J. Chem. Soc.-Chem. Commun.* **1981,** (14), 688-689.
21. Davies, P. W., Organometallics: transition metals in organic synthesis. In *Annual Reports on the Progress of Chemistry, Section B: Organic Chemistry, Vol 106*, Cunningham, I.; Page, P., Eds. 2010; Vol. 106, pp 98-119.
22. Muller, P.; Allenbach, Y.; Robert, E., Rhodium(II)-catalyzed olefin cyclopropanation with the phenyliodonium ylide derived from Meldrum's acid. *Tetrahedron-Asymmetry* **2003,** *14* (7), 779-785.
23. Baudoin, O., Transition metal-catalyzed arylation of unactivated C(sp(3))-H bonds. *Chem. Soc. Rev.* **2011,** *40* (10), 4902-4911.
24. Li, Y.; Huang, J. S.; Zhou, Z. Y.; Che, C. M., Isolation and X-ray crystal structure of an unusual biscarbene metal complex and its reactivity toward cyclopropanation and allylic C-H insertion of unfunctionalized alkenes. *J. Am. Chem. Soc.* **2001,** *123* (20), 4843-4844.
25. Li, Y.; Huang, J. S.; Zhou, Z. Y.; Che, C. M.; You, X. Z., Remarkably stable iron porphyrins bearing nonheteroatom-stabilized carbene or (Alkoxycarbonyl) carbenes: Isolation, X-ray crystal structures, and carbon atom transfer reactions with hydrocarbons. *J. Am. Chem. Soc.* **2002,** *124* (44), 13185-13193.
26. Aggarwal, V. K.; Alonso, E.; Fang, G. Y.; Ferrara, M.; Hynd, G.; Porcelloni, M., Application of chiral sulfides to catalytic asymmetric aziridination and cyclopropanation with in situ generation of the diazo compound. *Angew. Chem.-Int. Edit.* **2001,** *40* (8), 1433-+.
27. Soldi, C.; Lamb, K. N.; Squitieri, R. A.; Gonzalez-Lopez, M.; Di Maso, M. J.; Shaw, J. T., Enantioselective intramolecular C-H insertion reactions of donor-donor metal carbenoids. *J Am Chem Soc* **2014,** *136* (43), 15142-5.
28. Souza, L. W.; Squitieri, R. A.; Dimirjian, C. A.; Hodur, B. M.; Nickerson, L. A.; Penrod, C. N.; Cordova, J.; Fettinger, J. C.; Shaw, J. T., Enantioselective Synthesis of Indolines, Benzodihydrothiophenes, and Indanes by C-H Insertion of Donor/Donor Carbenes. *Angew Chem Int Ed Engl* **2018,** *57* (46), 15213-15216.
29. Lamb, K. N.; Squitieri, R. A.; Chintala, S. R.; Kwong, A. J.; Balmond, E. I.; Soldi, C.; Dmitrenko, O.; Castiñeira Reis, M.; Chung, R.; Addison, J. B.; Fettinger, J. C.; Hein, J. E.; Tantillo, D. J.; Fox, J. M.; Shaw, J. T., Synthesis of Benzodihydrofurans by Asymmetric C−H Insertion Reactions of Donor/Donor Rhodium Carbenes. *Chemistry – A European Journal* **2017,** *23* (49), 11843-11855.
30. Reddy, R. P.; Lee, G. H.; Davies, H. M. L., Dirhodium tetracarboxylate derived from adamantylglycine as a chiral catalyst for carbenoid reactions. *Org. Lett.* **2006,** *8* (16), 3437-3440.
31. Gao, M. C.; Ruiz, J. M.; Jimenez, E.; Lo, A.; Laconsay, C. J.; Fettinger, J. C.; Tantillo, D. J.; Shaw, J. T., Catalytic generation of ortho-quinone dimethides via donor/donor rhodium carbenes. *Chem. Sci.* **2023**, 6.

32. Dishman, S. N.; Laconsay, C. J.; Fettinger, J. C.; Tantillo, D. J.; Shaw, J. T., Divergent stereochemical outcomes in the insertion of donor/donor carbenes into the C-H bonds of stereogenic centers. *Chem Sci* **2022,** *13* (4), 1030-1036.
33. Werle, C.; Goddard, R.; Philipps, P.; Fares, C.; Furstner, A., Structures of Reactive Donor/Acceptor and Donor/Donor Rhodium Carbenes in the Solid State and Their Implications for Catalysis. *J Am Chem Soc* **2016,** *138* (11), 3797-805.
34. Becke, A. D., Density-Functional Exchange-Energy Approximation With Correct Asymptotic-Behavior. *Phys. Rev. A* **1988,** *38* (6), 3098-3100.
35. Lee, C. T.; Yang, W. T.; Parr, R. G., Development Of The Colle-Salvetti Correlation-Energy Formula Into A Functional Of The Electron-Density. *Phys. Rev. B* **1988,** *37* (2), 785-789.
36. Becke, A. D., Density-Functional Thermochemistry .3. The Role Of Exact Exchange. *J. Chem. Phys.* **1993,** *98* (7), 5648-5652.
37. Grimme, S.; Antony, J.; Ehrlich, S.; Krieg, H., A consistent and accurate ab initio parametrization of density functional dispersion correction (DFT-D) for the 94 elements H-Pu. *J. Chem. Phys.* **2010,** *132* (15), 19.
38. Barone, V.; Cossi, M., Quantum calculation of molecular energies and energy gradients in solution by a conductor solvent model. *J. Phys. Chem. A* **1998,** *102* (11), 1995-2001.
39. Cossi, M.; Rega, N.; Scalmani, G.; Barone, V., Energies, structures, and electronic properties of molecules in solution with the C-PCM solvation model. *J. Comput. Chem.* **2003,** *24* (6), 669-681.
40. Liu, H. X.; Wei, Y. Y.; Cai, C., Hypervalent-iodine(III) oxidation of hydrazones to diazo compounds and one-pot nickel(II)-catalyzed cyclopropanation. *New J. Chem.* **2016,** *40* (1), 674-678.
41. Baum, J. S.; Shook, D. A.; Davies, H. M. L.; Smith, H. D., Diazotransfer Reactions With Para-Acetamidobenzenesulfonyl Azide. *Synth. Commun.* **1987,** *17* (14), 1709-1716.
42. Zhang, J. D.; Bellomo, A.; Creamer, A. D.; Dreher, S. D.; Walsh, P. J., Palladium-Catalyzed C(sp(3))-H Arylation of Diarylmethanes at Room Temperature: Synthesis of Triarylmethanes via Deprotonative-Cross-Coupling Processes. *J. Am. Chem. Soc.* **2012,** *134* (33), 13765-13772.
43. Bordwell, F. G.; Matthews, W. S.; Vanier, N. R., Acidities of Carbon Acids .4. Kinetic Vs Equilibrium Acidities as Measures of Carbanion Stabilities - Relative Effects Of Phenylthio, Diphenylphosphino, And Phenyl Groups. *J. Am. Chem. Soc.* **1975,** *97* (2), 442-443.
44. Zhu, D.; Chen, L. F.; Fan, H. L.; Yao, Q. L.; Zhu, S. F., Recent Progress On Donor And Donor-Donor Carbenes. *Chem. Soc. Rev.* **2020,** *49* (3), 908-950.
45. Thoraval, J. Y.; Nagai, W.; Ko, Y.; Carrie, R., Cycloadditions of Disubstituted Diazo-Compounds To p-Chloro (Bistrimethylsilyl) Methylene Phosphine. *Tetrahedron* **1990,** *46* (11), 3859-3868.
46. Nicolle, S. M.; Moody, C. J., Potassium N-iodo p-toluenesulfonamide (TsNIK, Iodamine-T): a new reagent for the oxidation of hydrazones to diazo compounds. *Chemistry* **2014,** *20* (15), 4420-5.
47. Werner, H.; Schneider, M. E.; Bosch, M.; Wolf, J.; Teuben, J. H.; Meetsma, A.; Troyanov, S. I., Cationic and neutral diphenyldiazomethanerhodium(I) complexes as catalytically active species in the C-C coupling reaction of olefins and diphenyldiazomethane. *Chem.-Eur. J.* **2000,** *6* (16), 3052-3059.
48. Davies, H. M. L.; Grazini, M. V. A.; Aouad, E., Asymmetric intramolecular C-H insertions of aryldiazoacetates. *Org. Lett.* **2001,** *3* (10), 1475-1477.

49. Wei, B.; Sharland, J. C.; Lin, P.; Wilkerson-Hill, S. M.; Fullilove, F. A.; McKinnon, S.; Blackmond, D. G.; Davies, H. M. L., In Situ Kinetic Studies of Rh(II)-Catalyzed Asymmetric Cyclopropanation with Low Catalyst Loadings. *ACS Catalysis* **2019,** *10* (2), 1161-1170.
50. Nicolle, S. M.; Moody, C. J., Potassium N-Iodo p-Toluenesulfonamide (TsNIK, Iodamine-T): A New Reagent for the Oxidation of Hydrazones to Diazo Compounds. *Chem.-Eur. J.* **2014,** *20* (15), 4420-4425.
51. Humphreys, R. W. R.; Arnold, D. R., Substituent effects on the zero-field splitting parameters of diarylmethylene. Evidence for merostabilization in appropriately substituted diphenylmethylenes. *Canadian Journal of Chemistry* **1979,** *57* (19), 2652-2661.
52. Shaffer, M. W.; Leyva, E.; Soundararajan, N.; Chang, E.; Chang, D. H. S.; Capuano, V.; Platz, M. S., Contributions Of Quantum Mechanical Tunneling To The Rate Of Benzylic Hydrogen Atom Abstraction Reactions Of Triplet Diarylcarbenes In Fluid Solution. *The Journal of Physical Chemistry* **1991,** *95* (19), 7273-7277.
53. [3+2] Cycloaddition of cyclopropane with vinyl ether via photoinduced electron transfer. *Tetrahedron Letters* **1989,** *30* (35), 4685 - 4688.
54. Hideo, T.; Osamu, I., Effects of Aryl Substituents on Electron-Transfer-Mediated Photochemical Addition of Alcohol to 1,1,2-Triarylcyclopropanes. *Bulletin of the Chemical Society of Japan* **1988,** *61* (4), 1404-1406.
55. Sheldrick, G., SHELXT - Integrated space-group and crystal-structure determination. *Acta Crystallographica Section A* **2015,** *71* (1), 3-8.
56. Bourhis, L. J.; Dolomanov, O. V.; Gildea, R. J.; Howard, J. A. K.; Puschmann, H., The anatomy of a comprehensive constrained, restrained refinement program for the modern computing environment - Olex2 dissected. *Acta Crystallographica Section A* **2015,** *71* (1), 59-75.
57. Dolomanov, O. V.; Bourhis, L. J.; Gildea, R. J.; Howard, J. A. K.; Puschmann, H., OLEX2: a complete structure solution, refinement and analysis program. *J. Appl. Crystallogr.* **2009,** *42* (2), 339-341.

Chapter 3. C–H Functionalization Chemistry using Diaryl Diazo Compounds and their Application Toward Triarylmethane Compounds

The work discussed in this chapter has been published in the ACS journal Organic Letters.[1]

3.1 Introduction of Intermolecular Reactivity of Diaryl Diazo Compounds

Previous work on diaryl diazo compounds showcased that with electronic and steric manipulations, although previously thought of as donor/donor compounds, these compounds are capable of achieving high selectivity and reactivity in the cyclopropanation of styrene behaving more similarly to a donor/acceptor carbenes.[2] Shortly after the publication of our study discussed in Chapter 1 the Franz and Zhou groups concurrently published studies on the Si–H insertion reaction using the diaryl diazo system shown in Scheme 1.[3, 4] These reports represent the first stereoselective intermolecular Si–H insertion reaction with diaryl diazo compounds to generate chiral silicon products. The Franz group has previously published work on prochiral silanes[5, 6] and this work expands the scope of stereoselective intermolecular Si–H insertion yielding a variety of chiral-at-silicon benzhydryl silanes which allows access to silicon-stereogenic silanols, dehydrocoupling, and C–H silylation products. In addition, this method demonstrates that using a prochiral diazo the selectivity of Si–H insertion can be dramatically improved with up to 98:2 d.r. and 95:5 e.r. Metal catalysts Ru(II), Ir(I), Fe(II), Cu(II), and Rh(II), were screened but only Rh(II) gave the desired Si–H insertion product. Of the rhodium catalysts screened, Rh_2(*S*-TCPTTL)$_4$, a derived catalyst gave the highest levels of enantioselectivity.

The Zhu group highlights in their work that the level of enantioselectivity of Si–H insertion relies heavily on the electronic characteristics of the carbene precursor. They disclosed that when

the Hammett substituent constant is equal to or greater than 0.5 the enantioselectvity of the corresponding product is equal to or greater than 90% ee, meaning that the more different substituents or more donor/acceptor-like characteristics, the greater the selectivity. In addition, the authors developed a new class of D_4-symmetric dirhodium catalysts bearing chiral spiro phosphate ligands, which enabled unprecedented enantioselective transformations with the formation of 19 optically active silanes. These approaches both highlight the potential for diaryl diazo compounds to be synthetically useful and versatile intermediates, and demonstrates the need for further research into their synthetic utility in asymmetric intermolecular insertion reactions.

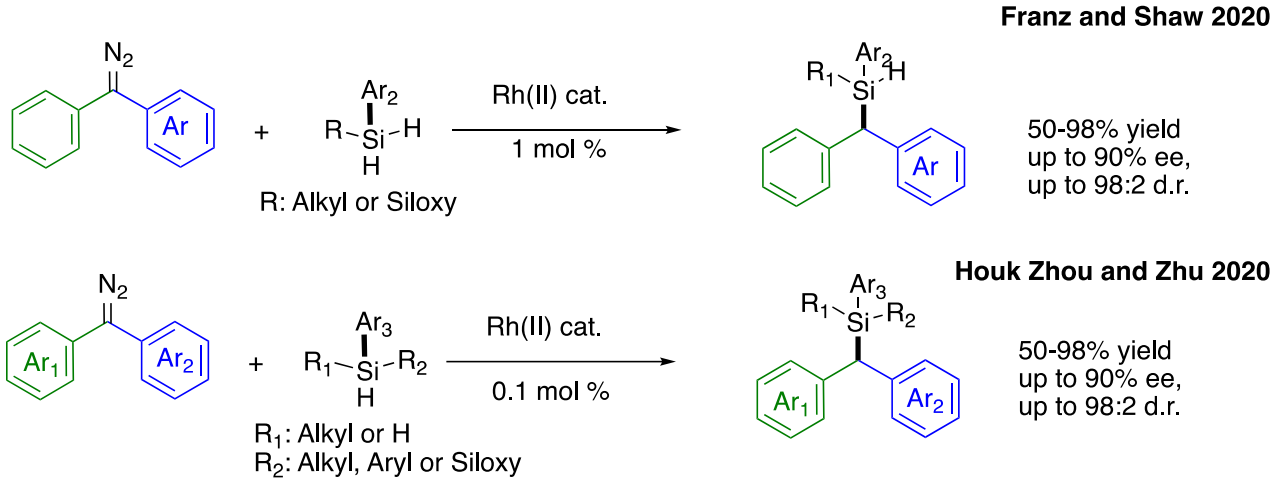

Scheme 1. Stereoselective Si–H insertions with Diaryl Diazo Compounds

3.2 Preliminary Results and Discussion of C–H Insertion

To this end, we sought to explore the potential for diaryl diazo compounds to perform C–H functionalization on varying C–H bonds. The Davies lab in 2001, calculated the relative rates of reactivity for select C–H bonds.[7] In competition studies, the cyclopropanation of styrene and the C–H insertion of the doubly activated cyclohexadiene C–H bond were both 28,000 times more reactive than the C–H insertion of unactivated cyclohexane. C–H bonds that are *alph*a to a heteroatom, such as oxygen or nitrogen, are more activated and react 2,700 or 1,700 times faster

than cyclohexane. Lastly, C–H bonds that are sterically crowded and have no electronic activation are less reactive than cyclohexane.

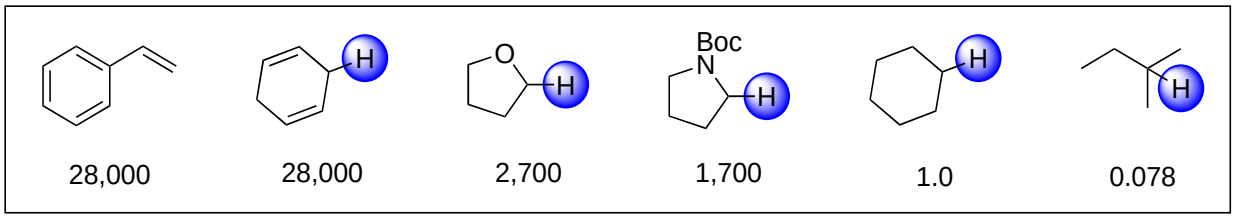

Figure 1. Relative Rates of Reactivity of C–H Functionalization Substrates

Based on this reactivity profile and our previous results showing that diaryl diazo compounds display umpolung reactivity and can easily dimerize, we decided to first screen reactions with more activated substrates such as 1,4-cyclohexadiene and tetrahydrofuran (Scheme 2). The reactions were conducted using the best-performing diaryl diazo compound in our previous studies, *p*-nitro-*p'*-methoxy diaryl diazo. The C–H insertion of tetrahydrofuran and cyclohexadiene was performed at 23 °C using Rh_2(*S*-NTTL)$_4$ as catalyst. In the reaction with tetrahydrofuran, the major outcome was the formation of carbene and azine dimer, which is a known byproduct in the use of diaryl diazo compounds. Although this is not an optimal result, it is not unexpected given the lower reactivity of the desired C–H bond. This reaction was able to deliver the product, **1**, in 5:1 d.r. and a high ee of 90%. With cyclohexadiene the C–H bond is much more activated, leading to a higher-yielding reaction of product **2** (61% yield). We suspected that the enantioselectivity was lower (65% ee) due to the reaction being run at 23 °C whereas previous reports have shown a significant increase in enantioselectivity when the temperature is lowered especially in the case of an activated bond such as cyclohexadiene.[8]

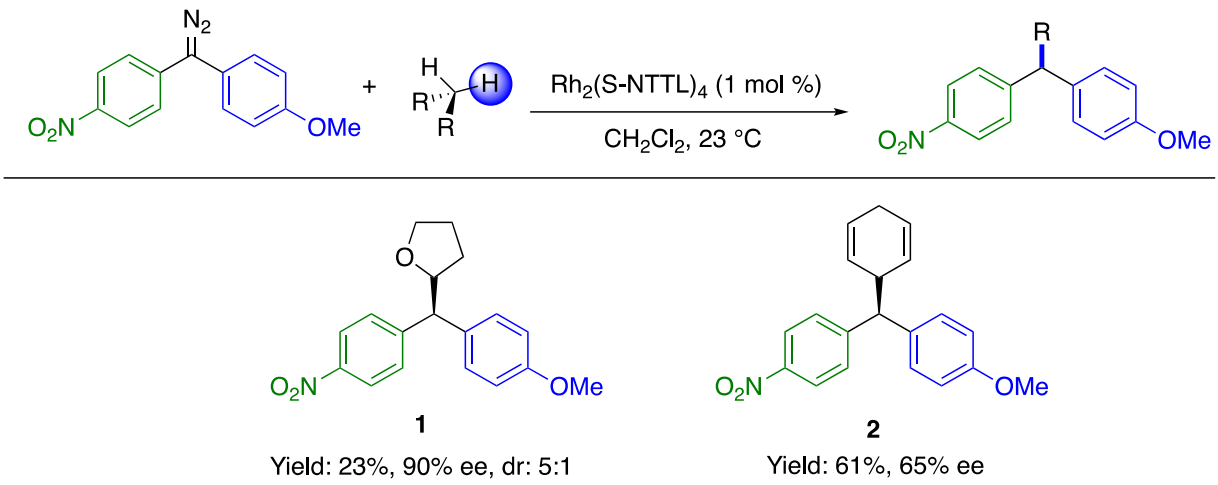

Reaction conditions: 0.20 mmol diazo was inversely added to a solution of 1 mol % Rh_2(*S*-NTTL)$_4$ and 4 equiv of substrate in 1 mL CH_2Cl_2 over 1h. [a] ee (%) was determined using chiral HPLC analysis. [b]. d.r. was determined by crude NMR analysis.

Scheme 2. C–H Functionalization of tetrahydrofuran and Cyclohexadiene

Product **2** was most intriguing due to its potential for further derivatization, namely, oxidation to triarylmethane compounds, as outlined in Scheme 3. We envisioned that the C–H insertion of a diaryl diazo compound **3** into cyclohexadiene **4** could form intermediate **5** in high selectivity and then be oxidized without epimerization to furnish general triarylmethanes, **6**. This would be a viable method to access highly asymmetric triarylmethanes rapidly. Due to their pharmaceutical relevance, methods for their enantioselective synthesis have been extensively explored, but it is still challenging to achieve a broad scope.[9] Our method would extend the range of triarylmethanes that can be readily formed with high enantioselectivity.

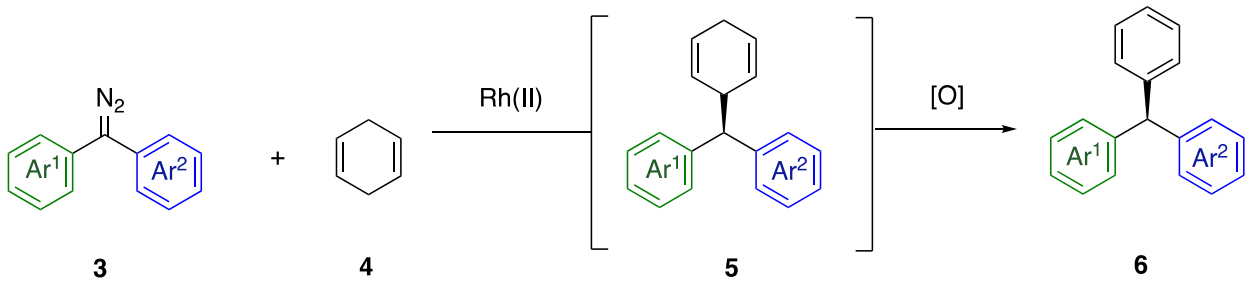

Scheme 3. Overview of C–H Insertion and Oxidation toward Triarylmethane Compounds

3.3 Background of the Synthesis and Utility of Triarylmethane Compounds

Triarylmethanes have been well studied in the literature and have garnered relevance due to their unique applications in dyes, materials, and pharmaceutical applications.[10, 11] Many methods have been developed to synthesize a variety of triarylmethanes, however, many methods make symmetric triarylmethanes or rely on employing stereospecific reactions.[12] One of the first methods developed by Jarvo and Watson concurrently employed stereospecific Ni-catalyzed cross coupling, shown in Scheme 4a, with either chiral dibenzylic ester or ether as electrophiles.[13] More recently, the Hazari group reported a Suzuki–Miyaura cross coupling of diarylbenzoates to generate triarylmethanes by selectively cleaving the C–O bond. While this report expanded the substrate scope allowed, only two enantioenriched products were disclosed.[14] Another route toward asymmetric triarylmethanes is shown in Scheme 4b, which goes through an enantiomerically enriched diaryl boron intermediate.[15] The Zhu group disclosed a Rh-catalyzed B–H insertion into a diarylcarbene to form the diaryl boron intermediate, and in a selected example could be further converted using Pd-catalyzed cross coupling. Rhodium catalysis was also disclosed by the Hayashi group through nucleophilic addition to quinone methides, scheme 4d.[16] This approach is limited due to the need for directing and blocking groups on the methides. Collectively these reports show the synthetic utility of triarylmethane compounds and the pursuit toward a general method for a wide variety of chiral triarylmethane compounds.

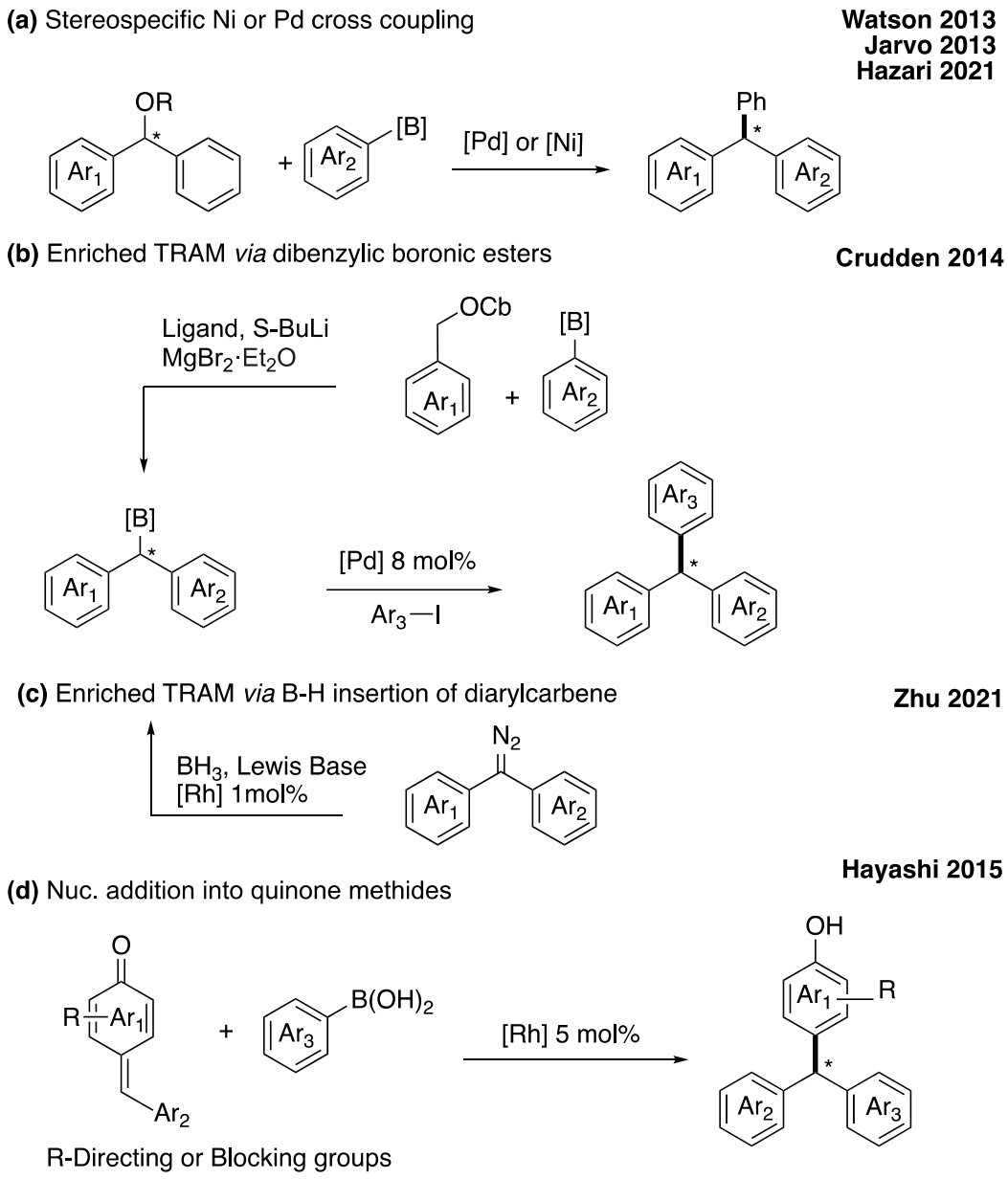

Scheme 4. Previous Asymmetric Synthesis of Triarylmethane Compounds

These methods provide a framework for the development of new asymmetric methods to access a variety of triarylmethanes without the use of directing group functionality prochiral starting materials. To this end, we began exploring the reaction of diayl diazo compounds with cyclohexadienefollowed by oxidation to afford a variety of asymmetric triarylmethane compounds in high enantioselectivity.

3.4 Synthetic Studies and Results

The study began via evaluation of the C−H insertion reaction of 1,4-cyclohexadiene, **4**, with 4-nitro-4′-methoxydiphenyldiazomethane (**7**), to generate product **2**. The initial reaction was run at 23 °C and gave only a moderate level of enantioselectivity (65% ee). Hence, further screens were performed at –20 °C and the enantioselectivity of the transformation was greatly enhanced. Rh_2(*S*-DOSP)$_4$ gave a very low level of asymmetric induction at 3% ee (Entry 1), which was not unexpected because previous literature shows an ester group is needed as the acceptor group to achieve a high degree of selectivity.[17] Rh_2(*S*-2-Cl-5-BrTPCP)$_4$, a triarylcyclopropane carboxylate catalyst (Entry 2) significantly boosted the asymmetric induction of the C−H insertion with 79% ee.

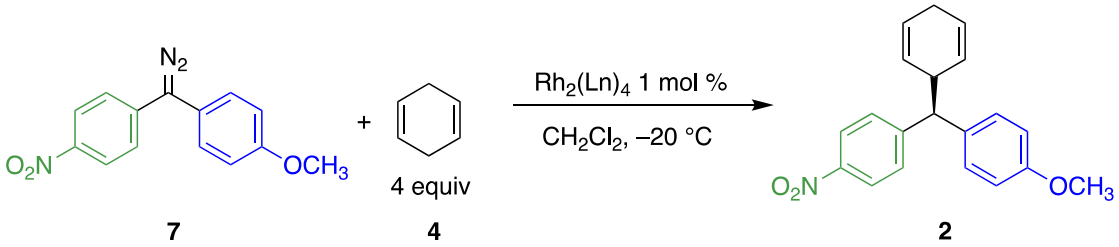

7 **4** **2**

Entry	Catalyst	yield (%)	ee (%)
1	Rh_2(*S*-DOSP)$_4$	64	3
2	Rh_2(*S*-2-Cl 5-BrTPCP)$_4$	60	-79
3	Rh_2(*S*-NTTL)$_4$	73	94
4	Rh_2(*S*-TPPTTL)$_4$	85	79
5	Rh_2(*S*-PTTL)$_4$	80	98
6	Rh_2(*S*-TCPTAD)$_4$	80	97
7	**Rh_2(*S*-PTAD)$_4$**	**77**	**99**

Reaction Conditions: **7** (0.20 mmol) in a solution of CH_2Cl_2 was inversely added to a solution of **4** (4 equiv) and $Rh_2(Ln)_4$ (1 mol %) in CH_2Cl_2 (1 mL) over 1 h at –20 °C under N_2.

Table 1. Screening of Dirhodium Catalyst for C–H insertion into 1,4-Cyclohexadiene

As seen in our cyclopropanation study, the best class of catalysts was the naphthylimido- and phthalimido-derived catalysts.[2, 18, 19] Rh_2(*S*-NTTL)$_4$, a napthylimido catalyst (Entry 3), generated **2** in 94% ee and 73% yield. The phthalimido-derived catalysts gave excellent results. For example, Rh_2(*S*-TCPTAD)$_4$ (Entry 6) gave 97% ee. Most impressively, Rh_2(*S*-PTAD)$_4$ (Entry 7) generated product **2** in 77% yield and 99% ee.

The oxidation of 1,4-cyclohexadienes to benzene compounds is well established.[20] It was expected that the C–H functionalization product 2 could be readily oxidized using established methods for convenient, asymmetric construction of triarylmethanes. Indeed, oxidation using 2,3-dichloro-5,6-dicyano-1,4-benzoquinone (DDQ) generated the desired triarylmethane product 8 with no racemization (Scheme 5).

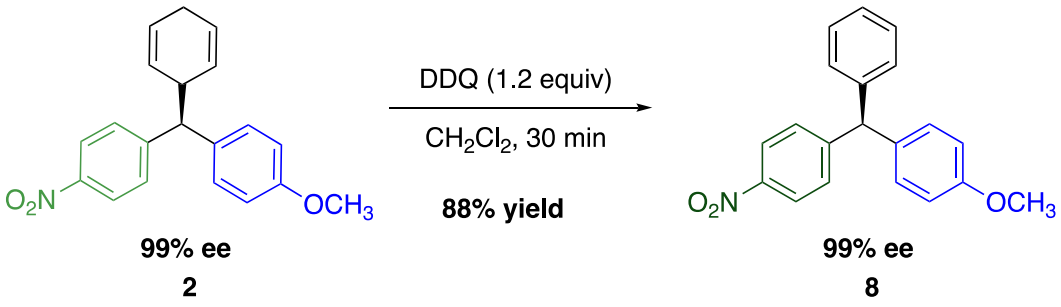

Scheme 5. Stereoretentive Oxdixation to Triarylmethane

With the optimized reaction conditions in hand, the rhodium-catalyzed C–H insertion reaction with cyclohexadiene followed by DDQ oxidation was applied to a series of diaryldiazomethanes lacking *ortho* substituents to generate triarylmethane products **9–13** (Scheme 6). The reaction conditions were compatible with a variety of substituents, but compounds with more donor/acceptor-like character gave the highest degree of asymmetric induction. Substrates containing a strong electron-withdrawing group such as nitro or trifluoromethyl gave the highest levels of asymmetric induction, as seen with **9** and **10**. The reactions with a *p*-CF_3 substituent gave triarylmethane **10** in 80% yield and 85% ee, whereas the

reaction with a *p*-chloro substituent afforded **11** in 61% yield and 79% ee. Electron-rich or electron-deficient heterocyclic substrates can be incorporated into the diazo compound as illustrated in the formation of **12** and **13**, although the enantioselectivity was lower (45 and 77% ee, respectively). Typical reactions were conducted on a 0.3 mmol scale, but the reaction is easily scalable and product **8** was prepared on a 1 mmol scale in 90% yield and 99% ee.

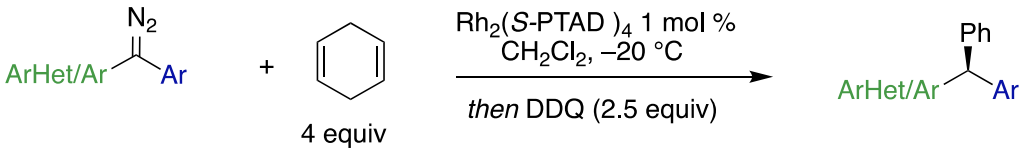

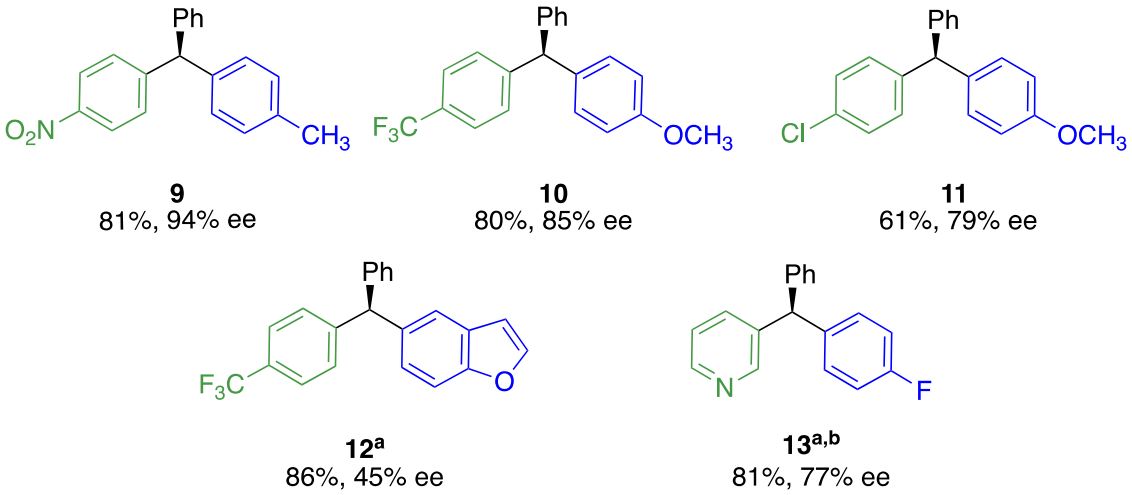

Reaction Conditions: 0.30 mmol of diazo was inversely added to a solution of Rh_2(*S*-PTAD)$_4$ and 4 equiv of the cyclohexadiene substrate in 1 mL of CH_2Cl_2. [a]Triarylmethane compound could not be resolved using chiral HPLC. The ee value is estimated from the analysis of the C–H insertion intermediate. [b] 20 equiv of HFIP added to the mixture.

Scheme 6. Scope of Triarylmethane Derivatives with Cyclohexadiene

Next, the scope of the cyclohexadiene substrate was expanded to 1-methyl-1,4-cyclohexadiene (Scheme 7). Products **14**–**17** did not contain *ortho* chloro substituents and were generated in moderate yield and ee. Diazo compound with only a *p*-nitro group generated **14** in 76% ee. When a *p*-methyl was added to the other ring (**15**) which does not highly increase electron density to the aryl ring, the ee remained unchanged at 76%. When diazo compounds containing

an *o*-Cl substituent were included, the enantioselectivity decreased. Triarylmethane product **17** was generated in excellent yield and a modest 74% ee. However, with the incorporation of a *p*-methoxy on the other aryl ring as seen in **18,** the enanatioselectivity of the reaction was only 20% ee. This result was initially perplexing, as in previous studies more electron-rich character with an ortho substituent increased the overall reaction performance.

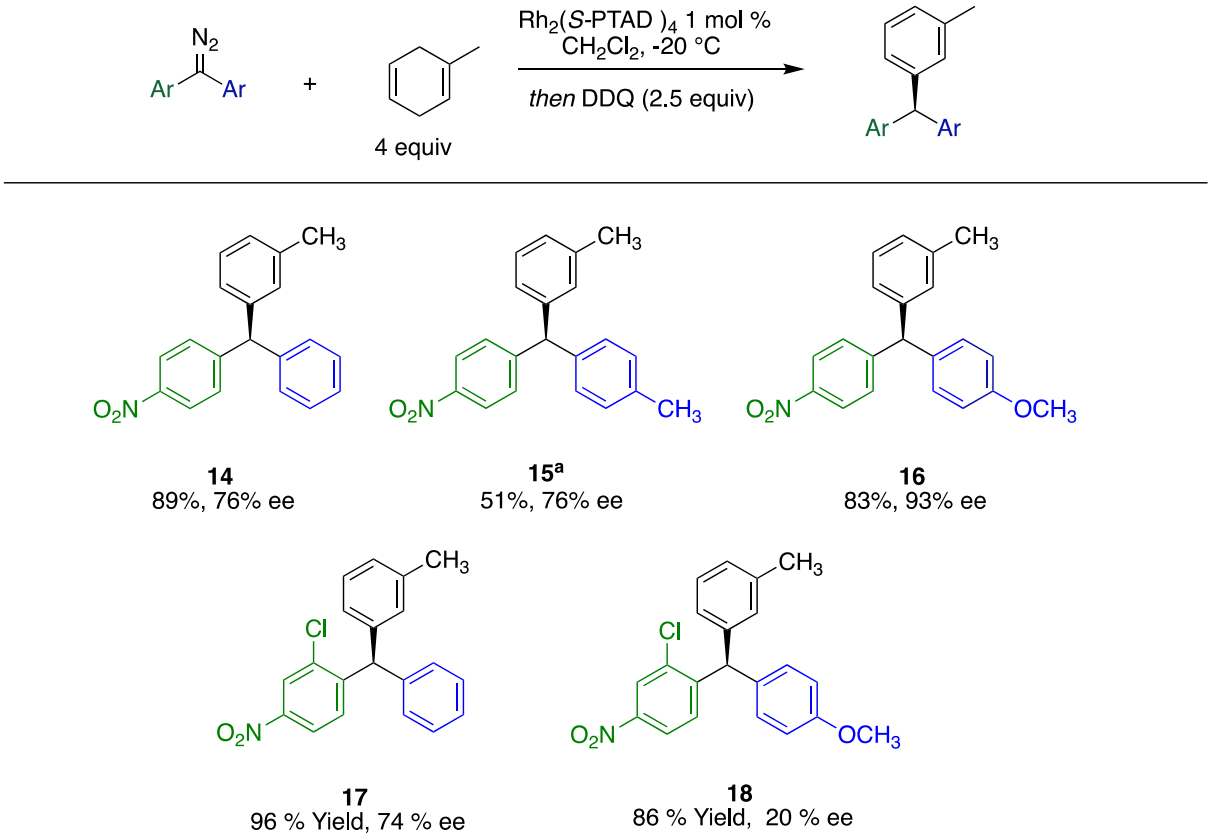

Reaction Conditions: 0.30 mmol of diazo was inversely added to a solution of Rh_2(*S*-PTAD)$_4$ and 4 equiv of the cyclohexadiene substrate in 1 mL of CH_2Cl_2.[a]The ee value is an estimated value due to the imperfect resolution of peaks in the HPLC spectrum.

Scheme 7. C−H Functionalization of 1-Methyl-1,4-cyclohexadiene

Based on the non-symmetric nature of the cyclohexadiene, we investigated if the C–H insertion step was not diastereoselective causing an overall decrease in the ee of the final triarylmethane compound. Diazo compound **19**, was chosen as a good substrate to investigate

because it has both an electron-donating *p*-OMe and an electron-withdrawing *p*-CF_3 group. This substrate was also chosen because the diastereomers were able to be resolved on chiral HPLC for analysis. The C−H functionalization reaction using diaryldiazomethane **19** produces a mixture of diastereomers **20a** and **20b** in a 3:1 ratio. On prolonged standing, the major diastereomer crystallized from the mixture, and the relative and absolute configuration of **20a** could be determined by X-ray crystallography. 2D NMR correlations also confirmed the *anti* relationship of the hydrogen atoms at the site of C–H insertion. The major diastereomer **20a** was produced with a higher level of asymmetric induction (86% ee) compared to the minor diastereomer **20b** (52% ee). The two diastereomers are difficult to separate by chromatography, and thus the combined mixture was oxidized to the corresponding triarylmethane compound **21** in 79% ee. This value agreed with the calculated value assuming that both **20a** and **20b** are generated with the same level of asymmetric induction and that the oxidation of both occurs without epimerization. The absolute configuration of **21** is assigned *R* because it is derived from **20a** of a known absolute configuration. All other absolute configurations of the triarylmethanes are tentatively assigned by analogy.

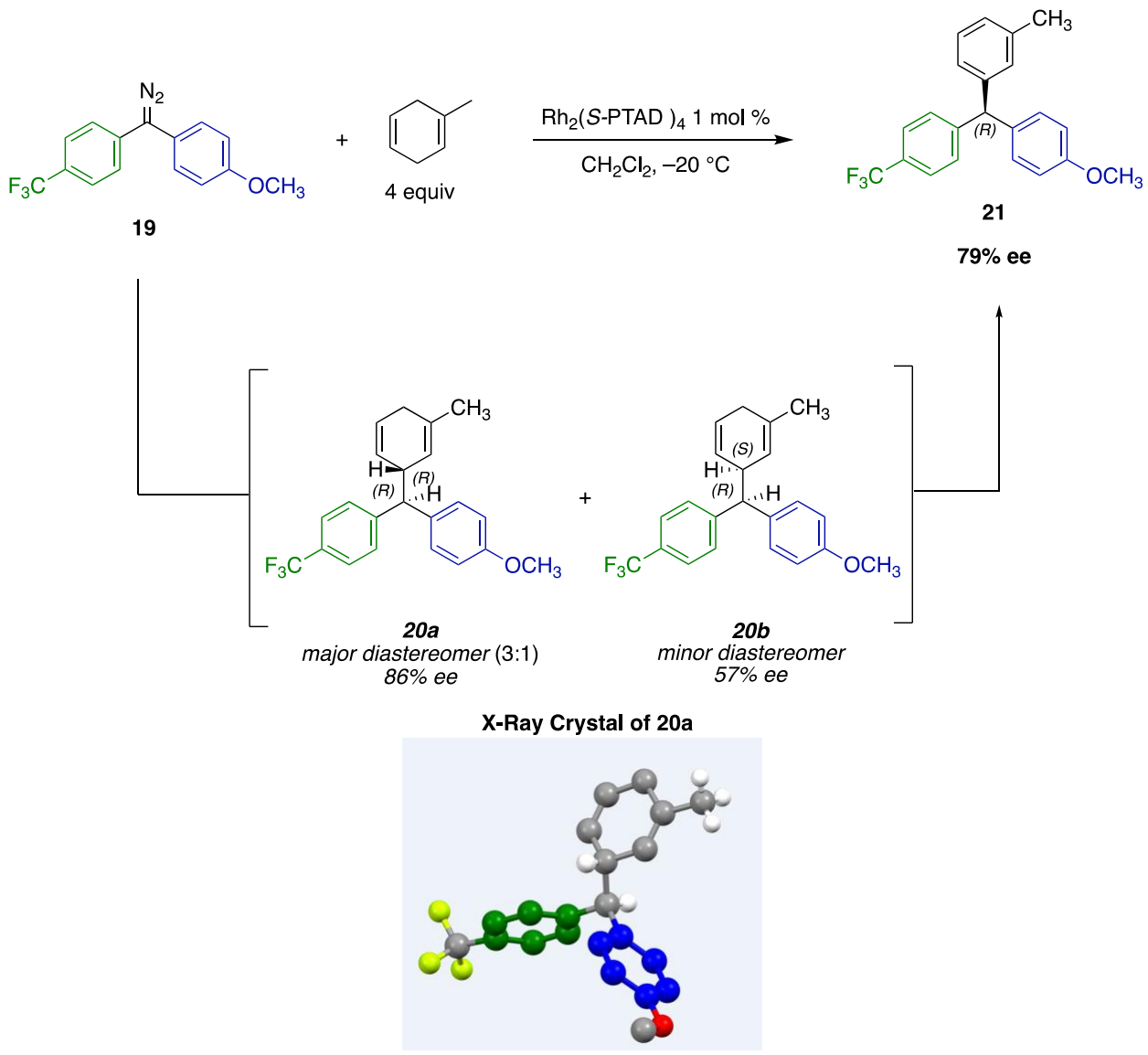

Scheme 8. Analysis of C–H Insertion of 1-Methyl-1,4-cyclohexadiene

The ultimate goal of this work is to generate highly asymmetric triarylmethanes in a straightforward manner. The one-pot oxidation is desirable, but would not be practical if the scope is limited to symmetric cyclohexadienes. We envisioned that with a different catalyst system, the diastereoselectivity of the intermediate could be enhanced which would lead to an overall highly asymmetric triarylmethane product. As such, a catalyst screening was employed on 1-methyl-1,4-cyclohexadiene using diaryl diazo compound **22**, bearing an *o*-chloro subsituent (Table 2). A

reference to the previously optimized catalyst with cyclohexadiene is shown in Entry 1.Rh_2(*S*-TCPTAD)$_4$, a chlorinated version of Rh_2(*S*-PTAD)$_4$ (Entry 2), gave only 6% ee. Rh_2(*S*-NTTL)$_4$ (Entry 3) also gave a very low level of asymmetric induction. Switching to Rh_2(*S*-PTTL)$_4$ gave a slight increase up to 51% ee (Entry 4), but was still lower than Rh_2(*S*-PTAD)$_4$. Finally, Rh_2(*S*-TPPTTL)$_4$ (Entry 5) significantly enhanced chiral induction to 88% ee. Rh_2(*S*-TPPTTL)$_4$ has been previously shown to give superior asymmetric induction in cyclopropanation reactions with *ortho*-substituted aryldiazoacetates, and similar characteristics are observed here in the reaction with *ortho*-substituted diaryldiazomethanes.[21]

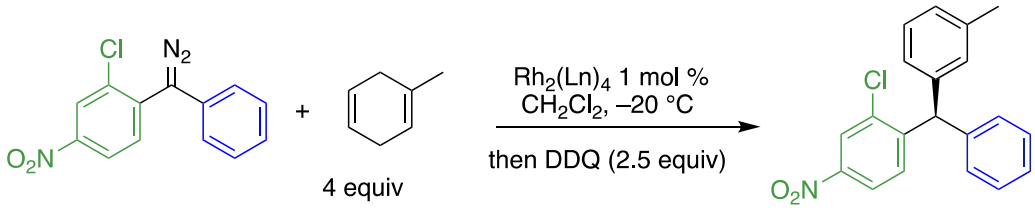

22 **17**

Entry	Catalyst	yield (%)	ee (%)
1	Rh_2(*S*-PTAD)$_4$	94	74
2	Rh_2(*S*-TCPTAD)$_4$	87	6
3	Rh_2(*S*-NTTL)$_4$	78	-6
4	Rh_2(*S*-PTTL)$_4$	92	51
5	**Rh_2(*S*-TPPTTL)$_4$**	**94**	**88**

Reaction Conditions: **22** (0.20 mmol) in a solution of CH_2Cl_2 was inversely added to a solution of cyclohexadiene substrate (4 equiv) and $Rh_2(Ln)_4$ (1 mol %) in CH_2Cl_2 (1 mL) over 1 h at –20 °C under N_2.

Table 2. Screening of Dirhodium Catalyst forC–H Insertion into 1-Methyl-1,4-cyclohexadiene

In Scheme 9, diazo compounds containing an *ortho*-substituent were employed for the C–H functionalization of a variety of substituted cyclohexadiene compounds, which could then be

oxidized to the desired triarylmethane. Triarylmethane **23**, derived from a diaryldiazomethane bearing an electron-donating methoxy group was produced in 82% yield and 87% ee. Triarylmethane **24**, which lacks the methoxy group, was generated with a slightly lower enantioselectivity (83% ee). Triarylmethanes **25** and **18**, derived from diaryldiazomethanes having an electron-donating group, an electron-withdrawing group, and an *o*-chloro group, were generated with the highest levels of enantioselectivity (98 and 91% ee, respectively). These trends are consistent with our understanding that diaryl diazo compounds that closely model that of a donor/acceptor diazo compound through electronic and steric properties give higher levels of asymmetric induction. This is an impressive result, particularly because triarylmethane **18**, catalyzed by Rh_2(*S*-PTAD)$_4$ gave a mere 20% ee. The reaction could be also extended to various substituted cyclohexadienes, resulting in the formation of **27**−**29**. Triarylmethane **27**, with a bulkier 1-naphthyl group gave moderate yield and asymmetric induction of 43% and 65% ee. Electron-rich 1-methoxy-1,4-cyclohexadiene gave rise to product **28** with 75% ee. The formation of **29** is an interesting transformation because the C−H functionalization was site selective, favoring by a 12:1 ratio insertion α to the methyl group versus insertion α to the isopropyl group in γ-terpene.

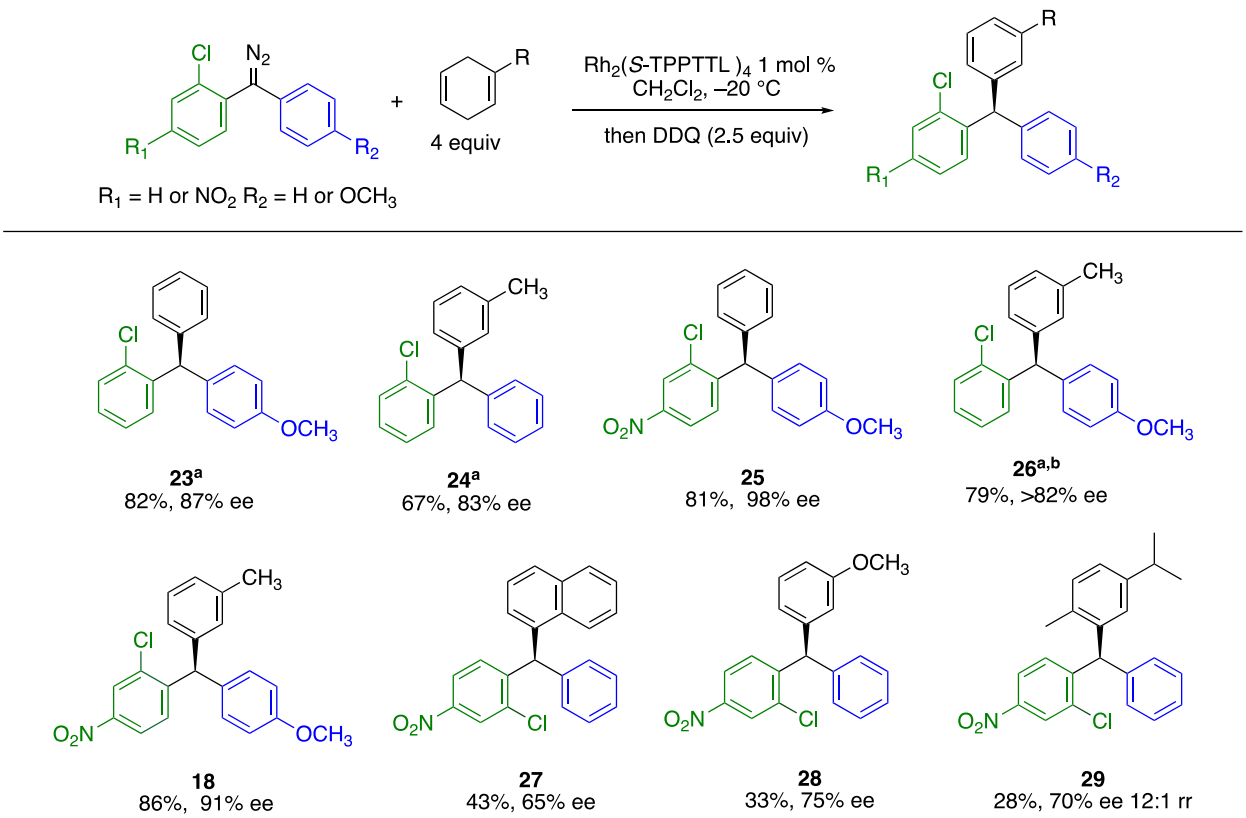

Reaction conditions: 0.30 mmol of diazo was inversely added to a solution of Rh_2(S-PTAD)$_4$ and 4 equiv of the cyclohexadiene substrate in 1 mL of CH_2Cl_2. [a]The triarylmethane compound could not be resolved using chiral HPLC. The ee value is estimated from the analysis of the C–H insertion intermediate. The ee value was assigned on the basis of the analysis shown in Scheme 8 and the crystal structure of 20a. [b]The ee value is an estimated value due to the imperfect resolution of peaks in the HPLC spectrum.

Scheme 9. C−H Functionalization of Cyclohexadienes with *o*-Cl Diaryldiazomethanes

3.4 Conclusions

This work demonstrates diaryl diazo compounds previously thought to be donor/donor carbenes can be highly selective and useful toward intermolecular C–H functionalization. We have developed a facile enantioselective synthesis of triarylmethanes using rhodium-catalyzed C–H insertion of cyclohexadienes with diaryldiazomethanes. This system is compatible with a variety of aryl substituents including examples of two heterocycles. This method can tolerate electron-rich and electron-poor aryl substituents and with Rh_2(*S*-TPPTTL)$_4$ *o*-chloro substituents. Furthermore, this work provides evidence that diaryl diazo compounds should be further explored and have broad synthetic potential in C–H functionalization reactions. The work discussed in this chapter

has been published in the ACS journal *Organic Letters*. Figures and analysis from this paper have been incorporated into this chapter.[1]

3.5 Experimental Procedures and Data

3.5.1 General Considerations

Caution: Diazo compounds are high energy compounds and should be handled with caution. Although we have had no difficulties with working with these compounds, it is advisable to carry out reactions on small scale behind a blast shield. Hydrazine hydrate is highly toxic compound and needs to be handled using the established safety protocols. In addition, Diaryl Diazo compounds are known to be unstable and must be handled with caution and stored in a -20 °C freezer to avoid decomposition over time.

Substrates and reagents were purchased from the following suppliers and used without further purification: Sigma-Aldrich, Alfa-Aesar, Oakwood Chemical America, and Fisher Scientific.

All solvents were purified and dried by a Glass Contour Solvent System, and stored over 4 Å molecular sieves 24 hours before use. All reactions were carried out in flamed-dried glassware unless otherwise stated. ^{1}H NMR spectra were recorded at 600 MHz on Bruker-600 spectrometer, Varian INOVA 500 MHz or Varian 400 MHz. ^{13}C NMR spectra were recorded at 150 MHz on Bruker-600. NMR spectra samples were prepared using deuterated chloroform($CDCl_3$) with residual solvent serving as internal standard 7.26 ppm for ^{1}H and 77.16 ppm for ^{13}C; or with Deuterated chloroform 0.03% TMS with residual TMS serving at internal standard (0.00 ppm). Abbreviations for signal multiplicity are as follows: s= singlet, d= doublet, t= triplet, m= multiplet, dd= doublet of doublets dt= doublet of triplets. The coupling constants J, are reported in Hertz and integration is provided, along with assignments, as indicated. Structural assignments were made with additional information from gCOSY, gHSQC, and gHMBC experiments. Optical rotations were measured on Autopol IV automatic polarimeter by Rudolph Research Analytical. Crystallographic data was obtaining through the Emory X-ray Crystallography center using the ShelXT 2018 solution program. IR spectra were collected on a Nicolet Is10 FT-IR spectrometer.

Mass spectra were taken on a Thermo Finnigan LTQ-FTMS spectrometer with APCI ESI or NSI. Thin layer chromatographic analysis (TLC) was performed on aluminum-sheet silica gel plates, and visualized with UV light. Racemic standards for enantiomeric determination were generated with reactions with $Rh_2(OAc)_4$ or from Rh_2((*R*) and (*S*)-DOSP)$_4$ which was generated by dissolving equimolar mixture of R and S catalyst in a minimal amount of benzene and lyophilizing. High performance liquid chromatography analysis (HPLC) was performed on Agilent 1100 Technologies HPLC instrument.

3.5.2 Preparation of diaryl/heteroaryl diazo compound

Procedure adopted from literature.[2] A 50 mL dried round bottom flask was charged with desired hydrazone (1.1 mmol) and THF (4 mL) followed by tsNIK(1.2 mmol) prepared by following the literature procedure.[4] Potassium hydroxide in 1 M solution (1 mL) was slowly added to the reaction flask. The reaction was monitored by TLC, with disappearance of all starting hydrazone derivatives by 1.5 h. The reaction was poured into 5 mL potassium hydroxide in 1 M solution and extracted with diethyl ether (2 x 30 mL). The organic layers were combined then washed with brine (2 x 30 mL) and dried over $MgSO_4$. After removal of the solvent, the desired diazo compound was obtained. If necessary, the diazo compound was purified using an alumina column with a solvent gradient of 0 to 5% diethyl ether in hexanes. The product was stored under argon at –20 °C.

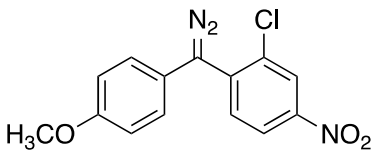

2-chloro-1-(diazo(4-methoxyphenyl)methyl)-4-nitrobenzene (SI 1)

The diazo compound was prepared from (*E*)-((2-chloro-4-nitrophenyl)(4-methoxyphenyl)-methylene)hydrazone and was obtained as a red solid on a 2.6 mmol scale in 71% yield (550 mg).

^{1}H NMR (600 MHz, $CDCl_3$) δ 8.33 (d, *J* = 2.4 Hz, 1H), 8.06 (dd, *J* = 8.8, 2.4 Hz, 1H), 7.39 (d, *J* = 8.8 Hz, 1H), 7.14 (d, *J* = 8.8 Hz, 2H), 6.99 (d, *J* = 8.8 Hz, 2H), 3.86 (s, 3H).

^{13}C NMR (151 MHz, $CDCl_3$) δ 158.7, 145.8, 136.7, 131.8, 128.6, 127.0, 126.5, 122.0, 120.3, 115.2, 55.5 (The resonance resulting from the diazo carbon was not observed).

IR: 3090, 3007, 2963, 2044, 1506, 1473, 1302, 1274, 1246, 1184, 1119, 875, 841, 739 $cm^{-1.}$

HRMS (+p APCl) *m/z*: calcd for $C_{14}H_{10}ClN_3O_3$ [M+H-N_2] 276.0427; found 276.0426.

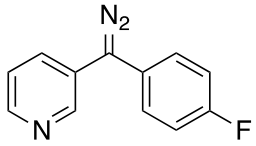

3-(diazo(4-fluorophenyl)methyl)pyridine (SI 2)

The diazo compound was prepared from (*Z*)-3-((4-fluorophenyl)(hydrazineylidene)methyl)-pyridine and was obtained as a red/purple solid at a 3.70 mmol scale in 69% yield (548 mg).

^{1}H NMR (400 MHz, $CDCl_3$) δ 8.49 (dd, *J* = 4.9, 1.7 Hz, 2H), 7.45 – 7.36 (m, 2H), 7.25 – 7.16 (m, 2H), 7.02 (dd, *J* = 6.3, 1.7 Hz, 2H).

C NMR: Compound was not stable enough in $CDCl_3$ to obtain ^{13}C.

^{19}F NMR (376 MHz, $CDCl_3$) δ -113.3.

IR: 3036, 2042, 1585, 1507, 1493, 1446, 1220, 1159, 988, 942 cm^{-1}

HRMS ($^{+}$APCl) *m/z*: calcd for $C_{12}H_9ONF$ [M+OH-N_2] 202.0663; found 202.0666.

3.5.3 General procedures

a.) C-H insertion reaction of C-H Insertions:

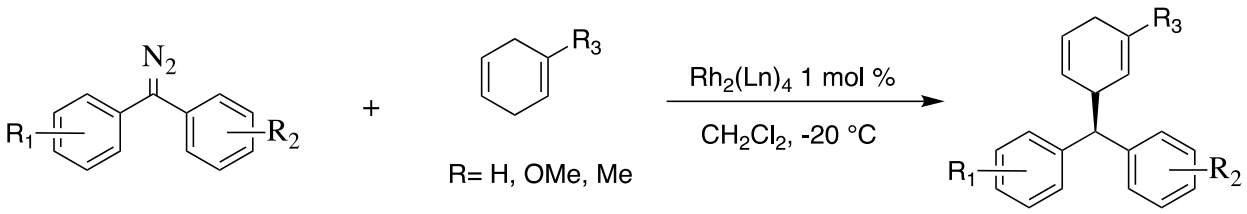

To a flame-dried 12 mL dram vial with a stir bar the desired dirhodium catalyst (1 mol %) was added, and the reaction vial was purged with nitrogen three times and then the catalyst was dissolved in CH_2Cl_2 (1.0 mL). The vial was placed in a salt/ice bath to reach –20 °C and was charged with substituted cyclohexadiene (4 equiv). The corresponding diazo compound (0.30 mmol) was weighed in a 20 mL vial and dissolved in dry degassed DCM (5.0 mL) under N_2. The diazo compound solution was then added to the reaction vial dropwise over 1 h at (–20 °C) *via* a syringe pump. The reaction was stopped after 14 h. The product was purified *via* flash column chromatography with a gradient of 0 to 15 % diethyl ether in hexanes.

b.) one-pot C-H insertion followed by oxidation to TRAM:

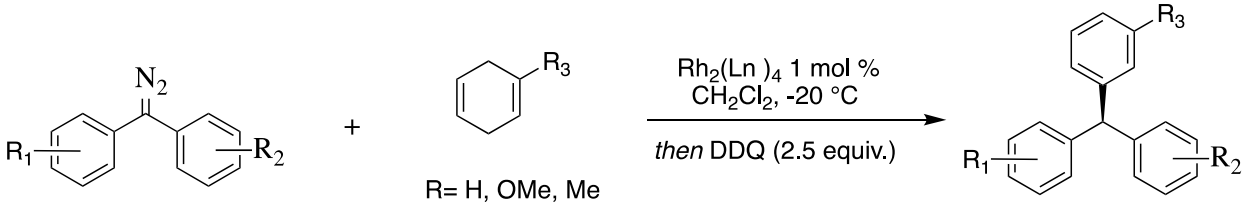

To a flame-dried 16 mL dram vial the desired dirhodium catalyst (1 mol %) was added, and the reaction vial was purged with nitrogen three times and dissolved in CH_2Cl_2 (1.0 mL). The vial was placed in a salt/ice bath to reach –20 °C and was charged with substituted cyclohexadiene (4 equiv) The corresponding diazo compound (0.30 mmol) was weighed in a 20 mL vial and dissolved in

dry degassed DCM (5.0 mL) under N_2. The diazo compound in DCM solution was then added to the reaction vial dropwise over 1 h at (–20 °C) *via* a syringe pump. In some cases, a small aliquot was kept for HPLC analysis of C-H insertion intermediate. After 14 h, 2,3-dichloro-5,6-dicyano-1,4-benzoquinone (*DDQ*) (2.5 equiv) was added into the mixture and allowed to stir for 2 h. The reaction was stopped, and filtered through a celite plug to remove excess DDQ. The mixture was purified *via* flash column chromatography with a gradient of 0 to 10% diethyl ether in hexanes to afford the desired triarylmethane compounds, as white solids (racemic compounds) or an oil (enantioenriched material).

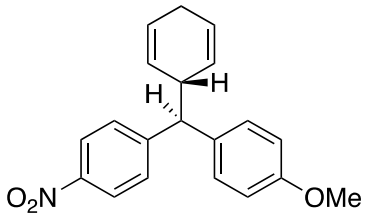

(*R*)-1-(cyclohexa-2,5-dien-1-yl(4-methoxyphenyl)methyl)-4-nitrobenzene (2)

Compound 2 was obtained according to general procedure a from the C–H functionalization reaction between 1,4-cyclohexadiene (0.1 mL, 0.2 mmol, 4 equiv) and 1-(diazo(4-methoxyphenyl)methyl)-4-nitrobenzene (54 mg, 0.2 mmol, 1.0 equiv), catalyzed by Rh_2(*S*-PTAD)$_4$ (3.12 mg, 0.002 mmol, 1.0 mol %). The product was purified by flash column chromatography on silica gel (gradient elution: 0 – 2% diethyl ether in pentane) to afford a white solid in 77% yield (49 mg).

^{1}H NMR (400 MHz, $CDCl_3$) δ 8.14 (d, *J* = 8.7 Hz, 3H), 7.45 (d, *J* = 8.8 Hz, 3H), 7.19 (d, *J* = 8.7 Hz, 3H), 6.85 (d, *J* = 8.7 Hz, 3H), 5.73 (dtd, *J* = 10.4, 3.3, 1.7 Hz, 4H), 5.53 (ddd, *J* = 10.8, 3.6, 2.0 Hz, 1H), 5.45 (ddd, *J* = 10.8, 3.7, 2.1 Hz, 1H), 3.91 (d, *J* = 9.7 Hz, 2H), 3.61 (ddt, *J* = 6.4, 3.3, 1.6 Hz, 1H), 2.63 (dtd, *J* = 8.3, 3.4, 1.7 Hz, 4H).

^{13}C NMR (101 MHz, $CDCl_3$) δ 158.4, 151.3, 146.4, 133.5, 129.2, 127.0, 126.7, 126.1, 125.8,

123.7, 114.2, 57.4, 55.3, 39.1, 26.5.

IR(in $CDCl_3$): 3030, 2836, 1605,1509,1345, 1253,1179, 1034, 806, 695 cm^{-1}.

HRMS ($^-$APCI) *m/z*: calcd for $C_{20}H_{18}NO_3^-$ $[M]^-$ 320.1292; found 320.1285.

$[\alpha]^{22}_D$ –27.5 (*c* 1.18, $CHCl_3$)

HPLC conditions: HPLC (ADH column, 1.0 mL/min 1% *i*-PrOH in *n*-hexane 30 min, UV 230 nm) retention times of

17.1 (minor) and 18.0min (major) 94 % ee with Rh_2(*S*-NTTL)$_4$.

17.1 (minor) and 18.0 min (major) 99 % ee with Rh_2(*S*-PTAD)$_4$.

17.8 (minor) and 18.8 min (major) 79 % ee with Rh_2(*S*-TPPTTL)$_4$.

17.6 (minor) and 18.5 min (major) 97 % ee with Rh_2(*S*-TCPTAD)$_4$.

17.4 (minor) and 18.3 min (major) -79 % ee with Rh_2(*S*-2-Cl-5-Br-TPCP)$_4$.

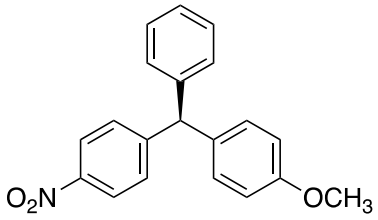

(*R*)-1-methoxy-4-((4-nitrophenyl)(phenyl)methyl)benzene (8)

Compound 8 was obtained through the oxidation of Compound **2.** Compound **2** was placed in a 16 mL dram vial charged with a stir bar. 1.2 equiv of 2,3-Dichloro-5,6-dicyano-1,4-benzoquinone (*DDQ*) was added and components were dissolved in 4 mL DCM. The reaction was complete after 2 h and the desired triarylmethane was observed by NMR. The crude mixture was filtered through a short pipette column to remove DDQ and desired product was obtained as an oil in 88 % yield (57 mg).

Compound **8** was also scaled up to a 1 mmol. To a flame-dried 50 mL round bottom flask charged with a stirbar Rh_2(*S*-PTAD)$_4$ (15.6 mg, 0.010 mmol, 1.0 mol %) and was added, and the reaction vial was purged with nitrogen three times and dissolved in CH_2Cl_2 (4.0 mL). The flask was placed in a salt/ice bath to reach –20 °C and was charged with 1,4-cyclohexadiene (0.38 mL,4 mmol, 4 equiv). In a 20mL vial 1-(diazo(4-methoxyphenyl)methyl)-4-nitrobenzene (269 mg, 1.00 mmol, 1 equiv) was dissolved in CH_2Cl_2 (16mL). The diazo solution was split into two 12mL syringes and was then added to the reaction vial dropwise over 1 h at (–20 °C) *via* a syringe pump. After 14 h, 2,3-dichloro-5,6-dicyano-1,4-benzoquinon*e (DDQ*) (568 mg, 2.5 equiv) was added into the mixture and allowed to stir for 2 h. The reaction was stopped, and filtered through a celite plug to remove excess DDQ. The mixture was purified *via* flash column chromatography with a gradient of 0 to 10% diethyl ether in hexanes to afford the desired triarylmethane compound in 90% yield (319 mg).

^{1}H NMR (400 MHz, $CDCl_3$) δ 8.13 (d, *J* = 8.7 Hz, 2H), 7.38 – 7.17 (m, 5H), 7.08 (d, *J* = 7.3 Hz, 2H), 7.00 (d, *J* = 8.4 Hz, 2H), 6.85 (d, *J* = 8.7 Hz, 2H), 5.58 (s, 1H), 3.79 (s, 3H).

^{13}C NMR (101 MHz, $CDCl_3$) δ 158.5, 152.0, 146.5, 142.7, 134.4, 130.3, 130.2, 129.3, 128.7, 126.9, 123.6, 114.1, 55.9, 55.3.

IR: 3027, 2932, 2835, 1605, 1510, 1345, 1302, 1248, 1178, 1032, 826 cm^{-1}.

HRMS ($^+$APCI) *m/z*: calcd for $C_{20}H_{17}NO_3$ $[M+H]^+$ 320.1286; found 320.1278.

$[\alpha]^{22}_D$ –2.7 (*c* 1.00, $CHCl_3$)

HPLC conditions: (OD column,1.0 mL/min 1% *i*-PrOH in *n*-hexane 30 min, UV 230 nm) retention times of 17.3 (major) and 22.5 min (minor) 99% ee with Rh_2(*S*-PTAD)$_4$.

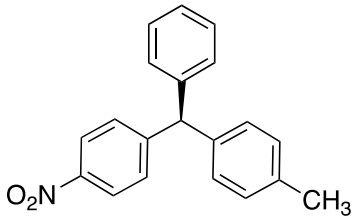

(*S*)-1-methyl-4-((4-nitrophenyl)(phenyl)methyl)benzene (9)

Compound 9 was obtained according to general procedure b from the C–H functionalization reaction between 1,4-cyclohexadiene (0.12 mL, 1.2 mmol, 4 equiv) and 1-(diazo(4-nitrophenyl)methyl)-4-methylbenzene (76 mg, 0.3 mmol, 1.0 equiv), catalyzed by Rh_2(*S*-PTAD)$_4$ (4.68 mg, 0.003 mmol, 1.0 mol %). The product was purified by flash column chromatography on silica gel (gradient elution: 0 – 5% diethyl ether in hexanes) to afford colorless oil in 81 % yield (73 mg).

^{1}H NMR (600 MHz, $CDCl_3$) δ 8.16 (d, *J* = 8.7 Hz, 2H), 7.37 – 7.25 (m, 5H), 7.16 (d, *J* = 7.9 Hz, 2H), 7.12 (d, *J* = 7.3 Hz, 2H), 7.01 (d, *J* = 8.1 Hz, 2H), 5.63 (s, 1H), 2.37 (s, 3H).

^{13}C NMR (151 MHz, $CDCl_3$) δ 151.9, 146.5, 142.5, 139.4, 136.6, 130.2, 129.4, 129.3, 129.2, 128.7, 126.9, 123.6, 56.3, 21.0.

IR: 3025, 2921, 1593, 1514, 1450, 1343, 1110, 820, 778 cm^{-1}.

HRMS ($^+$APCI) *m/z*: calcd for $C_{20}H_{17}NO_2[M+H]^+$ 304.1338; found 304.1334.

$[\alpha]^{23}_D$ 5.5 (*c* 1.28, $CHCl_3$)

HPLC conditions: HPLC (ODH column, 1.0 mL/min 0.5% *i*-PrOH in *n*-hexane 45 min, UV 230 nm) retention times of 12.3 (major) and 16.0 min (minor) 94% ee with Rh_2(S-PTAD)$_4$.

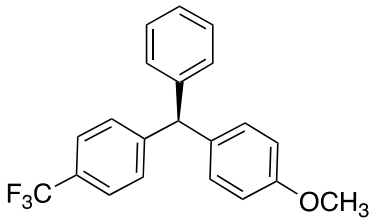

(*R*)-1-methoxy-4-(phenyl(4-(trifluoromethyl)phenyl)methyl)benzene (10)

Compound 10 was obtained according to general procedure b from the C–H functionalization reaction between 1,4-cyclohexadiene (0.12 mL, 1.2 mmol, 4 equiv) and 1-(diazo(4-(trifluoromethyl)phenyl)methyl)-4-methoxybenzene (88 mg, 0.3 mmol, 1.0 equiv), catalyzed by Rh_2(*S*-PTAD)$_4$ (4.68 mg, 0.003 mmol, 1.0 mol %). The product was purified by flash column chromatography on silica gel (gradient elution: 0 – 5% diethyl ether in hexanes) to afford **6** as a colorless oil in 80 % yield (83 mg).

^{1}H NMR: (600 MHz, $CDCl_3$) δ 7.55 (d, *J* = 8.2 Hz, 1H), 7.32 (t, *J* = 7.3 Hz, 1H), 7.30 – 7.23 (m, 1H), 7.11 (d, *J* = 7.3 Hz, 1H), 7.03 (d, *J* = 8.7 Hz, 1H), 6.86 (d, *J* = 8.7 Hz, 1H). This matches literature reported values.[4]

$[\alpha]^{22}_D$ –3.4 (*c* 1.22, $CHCl_3$)

HPLC (ODH column, hexane, 1.0 mL/min 0.5% *i*-PrOH in *n*-hexane 25 min, UV 230 nm) retention times of 6.2 (minor) and 7.2 min (major) 85 % ee with Rh_2(S-PTAD)$_4$.

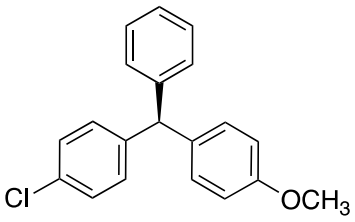

(*S*)-1-chloro-4-((4-methoxyphenyl)(phenyl)methyl)benzene (11)

Compound 11 was obtained according to general procedure b from the C–H functionalization reaction between 1,4-cyclohexadiene (0.12 mL, 1.2 mmol, 4 equiv) and 1-chloro-4-(diazo(4-methoxyphenyl)methyl)benzene (78 mg, 0.3 mmol, 1.0 equiv), catalyzed by Rh_2(*S*-PTAD)$_4$ (4.68 mg, 0.003 mmol, 1.0 mol %). The product was purified by flash column chromatography on silica gel (gradient elution: 0 – 5% diethyl ether in hexanes) to afford colorless oil in 61 % yield (57 mg).

^{1}H NMR (600 MHz, $CDCl_3$) δ 7.31 – 7.22 (m, 5H), 7.11 (d, *J* = 7.6 Hz, 2H), 7.06 (d, *J* = 8.3 Hz, 2H), 7.02 (d, *J* = 8.6 Hz, 2H), 6.86 (d, *J* = 8.6 Hz, 2H), 5.49 (s, 1H), 3.81 (s, 3H).

^{13}C NMR (151 MHz, $CDCl_3$) δ 158.2, 143.7, 142.8, 135.6, 132.1, 130.7, 130.5, 130.3, 129.3, 128.4, 126.5, 113.8, 55.4, 55.3.

IR: 3026, 2930, 2834, 1509, 1488, 1248, 1177, 1034, 819, 700 cm^{-1}.

HRMS ($^+$APCI) *m/z*: calcd for $C_{20}H_{17}ClO$ [M^+] 308.0968; found 308.0966.

HPLC conditions: HPLC (ODH column, hexane, 0.8 mL/min 0.2 *i*-PrOH in *n*-hexane 20 min, UV 230 nm) retention times of 14.4 (minor) and 15.6 min (major) 79 % ee with Rh_2(S-PTAD)$_4$.

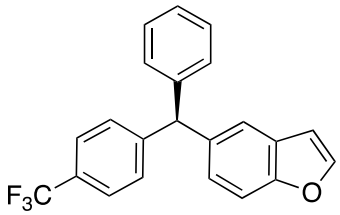

(*R*)-5-(phenyl(4-(trifluoromethyl)phenyl)methyl)benzofuran (12)

Compound 12 was obtained according to general procedure b from the C–H functionalization reaction between 1,4-cyclohexadiene (0.12 mL, 1.2 mmol, 4 equiv) and 5-(diazo(4-(trifluoromethyl)phenyl)methyl)benzofuran (91 mg, 0.3 mmol, 1.0 equiv), catalyzed by Rh_2(*S*-PTAD)$_4$ (4.68 mg, 0.003 mmol, 1.0 mol %). The product was purified by flash column chromatography on silica gel (gradient elution: 0 – 5% diethyl ether in hexanes) to afford a

colorless oil in 86% yield (91 mg).

^{1}H NMR (600 MHz, $CDCl_3$) δ 7.63 (d, *J* = 2.2 Hz, 1H), 7.56 (d, *J* = 7.9 Hz, 2H), 7.45 (d, *J* = 8.5 Hz, 1H), 7.33 (t, *J* = 7.6 Hz, 2H), 7.27-7.24 (m, 5 H), 7.14 (d, *J* = 7.6 Hz, 2H), 7.09 (dd, *J* = 8.5, 1.89 Hz, 1H), 6.71 (d, *J* = 2.2 Hz, 1H), 5.73 (s, 1H).

^{13}C NMR (151 MHz, $CDCl_3$) δ 153.8, 145.5, 143.3, 137.6, 129.8, 129.4, 128.7, 128.5, 127.6, 126.7, 125.9, 125.28, 125.25 (q, *J* = 3.8 Hz), 125.23, 121.7, 111.3, 106.6, 56.5.

^{19}F NMR (565 MHz, $CDCl_3$) δ -62.4.

IR: 2927, 2855, 1708, 1617, 1494, 1466, 1324, 1163, 1121, 1108, 1066, 1030, 1018, 887, 851 cm^{-1}.

$[\alpha]^{22}_{D}$ –6.8 (*c* 1.00, $CHCl_3$)

HRMS ($^{+}$APCI) *m/z*: calcd for $C_{22}H_{15}F_3O$ $[M+H]^+$ 353.1153; found 353.1167.

HPLC conditions: HPLC (ADH column, hexane, 0.5 Ml/min, 1.0% *i*-PrOH in *n*-hexane 30 min, UV 230) retention times of 10.5 min (minor) and 11.3 min (major) 40 % ee with Rh_2(S-PTAD)$_4$.

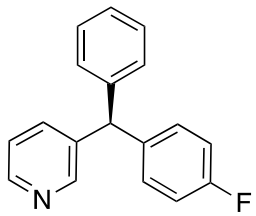

(*S*)-3-((4-fluorophenyl)(phenyl)methyl)pyridine (13)

Compound 13 was obtained according to general procedure b from the C–H functionalization reaction between 1,4-cyclohexadiene (0.12 mL, 1.2 mmol, 4 equiv) and 3-(diazo(4-fluorophenyl)methyl)pyridine (64 mg, 0.3 mmol, 1.0 equiv), catalyzed by Rh_2(*S*-PTAD)$_4$ (4.68 mg, 0.003 mmol, 1.0 mol %). The product was purified by flash column chromatography on silica gel (gradient elution: 0 – 5% diethyl ether in hexanes) to afford colorless oil in 81 % yield (64 mg).

^{1}H NMR (600 MHz, $CDCl_3$) δ 8.55 (d, *J* = 5.2 Hz, 2H), 7.37 – 7.31 (m, 2H), 7.30 – 7.27 (m, 1H), 7.14 – 6.99 (m, 8H), 5.51 (s, 1H).

^{13}C NMR (151 MHz, $CDCl_3$) δ 162.5, 160.9, 152.6, 149.9, 141.9, 137.9 (d, *J* = 3.1 Hz), 130.8 (d, *J* = 7.9 Hz), 129.2, 128.7, 128.6, 127.0, 124.5, 115.5, 115.4, 55.5.

^{19}F NMR (565 MHz, $CDCl_3$) δ -115.8.

IR: 3026, 2922, 2850, 1594, 1506, 1412, 1224, 1159, 1014, 816, 788 cm^{-1}.

HRMS ($^{+}$APCI) *m/z*: calcd for $C_{18}H_{14}FN[M+H]^+$ 264.1188; found 264.1187.

HPLC conditions: via CH insertion product HPLC (ODH column, 1.0 mL/min 2.25 % *i*-PrOH in *n*-hexane 30 min, UV 230 nm) retention times of 16.2 (major) and 25.0 min (minor) 77 % ee with Rh_2(*S*-PTAD)$_4$.

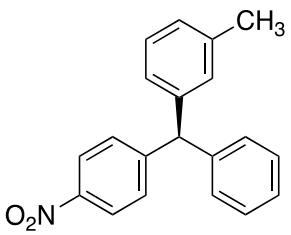

(*S*)-1-Methyl-3-((4-nitrophenyl)(phenyl)methyl)benzene (14)

Compound 14 was obtained according to general procedure b from the C–H functionalization reaction between 1-methyl,1,4-cyclohexadiene (0.1 mL, 1.2 mmol, 4 equiv) 1-(diazo(phenyl)methyl)-4-nitrobenzene (72 mg, 0.3 mmol, 1.0 equiv), catalyzed by Rh_2(*S*-PTAD)$_4$ (4.68 mg, 0.003 mmol, 1.0 mol %). The product was purified by flash column chromatography on silica gel (gradient elution: 0 – 5% diethyl ether in hexanes) to afford **21** as a colorless oil in 89 % yield (81 mg).

^{1}H NMR (600 MHz, $CDCl_3$) δ 8.14 (d, *J* = 8.7 Hz, 2H), 7.35 – 7.24 (m, 5H), 7.21 (t, *J* = 7.6 Hz, 1H), 7.12 – 7.06 (m, 3H), 6.92 (s, 1H), 6.88 (d, *J* = 7.9 Hz, 1H), 5.60 (s, 1H), 2.31 (s, 3H).

^{13}C NMR (151 MHz, $CDCl_3$) δ 151.8, 146.5, 142.4, 142.3, 138.4, 130.3, 130.1, 129.3, 128.7, 128.6, 127.7, 126.9, 126.4, 123.6, 56.7, 21.5.

IR: 3026, 2902, 1602, 1514,1343, 1108, 1076, 1030, 1015, 857, 748 cm^{-1}.

HRMS ($^+$APCI) *m/z*: calcd for $C_{20}H_{17}NO_2$ $[M+H]^+$ 304.1337; found 304.1329.

$[\alpha]^{23}_D$ –5.1 (*c* 1.09 $CHCl_3$)

HPLC conditions: HPLC (OD column, 1.0 mL/min 0.5 % *i*-PrOH in *n*-hexane 30 min, UV 210 nm) retention times of 13.5 (minor) and 16.0 min (major) 76 % ee with Rh_2(S-PTAD)$_4$.

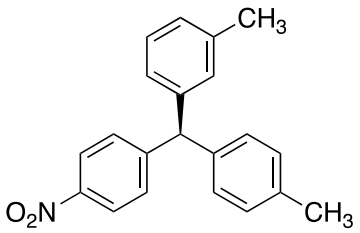

(*S*)-1-Methyl-3-((4-nitrophenyl)(*p*-tolyl)methyl)benzene (15)

Compound 15 was obtained according to general procedure b from the C–H functionalization reaction between 1-methyl,1,4-cyclohexadiene (0.1 mL, 1.2 mmol, 4 equiv) 1-(diazo(4-nitrophenyl)methyl)-4-methylbenzene (76mg, 0.3 mmol, 1.0 equiv), catalyzed by Rh_2(*S*-PTAD)$_4$ (4.68 mg, 0.003 mmol, 1.0 mol %). The product was purified by flash column chromatography on silica gel (gradient elution: 0 – 5% diethyl ether in hexanes) to afford colorless oil in 51% yield (48 mg).

^{1}H NMR (600 MHz, $CDCl_3$) δ 8.16 (d, *J* = 8.7 Hz, 2H), 7.30 (d, *J* = 8.7 Hz, 2H), 7.22 (t, *J* = 7.6 Hz, 1H), 7.15 (d, *J* = 7.8 Hz, 2H), 7.09 (d, *J* = 7.5 Hz, 1H), 7.00 (d, *J* = 8.0 Hz, 2H), 6.94 (s, 1H), 6.89 (d, *J* = 7.6 Hz, 1H), 5.58 (s, 1H), 2.37 (s, 3H), 2.33 (s, 3H).

^{13}C NMR (151 MHz, $CDCl_3$) δ 152.0, 146.5, 142.5, 139.4, 138.3, 136.6, 130.2, 130.0, 129.4, 129.2, 128.5, 127.7, 126.4, 123.5, 56.3, 21.5, 21.0.

IR: 3021, 2920, 1603, 1514, 1489, 1455, 1343, 1109, 841, 763 cm^{-1}.

$[\alpha]^{23}_{D}$ –3.9 (*c* 0.75, $CHCl_3$)

HRMS ($^{+}$APCI) *m/z*: calcd for $C_{21}H_{19}NO_2$ $[M+H]^+$ 318.1494; found 318.1491.

HPLC conditions: (ADH column, 0.5 mL/min 0.5% *i*-PrOH in *n*-hexane 25 min, UV 230 nm) retention times of 16.3 (major) and 17.1 min (minor) 76 % ee with Rh_2(S-PTAD)$_4$.

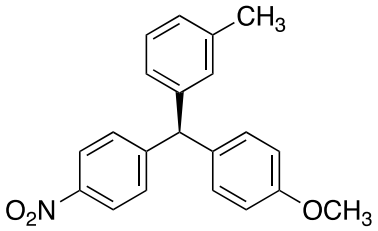

(*R*)-1-((4-methoxyphenyl)(4-nitrophenyl)methyl)-3-methylbenzene(16)

Compound 16 was obtained according to general procedure b from the C–H functionalization reaction between 1-methyl,1,4-cyclohexadiene (0.1 mL, 1.2 mmol, 4 equiv) and 1-(diazo(4-methoxyphenyl)methyl)-4-nitrobenzene (81 mg, 0.3 mmol, 1.0 equiv), catalyzed by Rh_2(*S*-PTAD)$_4$ (4.68 mg, 0.003 mmol, 1.0 mol %). The product was purified by flash column chromatography on silica gel (gradient elution: 0 – 5% diethyl ether in hexanes) to afford colorless oil in 83 % yield (83 mg).

^{1}H NMR (600 MHz, $CDCl_3$) δ 8.16 (d, *J* = 8.8 Hz, 2H), 7.30 (s, 1H), 7.28 (d, *J* = 2.9 Hz, 2H), 7.22 (t, *J* = 7.6 Hz, 1H), 7.09 (d, *J* = 7.6 Hz, 1H), 7.02 (d, *J* = 8.6 Hz, 2H), 6.92 (s, 1H), 6.87 (d, *J* = 8.6 Hz, 2H), 5.56 (s, 1H), 3.82 (s, 3H), 2.32 (s, 3H).

^{13}C NMR (151 MHz, $CDCl_3$) δ 158.4, 152.2, 146.5, 142.6, 138.3, 134.5, 130.3, 130.2, 130.0, 128.5, 127.6, 126.3, 123.5, 114.0, 55.8, 55.3, 21.5.

IR: 2930, 1605, 1489, 1346,1302,1249, 1179, 1110, 849 cm^{-1}.

HRMS ($^{+}$APCI) *m/z*: calcd for $C_{21}H_{19}NO_3$$[M+H]^+$ 334.1443; found 334.1439.

$[\alpha]^{22}_{D}$ –6.6 (*c* 1.00, $CHCl_3$)

HPLC conditions: HPLC (ODH column, 0.8 mL/min 2.25 *i*-PrOH in *n*-hexane 30 min, UV 230 nm) retention times of:

12.4 (major) and 14.1 min (minor) 93 % ee with Rh_2(S-PTAD)$_4$.

12.3 (major) and 14.0 min (minor) 91 % ee with Rh_2(S-NTTL)$_4$.

12.3 (major) and 14.0 min (minor) 77 % ee with Rh_2(S-TPPTTL)$_4$.

12.3 (major) and 14.0 min (minor) 84 % ee with Rh_2(S-PTTL)$_4$.

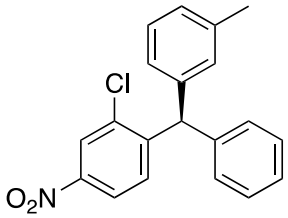

(*R*)-2-chloro-4-nitro-1-(phenyl(*m*-tolyl)methyl)benzene(17)

Compound 17 was obtained according to general procedure b from the C–H functionalization reaction between 1-methyl, 1,4-cyclohexadiene (0.1mL, 1.2 mmol, 4 equiv) and 2-chloro-1-(diazo(phenyl)methyl)-4-nitrobenzene (82 mg, 0.3 mmol, 1.0 equiv), catalyzed by Rh_2(*S*-TPPTTL)$_4$ (4.93 mg, 0.003 mmol, 1.0 mol %). The product was purified by flash column chromatography on silica gel (gradient elution: 0 – 2% diethyl ether in pentane) to afford colorless oil in 94 % yield (96 mg).

^{1}H NMR (600 MHz, $CDCl_3$) δ 8.30 (d, *J* = 2.4 Hz, 1H), 8.05 (dd, *J* = 8.6, 2.36 Hz, 1H), 7.35 (t, *J* = 7.5 Hz, 2H), 7.32 – 7.27 (m, 1H), 7.23 (t, *J* = 7.6 Hz, 1H), 7.17 (d, *J* = 8.6 Hz, 1H), 7.11 (d, *J* = 7.5 Hz, 1H), 7.07 (d, *J* = 7.4 Hz, 2H), 6.90 (s, 1H), 6.85 (d, *J* = 7.6 Hz, 1H), 5.98 (s, 1H), 2.33 (s, 3H).

^{13}C NMR (151 MHz, $CDCl_3$) δ 149.3, 146.8, 141.1, 140.9, 138.4, 135.5, 131.7, 130.1, 129.4, 128.7, 128.6, 127.9, 127.1, 126.5, 124.9, 121.5, 53.6, 21.5.

IR: 3027, 2922, 1600, 1518,1395, 1137, 1045, 892 cm^{-1}.

$[\alpha]^{22}_D$ 16.9 (*c* 0.83, $CHCl_3$)

HRMS ($^+$APCI) *m/z*: calcd for $C_{20}H_{16}ClNO_2$ $[M+H]^+$ 338.0948; found 338.0946.

HPLC conditions: (ODH column, 0.8 mL/min 0.3 % *i*-PrOH in *n*-hexane 30 min, UV 230 nm) retention times of:

17.1 min (minor) and 23.3 min (major) 74 % ee with Rh_2(*S*-PTAD)$_4$.

17.2 (minor) and 22.9 min (major) 6 % ee with Rh_2(*S*-TCPTAD)$_4$.

17.3 (major) and 22.5 min (minor) -6 % ee with Rh_2(*S*-NTTL)$_4$.

17.8 (minor) and 22.6 min (major) 51 % ee with Rh_2(*S*-PTTL)$_4$.

18.2 (minor) and 22.7 min (major) 88 % ee with Rh_2(*S*-TPPTTL)$_4$.

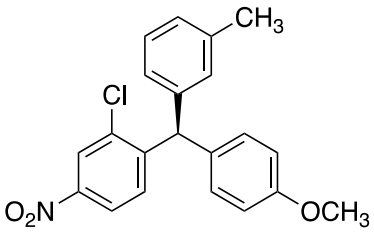

(*R*)-2-chloro-1-((4-methoxyphenyl)(*m*-tolyl)methyl)-4-nitrobenzene (18)

Compound 18 was obtained according to general procedure b from the C–H functionalization reaction between 1-methyl, 1,4-cyclohexadiene (0.1mL, 1.2 mmol, 4 equiv) 2-chloro-1-(diazo(4-methoxyphenyl)methyl)-4-nitrobenzene (92 mg, 0.3 mmol, 1.0 equiv), catalyzed by Rh_2(*S*-TPPTTL)$_4$ (4.93 mg, 0.003 mmol, 1.0 mol %). The product was purified by flash column chromatography on silica gel (gradient elution: 0 – 2% diethyl ether in pentane) to afford colorless oil in 86% yield (95 mg).

^{1}H NMR (600 MHz, $CDCl_3$) δ 8.29 (d, *J* = 2.3 Hz, 1H), 8.05 (dd, *J* = 8.7, 2.35 Hz, 1H), 7.22 (t, *J* = 7.61 Hz, 1H), 7.17 (d, *J* = 8.6 Hz, 1H), 7.10 (d, *J* = 7.5 Hz, 1H), 6.98 (d, *J* = 8.5 Hz, 2H), 6.88 (d, *J* = 8.8 Hz, 2H), 6.84 (d, *J* = 7.7 Hz, 1H), 5.92 (s, 1H), 3.82 (s, 3H), 2.33 (s, 3H).

^{13}C NMR (151 MHz, $CDCl_3$) δ 158.6, 149.7, 146.8, 141.3, 138.4, 135.4, 133.1, 131.6, 130.4, 130.1, 128.5, 127.8, 126.4, 124.9, 121.5, 114.1, 55.3, 52.8, 21.5.

IR: 2929,2836, 1607, 1510, 1462, 1348, 1248, 1178, 1034, 892 cm^{-1}.

HRMS ($^{+}$APCI) *m/z*: calcd for $C_{21}H_{18}ClNO_3[M+H]^+$ 368.1053 found 368.1048.

$[\alpha]^{23}_D$ –4.1 (*c* 1.00, $CHCl_3$)

HPLC conditions: HPLC (ODH column, 1.0mL/min 1.0% *i*-PrOH in *n*-hexane 15 min, UV 230 nm) retention times of 9.5 (minor) and 11.0 min (major) 91% ee with Rh_2(*S*-TPPTTL)$_4$.

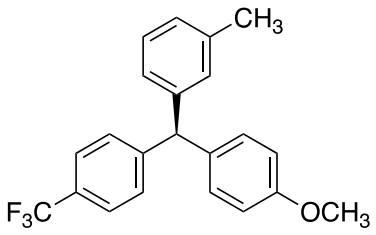

(*R*)-1-((4-methoxyphenyl)(4-(trifluoromethyl)phenyl)methyl)-3-methylbenzene (21)

Compound 21 was obtained according to general procedure b from the C–H functionalization reaction between 1-methyl,1,4-cyclohexadiene (0.1mL, 1.2 mmol, 4 equiv) and 1-(diazo(4-(trifluoromethyl)phenyl)methyl)-4-methoxybenzene (88 mg, mg, 0.3 mmol, 1.0 equiv), catalyzed by Rh_2(*S*-PTAD)$_4$ (4.68 mg, 0.003 mmol, 1.0 mol %). The product was purified by flash column chromatography on silica gel (gradient elution: 0 – 5% diethyl ether in hexanes) to afford colorless oil in 85 % yield (91 mg).

^{1}H NMR (600 MHz, $CDCl_3$) δ 7.52 (d, *J* = 8.0 Hz, 2H), 7.22 (d, *J* = 8.0 Hz, 2H), 7.18 (t, *J* = 7.5 Hz, 1H), 7.04 (d, *J* = 7.5 Hz, 1H), 7.00 (d, *J* = 8.7 Hz, 2H), 6.91 (s, 1H), 6.86 (d, *J* = 7.5 Hz, 1H), 6.84 (d, *J* = 8.7 Hz, 2H), 5.50 (s, 1H), 3.79 (s, 3H), 2.29 (s, 3H).

^{13}C NMR (151 MHz, $CDCl_3$) δ 158.3, 148.5, 143.2, 138.1, 135.2, 130.3, 130.0, 129.7, 128.4, 127.4, 126.4, 125.2, 125.24(q, *J* = 3.71 Hz), 125.22, 125.19, 113.9, 55.8, 55.3, 21.5.

^{19}F NMR (565 MHz, $CDCl_3$) δ -62.4.

IR: 2930, 1606, 1510, 1323, 1250, 1067, 1035, 834, 792 cm^{-1}.

HRMS ($^{-}$APCI) *m/z*: calcd for $C_{22}H_{18}F_3O$ [M^-] 355.1315; found 355.1308.

$[\alpha]^{23}_D$ –10.7 (*c* 1.00, $CHCl_3$)

HPLC conditions: HPLC (ODH column, 1.0 mL/min 1% *i*-PrOH in *n*-hexane 25 min, UV 230 nm) retention times of 4.8 (minor) and 5.3 min (major) 79 % ee with Rh_2(S-PTAD)$_4$.

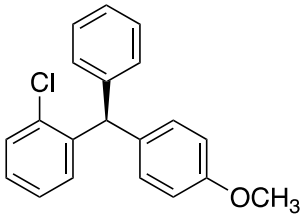

(*S*)-1-chloro-2-((4-methoxyphenyl)(phenyl)methyl)benzene(23)

Compound 23 was obtained according to general procedure b from the C–H functionalization reaction between 1,4-cyclohexadiene (0.12 mL, 1.2 mmol, 4 equiv) and 1-chloro-2-(diazo(4-methoxyphenyl)methyl)benzene (78 mg, 0.3 mmol, 1.0 equiv), catalyzed by Rh_2(*S*-TPPTTL)$_4$ (4.93 mg, 0.003 mmol, 1.0 mol %). The product was purified by flash column chromatography on silica gel (gradient elution: 0 – 2% diethyl ether in pentane) to afford colorless oil in 82 % yield (76 mg).

^{1}H NMR (600 MHz, $CDCl_3$) δ 7.43 – 7.38 (m, 1H), 7.31 (t, *J* = 7.5 Hz, 2H), 7.25 (t, *J* = 7.3 Hz, 1H), 7.21 – 7.18 (m, 2H), 7.10 (d, *J* = 7.4 Hz, 2H), 7.02 (d, *J* = 8.7 Hz, 2H), 6.99 – 6.95 (m, 1H), 6.86 (d, *J* = 8.7 Hz, 2H), 5.94 (s, 1H), 3.82 (s, 3H).

^{13}C NMR (151 MHz, $CDCl_3$) δ 158.2, 143.0, 141.9, 134.7, 134.5, 131.1, 130.5, 129.7, 129.5, 128.3, 127.7, 126.6, 126.4, 113.7, 55.2, 52.6.

IR: 3060, 3025, 2930, 2834, 1608, 1508, 1450, 1246, 1177, 1050, 1035 cm^{-1}.

HRMS ($^{+}$APCI) *m/z*: calcd for $C_{20}H_{17}ClO$ $[M]^+$ 308.0968 found 308.0965.

$[\alpha]^{22}_{D}$ –8.8 (*c* 1.06, $CHCl_3$)

HPLC conditions (Characterized as C-H intermediate): (ADH column, 0.5 mL/min 0.5 % *i*-PrOH in *n*-hexane 30 min, UV 230 nm) retention times of 13.9 (major) and 14.9 min (minor) 87 % ee with Rh_2(*S*-TPPTTL)$_4$, and retention times of 13.9 (major) and 15.8 min (minor) 98 % ee with Rh_2(*S*-PTAD)$_4$.

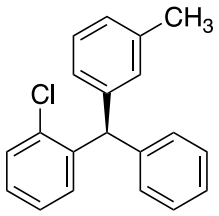

(*R*)-1-chloro-2-(phenyl(*m*-tolyl)methyl)benzene(24)

Compound 24 was obtained according to general procedure b from the C–H functionalization reaction between 1-methyl, 1,4-cyclohexadiene (0.1mL, 1.2 mmol, 4 equiv) and 1-chloro-2-(diazo(phenyl)methyl)benzene (69 mg, 0.3 mmol, 1.0 equiv), catalyzed by Rh_2(*S*-TPPTTL)$_4$ (4.93 mg, 0.003 mmol, 1.0 mol %). The product was purified by flash column chromatography on silica gel (gradient elution: 0 – 2% diethyl ether in pentane) to afford colorless oil in 67 % yield (59 mg).

^{1}H NMR (400 MHz, $CDCl_3$) δ 7.46 – 7.39 (m, 1H), 7.34 (t, *J* = 7.5 Hz, 2H), 7.30 – 7.18 (m, 4H), 7.15 – 7.06 (m, 3H), 7.03 – 6.98 (m, 1H), 6.96 (s, 1H), 6.90 (d, *J* = 7.9 Hz, 1H), 5.98 (s, 1H), 2.34 (s, 3H).

^{13}C NMR (151 MHz, $CDCl_3$) δ 142.7, 142.5, 141.7, 138.0, 134.6, 131.2, 130.4, 129.7, 129.6, 128.4, 128.2, 127.7, 127.3, 126.64, 126.59, 126.5, 53.4, 21.5.

HRMS ($^{+}$APCI) *m/z*: calcd for $C_{20}H_{17}Cl[M]^{+}$ 292.1019 found 292.1013.

IR: 3059, 3024, 2919, 1600, 1589, 1493, 1467, 1125, 1050, 1039 cm^{-1}.

$[\alpha]^{23}_{D}$ 2.1 (*c* 1.55, $CHCl_3$)

HPLC conditions as C-H Insertion product: HPLC (ODH column, 0.8 mL/min .1 % *i*-PrOH in *n*-hexane 45 min, UV 230 nm) retention times of 9.5 (major) and 15.2 min (minor) 83% ee with Rh_2(*S*-TPPTTL)$_4$.

The major enantiomer was assigned to the major peak based on the assumption that this compound will follow the pattern shown in Scheme 5. The major enantiomer is assigned based on the crystal structure obtained from compound **20a,** however which peak corresponds to the minor enantiomer is unclear. Based on the oxidation of both diasteromers to the subsequent TRAM compound, we obtain a calculated ee of 83% based on the 90:10 ratio and an estimated ee value of 83% was assigned.

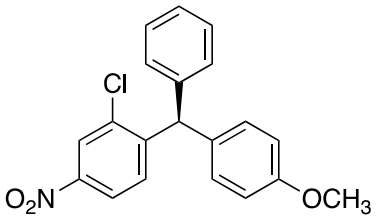

(*S*)-2-chloro-1-((4-methoxyphenyl)(phenyl)methyl)-4-nitrobenzene(25)

Compound 25 was obtained according to general procedure b from the C–H functionalization reaction between 1,4-cyclohexadiene (0.12mL, 1.2 mmol, 4 equiv) 2-chloro-1-(diazo(4-methoxyphenyl)methyl)-4-nitrobenzene (92 mg, 0.3 mmol, 1.0 equiv), catalyzed by Rh_2(*S*-TPPTTL)$_4$ (4.93 mg, 0.003 mmol, 1.0 mol %). The product was purified by flash column chromatography on silica gel (gradient elution: 0 – 2% diethyl ether in pentane) to afford a colorless oil in 81 % yield (90 mg).

^{1}H NMR (600 MHz, $CDCl_3$) δ 8.29 (d, *J* = 2.4 Hz, 1H), 8.05 (dd, *J* = 8.6, 2.4 Hz, 1H), 7.35 (t, *J* = 7.4 Hz, 2H), 7.29 (t, *J* = 7.5 Hz, 1H), 7.17 (d, *J* = 8.6 Hz, 1H), 7.08 (d, *J* = 7.3 Hz, 2H), 6.99 (d, *J* = 8.7 Hz, 2H), 6.89 (d, *J* = 8.7 Hz, 2H), 5.96 (s, 1H), 3.83 (s, 3H).

^{13}C NMR (151 MHz, $CDCl_3$) δ 158.6, 149.6, 146.8, 141.4, 135.4, 133.0, 131.6, 130.4, 129.3, 128.7, 127.1, 124.9, 121.5, 114.1, 55.3, 52.9.

IR: 3027, 2931, 2835, 1608, 1509, 1346, 1247, 1177, 1360, 1031, 824,736 cm^{-1}.

HRMS ($^+$APCI) *m/z*: calcd for $C_{20}H_{16}ClNO_3[M+H]^+$ 354.0897 found 354.0889.

$[\alpha]^{23}_D$ –9.4 (*c* 1.00, $CHCl_3$)

HPLC conditions: HPLC (ODH column, 0.25 mL/min 2.0 % *i*-PrOH in *n*-hexane 60 min, UV 230 nm) retention times of 35.0 (minor) and 41.9 min (major) 98 % ee with Rh_2(*S*-TPPTTL)$_4$.

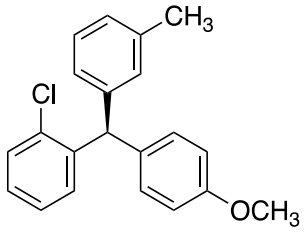

(*R*)-1-chloro-2-((4-methoxyphenyl)(*m*-tolyl)methyl)benzene(26)

Compound 26 was obtained according to general procedure b from the C–H functionalization reaction between 1-methyl, 1,4-cyclohexadiene (0.1mL, 1.2 mmol, 4 equiv) and 1-chloro-2-

(diazo(4-methoxyphenyl)methyl)benzene (78 mg, 0.3 mmol, 1.0 equiv), catalyzed by Rh_2(*S*-TPPTTL)$_4$ (4.93 mg, 0.003 mmol, 1.0 mol %). The product was purified by flash column chromatography on silica gel (gradient elution: 0 – 2% diethyl ether in pentane) to afford a colorless oil in 79 % yield (77 mg).

^{1}H NMR (600 MHz, $CDCl_3$) δ 7.42 – 7.38 (m, 1H), 7.22 – 7.18 (m, 3H), 7.07 (d, *J* = 7.5 Hz, 1H), 7.02 (d, *J* = 8.6 Hz, 2H), 7.00 – 6.97 (m, 1H), 6.94 (s, 1H), 6.90 – 6.85 (m, 3H), 5.91 (s, 1H), 3.82 (s, 3H), 2.33 (s, 3H).

^{13}C NMR (151 MHz, $CDCl_3$) δ 158.1, 142.9, 142.0, 137.9, 134.8, 134.5, 131.1, 130.5, 130.2, 129.7, 128.2, 127.6, 127.2, 126.55, 126.52, 113.7, 55.2, 52.5, 21.5.

IR: 3003, 2927, 2834, 1608, 1509, 1465, 1440,1281, 1247, 1177, 1037 cm^{-1}.

HRMS ($^+$APCI) *m/z*: calcd for $C_{21}H_{19}ClO[M+H]^+$ 323.1203 found 323.1198.

HPLC condition as the C-H Insertion intermediate: HPLC (ADH column, 0.25 mL/min 0.5 % *i*-PrOH in *n*-hexane 45 min, UV 230 nm) retention times of 23.0 min (major) and 29.5 min (minor) >83% ee with Rh_2(*S*-TPPTTL)$_4$.

The major enantiomer was assigned to the major peak based on the assumption that this compound will follow the pattern shown in Scheme 8. The major enantiomer is assigned based on the crystal structure obtained from compound **20a,** however which peak corresponds to the minor enantiomer is unclear.

Ee was calculated to be >82% based on the assumption that the diasteriomeric peak could be any of the minor peaks, and the ee is then assumed subtracting the sum of the 3 minor peaks.

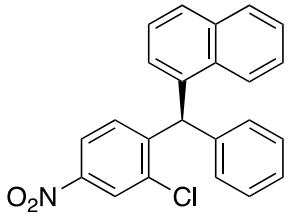

(*R*)-1-((2-chloro-4-nitrophenyl)(phenyl)methyl)naphthalene (27)

Compound 27 was obtained according to general procedure b from the C–H functionalization reaction between 1,8a-dihydronaphthalene (0.16 mL, 1.2 mmol, 4 equiv) and 2-chloro-1-(diazo(phenyl)methyl)-4-nitrobenzene (82 mg, 0.3 mmol, 1.0 equiv), catalyzed by Rh_2(*S*-TPPTTL)$_4$ (4.93 mg, 0.003 mmol, 1.0 mol %). The product was purified by flash column chromatography on silica gel (gradient elution: 0 – 10% diethyl ether in pentane) to afford an oil in 43% yield (49 mg).

^{1}H NMR (600 MHz, $CDCl_3$) δ 8.34 (d, *J* = 2.4 Hz, 1H), 7.99 (dd, *J* = 8.6, 2.4 Hz, 1H), 7.91 (d, *J* =7.9 Hz, 1H), 7.83 (t, *J* = 7.6 Hz, 2H), 7.50 (ddd, *J* = 8.2, 6.8, 1.3 Hz, 1H), 7.46 (ddd, *J* = 7.6, 6.4, 1.3 Hz, 1H), 7.42 – 7.30 (m, 4H), 7.11 (d, *J* = 6.9 Hz, 2H), 7.07 (d, *J* = 8.6 Hz, 1H), 6.89 (d, *J* = 7.2 Hz, 1H), 6.65 (s, 1H).

^{13}C NMR (151 MHz, $CDCl_3$) δ 149.1, 147.0, 140.5, 137.5, 135.3, 134.1, 131.7, 131.5, 129.7, 129.0, 128.9, 128.2, 127.3, 127.2, 126.7, 125.9, 125.2, 125.0, 123.6, 121.6, 50.4.

IR: 3063, 2962, 2358,1738, 1558,1395, 1136, 894 cm^{-1}.

HRMS ($^+$APCI) *m/z*: calcd for $C_{23}H_{16}ClNO_2$ $[M+H]^+$ 374.0948 found 374.0942.

$[\alpha]^{22}_D$ 3.5 (*c* 1.32, $CHCl_3$)

HPLC conditions: HPLC (ADH column, 1.0 mL/min 1% *i*-PrOH in *n*-hexane 30 min, UV 230 nm) retention times of 10.5 (minor) min and 12.9 (major) min with 65 % ee Rh_2(*S*- TPPTTL)$_4$.

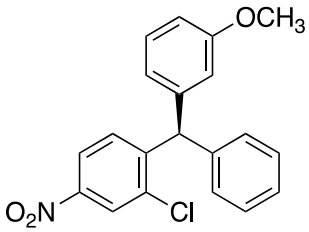

(*R*)-2-chloro-1-((3-methoxyphenyl)(phenyl)methyl)-4-nitrobenzene (28)

Compound 28 was obtained according to general procedure b from the C–H functionalization reaction between 1-methoxycyclohexa-1,4-diene (0.16mL, 1.2 mmol, 4 equiv) and 2-chloro-1-(diazo(phenyl)methyl)-4-nitrobenzene (82mg, 0.3 mmol, 1.0 equiv), catalyzed by Rh_2(*S*-TPPTTL)$_4$ (4.93 mg, 0.003 mmol, 1.0 mol %). The product was purified by flash column chromatography on silica gel (gradient elution: 0 – 5% diethyl ether in pentane) to afford an oil in 33% yield (36 mg).

^{1}H NMR (400 MHz, $CDCl_3$) δ 8.29 (d, *J* = 2.4 Hz, 1H), 8.05 (dd, *J* = 8.6, 2.37 Hz, 1H), 7.37 – 7.26 (m, 4H), 7.17 (d, *J* = 8.6 Hz, 1H), 7.08 (d, *J* = 6.7 Hz, 2H), 6.84 (dd, *J* = 8.3, 2.6 Hz, 1H), 6.65 (d, *J* = 7.6 Hz, 1H), 6.61 (t, *J* = 2.2 Hz, 1H), 5.97 (s, 1H), 3.78 (s, 3H).

^{13}C NMR (101 MHz, $CDCl_3$) δ 159.9, 149.0, 146.9, 142.6, 140.8, 135.5, 131.7, 129.7, 129.4, 128.7, 127.2, 124.9, 121.9, 121.5, 115.8, 111.9, 55.2, 53.6.

IR: 2920, 2851, 1735, 1598, 1519, 1493, 1454, 1376, 1348, 1136, 1075, 1046, 893 cm^{-1}.

HRMS ($^+$APCI) *m/z*: calcd for $C_{20}H_{17}ClNO_3$ $[M+H]^+$ 354.0897 found 354.0892.

$[\alpha]^{23}_D$ 4.2 (*c* 0.99, $CHCl_3$)

HPLC: (ODH column, 1.0 mL/min 1% *i*-PrOH in *n*-hexane 30 min, UV 230 nm) retention times of: 15.3 (major) and 18.9 min (minor) 75 % ee with Rh_2(*S*-TPPTTL)$_4$.

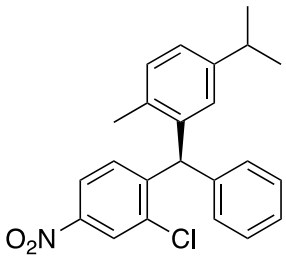

(*R*)-2-chloro-1-((5-isopropyl-2-methylphenyl)(phenyl)methyl)-4-nitrobenzene (29)

Compound 29 was obtained according to general procedure b from the C–H functionalization reaction between 1-isopropyl-4-methylcyclohexa-1,4-diene (0.19 mL, 1.2 mmol, 4 equiv) and 2-

chloro-1-(diazo(phenyl)methyl)-4-nitrobenzene (82mg, 0.3 mmol, 1.0 equiv), catalyzed by Rh_2(*S*-TPPTTL)$_4$ (4.93 mg, 0.003 mmol, 1.0 mol %). The product was purified by flash column chromatography on silica gel (gradient elution: 0 – 5% diethyl ether in pentane) to afford an oil in 28% yield (32 mg).

^{1}H NMR (400 MHz, $CDCl_3$) δ 8.30 (d, *J* = 2.3 Hz, 1H), 8.05 (dd, *J* = 8.6, 2.37 Hz, 1H), 7.37 – 7.24 (m, 3H), 7.16 (d, *J* = 7.8 Hz, 1H), 7.13 – 7.05 (m, 2H), 7.06 – 6.99 (m, 2H), 6.54 (d, *J* = 1.9 Hz, 1H), 6.02 (s, 1H), 2.76 (hept, *J* = 6.9 Hz, 1H), 2.16 (s, 3H), 1.14 (dd, *J* = 6.9, 1.66 Hz, 6H)

^{13}C NMR (101 MHz, $CDCl_3$) δ 149.2, 146.7, 140.4, 139.3, 135.5, 134.0, 131.5, 130.7, 129.59, 129.56, 128.7, 127.2, 127.1, 124.9, 124.8, 121.5, 50.9, 33.6, 24.1, 24.0, 19.2.

IR: 2961, 1526, 1450,1347, 1258, 1020, 861 cm^{-1}.

HRMS ($^+$APCI) *m/z*: calcd for $C_{23}H_{22}ClNO_2$ $[M+H]^+$ 380.1417 found 380.1407.

$[\alpha]^{23}_D$ –4.7 (*c* 1.00, $CHCl_3$)

HPLC (ODH column, 1.5 mL/min 0% *i*-PrOH in *n*-hexane 60 min, UV 230 nm) retention times of 17.34 (minor) and 21.74 min (major) 73 % ee with Rh_2(*S*-TPPTTL)$_4$.

3.6. ^{1}H ^{13}C and ^{19}F NMR Spectra for Characterization of Compounds.

Determination of Diastereomers of compound **20a** and **20b.**

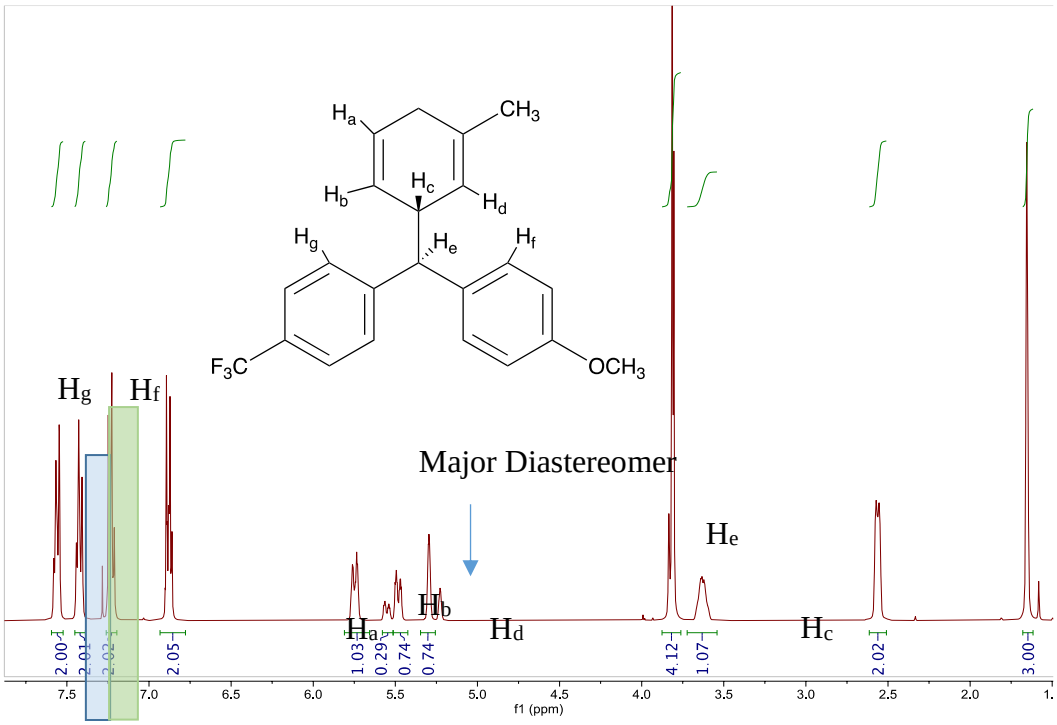

2D NOESY:

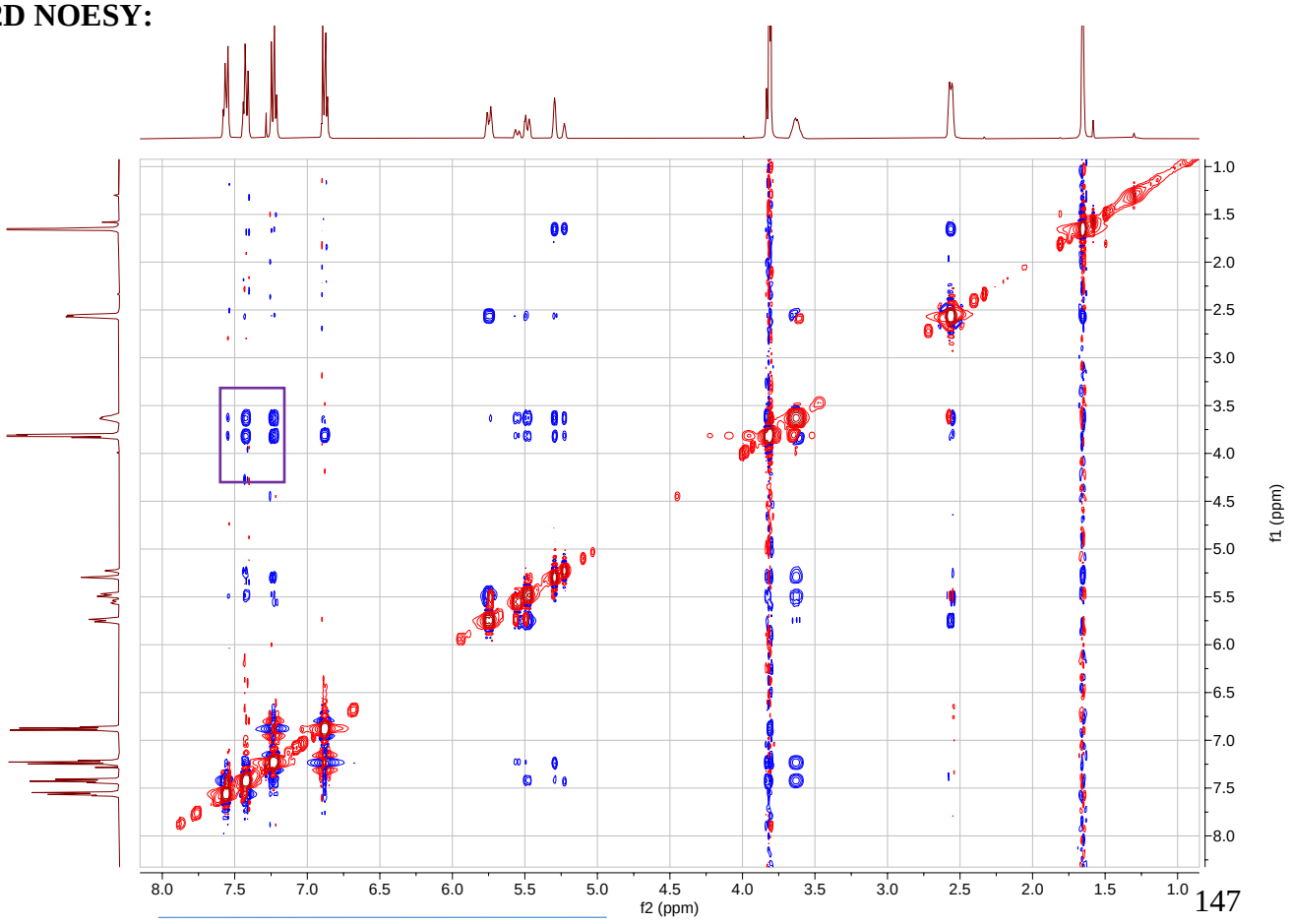

Boxed in purple is major diastereomer, showing correlation on zoomed in region of 2D NOESY.

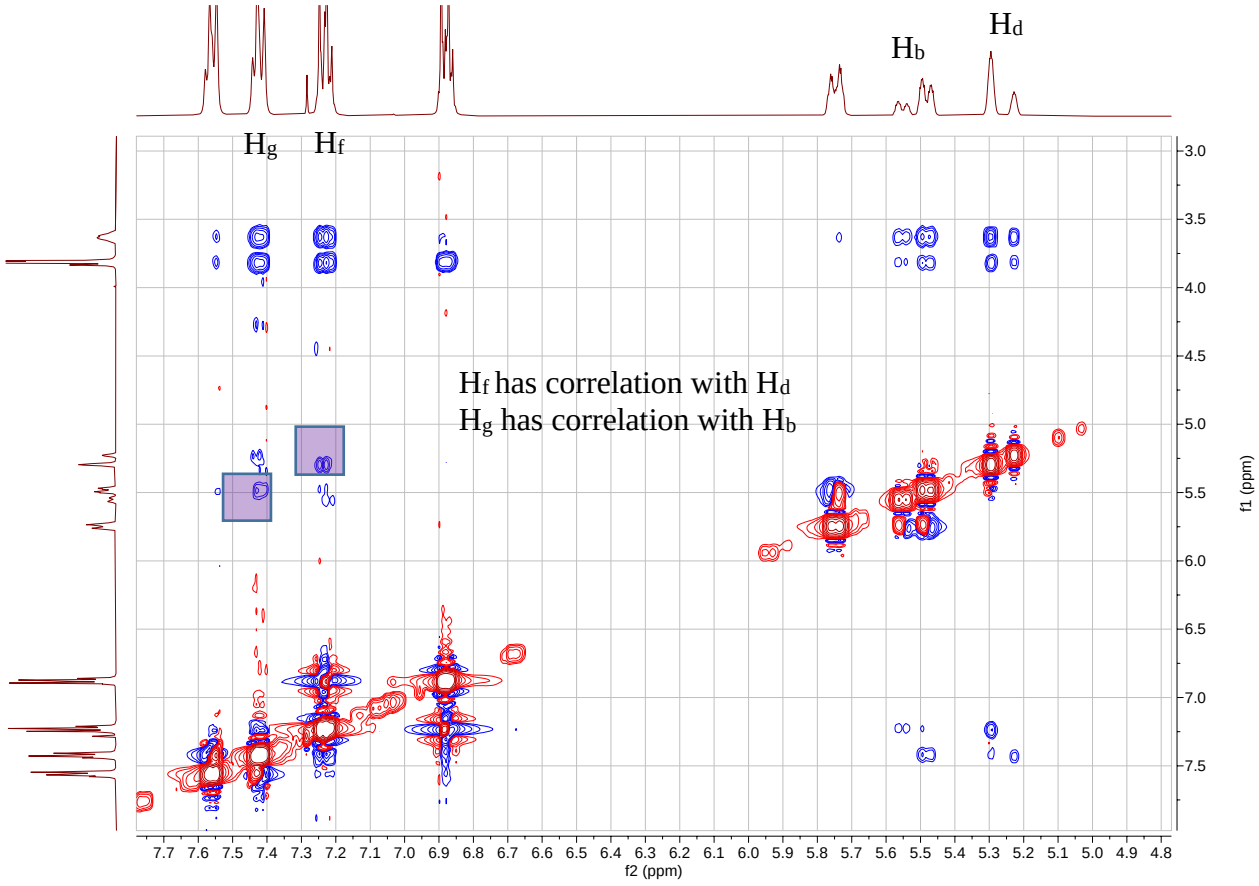

2D COSY:

Correlation between methyl group and H_d boxed in purple.

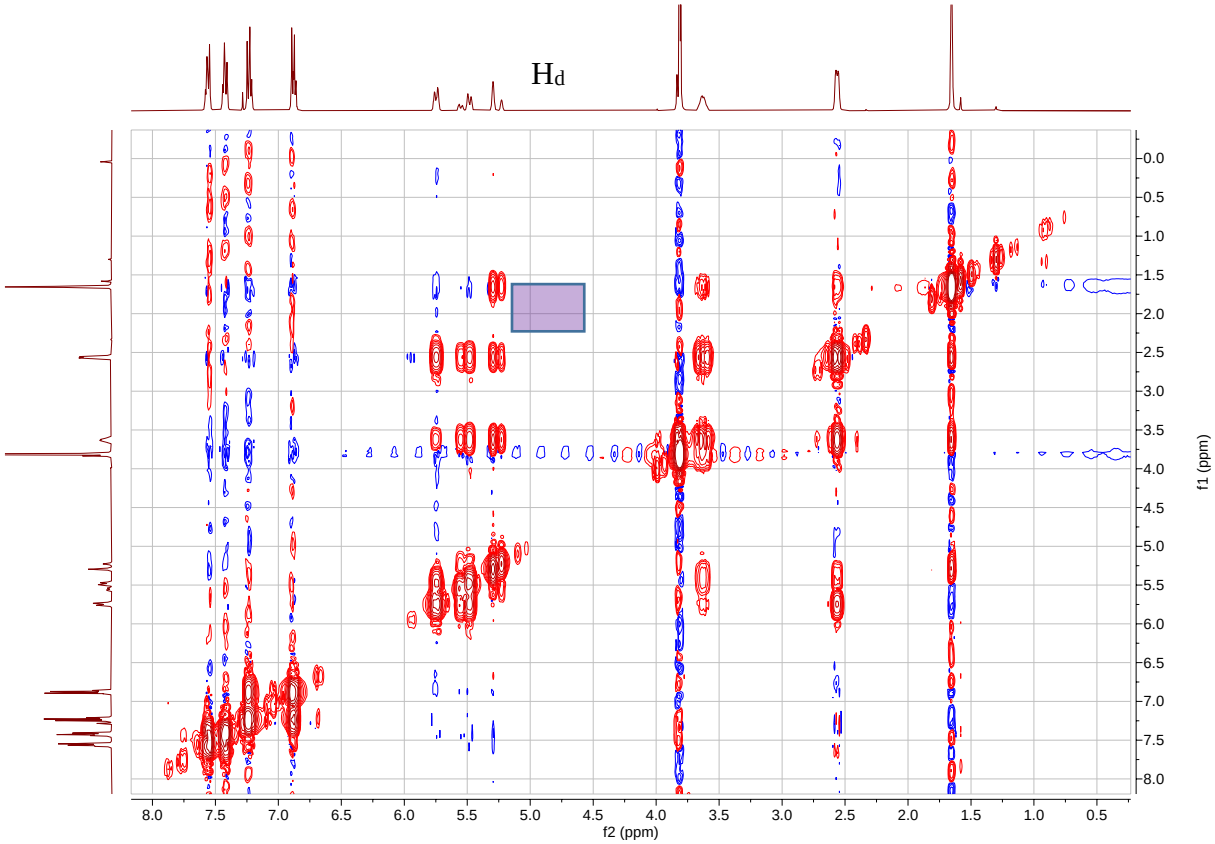

2-chloro-1-(diazo(4-methoxyphenyl)methyl)-4-nitrobenzene (SI-1)

^{1}H NMR (600 MHz, $CDCl_3$)

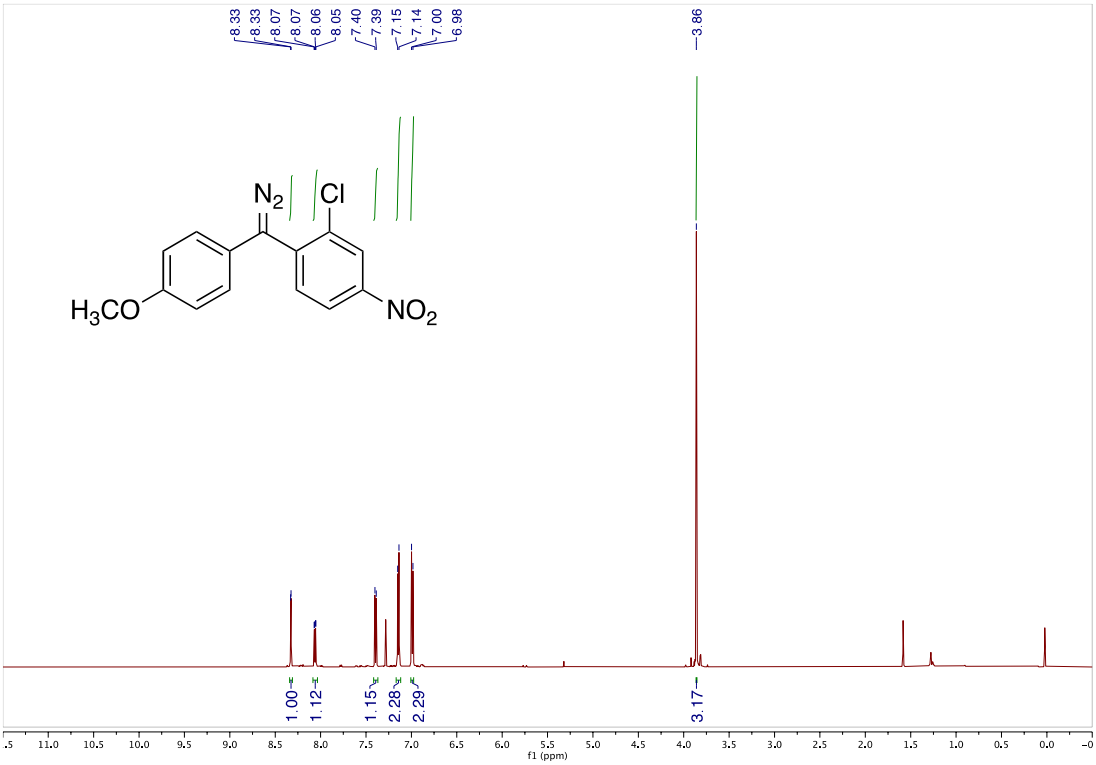

^{13}C NMR (600 MHz, $CDCl_3$)

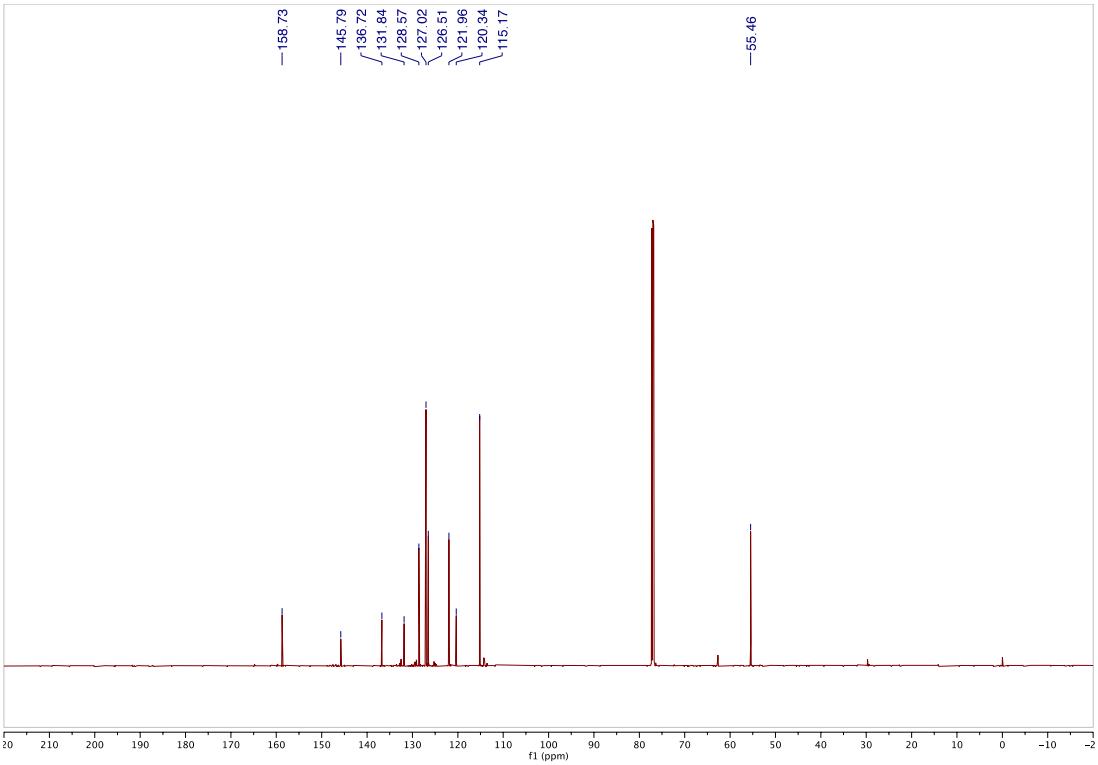

3-(diazo(4-fluorophenyl)methyl)pyridine (SI-2)

^{1}H NMR (400 MHz, $CDCl_3$)

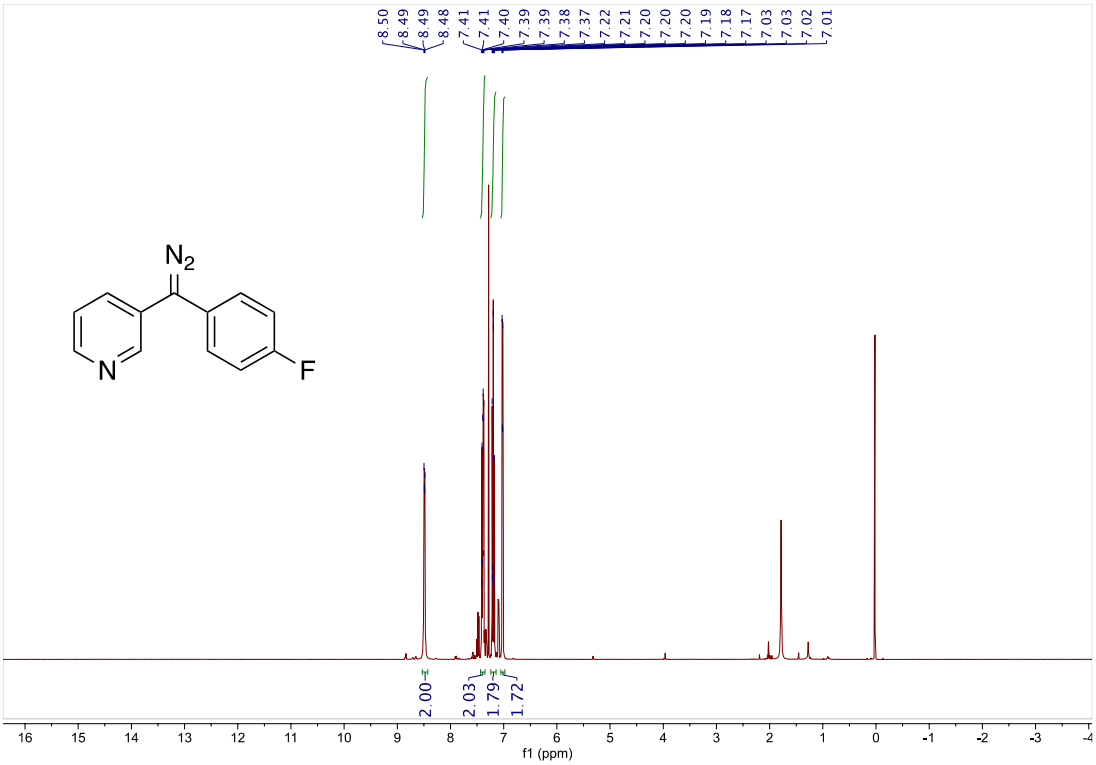

^{19}F NMR (400 MHz, $CDCl_3$)

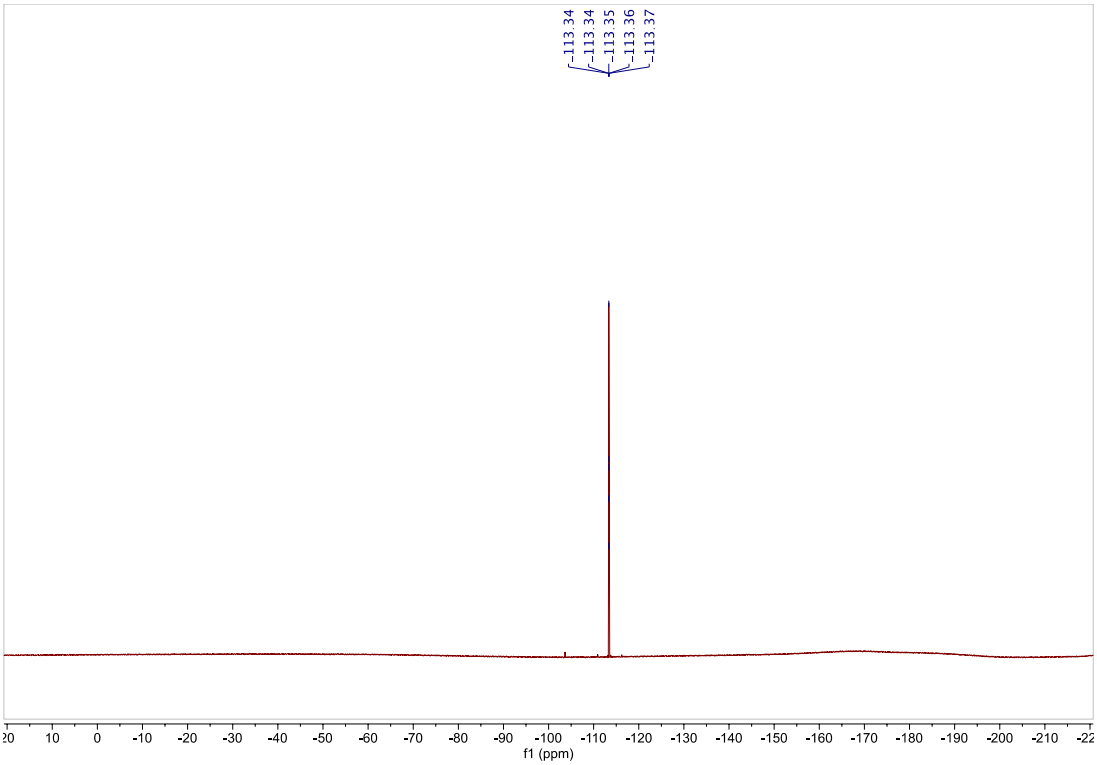

Compound 2

^{1}H NMR (400 MHz, $CDCl_3$)

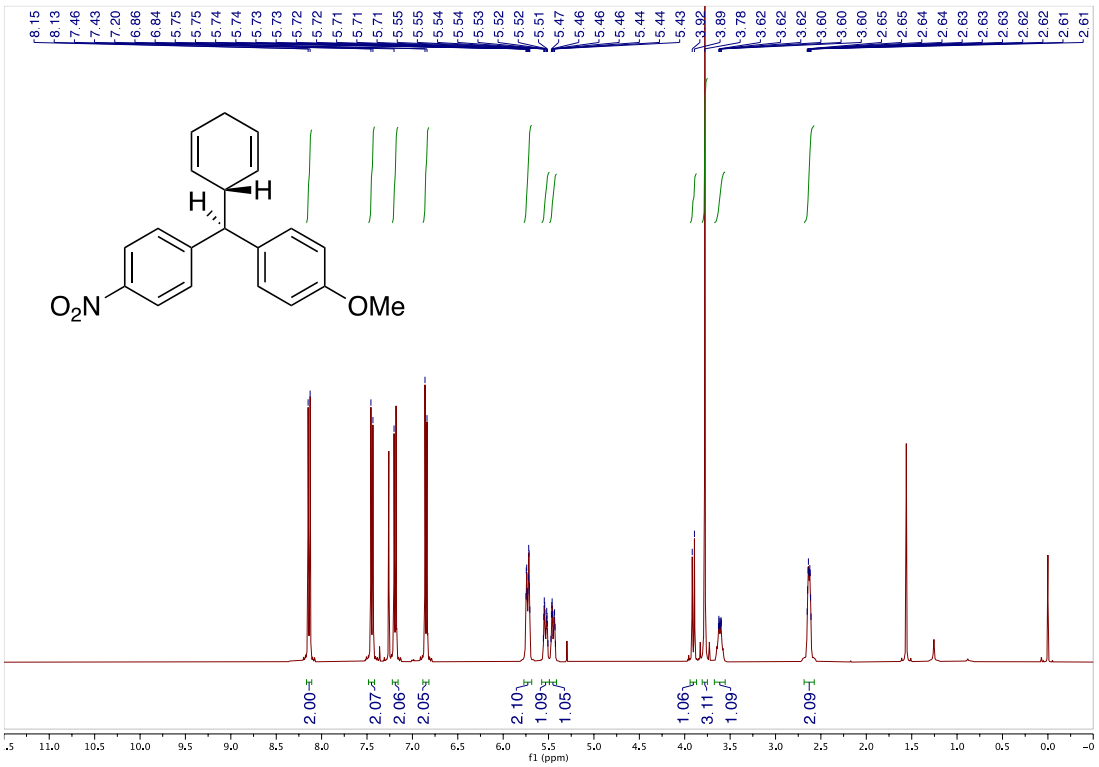

^{13}C NMR (400 MHz, $CDCl_3$)

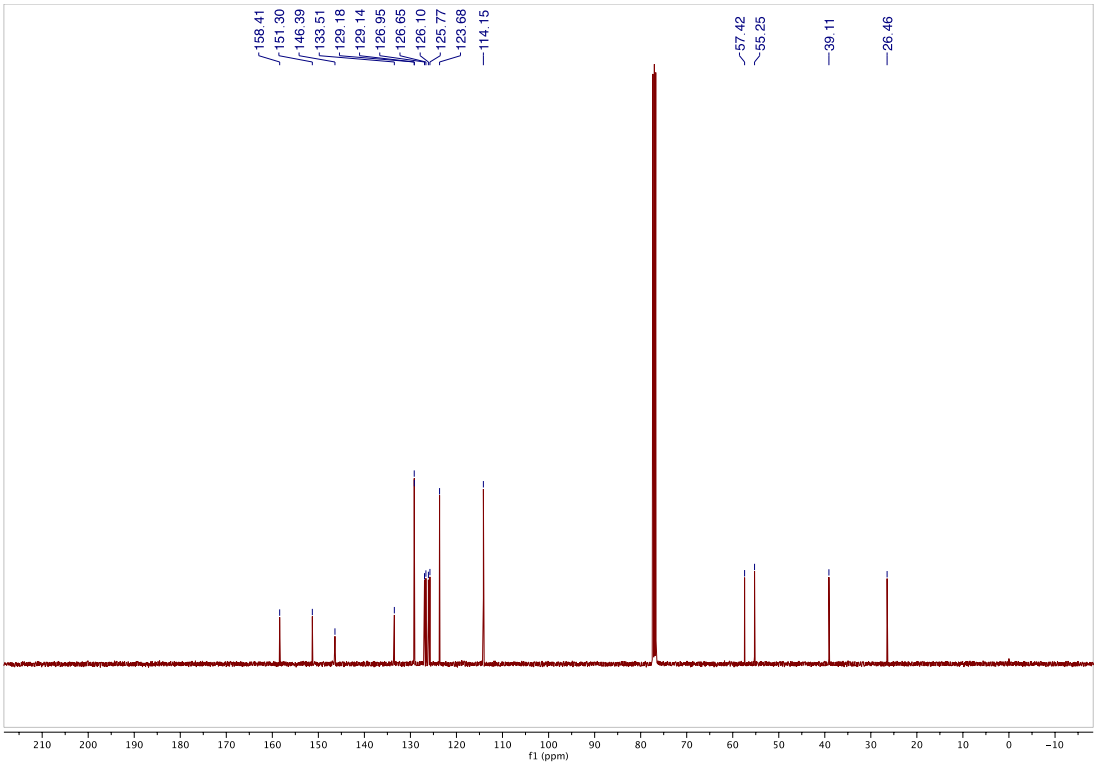

Compound 8

^{1}H NMR (400 MHz, $CDCl_3$)

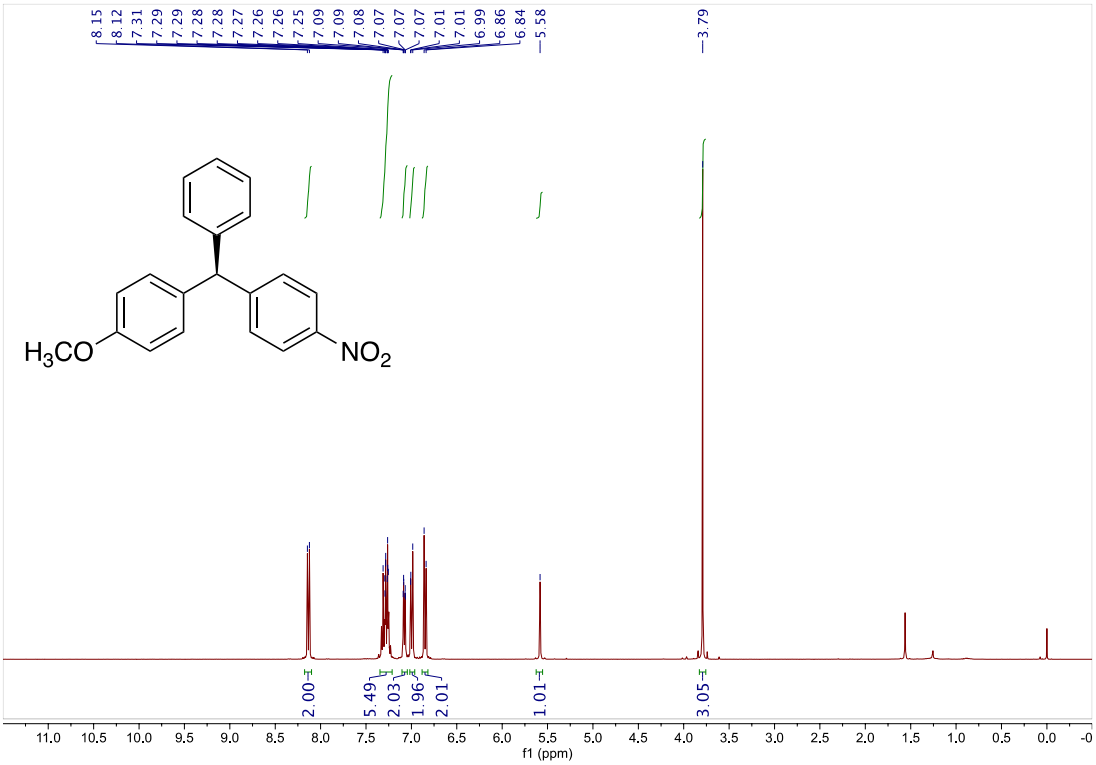

^{13}C NMR (400 MHz, $CDCl_3$)

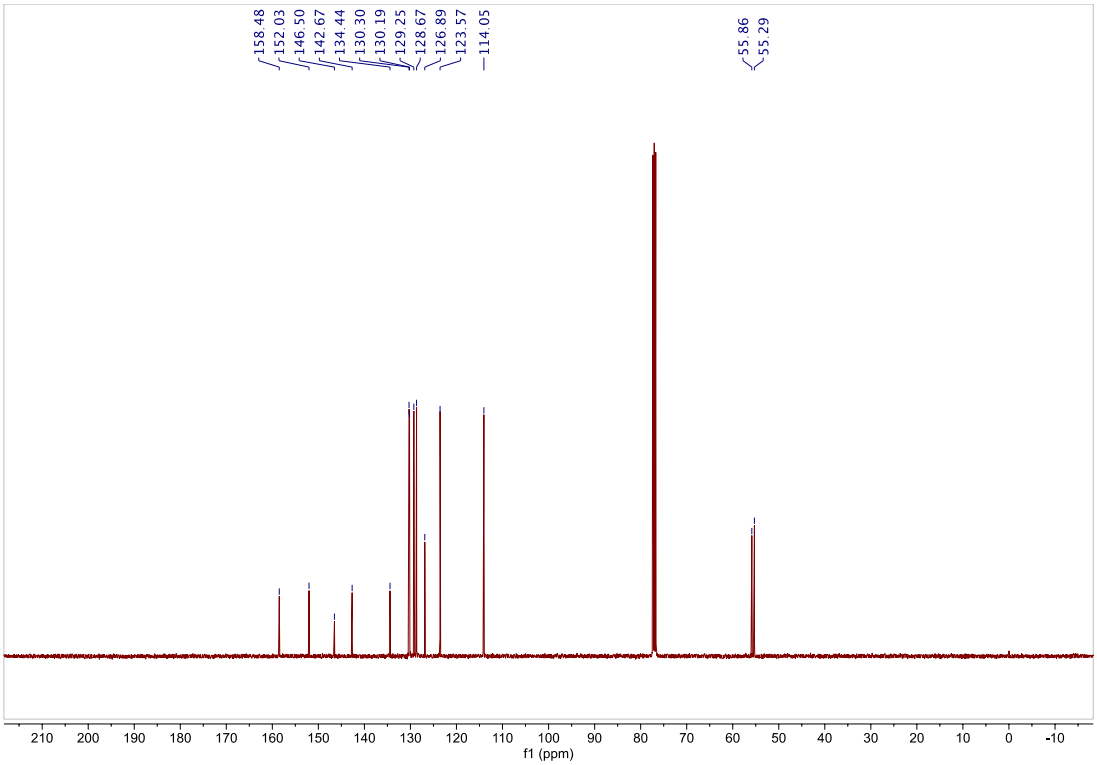

Compound 9

^{1}H NMR (600 MHz, $CDCl_3$)

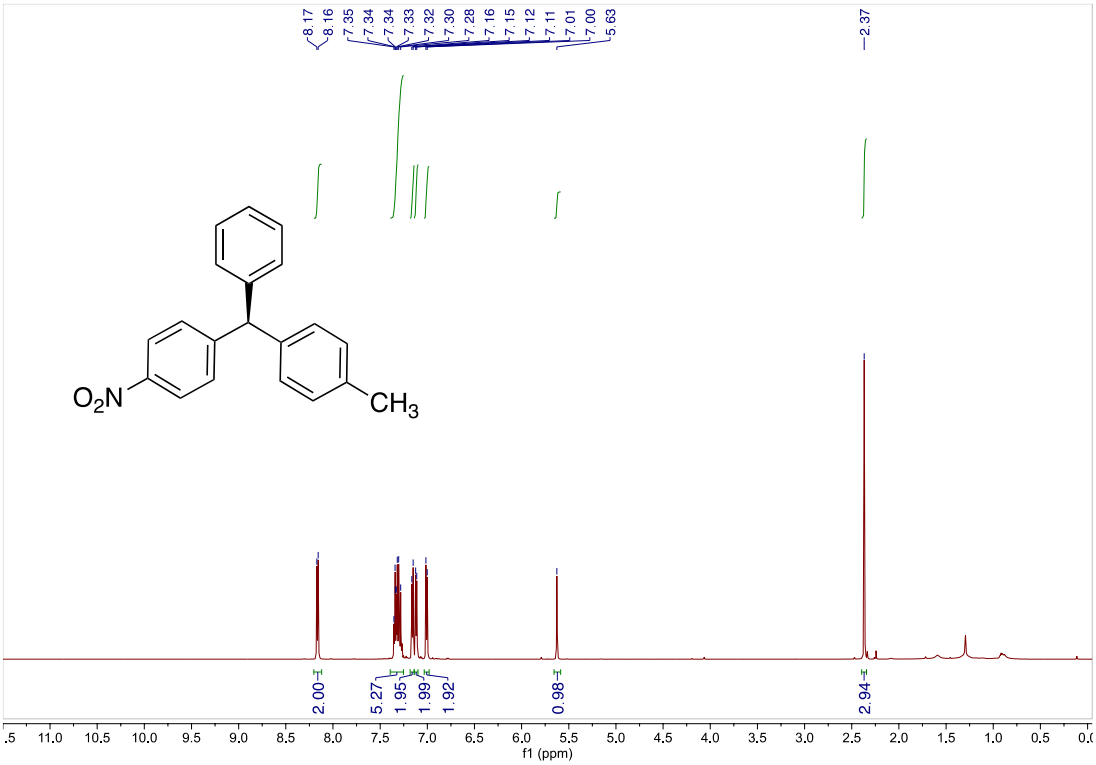

^{13}C NMR (600 MHz, $CDCl_3$)

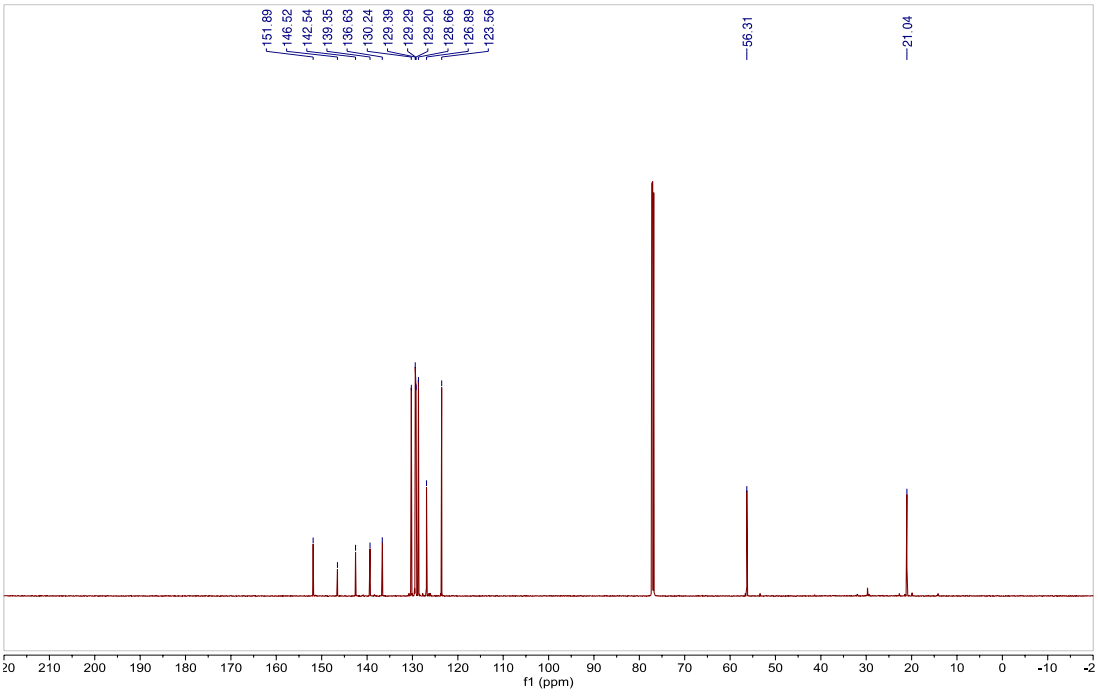

Compound 11

^{1}H NMR (600 MHz, $CDCl_3$)

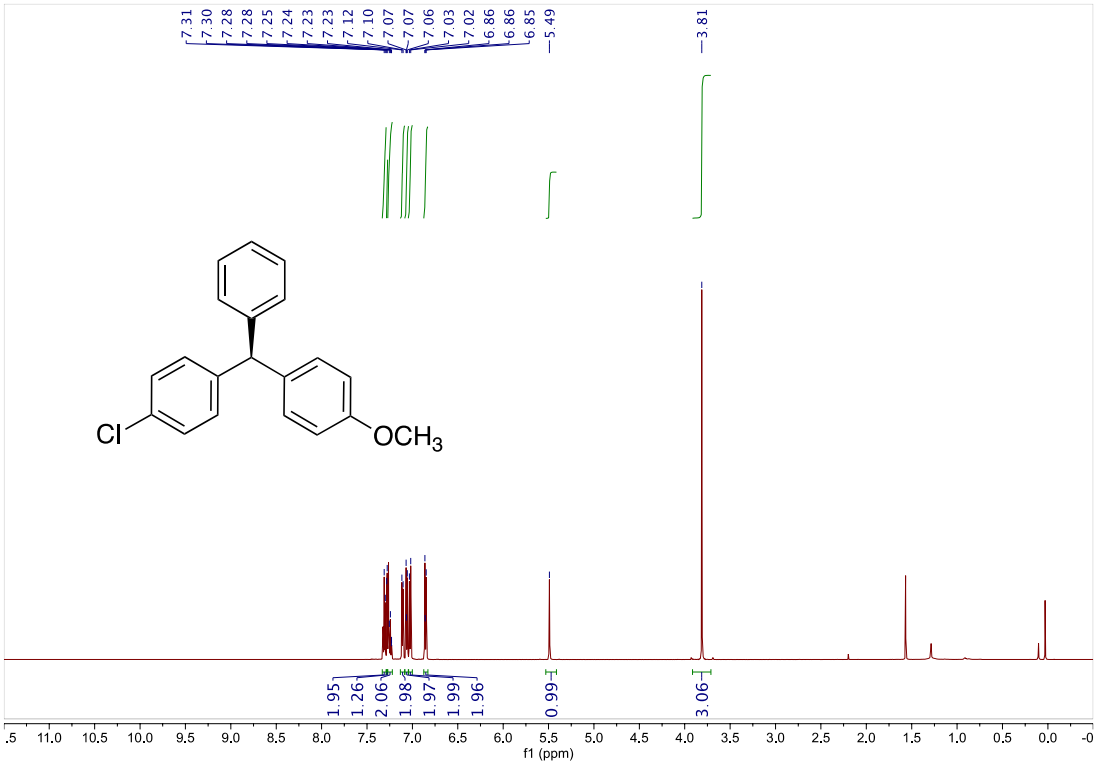

^{13}C NMR (600 MHz, $CDCl_3$)

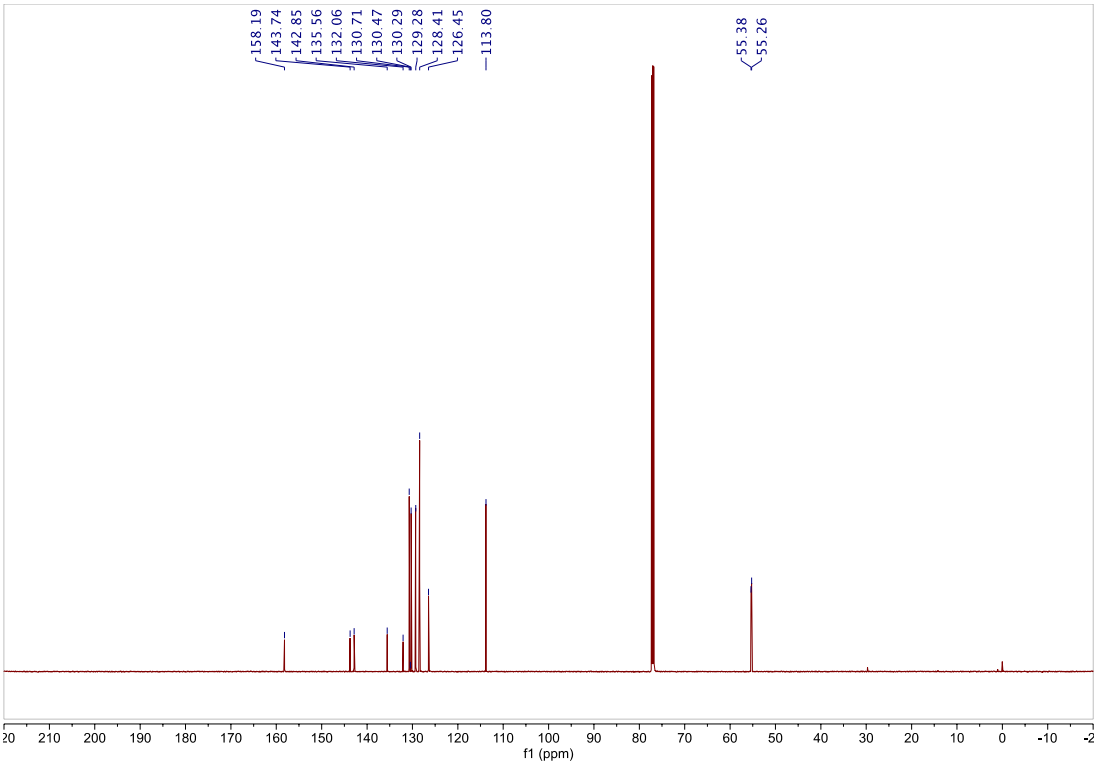

Compound 12
^{1}H NMR (600 MHz, $CDCl_3$)

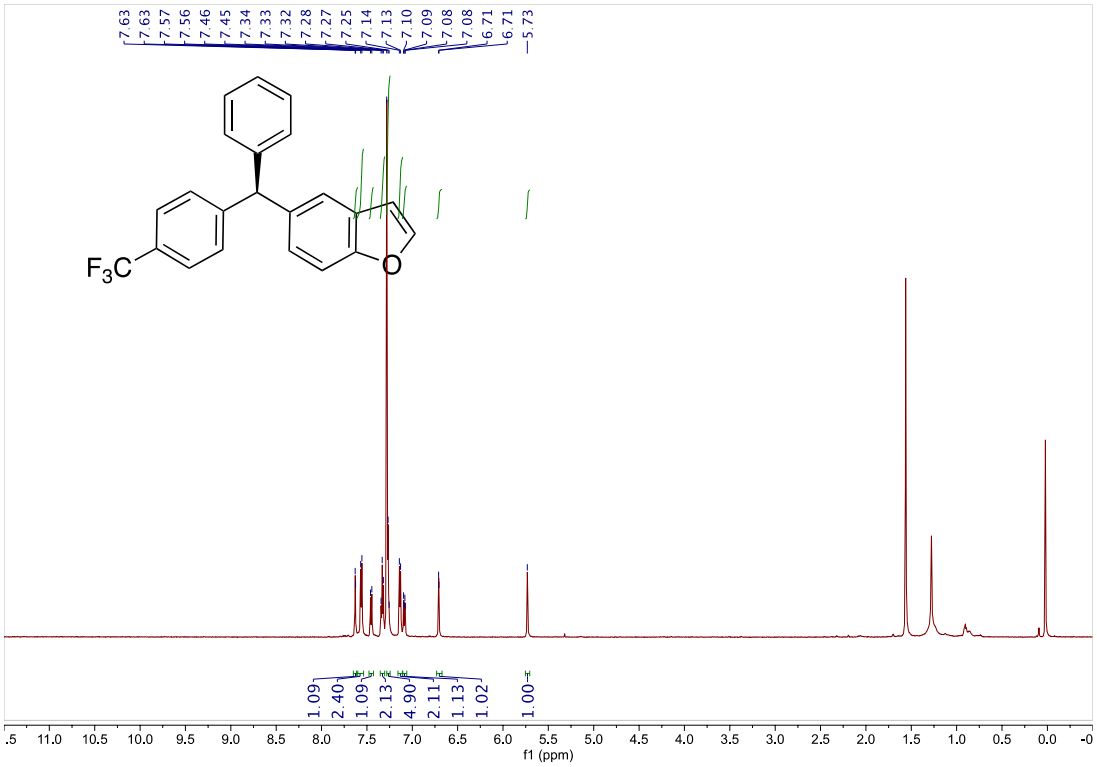

^{13}C NMR (600 MHz, $CDCl_3$)

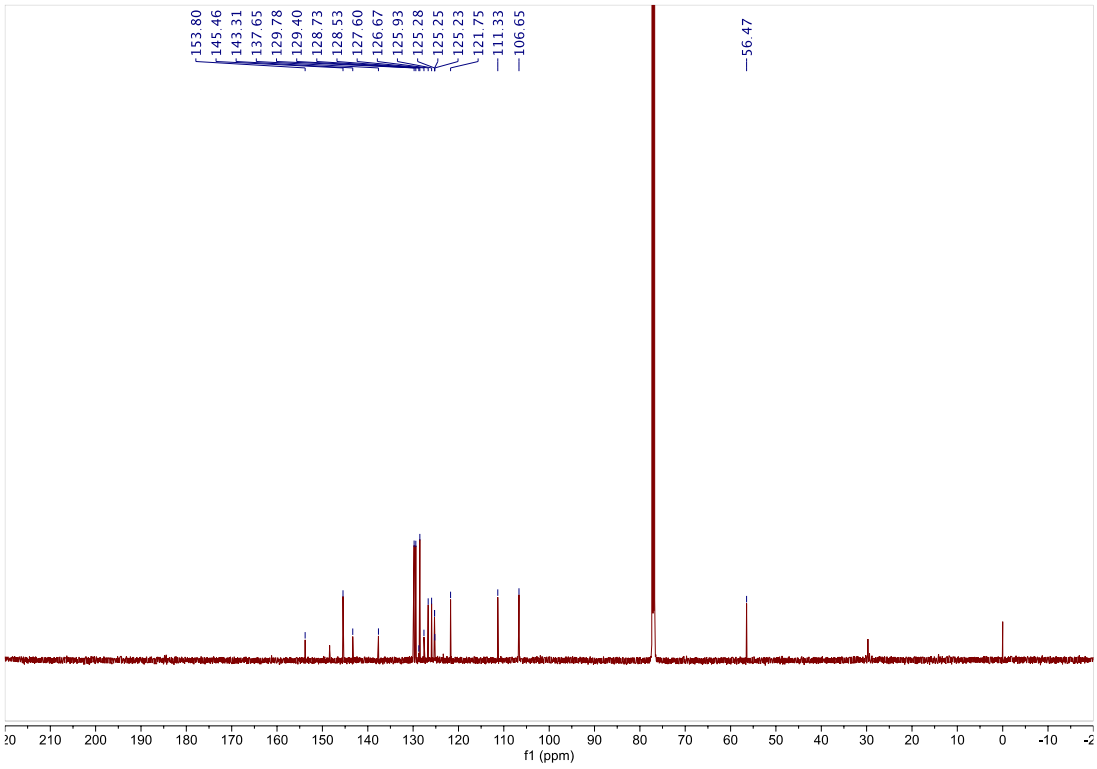

^{19}F NMR (600 MHz, $CDCl_3$) of compound 8.

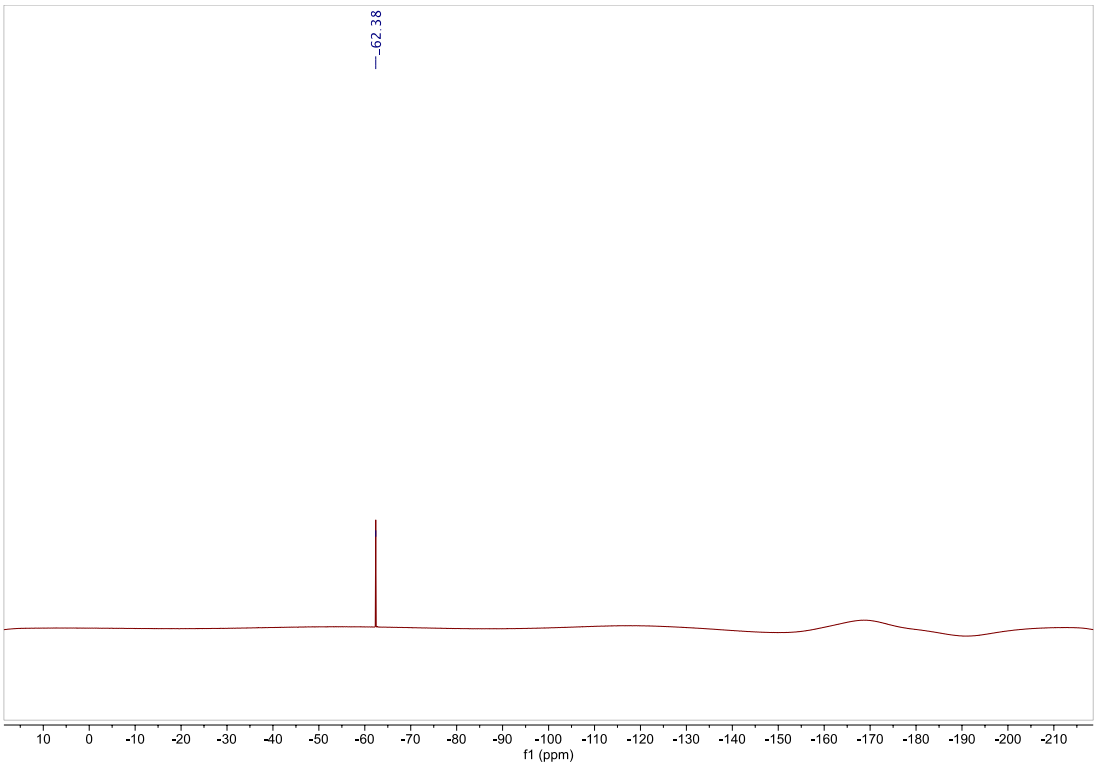

Compound 13

^{1}H NMR (600 MHz, $CDCl_3$)

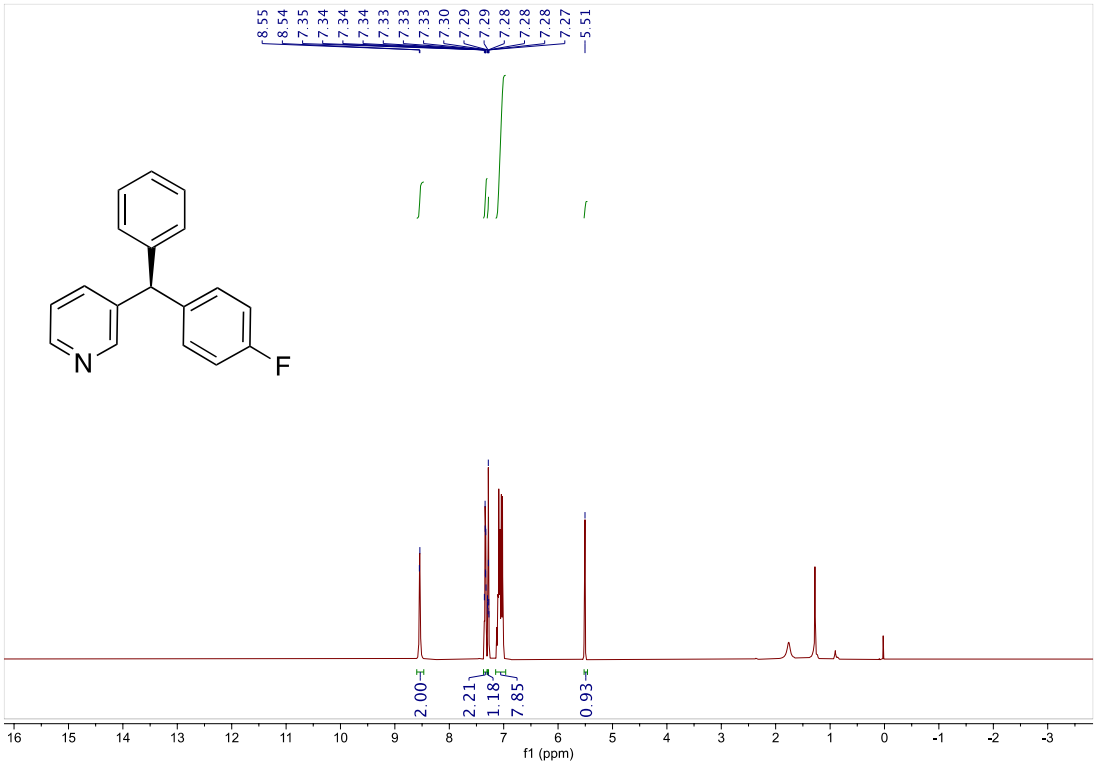

^{13}C NMR (600 MHz, $CDCl_3$)

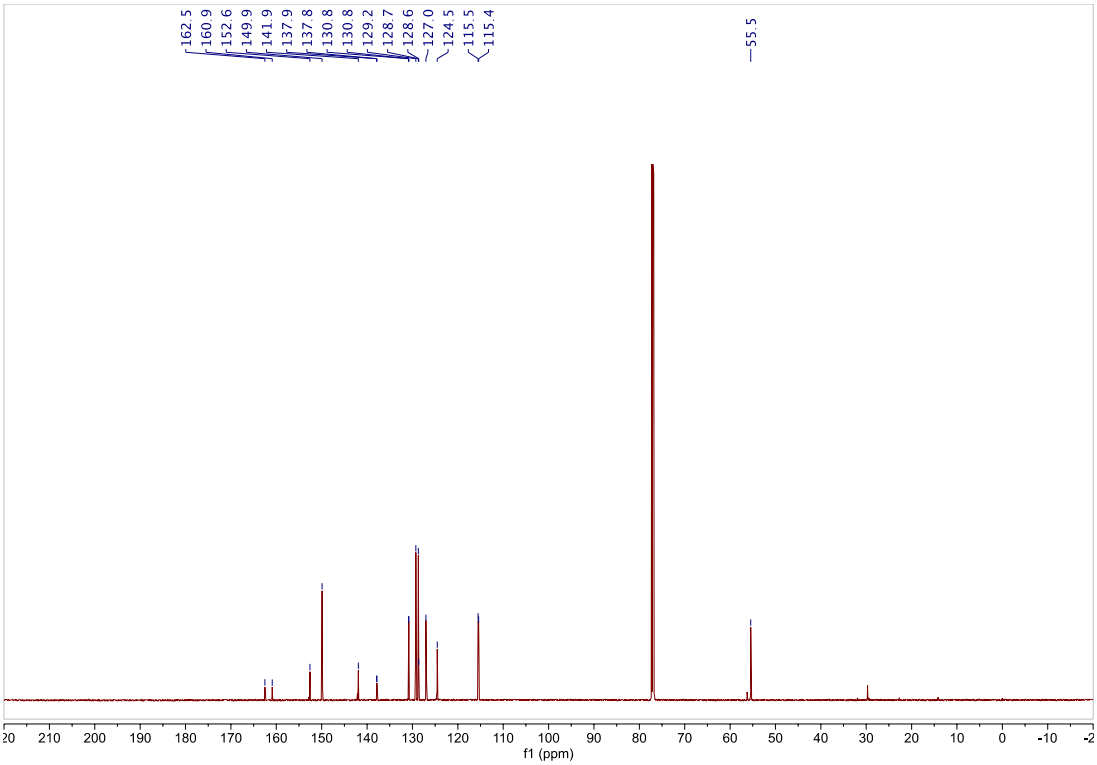

^{19}F NMR (600 MHz, $CDCl_3$) of compound **9**.

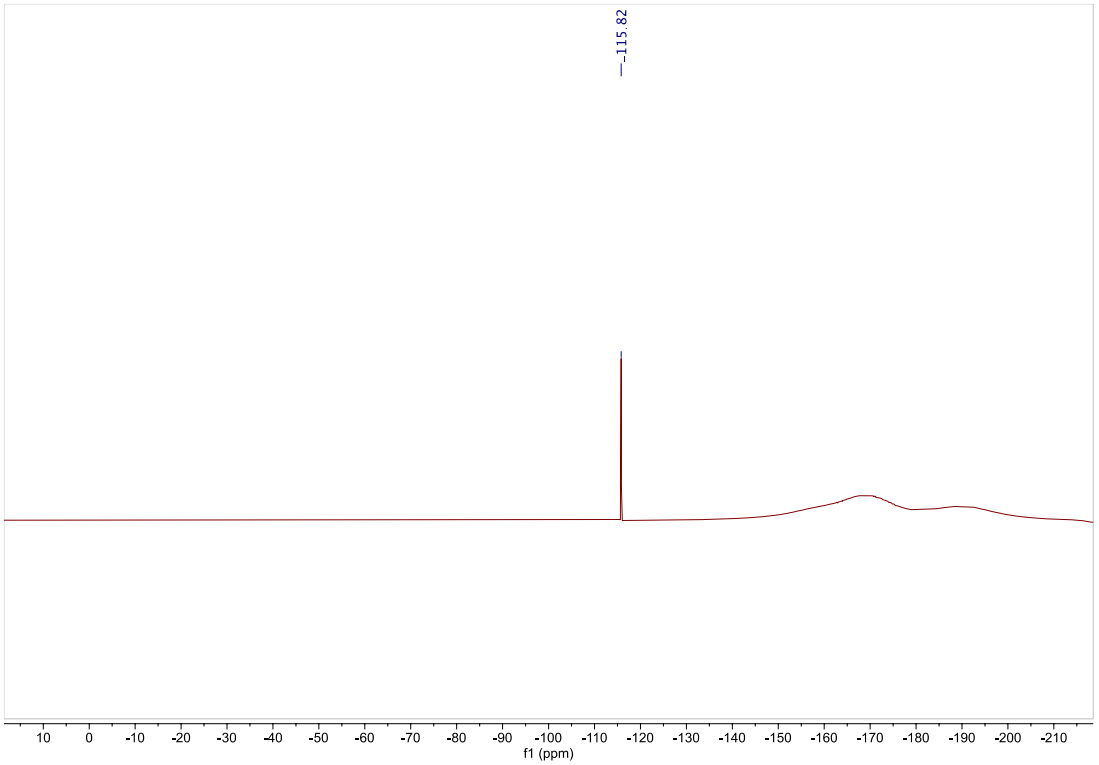

Compound 14

^{1}H NMR (600 MHz, $CDCl_3$)

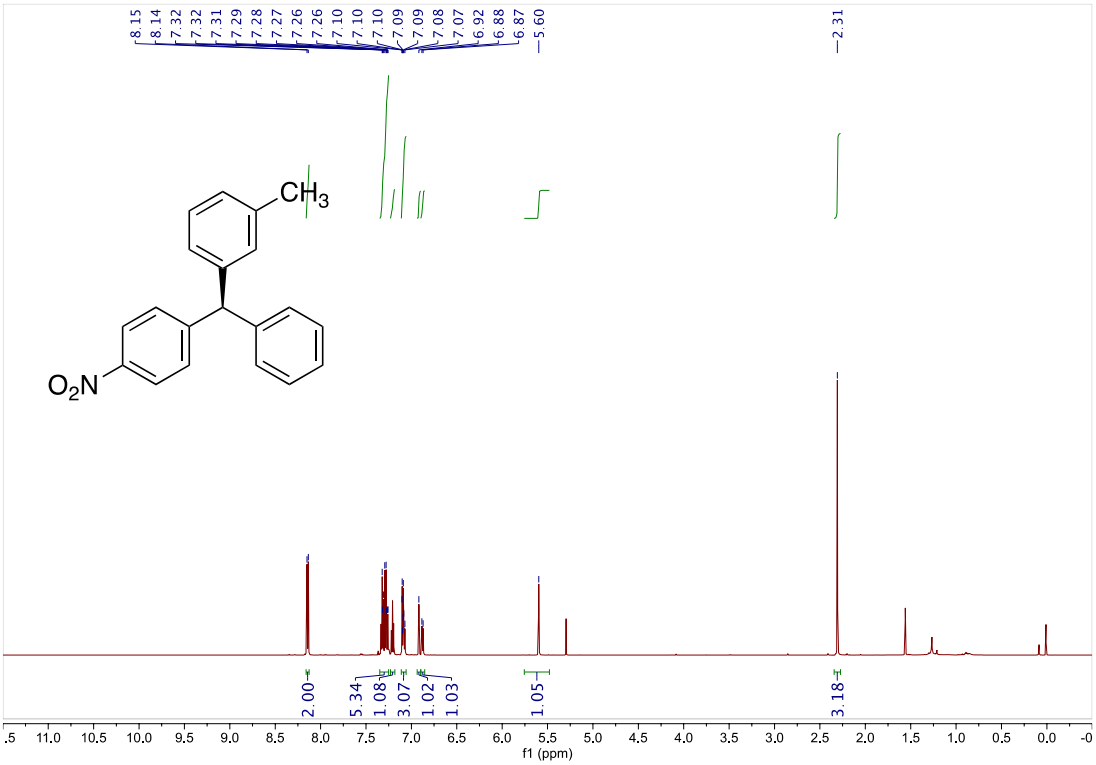

^{13}C NMR (600 MHz, $CDCl_3$)

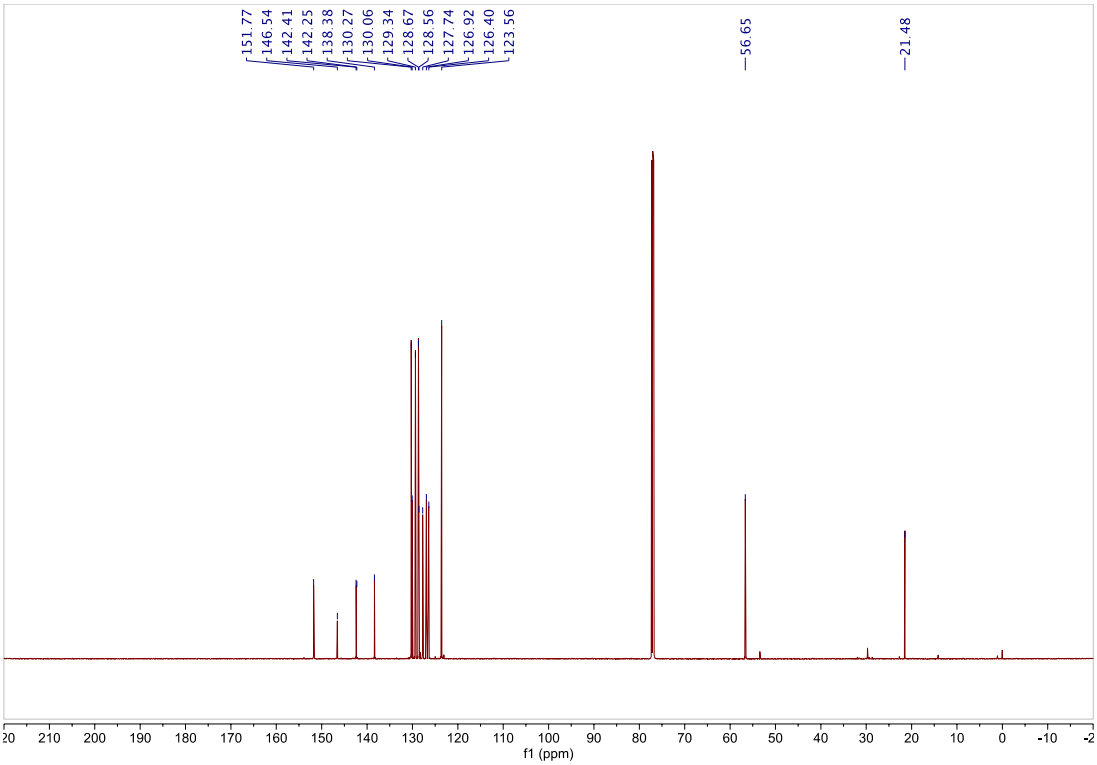

Compound 14

^{1}H NMR (600 MHz, $CDCl_3$)

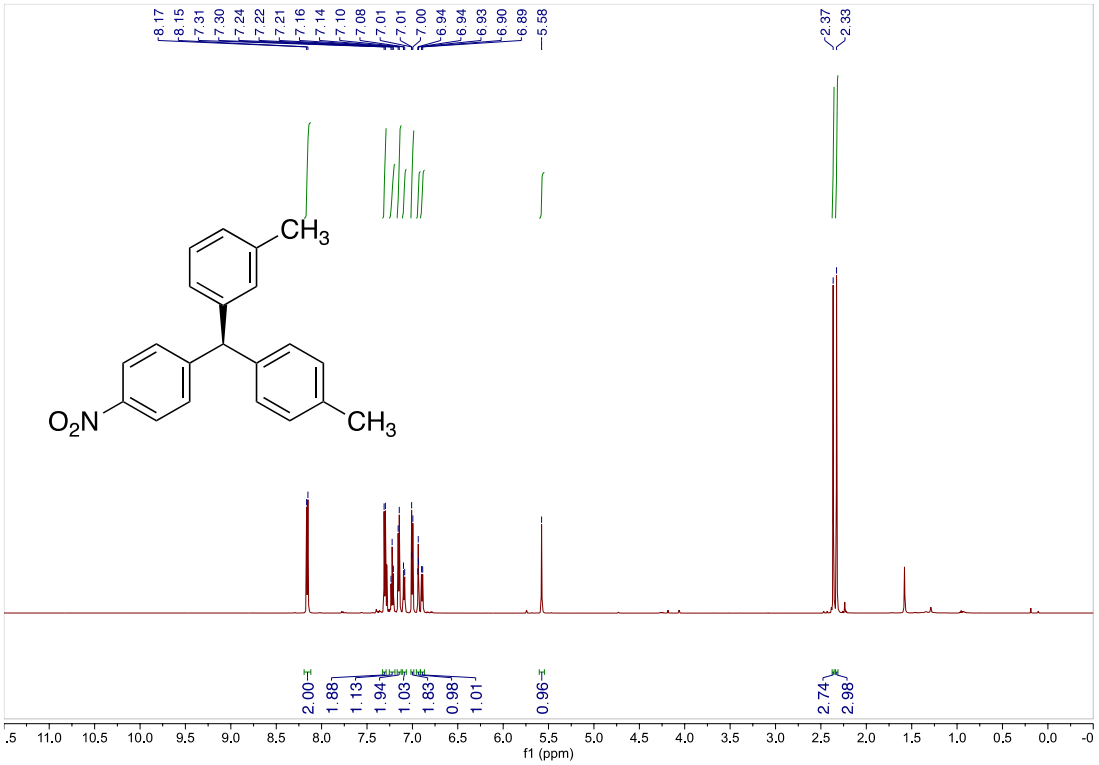

^{13}C NMR (600 MHz, $CDCl_3$)

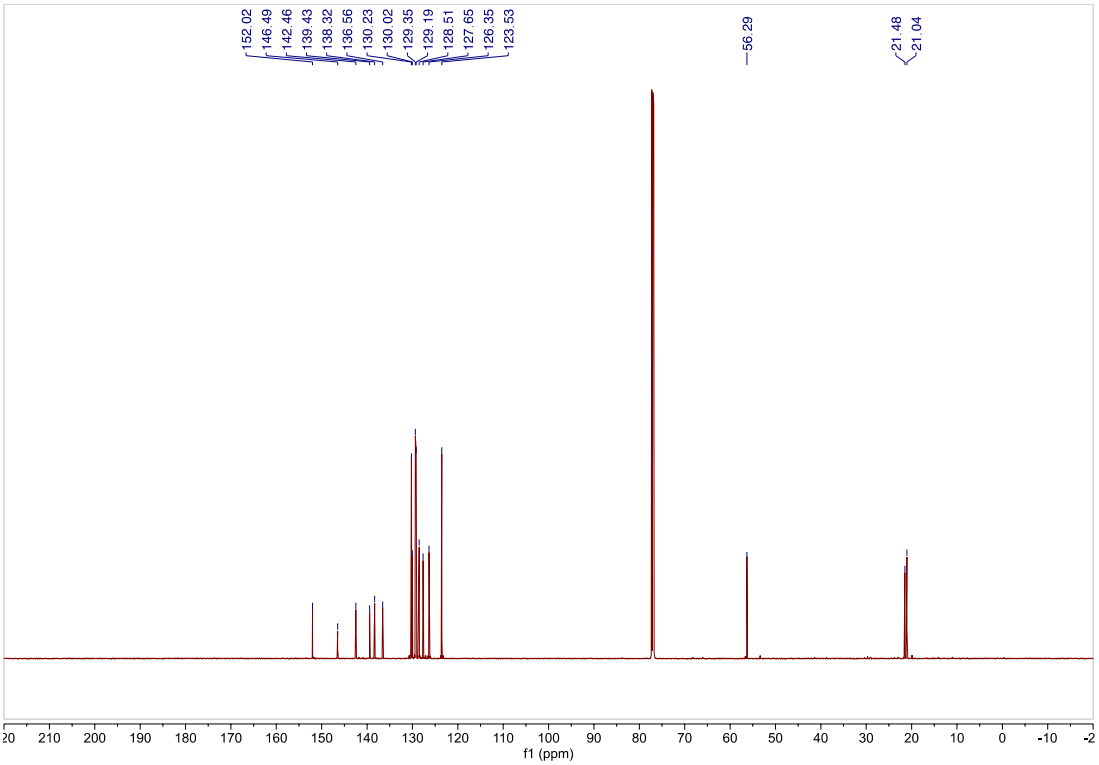

Compound 15

^{1}H NMR (600 MHz, $CDCl_3$)

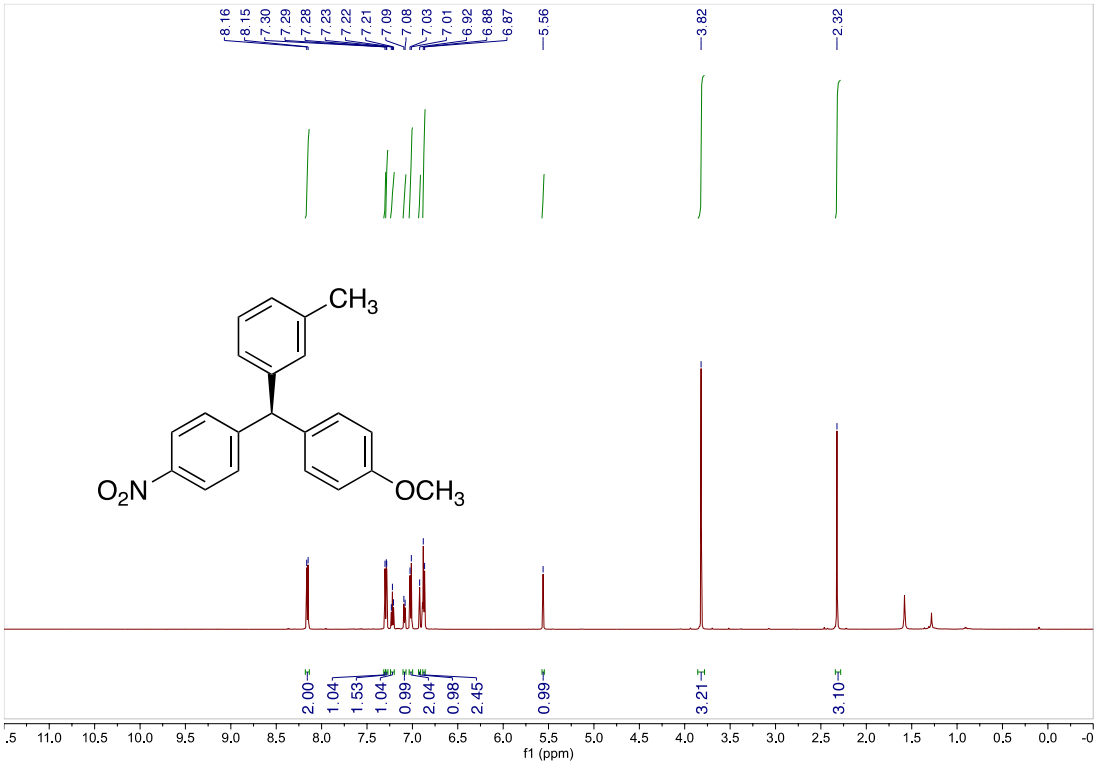

^{13}C NMR (600 MHz, $CDCl_3$)

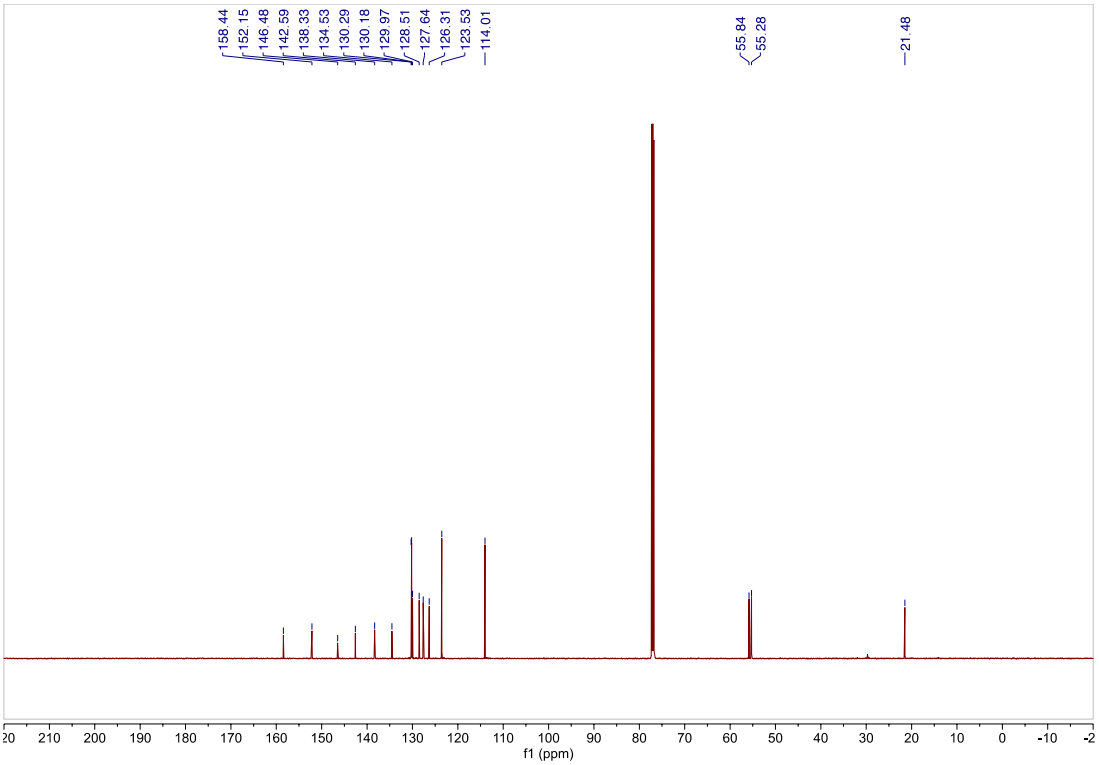

Compound 17

^{1}H NMR (600 MHz, $CDCl_3$)

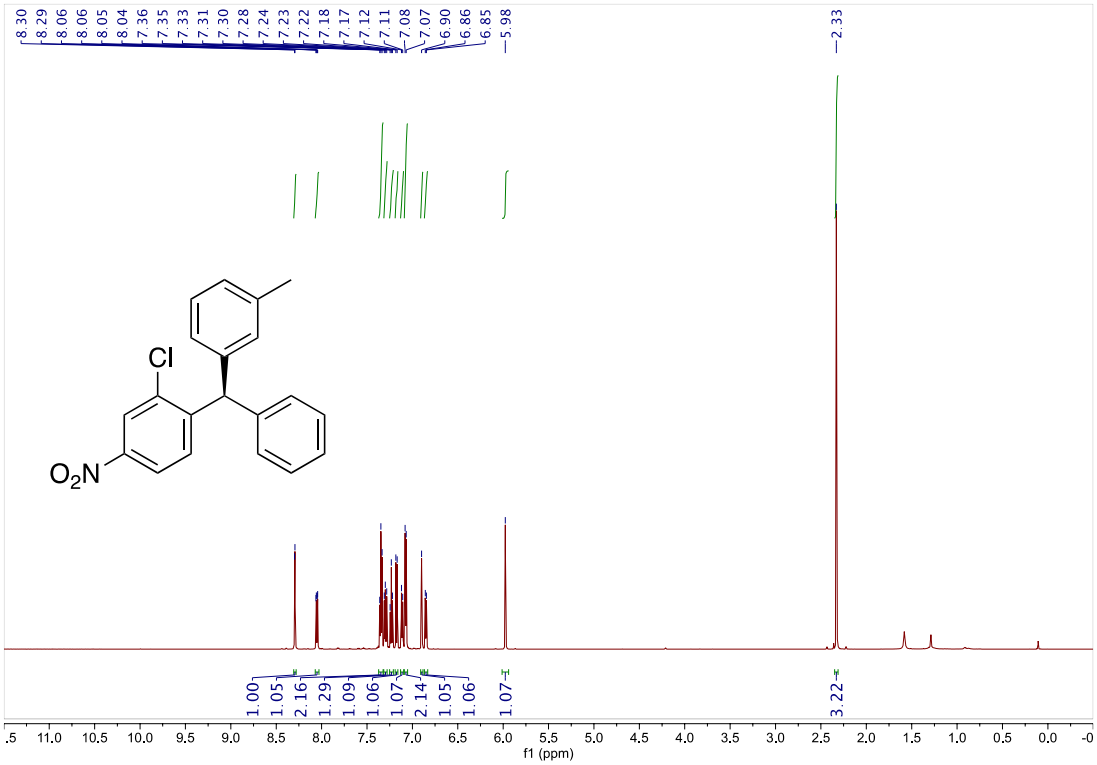

^{13}C NMR (600 MHz, $CDCl_3$)

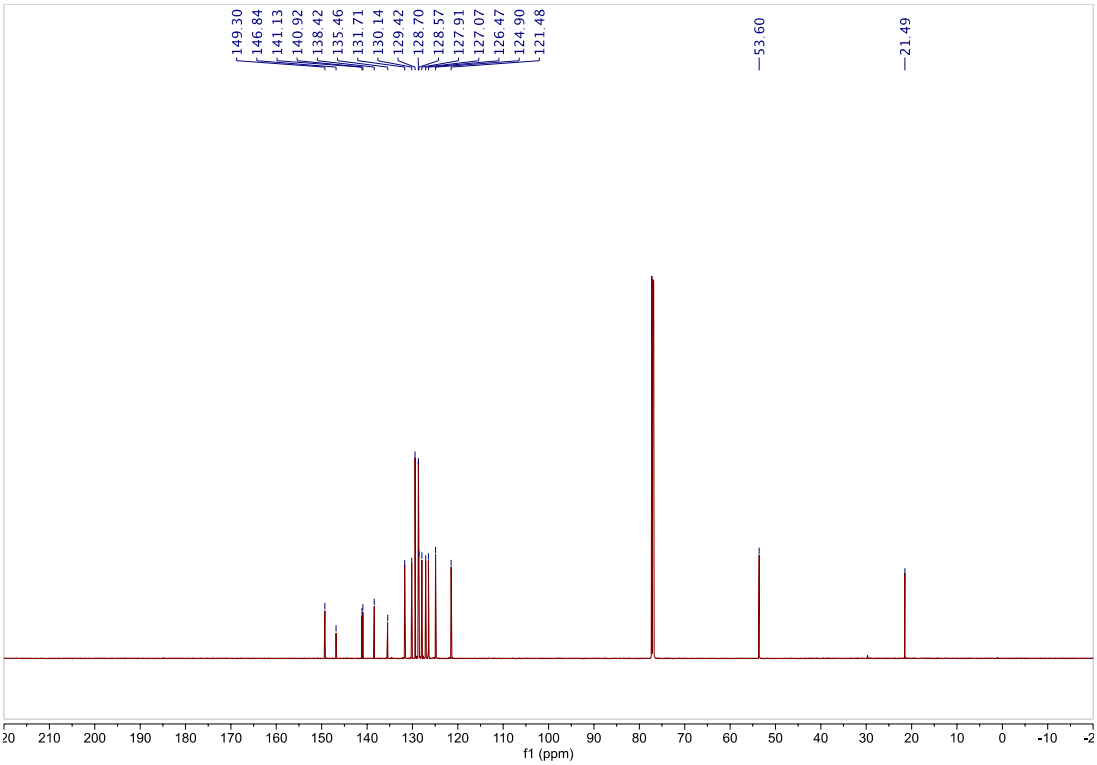

Compound 18

^{1}H NMR (600 MHz, $CDCl_3$)

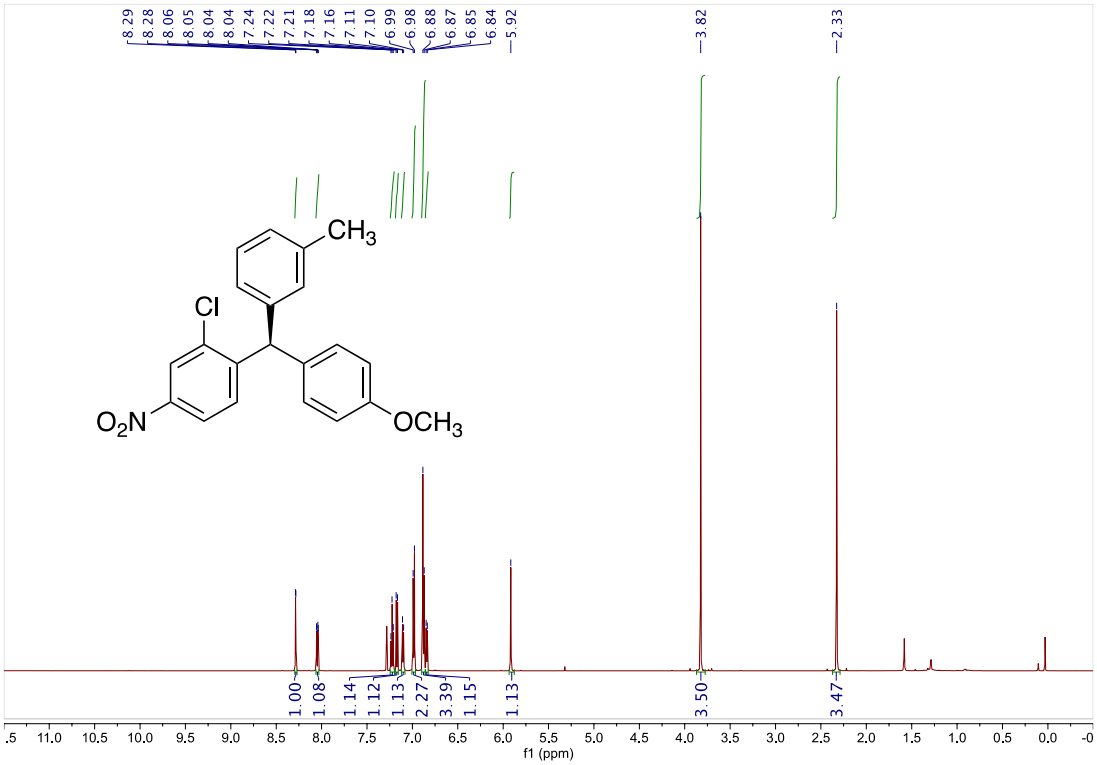

^{13}C NMR (600 MHz, $CDCl_3$)

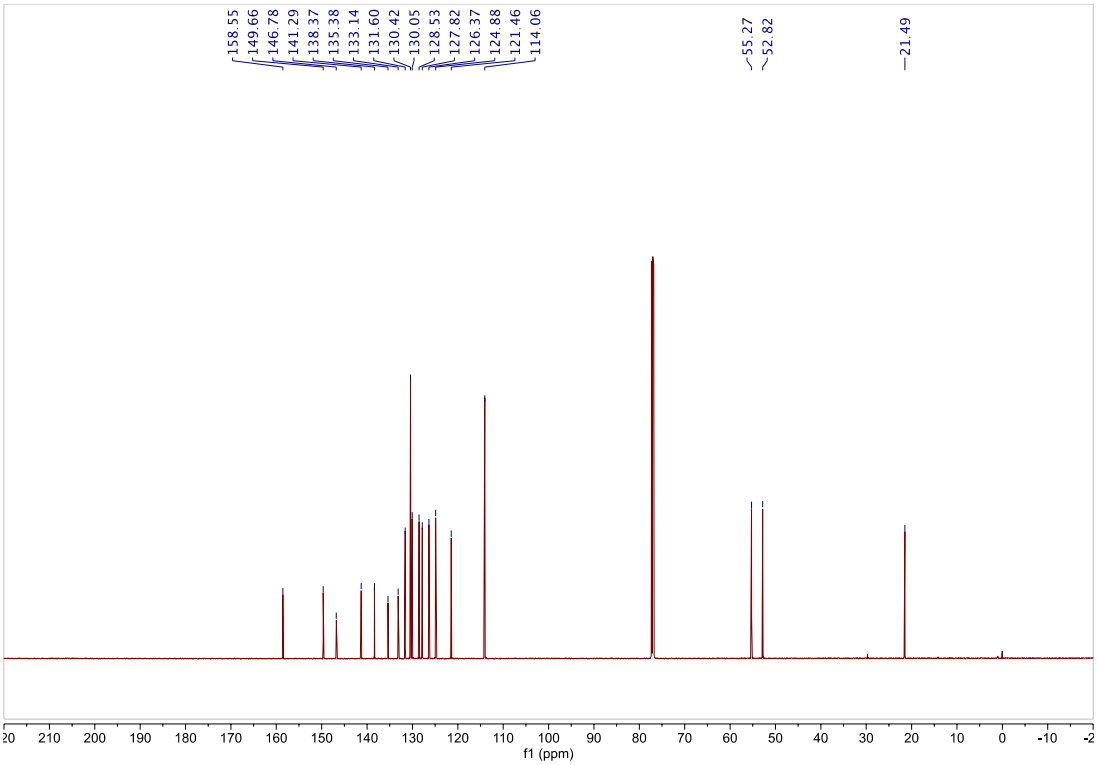

Compound 21

^{1}H NMR (600 MHz, $CDCl_3$)

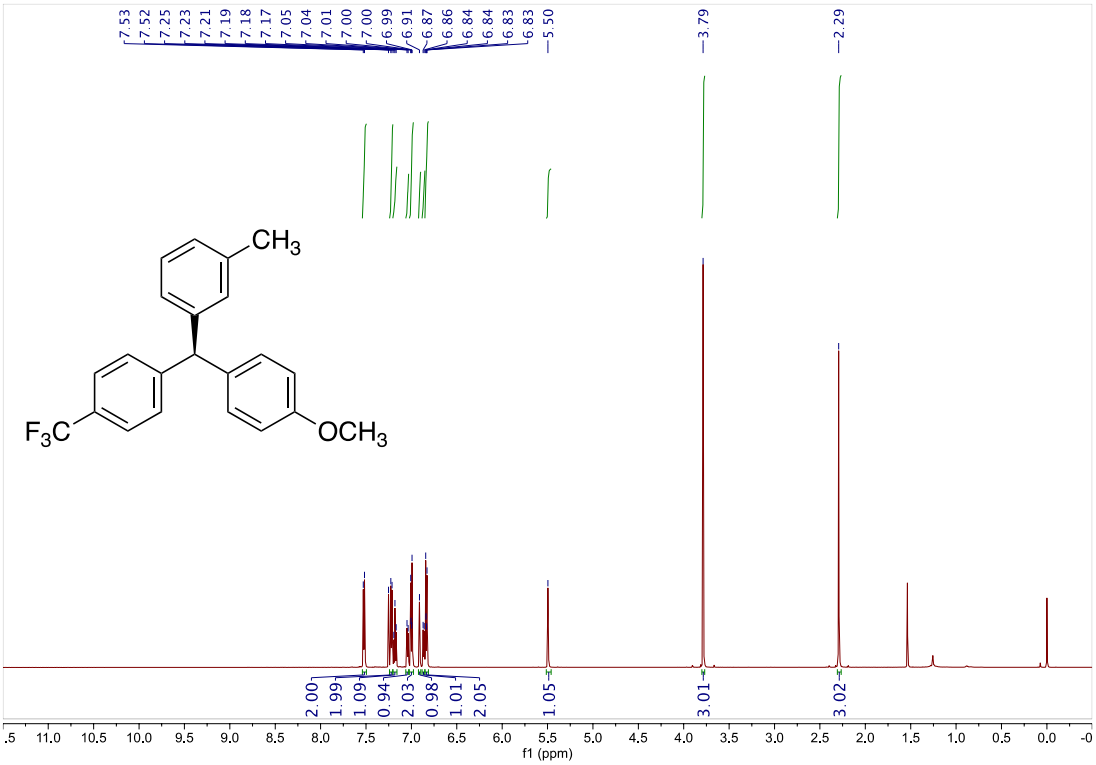

^{13}C NMR (600 MHz, $CDCl_3$)

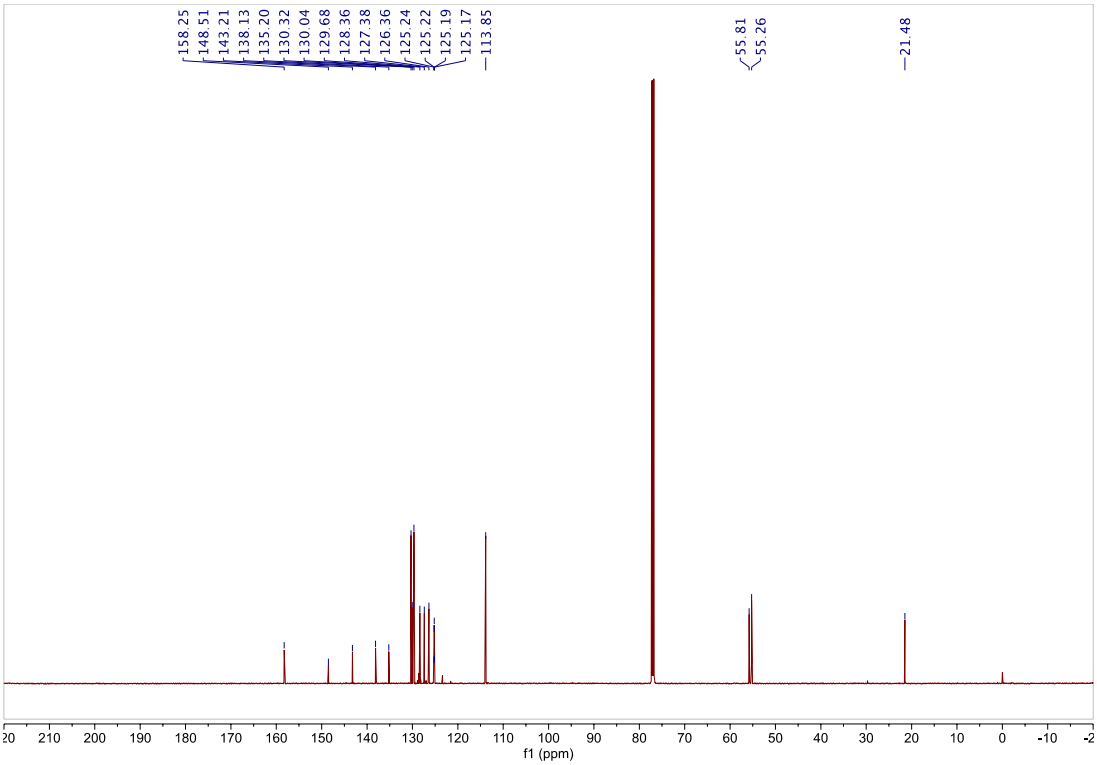

^{19}F NMR (600 MHz, $CDCl_3$) of compound **21**.

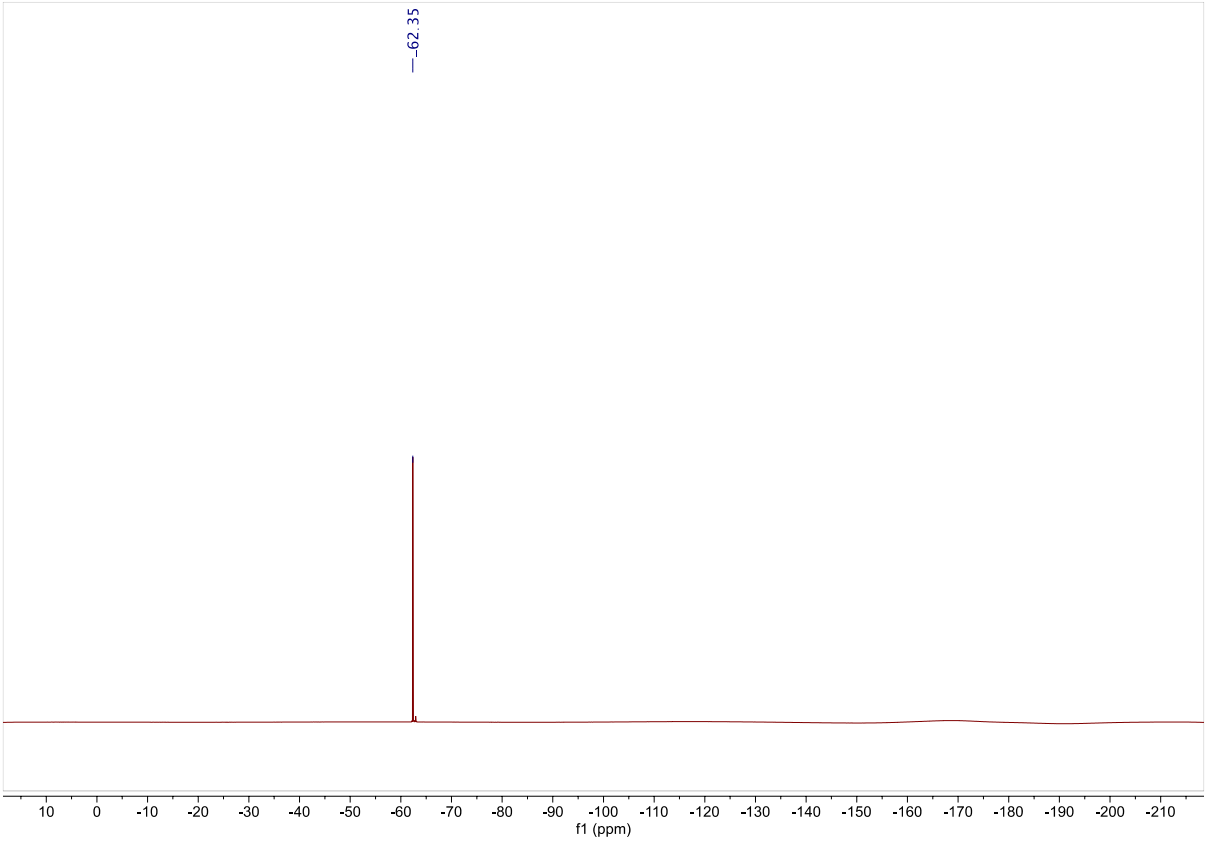

Compound 23

^{1}H NMR (600 MHz, $CDCl_3$)

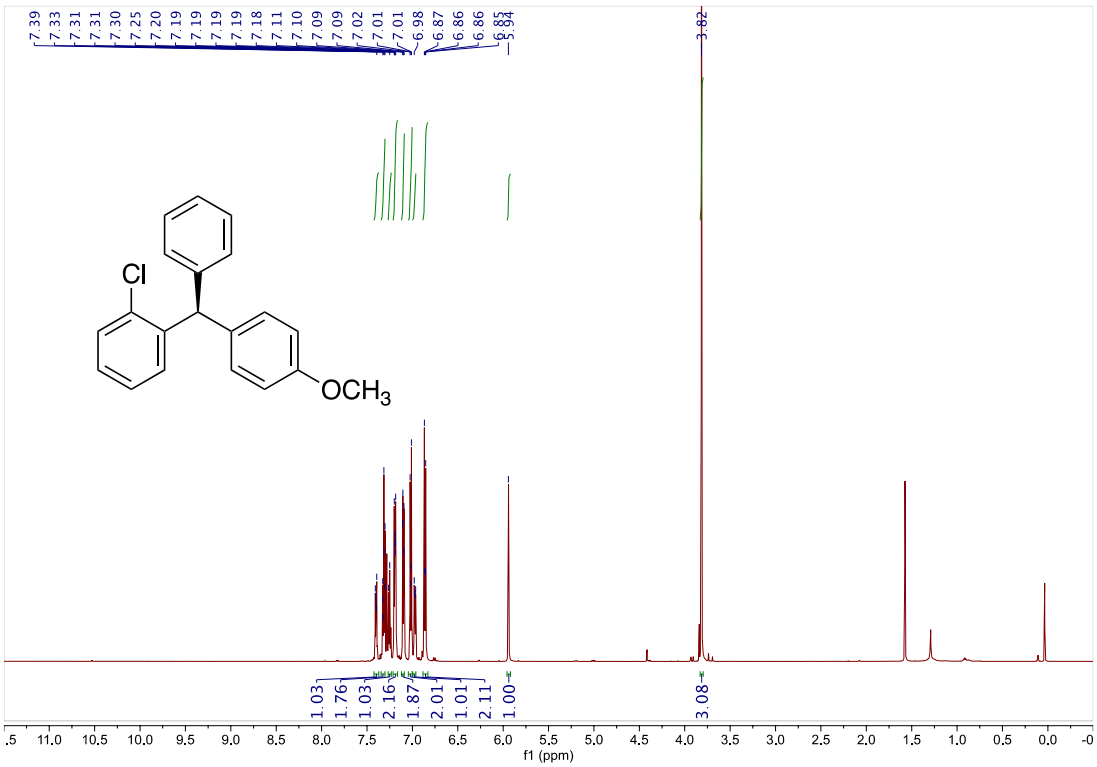

^{13}C NMR (600 MHz, $CDCl_3$)

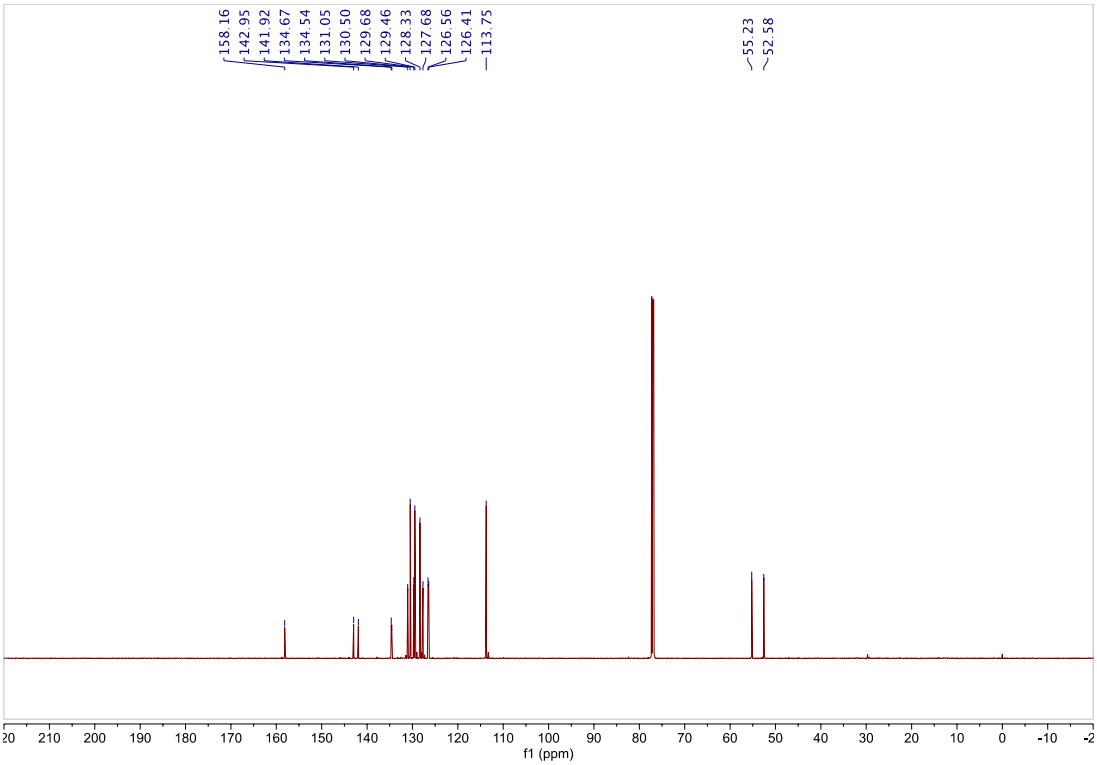

Compound 24

^{1}H NMR (400 MHz, $CDCl_3$)

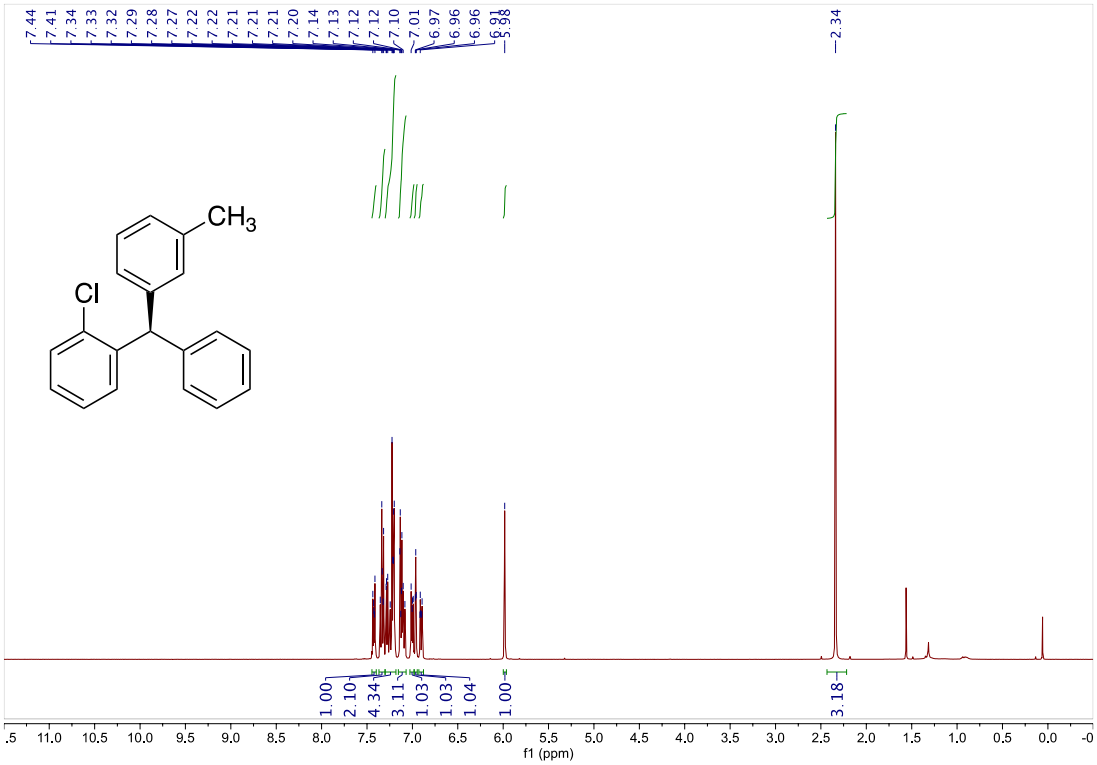

^{13}C NMR (600 MHz, $CDCl_3$)

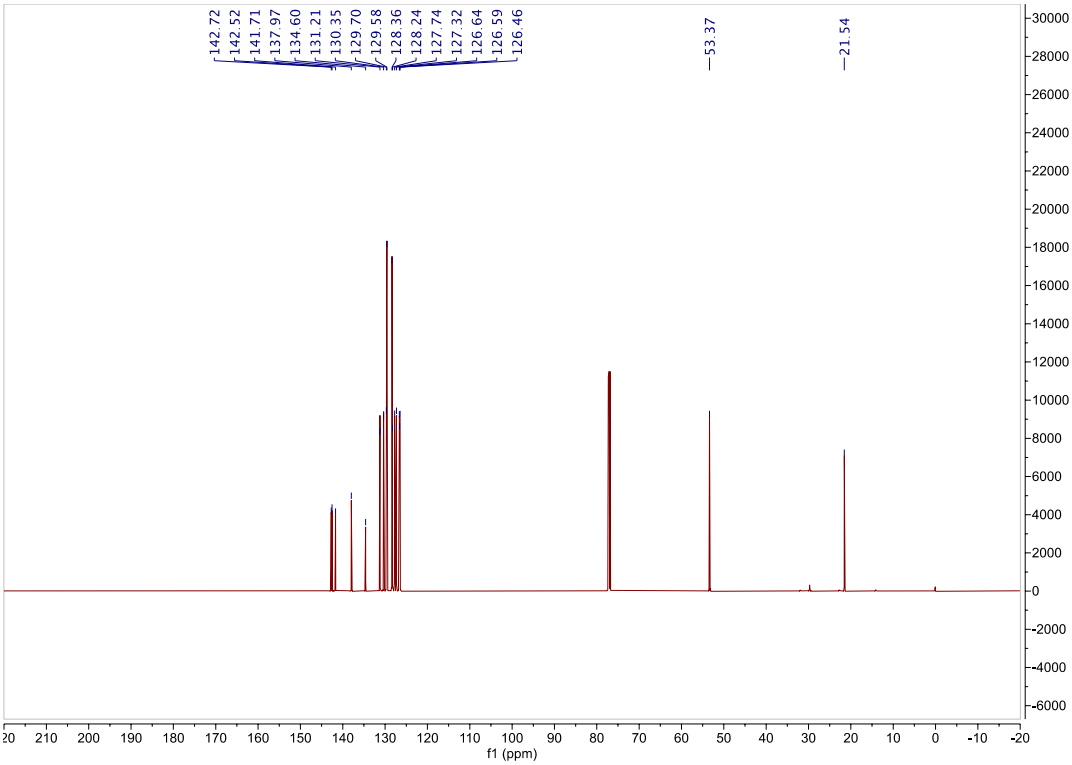

Compound 25

^{1}H NMR (600 MHz, $CDCl_3$)

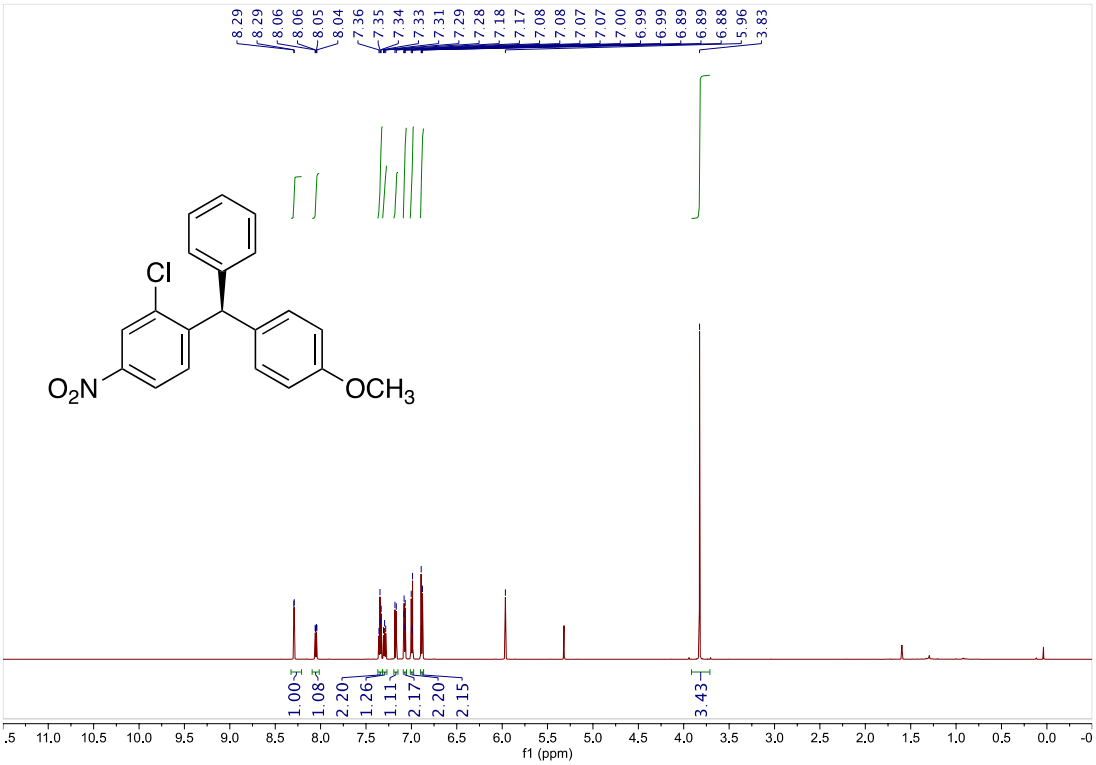

^{13}C NMR (600 MHz, $CDCl_3$)

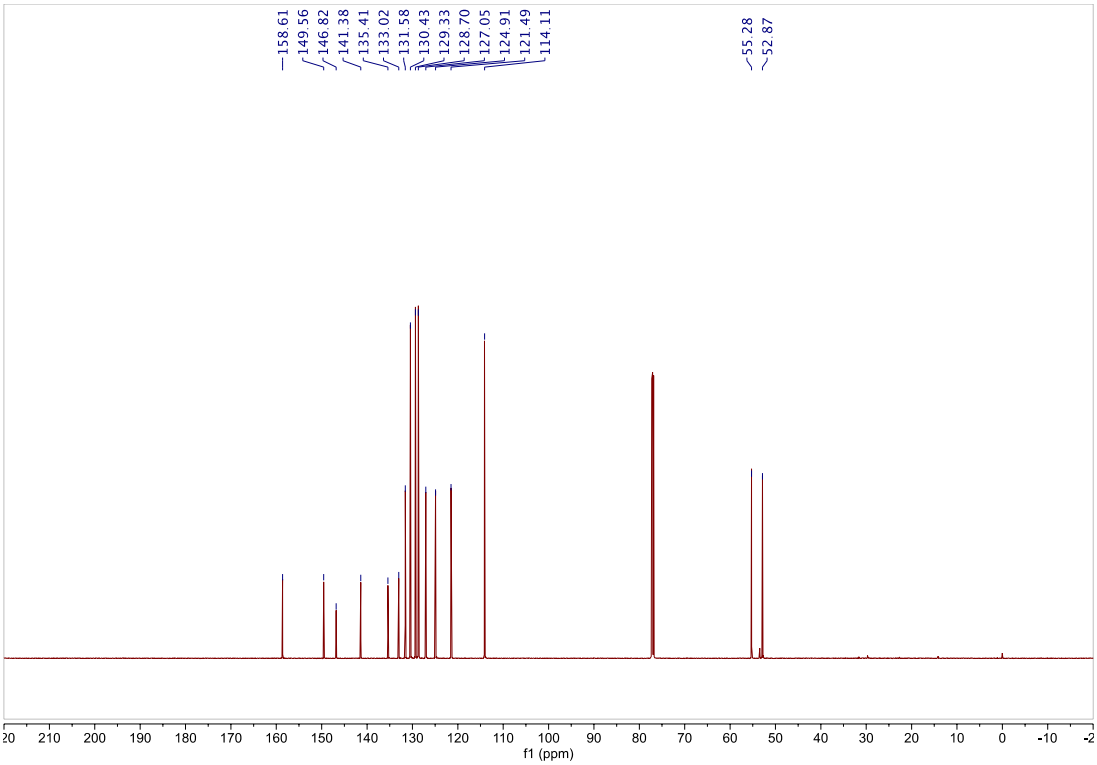

Compound 26

^{1}H NMR (600 MHz, $CDCl_3$)

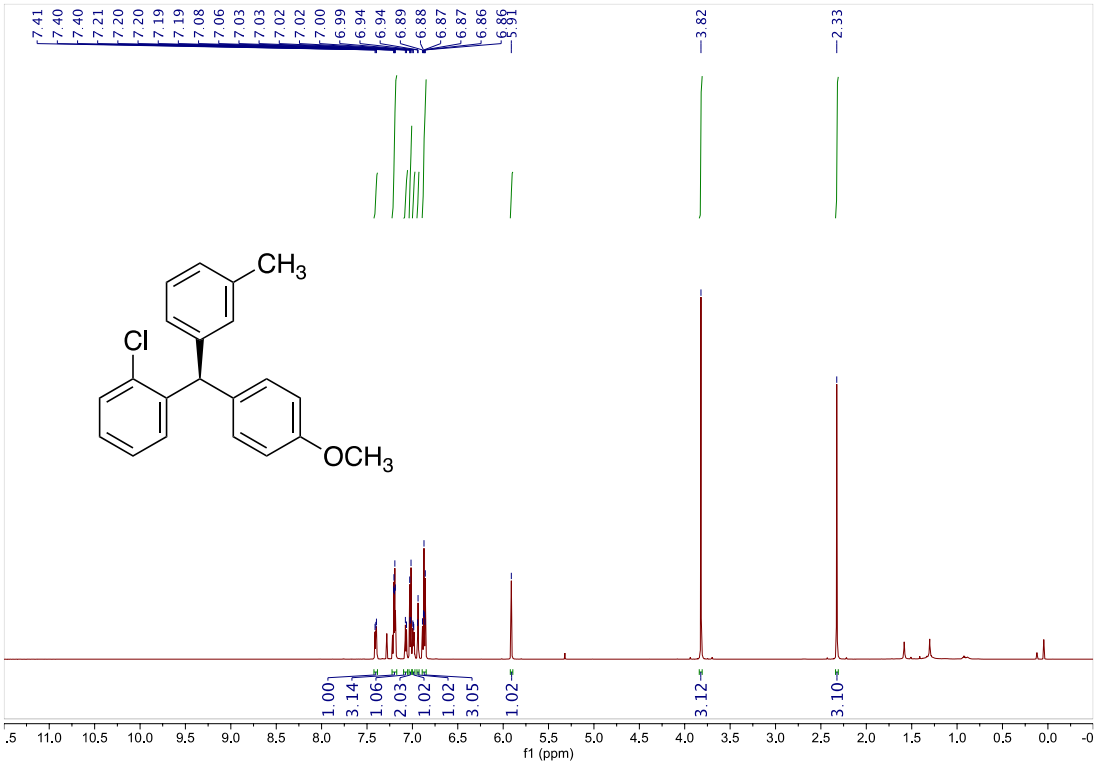

^{13}C NMR (600 MHz, $CDCl_3$)

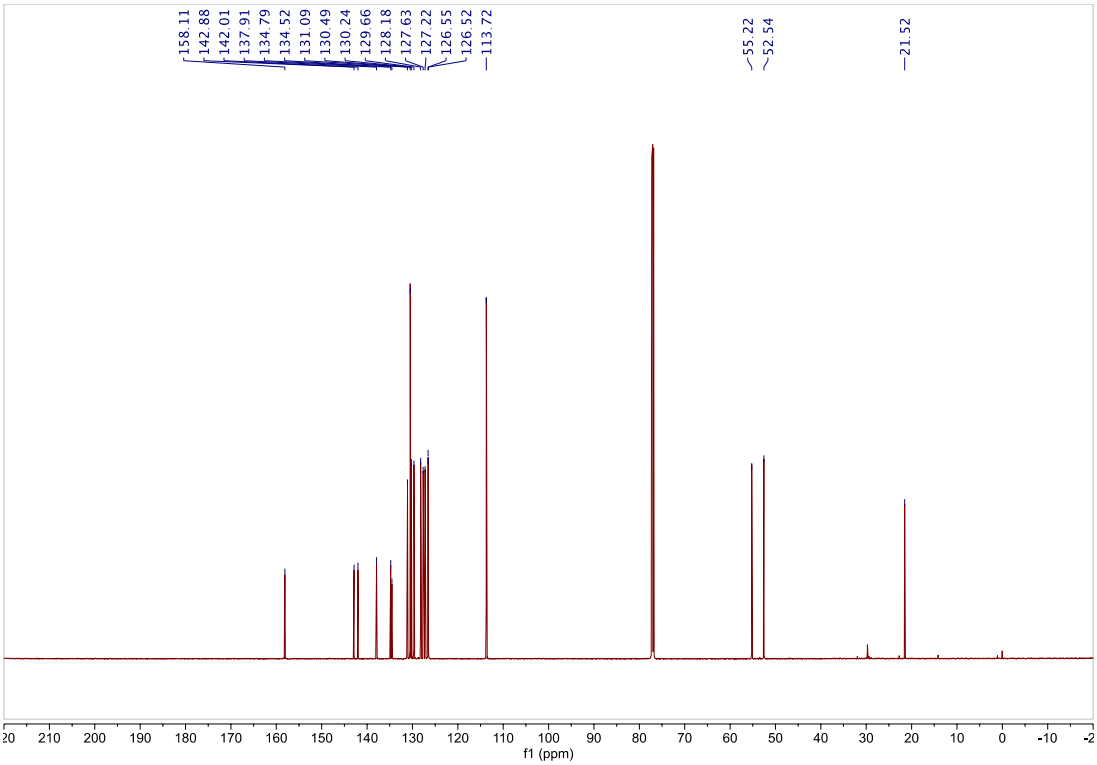

Compound 27

^{1}H NMR (600 MHz, $CDCl_3$)

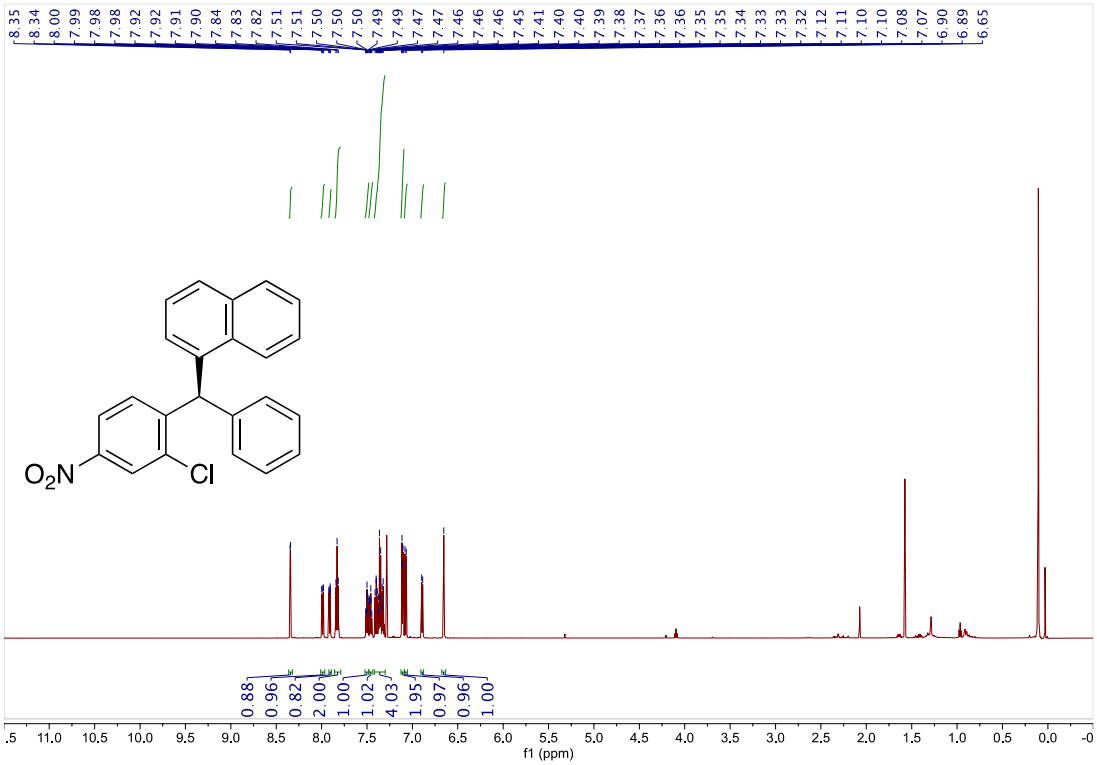

^{13}C NMR (600 MHz, $CDCl_3$)

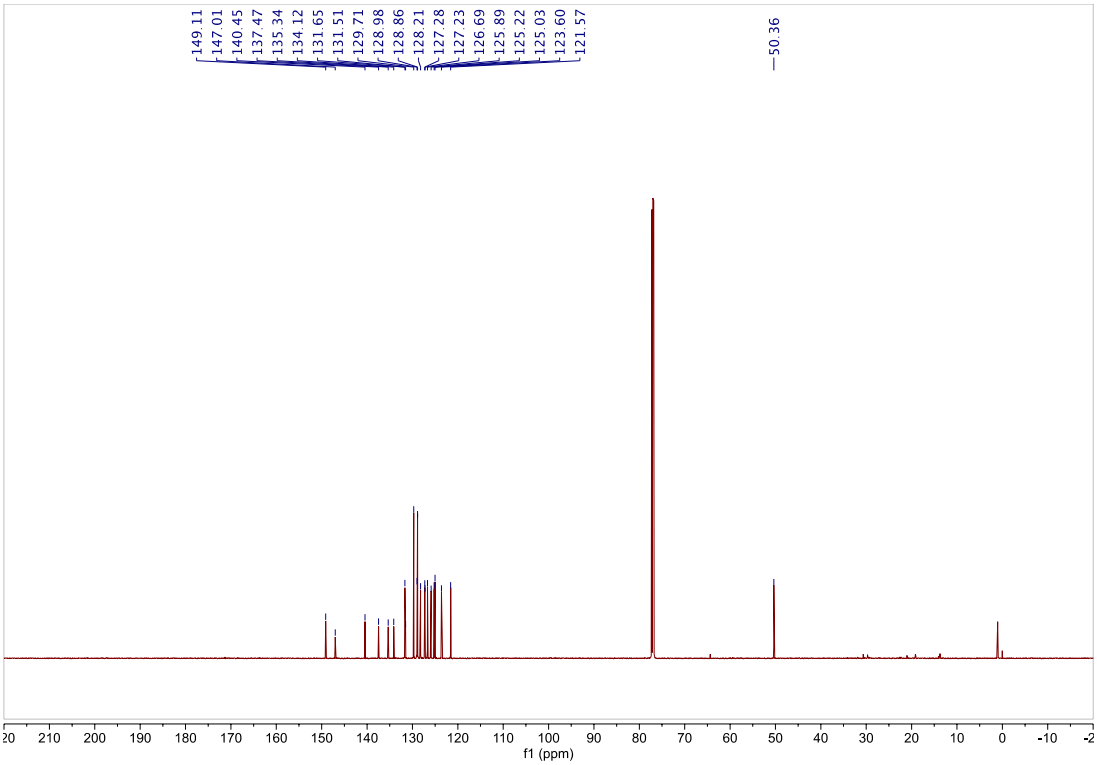

Compound 28

^{1}H NMR (400 MHz, $CDCl_3$)

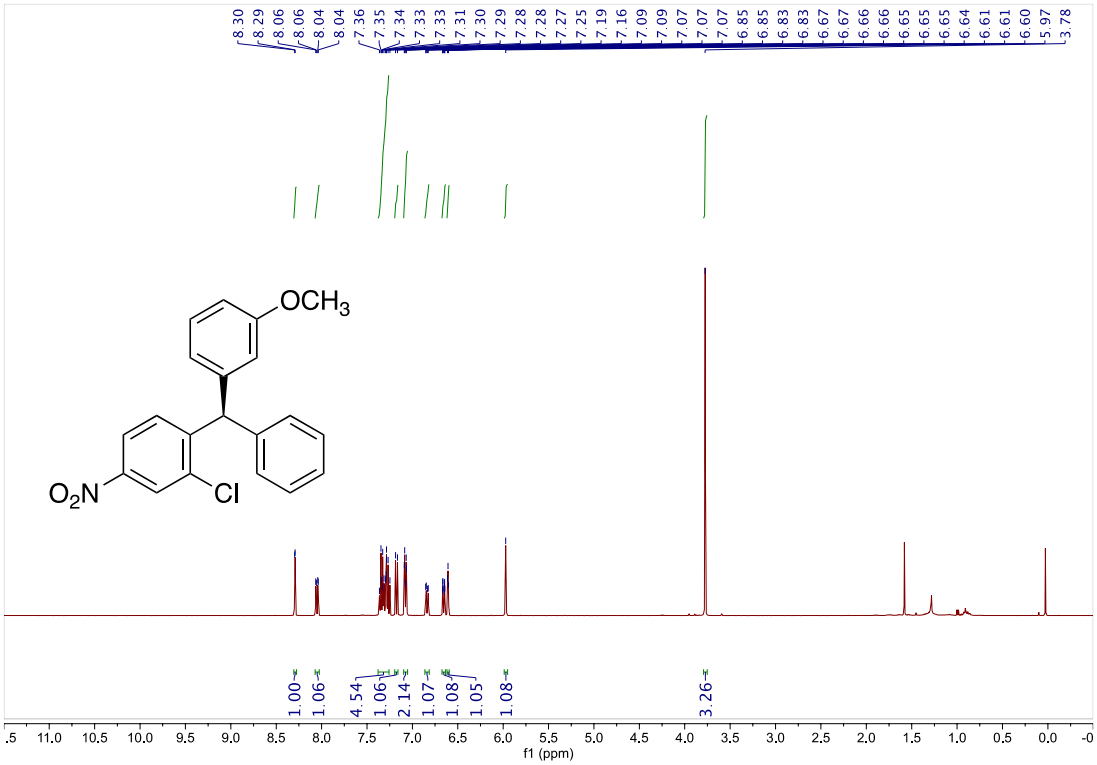

^{13}C NMR (400 MHz, $CDCl_3$)

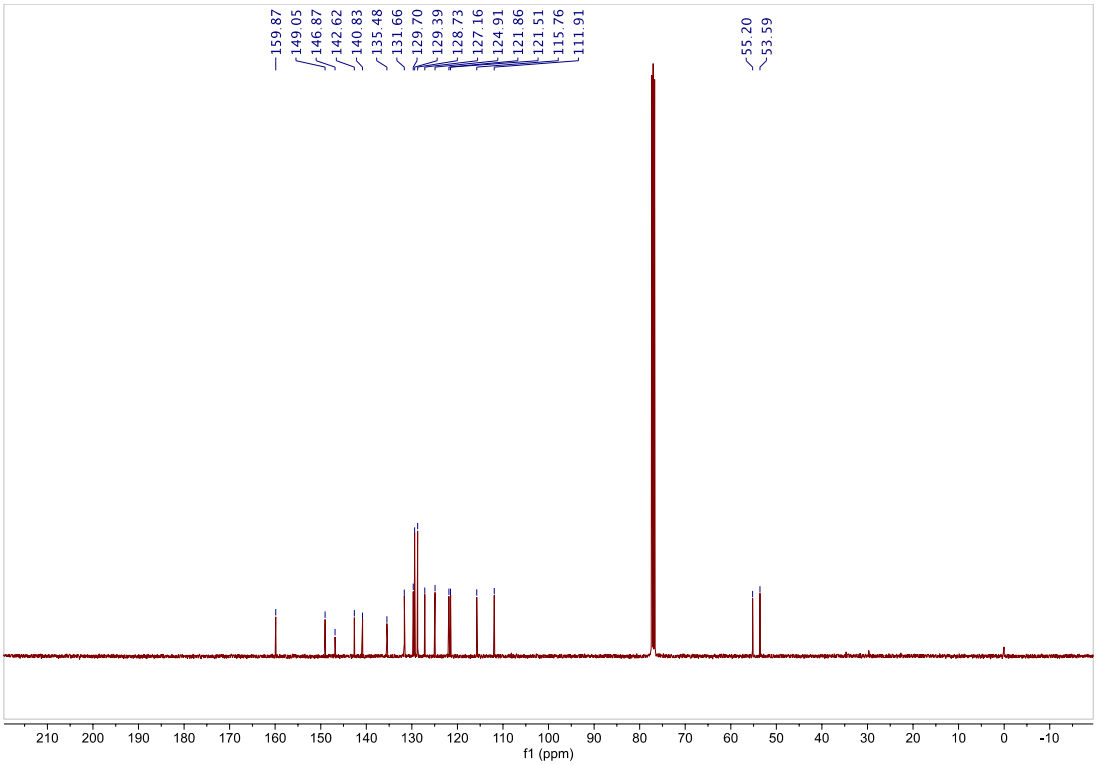

Compound 29

^{1}H NMR (400 MHz, $CDCl_3$)

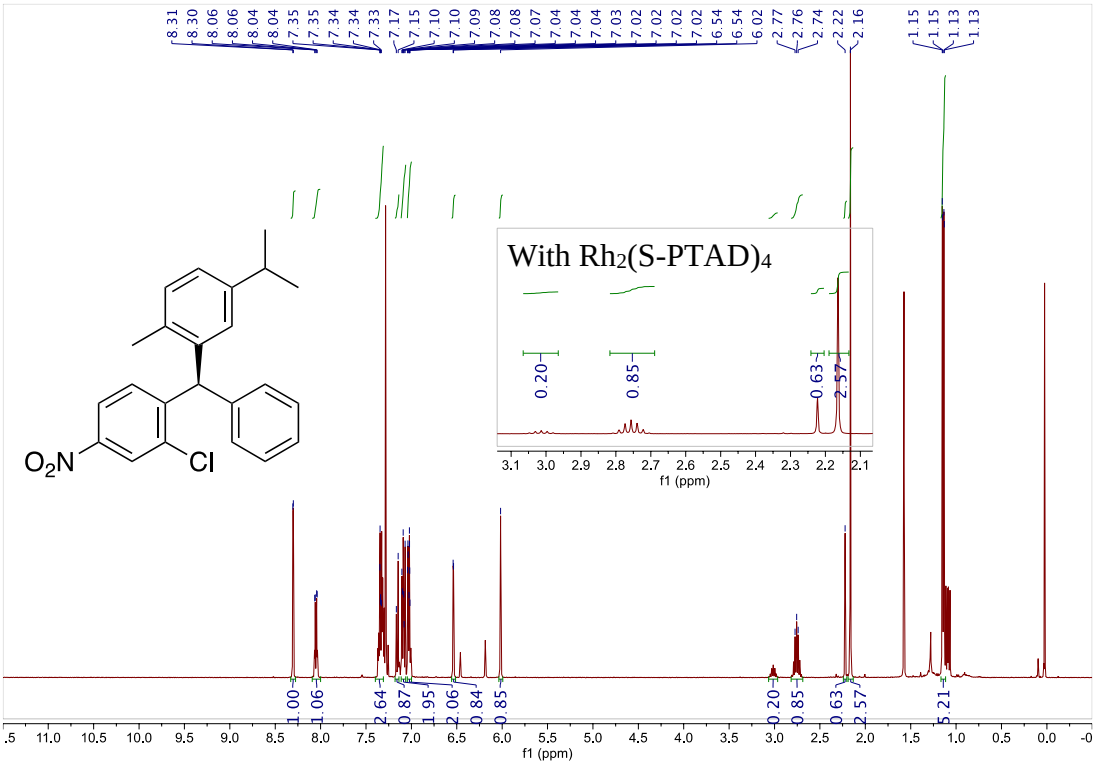

^{13}C NMR (400 MHz, $CDCl_3$)

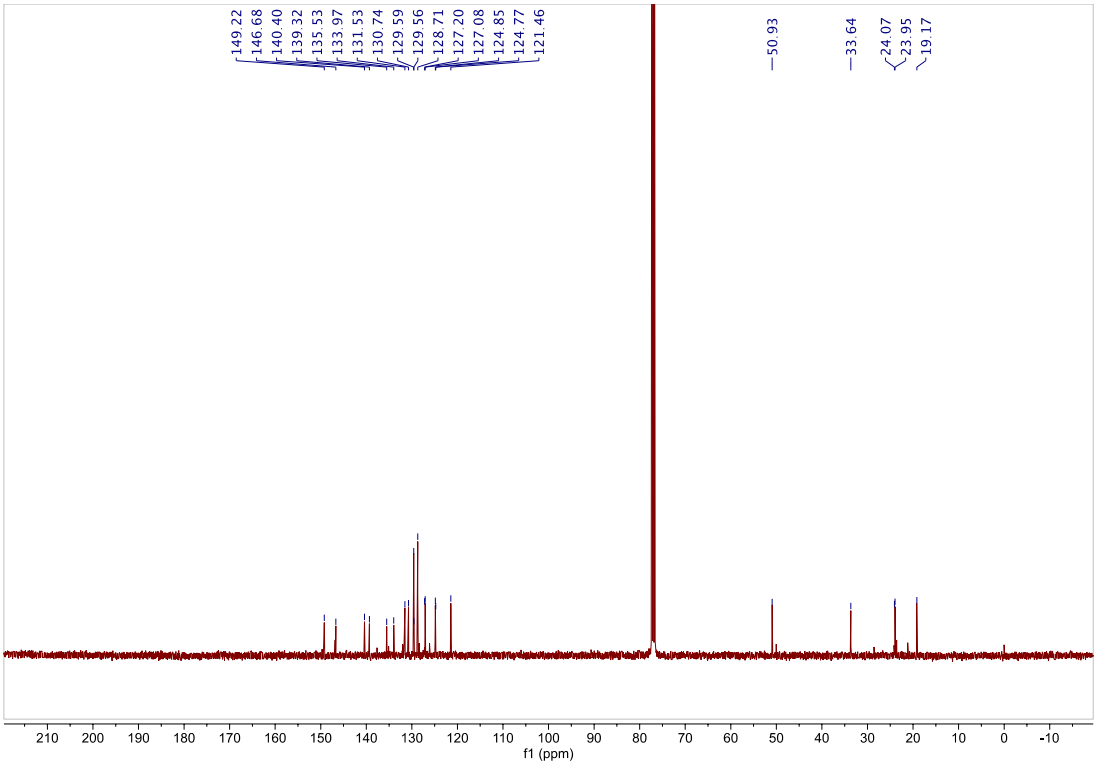

Compound 29 NOE
^{1}H-^{1}H COSY NMR (400 MHz, $CDCl_3$)

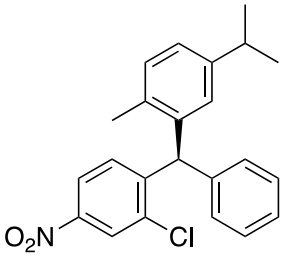

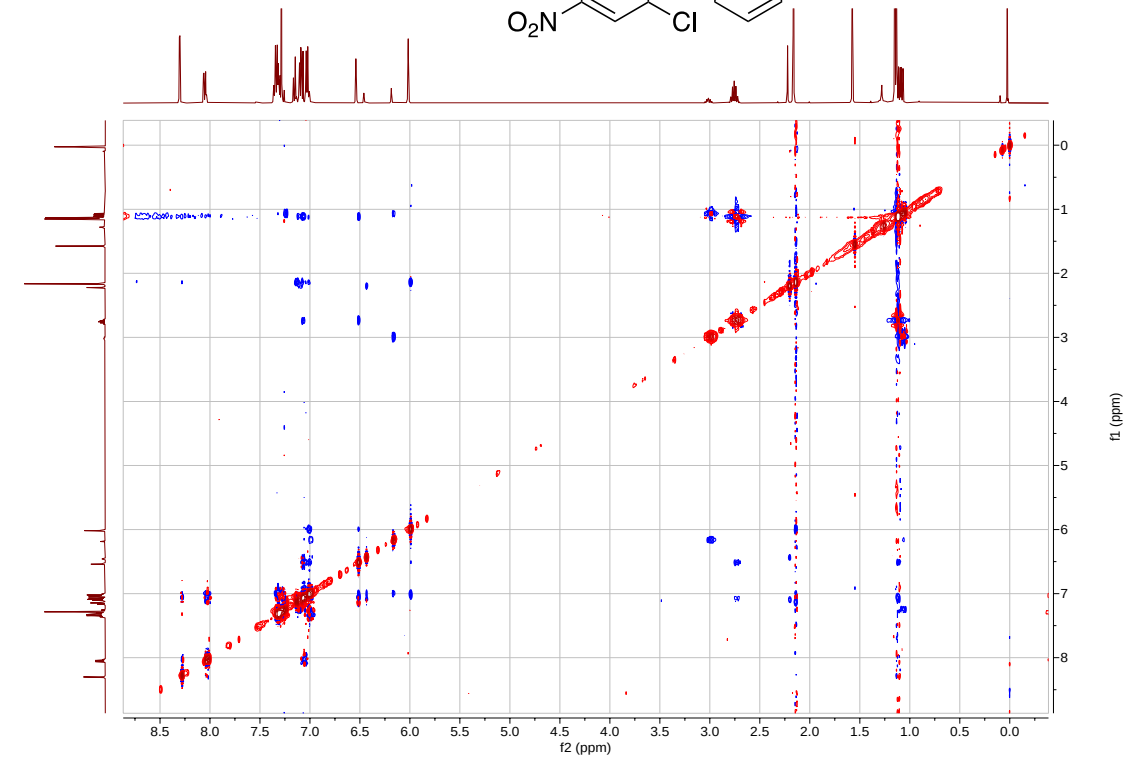

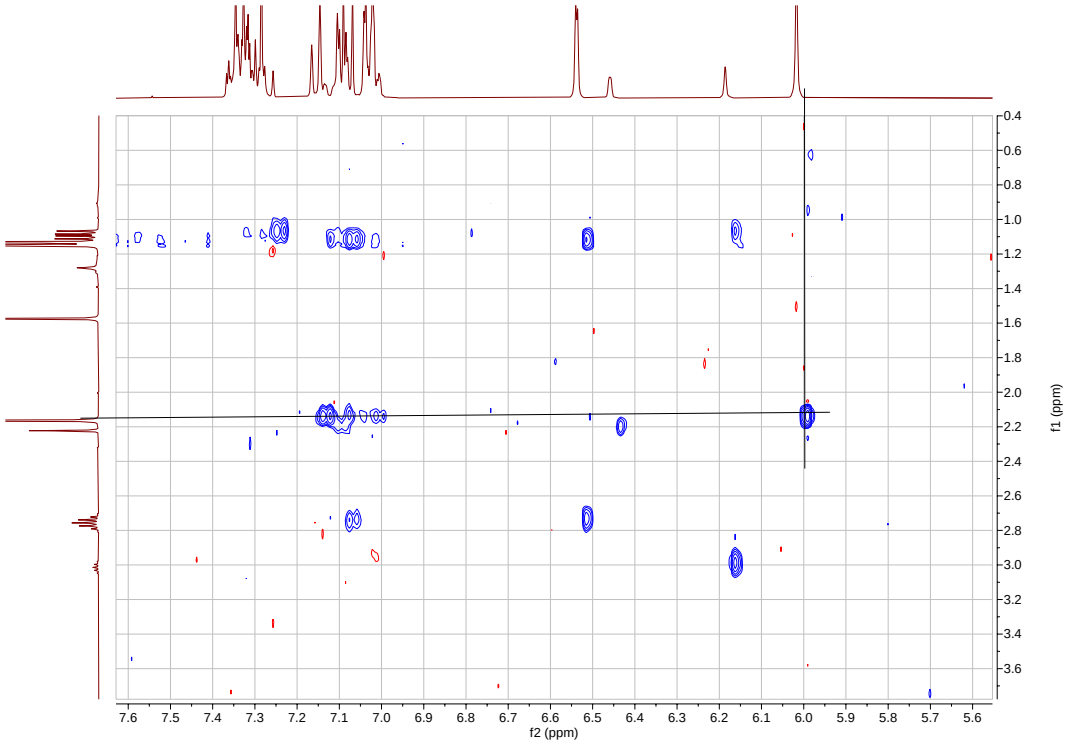

Compound 29
Crude **^{1}H NMR** (400 MHz, $CDCl_3$)
Selectivity with Rh_2(S-TPPTTL)$_4$

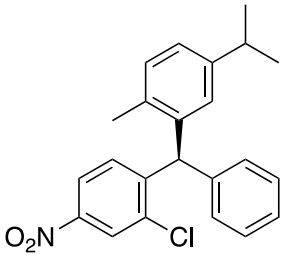

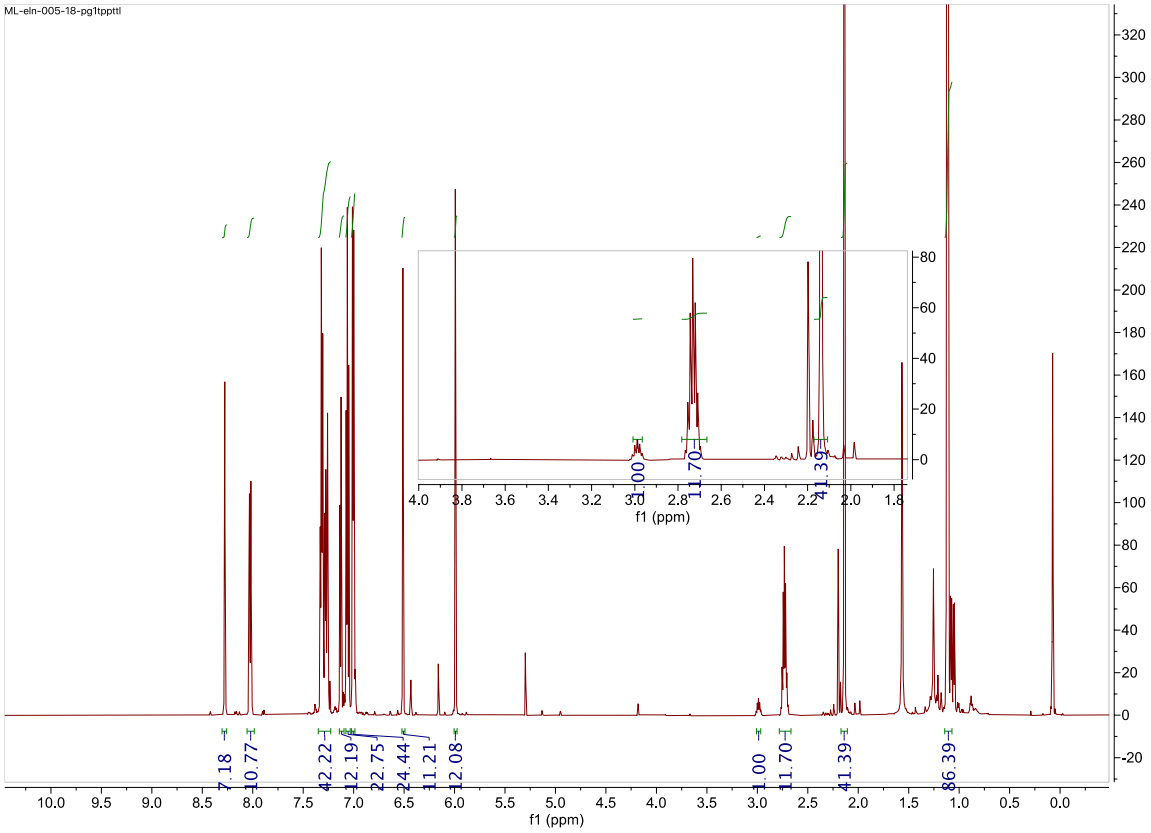

3.7 X-Ray Crystallographic Data for Compound 20a.

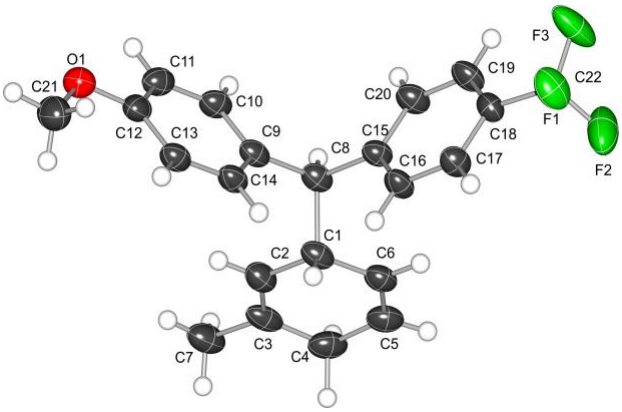

Experimental. Single colorless plate-shaped crystals of **Compound 20a.** were chosen from the sa mple as supplied. A suitable crystal with dimensions 0.36 × 0.27 × 0.14 mm^3 was selected and mounted on a loop with paratone on a XtaLAB Synergy diffractometer. The crystal was kept at a steady T = 100.00(10) K during data collection. The structure was solved with the ShelXT 2018/2 (Sheldrick, 2018) solution program using dual methods. The model was refined with **Jana2020** (Palatinus, 2020) using least squares minimisation on $\boldsymbol{F^2}$.

Crystal Data. $C_{22}H_{21}F_3O$, M_r = 358.4, monoclinic, $P2_1$ (No. 4), a = 7.331(2) Å, b = 6.002(2) Å, c = 21.088(4) Å, □ = 105.13(3)˚, □ = □ = 90˚, V = 895.7(4) $Å^3$, T = 100.00(10) K, Z = 2, Z' = 1, □(Cu K□) = 0.846, 11165 reflections measured, 3291 unique (R_{int} = 0.0536) which were used in all calculations. The final wR_2 was 0.1293 (all data) and R_1 was 0.0513 (I≥3 □(I)).

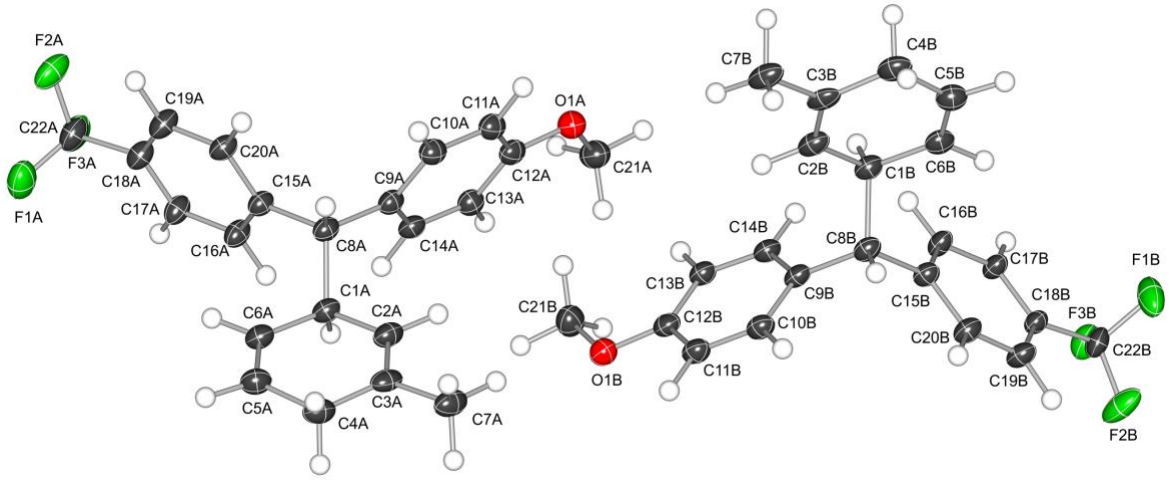

The repeating unit for the two overlapping twin domains treated as a single crystal .

3.8 HPLC Spectra for Enantioselectivity Determination

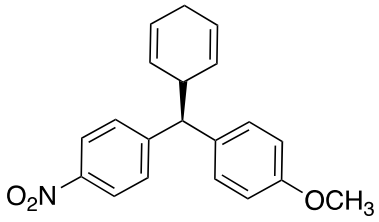

Compound 2-Table 1 Racemic Trace:

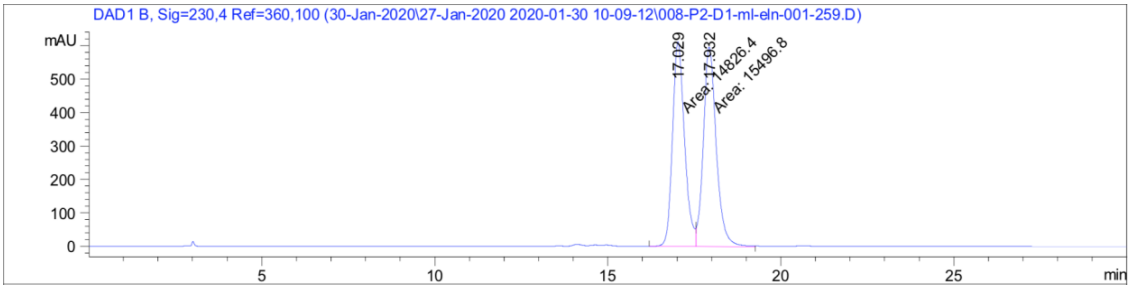

Signal 2: DAD1 B, Sig=230,4 Ref=360,100

Peak #	RetTime [min]	Type	Width [min]	Area [mAU*s]	Height [mAU]	Area %
1	17.029	MF	0.4038	1.48264e4	611.92981	48.8946
2	17.932	FM	0.4331	1.54968e4	596.41248	51.1054
Totals :				3.03232e4	1208.34229	

Compound 2- Table 1 Trace with Rh_2(*S*-DOSP)$_4$:

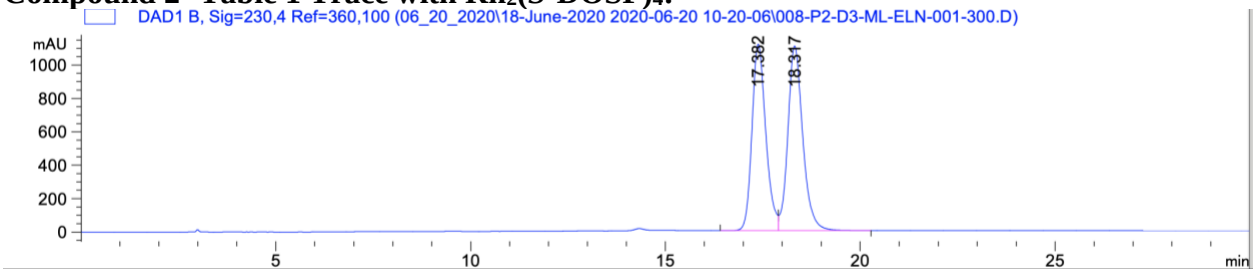

Signal 2: DAD1 B, Sig=230,4 Ref=360,100

Peak #	RetTime [min]	Type	Width [min]	Area [mAU*s]	Height [mAU]	Area %
1	17.382	BV	0.3794	2.76866e4	1116.22778	48.3530
2	18.317	VB	0.4061	2.95726e4	1105.29822	51.6470
Totals :				5.72592e4	2221.52600	

HPLC (ADH column, 1.0 mL/min 1% i-PrOH in n-hexane 30 min, UV 230 nm) retention times of 17.38 (minor) and 18.32 min (major) 3 % ee with Rh_2(*S*-DOSP)$_4$.

Compound 2- Table 1 Trace with Rh_2(*S*-2Cl-5BRTPCP)$_4$:

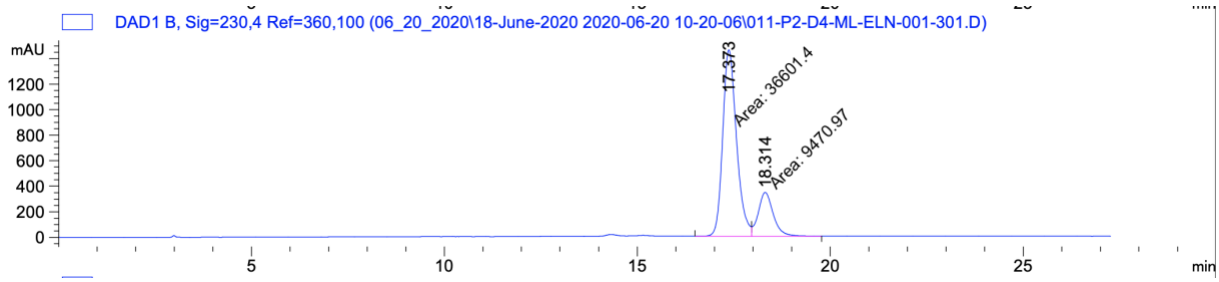

Signal 2: DAD1 B, Sig=230,4 Ref=360,100

Peak #	RetTime [min]	Type	Width [min]	Area [mAU*s]	Height [mAU]	Area %
1	17.373	MF	0.4172	3.66014e4	1462.27087	79.4433
2	18.314	FM	0.4577	9470.96973	344.90491	20.5567
Totals :				4.60724e4	1807.17578	

HPLC (ADH column, 1.0 mL/min 1% i-PrOH in n-hexane 30 min, UV 230 nm) retention times of 17.37 (minor) and 18.31 min (major) -79 % ee with Rh_2(*S*-2CL5BrTPCP)$_4$.

Compound 2- Table 1 Trace with Rh_2(*S*-NTTL)$_4$:

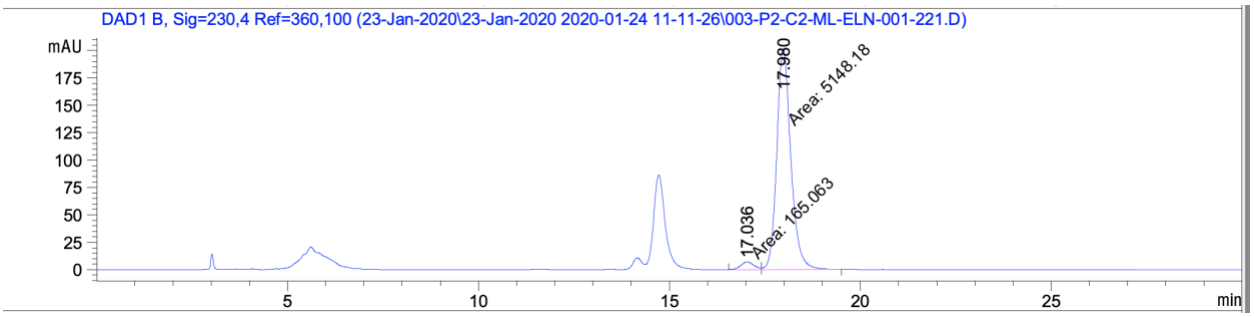

Signal 2: DAD1 B, Sig=230,4 Ref=360,100

Peak #	RetTime [min]	Type	Width [min]	Area [mAU*s]	Height [mAU]	Area %
1	17.036	MF	0.3915	165.06316	7.02773	3.1066
2	17.980	FM	0.4257	5148.18408	201.54683	96.8934
Totals :				5313.24724	208.57456	

HPLC (ADH column, 1.0 mL/min 1% i-PrOH in n-hexane 30 min, UV 230 nm) retention times of 17.1(minor) and 18.0min (major) 94 % ee with Rh_2(*S*-TPPTTL)$_4$.

Compound 2- Table 1 Trace with Rh_2(*S*-TPPTTL)$_4$:

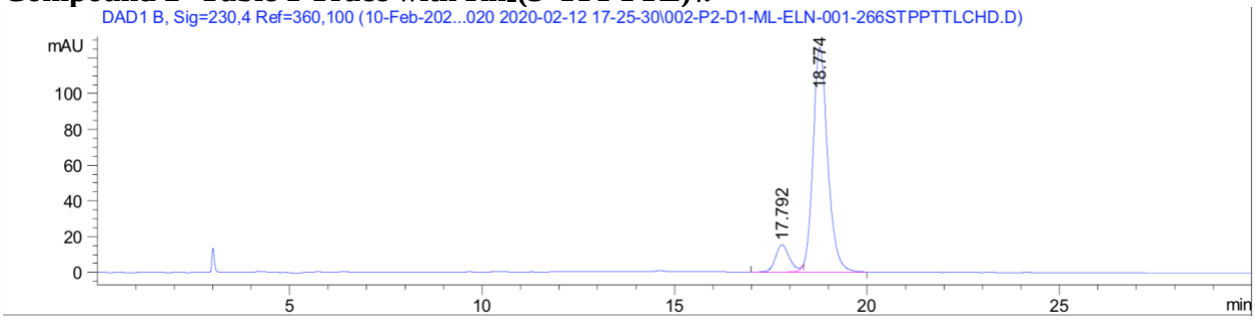

Signal 2: DAD1 B, Sig=230,4 Ref=360,100

Peak #	RetTime [min]	Type	Width [min]	Area [mAU*s]	Height [mAU]	Area %
1	17.792	BV E	0.3768	378.00079	15.27041	10.1628
2	18.774	VB R	0.4041	3341.45801	125.69870	89.8372
Totals :				3719.45880	140.96911	

HPLC (ADH column, 1.0 mL/min 1% i-PrOH in n-hexane 30 min, UV 230 nm) retention times of 17.80 (minor) and 18.77 min (major) 79 % ee with Rh_2(*S*-TPPTTL)$_4$.

Compound 2- Table 1 Trace with Rh_2(*S*-PTTLL)$_4$:

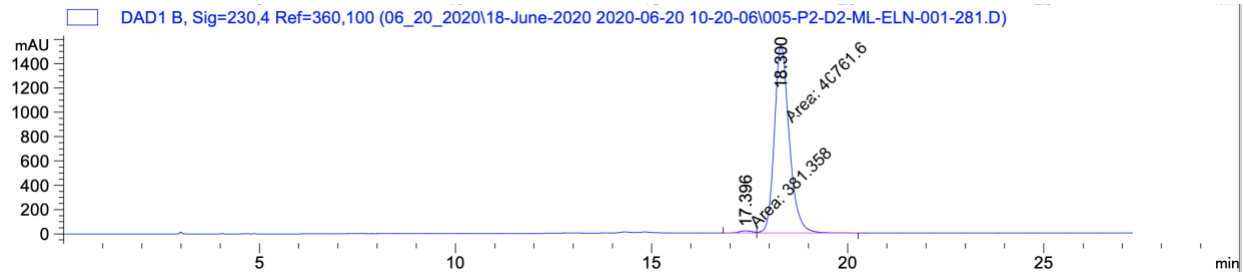

Signal 2: DAD1 B, Sig=230,4 Ref=360,100

Peak #	RetTime [min]	Type	Width [min]	Area [mAU*s]	Height [mAU]	Area %
1	17.396	MF	0.3778	381.35757	16.82251	0.9269
2	18.300	FM	0.4406	4.07616e4	1541.95007	99.0731
Totals :				4.11430e4	1558.77259	

HPLC (ADH column, 1.0 mL/min 1% i-PrOH in n-hexane 30 min, UV 230 nm) retention times of 17.40 (minor) and 18.3 min (major) 98 % ee with Rh_2(*S*-PTTL)$_4$.

Compound 2- Table 1 Trace with Rh_2(*S*-TCPTAD)$_4$:

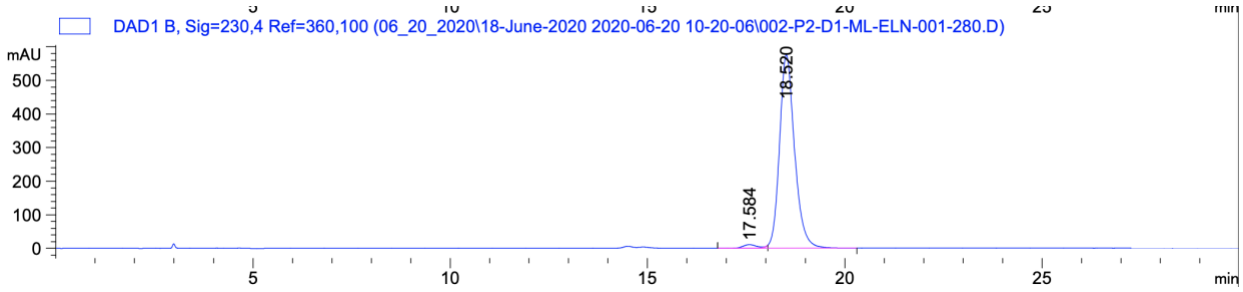

Signal 2: DAD1 B, Sig=230,4 Ref=360,100

Peak #	RetTime [min]	Type	Width [min]	Area [mAU*s]	Height [mAU]	Area %
1	17.584	BV E	0.3710	262.74722	10.83318	1.6928
2	18.520	VB R	0.4034	1.52584e4	575.31097	98.3072
Totals :				1.55211e4	586.14416	

HPLC (ADH column, 1.0 mL/min 1% i-PrOH in n-hexane 30 min, UV 230 nm) retention times of 17.58 (minor) and 18.52 min (major) 97 % ee with Rh_2(*S*-TCPTAD)$_4$.

Compound 2- Table 1 Trace with Rh_2(*S*-PTAD)$_4$:

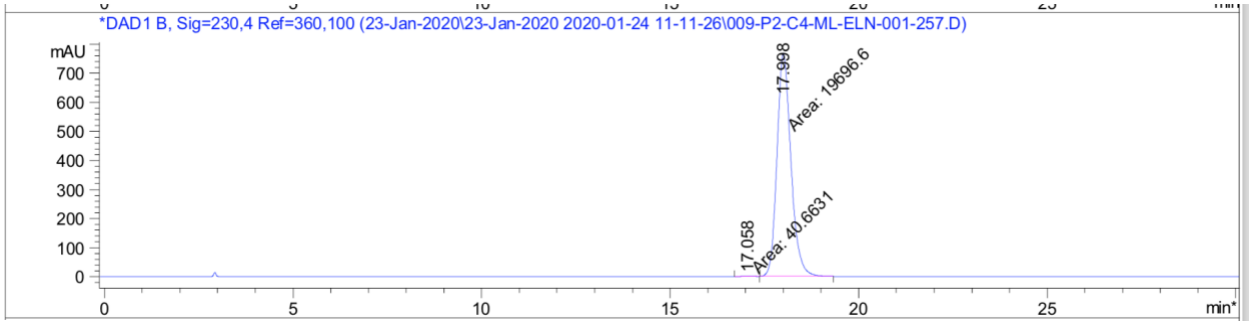

Peak #	Ret Time [min]	Type	Width [min]	Area [mAU*s]	Height [mAU]	Area %
1	17.058	MM	0.3362	40.66310	2.01585	0.2060
2	17.998	MM	0.4271	1.96966e4	768.57556	99.7940
Totals :				1.97372e4	770.59141	

HPLC (ADH column,1.0 mL/min 1% i-PrOH in n-hexane 30 min, UV 230 nm) retention times of 17.06 (minor) and 18.00 min (major) 99 % ee with Rh_2(*S*-PTAD)$_4$.

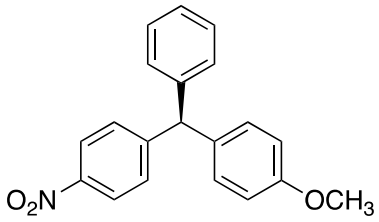

Compound 8-Racemic:

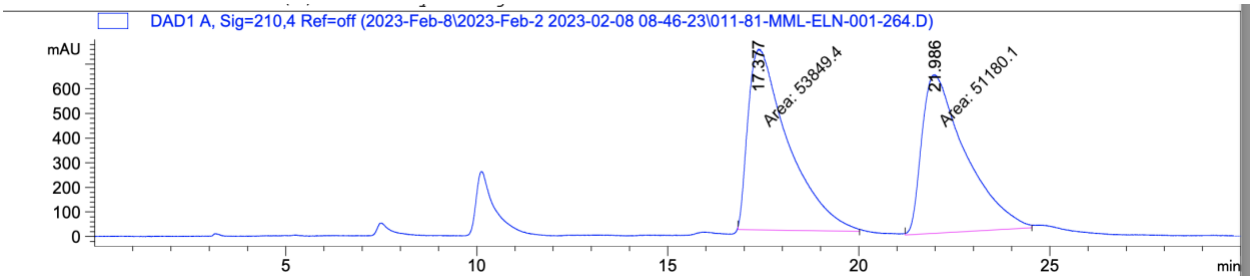

Peak #	RetTime [min]	Type	Width [min]	Area [mAU*s]	Height [mAU]	Area %
1	17.390	MM	1.2610	2.61256e4	345.30624	50.7963
2	21.995	MM	1.4203	2.53064e4	296.96356	49.2037
Totals :				5.14320e4	642.26981	

Compound 8 Trace with Rh_2(*S*-PTAD)$_4$:

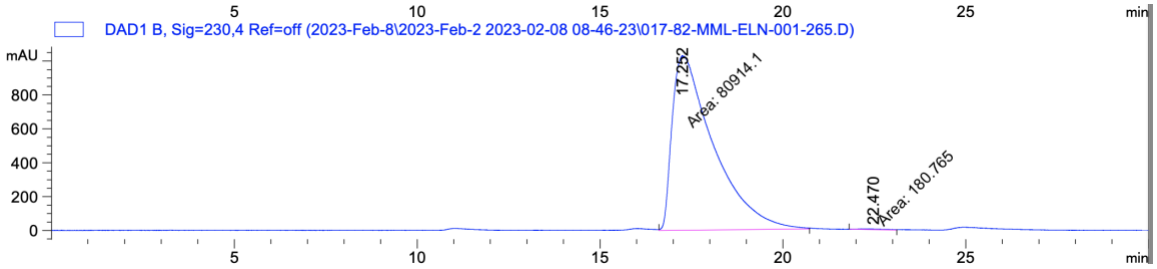

Signal 2: DAD1 B, Sig=230,4 Ref=off

Peak #	RetTime [min]	Type	Width [min]	Area [mAU*s]	Height [mAU]	Area %
1	17.252	MM	1.3081	8.09141e4	1030.96216	99.7771
2	22.470	MM	0.8065	180.76530	3.73546	0.2229
Totals :				8.10949e4	1034.69762	

HPLC (OD column,1.0 mL/min 1% i-PrOH in n-hexane 30 min, UV 230 nm) retention times of 17.3 (major) and 22.5 min (minor) 99% ee with Rh_2(*S*-PTAD)$_4$.

Compound 8- Rh_2(*S*-PTAD)$_4$: 1mmol scale

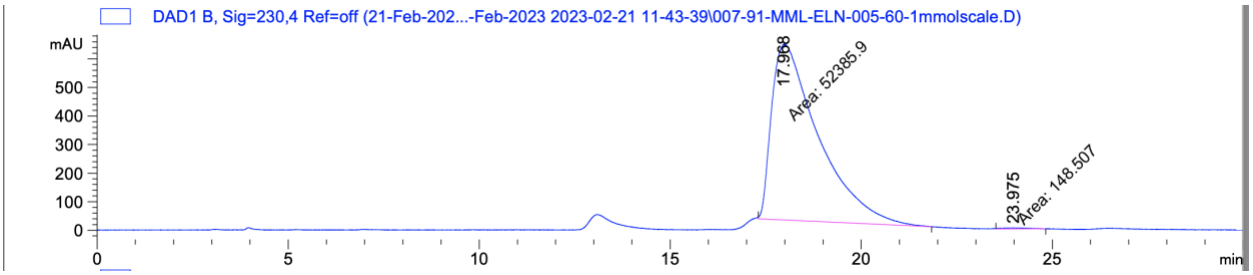

Peak #	RetTime [min]	Type	Width [min]	Area [mAU*s]	Height [mAU]	Area %
1	17.968	MM	1.4183	5.23859e4	615.59192	99.7173
2	23.975	MM	0.6302	148.50720	3.92752	0.2827
Totals :				5.25345e4	619.51944	

HPLC (OD column,1.0 mL/min 1% i-PrOH in n-hexane 30 min, UV 230 nm) retention times of 17.9 (major) and 23.9 min (minor) 99% ee with Rh_2(*S*-PTAD)$_4$.

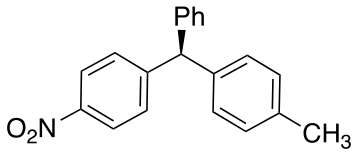

Compound 9-Racemic

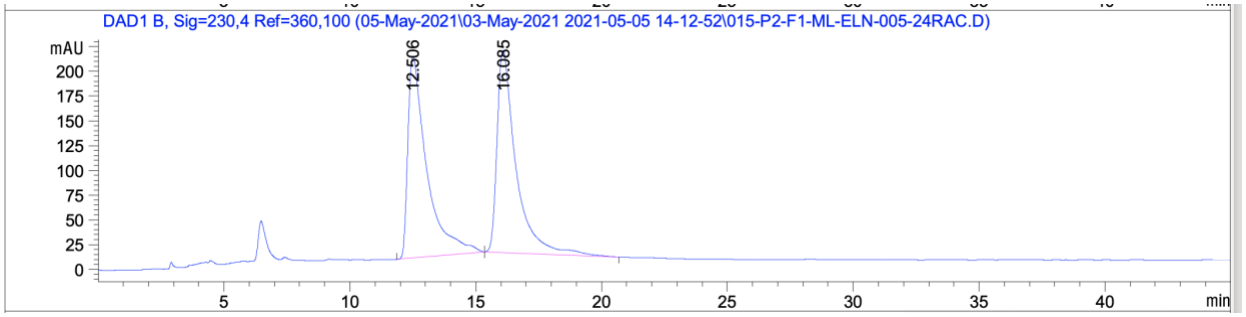

Signal 2: DAD1 B, Sig=230,4 Ref=360,100

Peak #	RetTime [min]	Type	Width [min]	Area [mAU*s]	Height [mAU]	Area %
1	12.506	BB	0.7440	1.06622e4	203.26964	49.9128
2	16.085	BB	0.7555	1.06995e4	204.14397	50.0872
Totals :				2.13617e4	407.41360	

Compound 9 Trace with Rh_2(*S*-PTAD)$_4$:

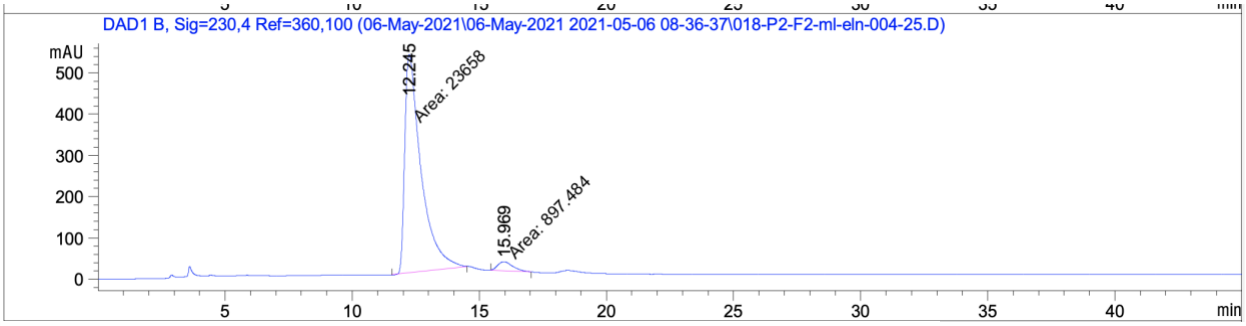

Signal 2: DAD1 B, Sig=230,4 Ref=360,100

Peak #	RetTime [min]	Type	Width [min]	Area [mAU*s]	Height [mAU]	Area %
1	12.245	MM	0.7448	2.36580e4	529.37201	96.3451
2	15.969	MM	0.6764	897.48407	22.11265	3.6549
Totals :				2.45555e4	551.48466	

HPLC (ODH column, 1.0 mL/min 0.5 % i-PrOH in n-hexane 45 min, UV 230 nm) retention times of 12.25 (major) and 15.97 min (minor) 93 % ee with Rh_2(S-PTAD)$_4$.

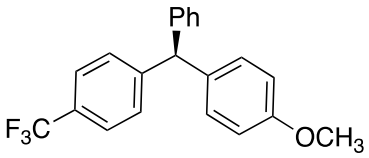

Compound 10 Racemic:

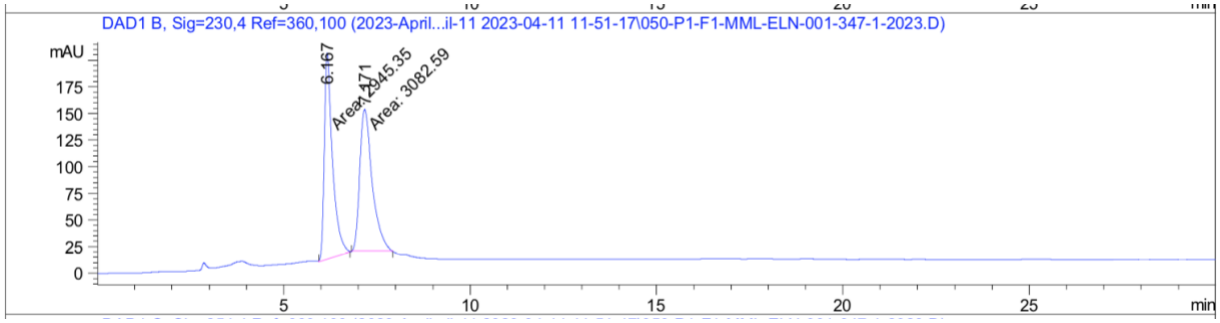

Signal 2: DAD1 B, Sig=230, 4 Ref=360, 100

Peak #	Ret Time [min]	Type	Width [min]	Area [mAU*s]	Height [mAU]	Area %
1	6.167	MM	0.2535	2945.35327	193.61526	48.8617
2	7.171	MM	0.3869	3082.59058	132.77647	51.1383
Totals :				6027.94385	326.39174	

Compound 10 Trace with Rh_2(*S*-PTAD)$_4$:

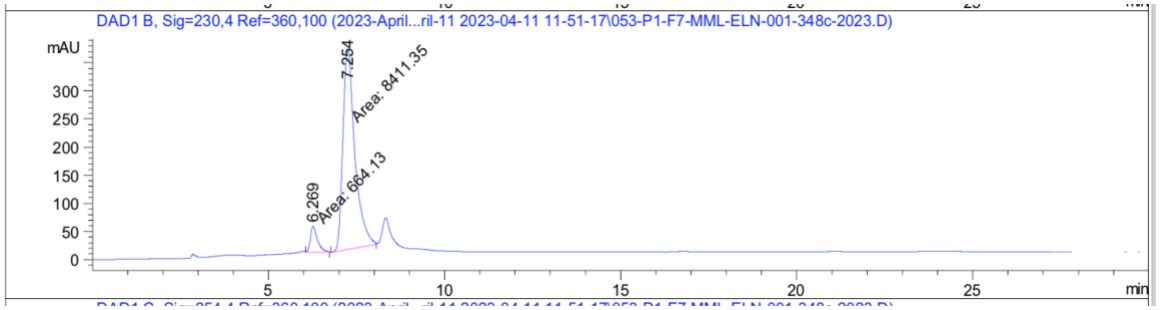

Signal 2: DAD1 B, Sig=230, 4 Ref=360, 100

Peak #	Ret Time [min]	Type	Width [min]	Area [mAU*s]	Height [mAU]	Area %
1	6.269	MM	0.2369	664.13013	46.72340	7.3179
2	7.254	MM	0.3939	8411.34668	355.90387	92.6821
Totals :				9075.47681	402.62727	

HPLC (ODH column, hexane, 1.0 mL/min 0.5% *i*-PrOH in *n*-hexane 25 min, UV 230 nm) retention times of 6.2 (minor) and 7.2 min (major) 85 % ee with Rh_2(S-PTAD)$_4$

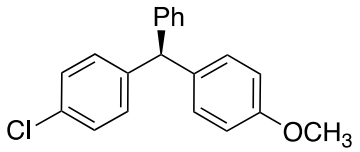

Compound 11 Racemic:

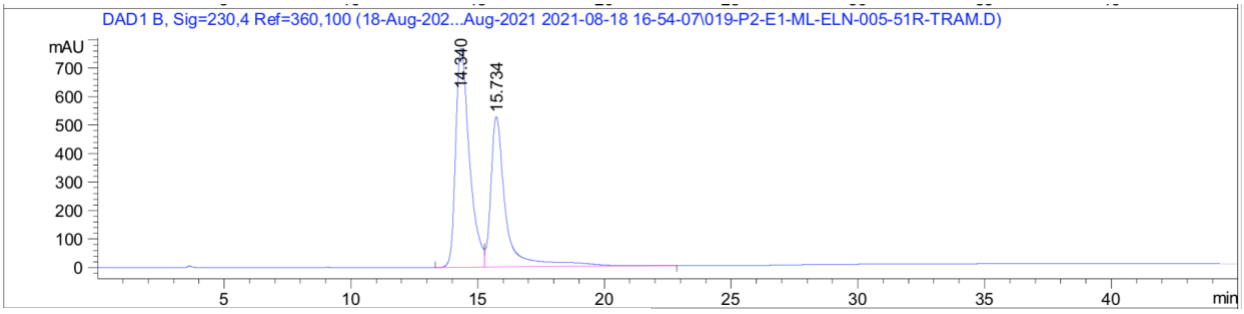

Signal 2: DAD1 B, Sig=230, 4 Ref=360, 100

Peak #	Ret Time [min]	Type	Width [min]	Area [mAU*s]	Height [mAU]	Area %
1	14.340	BV	0.5670	2.90592e4	768.75085	56.6860
2	15.734	VB	0.6112	2.22043e4	527.37427	43.3140
Totals :				5.12636e4	1296.12512	

Compound 11 Trace with Rh_2(*S*-PTAD)$_4$:

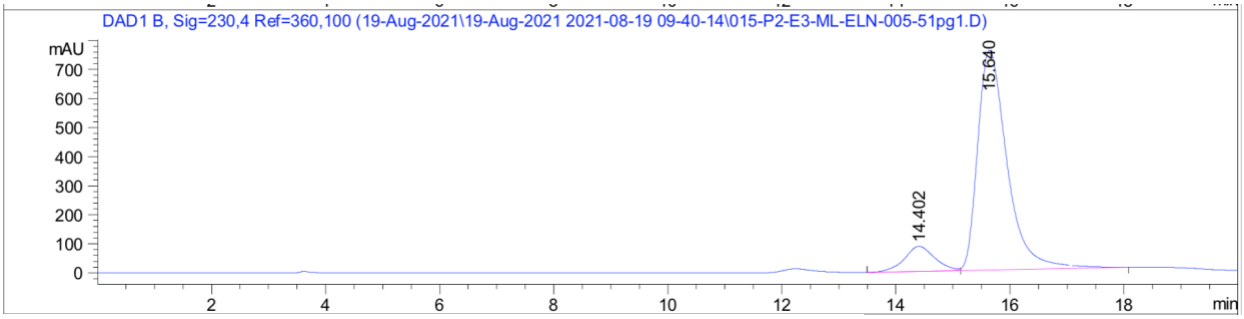

Signal 2: DAD1 B, Sig=230, 4 Ref=360, 100

Peak #	Ret Time [min]	Type	Width [min]	Area [mAU*s]	Height [mAU]	Area %
1	14.402	BV E	0.5514	3197.94141	86.48994	10.5457
2	15.640	VB R	0.5489	2.71266e4	755.56897	89.4543
Totals :				3.03246e4	842.05891	

HPLC (ODH column, hexane, 0.8 mL/min 0.2% i-PrOH in n-hexane 20 min, UV 230 nm) retention times of 14.40 (minor) and 15.64 min (major) 79 % ee with Rh_2(S-PTAD)$_4$.

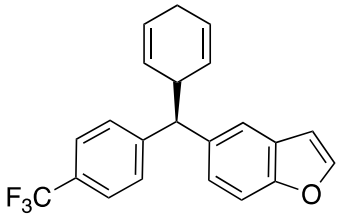

Compound 12-C-H insertion product Racemic:

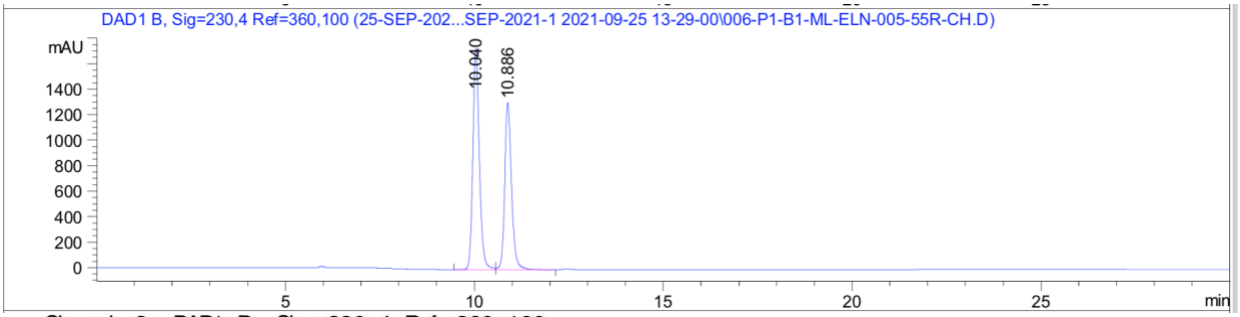

Signal 2: DAD1 B, Sig=230, 4 Ref=360, 100

Peak #	Ret Time [min]	Type	Width [min]	Area [mAU*s]	Height [mAU]	Area %
1	10.040	VV R	0.1827	2.09414e4	1733.34412	55.9860
2	10.886	VB	0.1884	1.64633e4	1312.39636	44.0140
Totals :				3.74048e4	3045.74048	

Compound 12-C-H insertion Trace with Rh_2(*S*-PTAD)$_4$:

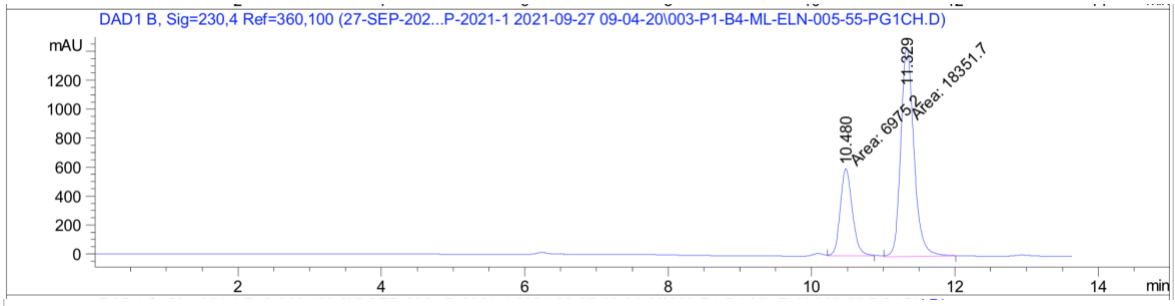

Signal 2: DAD1 B, Sig=230, 4 Ref=360, 100

Peak #	Ret Time [min]	Type	Width [min]	Area [mAU*s]	Height [mAU]	Area %
1	10.480	MM	0.1932	6975.20166	601.83905	27.5407
2	11.329	MM	0.2114	1.83517e4	1446.64294	72.4593
Totals :				2.53269e4	2048.48199	

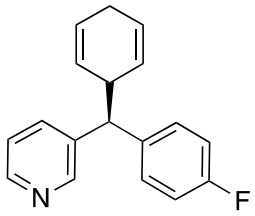

Compound C-H insertion product -Racemic

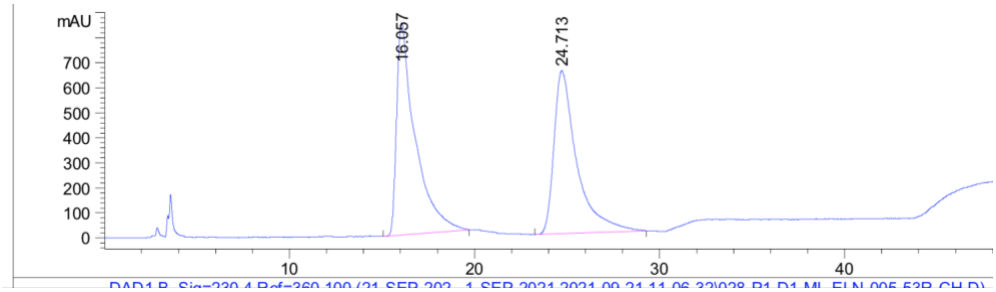

Signal 2: DAD1 B, Sig=230,4 Ref=360,100

Peak #	RetTime [min]	Type	Width [min]	Area [mAU*s]	Height [mAU]	Area %
1	16.057	BB	0.9639	1.82063e4	264.89426	50.8038
2	24.711	BB	1.2796	1.76302e4	204.14148	49.1962

1290 LC 9/22/2021 9:42:37 AM SYSTEM

Data File C:\Users\P...-2021\21-SEP-2021 2021-09-21 11-06-32\0
Sample Name: ML-ELN-005-53R-CH

Peak #	RetTime [min]	Type	Width [min]	Area [mAU*s]	Height [mAU]	Area %
Totals :				3.58366e4	469.03574	

Compound 13 C-H insertion product Rh_2(*S*-PTAD)$_4$:

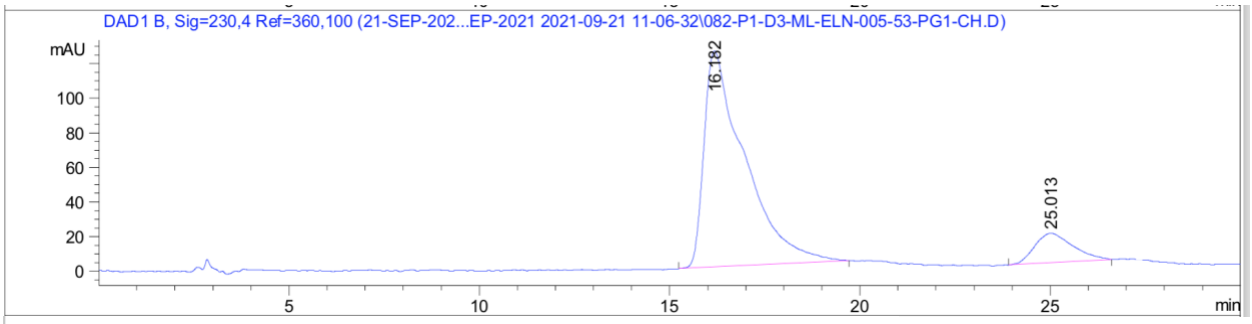

Signal 2: DAD1 B, Sig=230, 4 Ref=360, 100

Peak #	Ret Time [min]	Type	Width [min]	Area [mAU*s]	Height [mAU]	Area %
1	16.182	BB	1.0178	9286.60059	124.84396	88.5410
2	25.013	BB	0.9458	1201.87012	17.10319	11.4590
Totals :				1.04885e4	141.94715	

HPLC (ADH column, 1.0 mL/min 2.25 % i-PrOH in n-hexane 30 min, UV 230 nm) retention times of 16.2 (major) and 25.03 min (minor) 77 % ee with Rh_2(S-PTAD)$_4$.

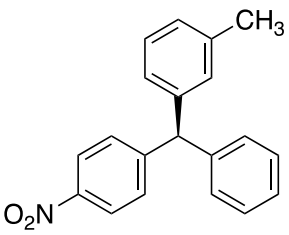

Compound 14 -Racemic

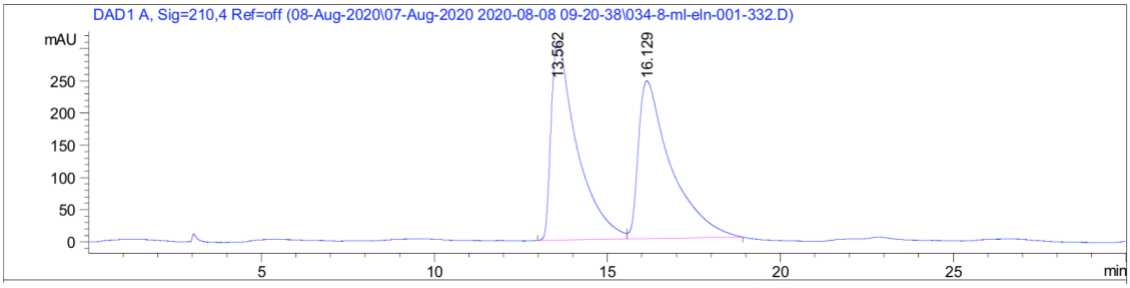

Signal 1: DAD1 A, Sig=210,4 Ref=off

Peak #	RetTime [min]	Type	Width [min]	Area [mAU*s]	Height [mAU]	Area %
1	13.562	VV R	0.6122	1.60869e4	308.32913	50.0392
2	16.129	VV R	0.7686	1.60617e4	245.07031	49.9608
Totals :				3.21485e4	553.39944	

Compound 14 Trace with Rh_2(*S*-PTAD)$_4$:

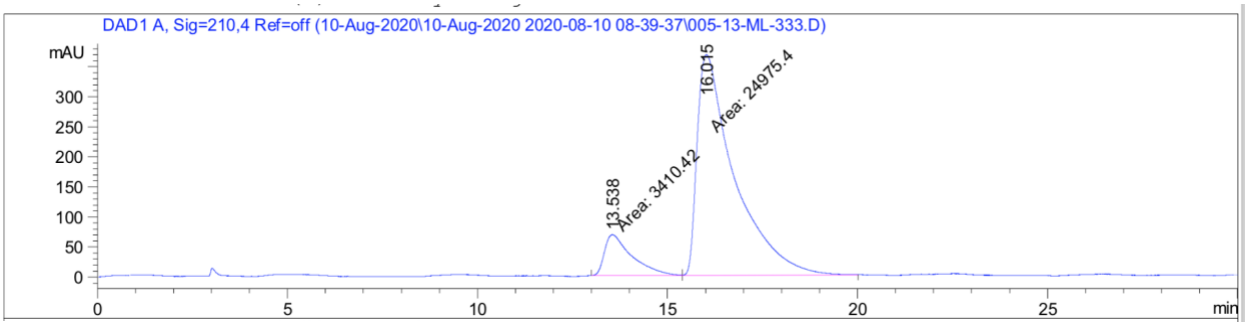

Signal 1: DAD1 A, Sig=210,4 Ref=off

Peak #	RetTime [min]	Type	Width [min]	Area [mAU*s]	Height [mAU]	Area %
1	13.538	MF	0.8326	3410.42017	68.26711	12.0145
2	16.015	FM	1.1330	2.49754e4	367.40823	87.9855
Totals :				2.83858e4	435.67534	

HPLC (OD column, 1.0 mL/min 0.5 % i-PrOH in n-hexane 30 min, UV 210 nm) retention times of 13.54 (minor) and 16.02 min (majorr) 76 % ee with Rh_2(S-PTAD)$_4$.

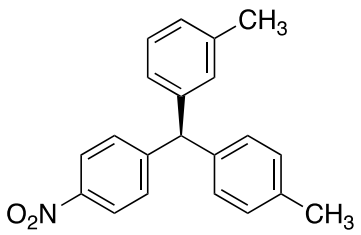

Compound 15 -Racemic

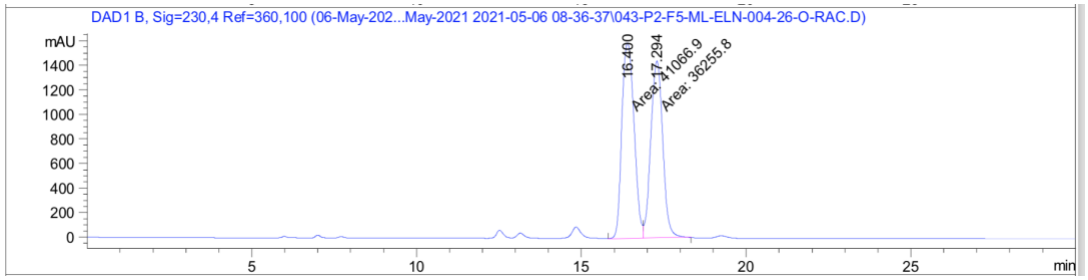

Signal 2: DAD1 B, Sig=230, 4 Ref=360, 100

Peak #	Ret Time [min]	Type	Width [min]	Area [mAU*s]	Height [mAU]	Area %
1	16.400	MF	0.4299	4.10669e4	1592.10583	53.1110
2	17.294	FM	0.4195	3.62558e4	1440.44507	46.8890
Totals :				7.73227e4	3032.55090	

Compound 15 Trace with Rh_2(*S*-PTAD)$_4$:

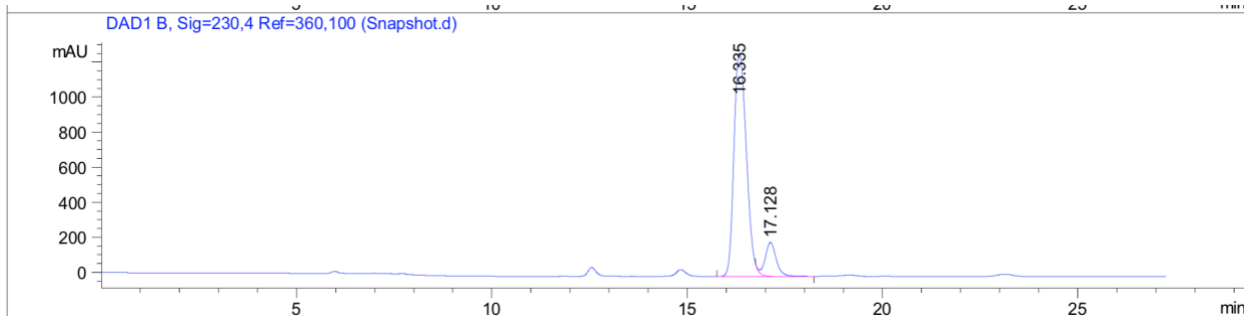

Signal 2: DAD1 B, Sig=230, 4 Ref=360, 100

Peak #	Ret Time [min]	Type	Width [min]	Area [mAU*s]	Height [mAU]	Area %
1	16.335	BV R	0.3530	2.82586e4	1272.74890	88.2069
2	17.128	VB E	0.2953	3778.10498	193.92400	11.7931
Totals :				3.20367e4	1466.67290	

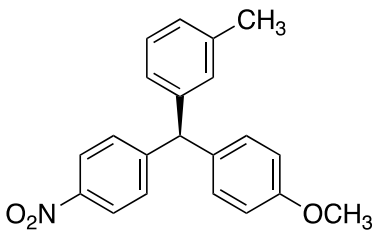

Compound 16 –Racemic.

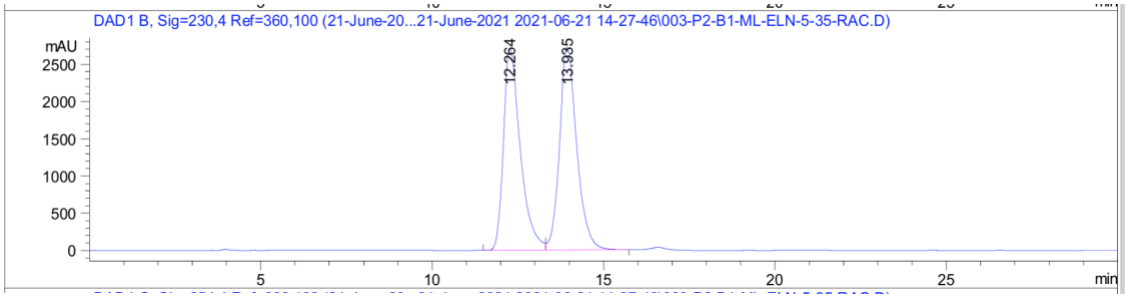

Signal 2: DAD1 B, Sig=230,4 Ref=360,100

Peak #	Ret Time [min]	Type	Width [min]	Area [mAU*s]	Height [mAU]	Area %
1	12.264	BV	0.5077	9.25909e4	2702.52637	49.1916
2	13.935	VB	0.5229	9.56341e4	2715.59790	50.8084
Totals :				1.88225e5	5418.12427	

Compound 16 Trace with Rh_2(*S*-PTAD)$_4$:

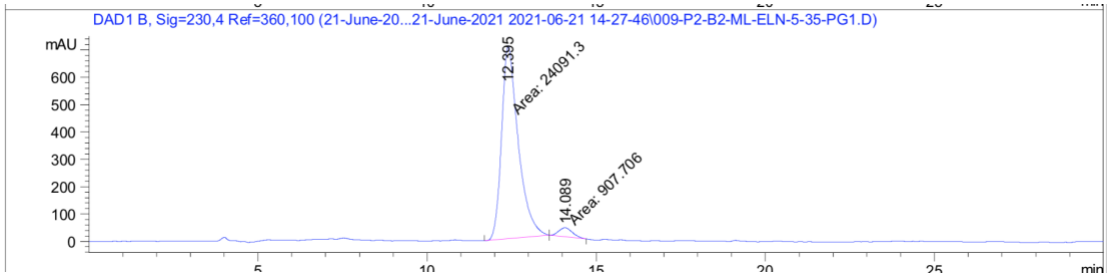

Signal 2: DAD1 B, Sig=230,4 Ref=360,100

Peak #	Ret Time [min]	Type	Width [min]	Area [mAU*s]	Height [mAU]	Area %
1	12.395	MM T	0.6539	2.40913e4	705.28912	96.3690
2	14.089	MM T	0.4632	907.70624	32.66312	3.6310
Totals :				2.49990e4	737.95225	

HPLC (ODH column, 0.8 mL/min 2.25 % i-PrOH in n-hexane 30 min, UV 230 nm) retention times of 12.40 (major) and 14.09 min (minor) 93 % ee with Rh_2(S-PTAD)$_4$.

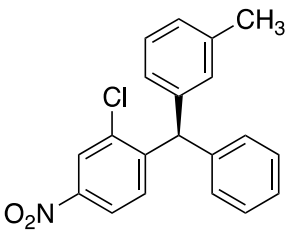

Compound 18 –Racemic

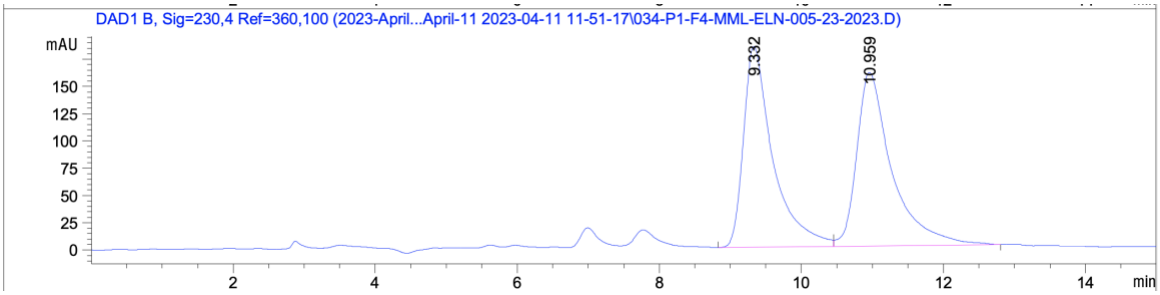

Signal 2: DAD1 B, Sig=230,4 Ref=360,100

Peak #	RetTime [min]	Type	Width [min]	Area [mAU*s]	Height [mAU]	Area %
1	9.332	BV	0.4152	5286.01904	183.98650	49.1916
2	10.959	VB	0.4965	5459.74756	159.04063	50.8084
Totals :				1.07458e4	343.02713	

Compound 18 Trace with Rh_2(*S*-PTAD)$_4$:

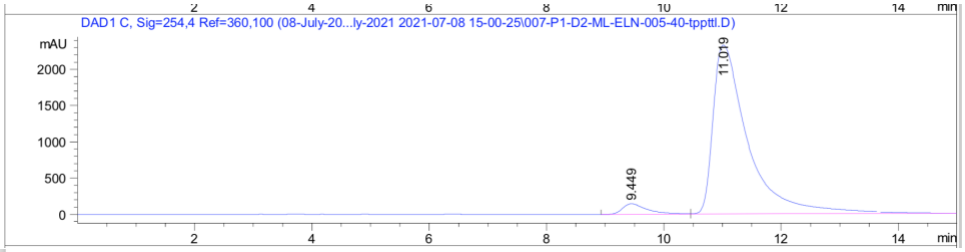

Signal 3: DAD1 C, Sig=254,4 Ref=360,100

Peak #	RetTime [min]	Type	Width [min]	Area [mAU*s]	Height [mAU]	Area %
1	9.449	BV	0.4316	4328.86230	146.15254	4.2674
2	11.019	VBA	0.6084	9.71105e4	2329.03613	95.7326
Totals :				1.01439e5	2475.18867	

HPLC (ODH column, 1.0mL/min 1.0 % i-PrOH in n-hexane 15 min, UV 230 nm) retention times of 9.45 (minor) and 11.02 min (major) 91 % ee with Rh_2(S-TPPTTL)$_4$

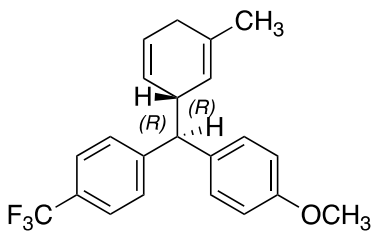

Compound 20 (C-H) intermediate -Racemic

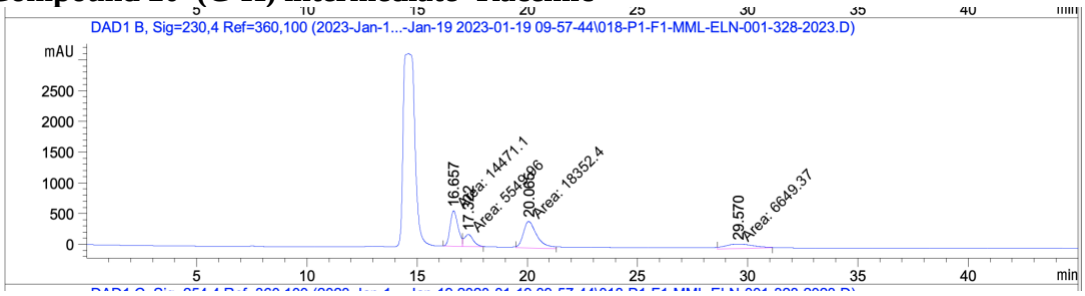

Signal 2: DAD1 B, Sig=230,4 Ref=360,100

Peak #	RetTime [min]	Type	Width [min]	Area [mAU*s]	Height [mAU]	Area %
1	16.657	MF	0.4187	1.44711e4	576.01093	32.1417
2	17.322	FM	0.4712	5549.96289	196.31697	12.3270
3	20.065	MM	0.7132	1.83524e4	428.88205	40.7624
4	29.570	MM	1.4402	6649.37451	76.95222	14.7689
Totals :				4.50229e4	1278.16217	

This trace tells us peaks 1 and 3 are enantionmers and 2 and 4 are the other set of diastereomers.

Compound 20 (C-H) intermediate Trace with Rh_2(*S*-PTAD)$_4$:

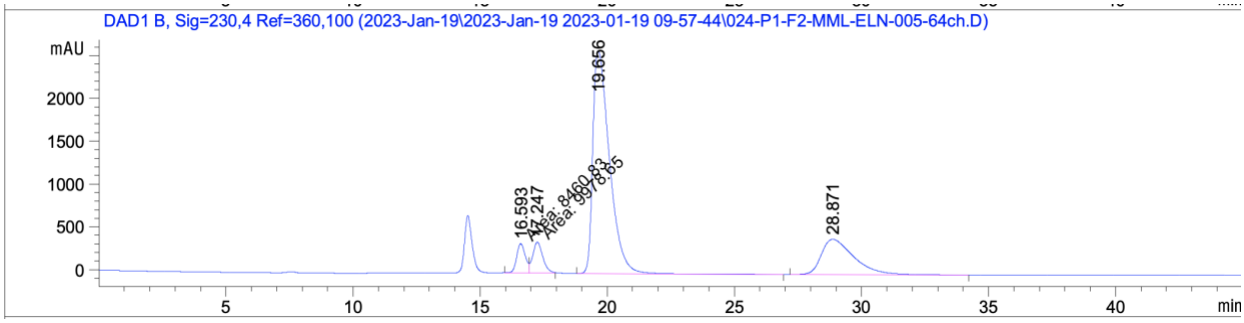

Signal 2: DAD1 B, Sig=230,4 Ref=360,100

Peak #	RetTime [min]	Type	Width [min]	Area [mAU*s]	Height [mAU]	Area %
1	16.593	MF	0.4102	8460.83008	343.75934	4.8815
2	17.247	FM	0.4557	9978.64746	364.95328	5.7572
3	19.656	BB	0.6851	1.18426e5	2601.37769	68.3262
4	28.871	BB	1.3181	3.64587e4	411.30997	21.0350
Totals :				1.73324e5	3721.40027	

Major Diasteriomer: peak 3 and 1. Minor Diasteriomer peak 4 and 2.

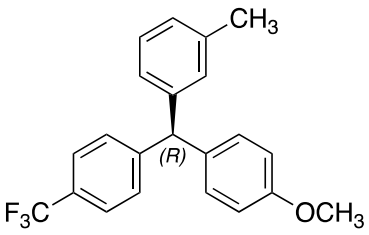

Compound 21 -Racemic

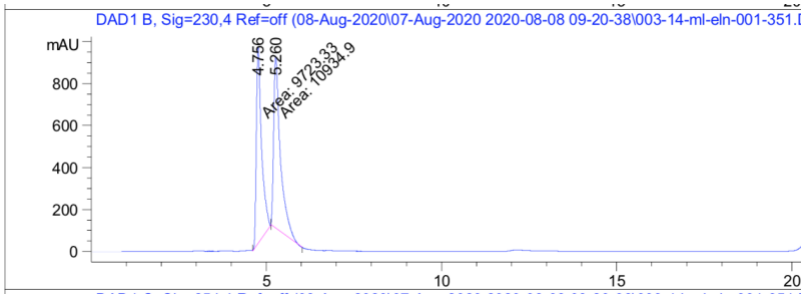

Signal 2: DAD1 B, Sig=230,4 Ref=off

Peak #	RetTime [min]	Type	Width [min]	Area [mAU*s]	Height [mAU]	Area %
1	4.756	MM	0.1732	9723.33008	935.85950	47.0675
2	5.260	MM	0.2226	1.09349e4	818.84296	52.9325
Totals :				2.06583e4	1754.70245	

Compoun 21 Trace with Rh_2(*S*-PTAD)$_4$:

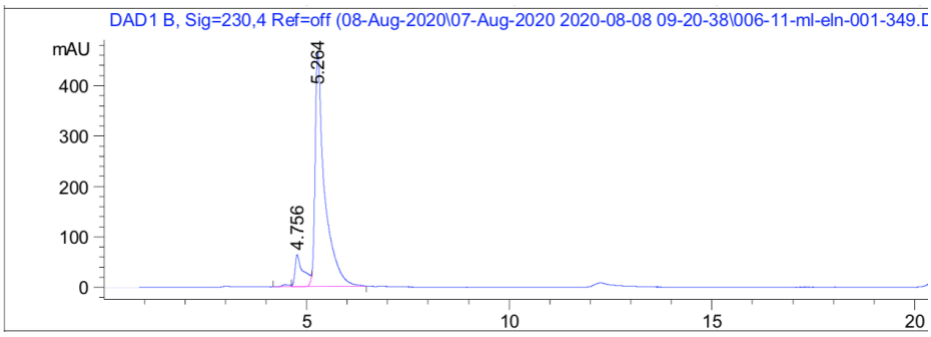

Signal 2: DAD1 B, Sig=230,4 Ref=off

Peak #	RetTime [min]	Type	Width [min]	Area [mAU*s]	Height [mAU]	Area %
1	4.756	VV E	0.1864	897.16034	63.45586	10.4860
2	5.264	VV R	0.2241	7658.66748	466.45120	89.5140
Totals :				8555.82782	529.90706	

HPLC (ODH column, 1.0 mL/min 1% i-PrOH in n-hexane 25 min, UV 230 nm) retention times of 4.76 (minor) and 5.26 min (major) 79 % ee with Rh_2(S-PTAD)$_4$.

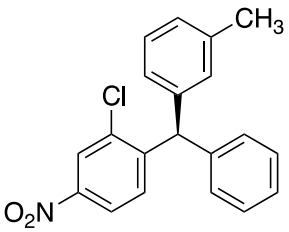

Compound 17 -Racemic Table 2. Catalyst Screen

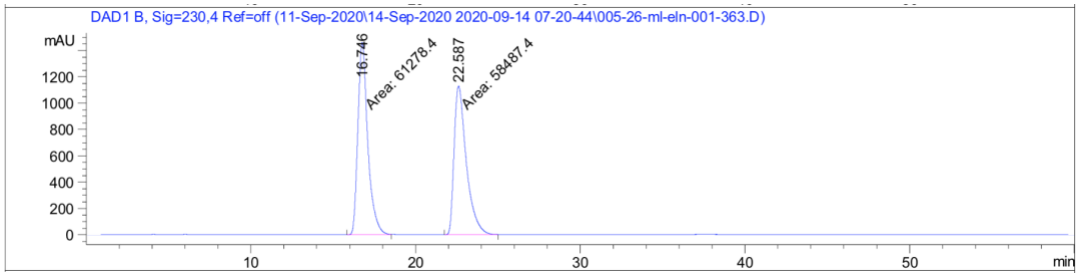

Signal 2: DAD1 B, Sig=230,4 Ref=off

Peak #	RetTime [min]	Type	Width [min]	Area [mAU*s]	Height [mAU]	Area %
1	16.746	MM	0.6988	6.12784e4	1461.53943	51.1652
2	22.587	MM	0.8622	5.84874e4	1130.60669	48.8348
Totals :				1.19766e5	2592.14612	

Compound 17 Trace with Rh_2(*S*-PTAD)$_4$:

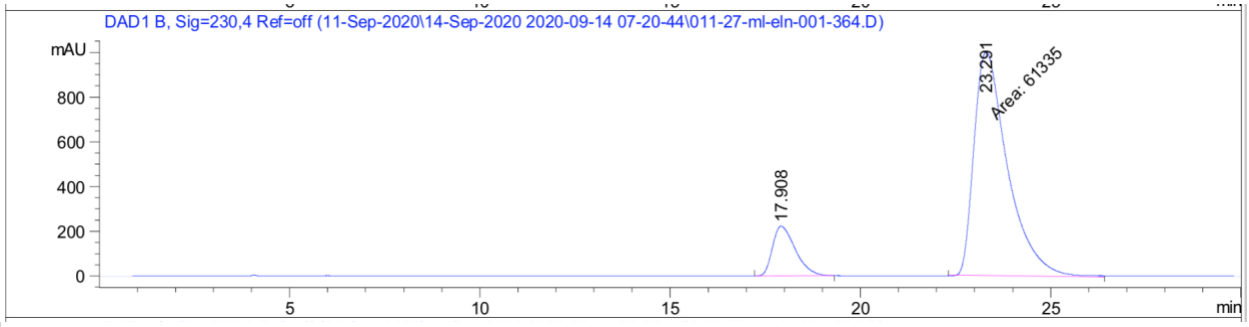

Signal 2: DAD1 B, Sig=230,4 Ref=off

Peak #	RetTime [min]	Type	Width [min]	Area [mAU*s]	Height [mAU]	Area %
1	17.908	VV R	0.4904	9232.09668	222.14276	13.0827
2	23.291	MM	1.0208	6.13350e4	1001.42139	86.9173
Totals :				7.05671e4	1223.56415	

Compound 17 Trace with Rh_2(*S*-TCPTAD)$_4$:

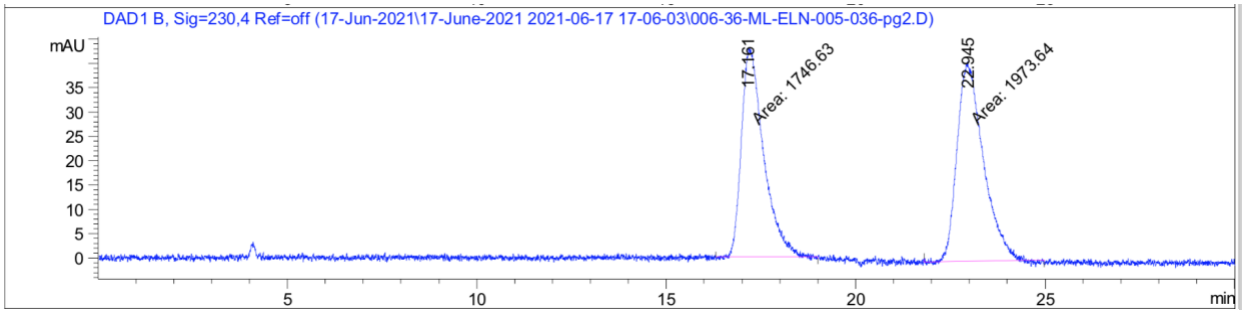

Signal 2: DAD1 B, Sig=230,4 Ref=off

Peak #	RetTime [min]	Type	Width [min]	Area [mAU*s]	Height [mAU]	Area %
1	17.161	MM	0.6777	1746.63354	42.95704	46.9490
2	22.945	MM	0.8026	1973.64307	40.98562	53.0510
Totals :				3720.27661	83.94266	

Compound 17 Trace with Rh_2(*S*-NTTL)$_4$:

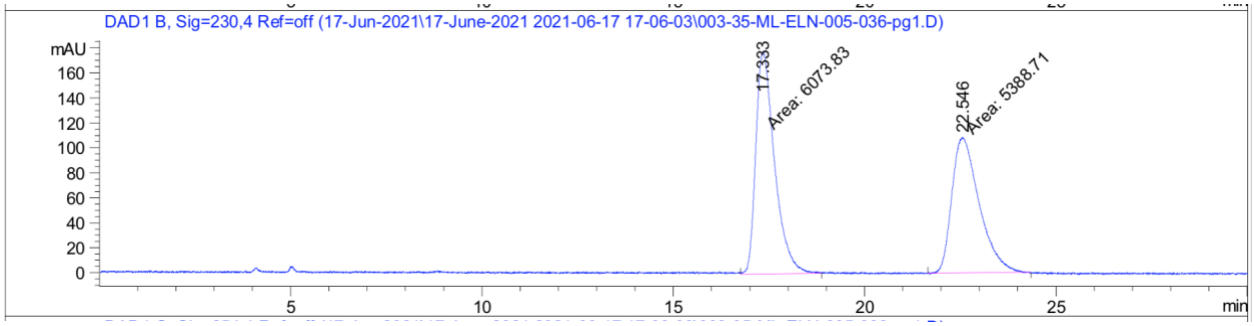

Signal 2: DAD1 B, Sig=230,4 Ref=off

Peak #	RetTime [min]	Type	Width [min]	Area [mAU*s]	Height [mAU]	Area %
1	17.333	MM	0.5676	6073.83252	178.35365	52.9885
2	22.546	MM	0.8256	5388.71484	108.78693	47.0115
Totals :				1.14625e4	287.14058	

Compound 17 Trace with Rh_2(*S*-PTTL)$_4$:

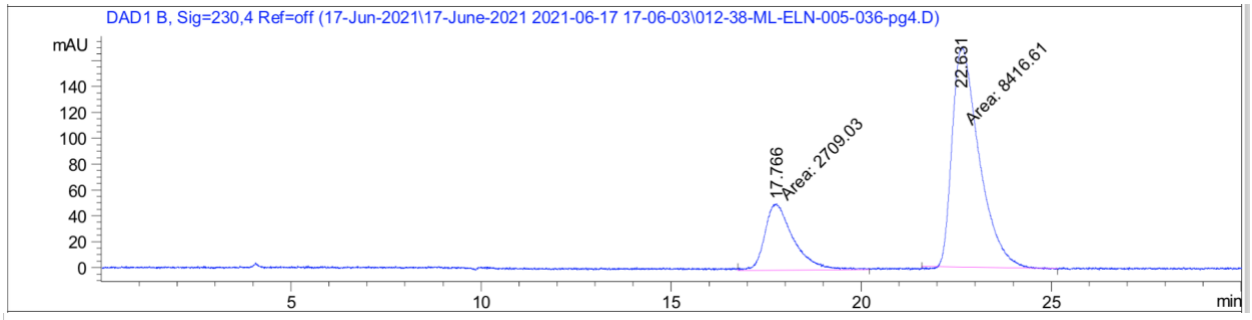

Signal 2: DAD1 B, Sig=230,4 Ref=off

Peak #	RetTime [min]	Type	Width [min]	Area [mAU*s]	Height [mAU]	Area %
1	17.766	MM	0.8732	2709.02710	51.70412	24.3494
2	22.631	MM	0.8247	8416.60938	170.09402	75.6506
Totals :				1.11256e4	221.79815	

Compound 17 Trace with Rh_2(*S*-TPPTTL)$_4$:

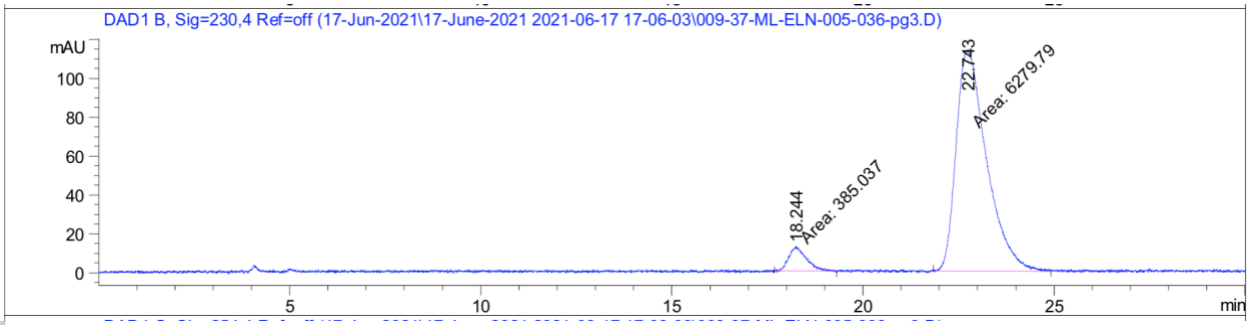

Signal 2: DAD1 B, Sig=230,4 Ref=off

Peak #	RetTime [min]	Type	Width [min]	Area [mAU*s]	Height [mAU]	Area %
1	18.244	MM	0.5177	385.03741	12.39615	5.7772
2	22.743	MM	0.9188	6279.78906	113.91827	94.2228
Totals :				6664.82648	126.31442	

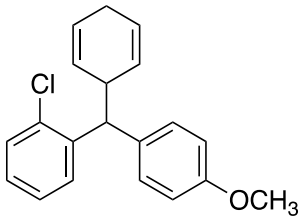

Compound 23 –Racemic

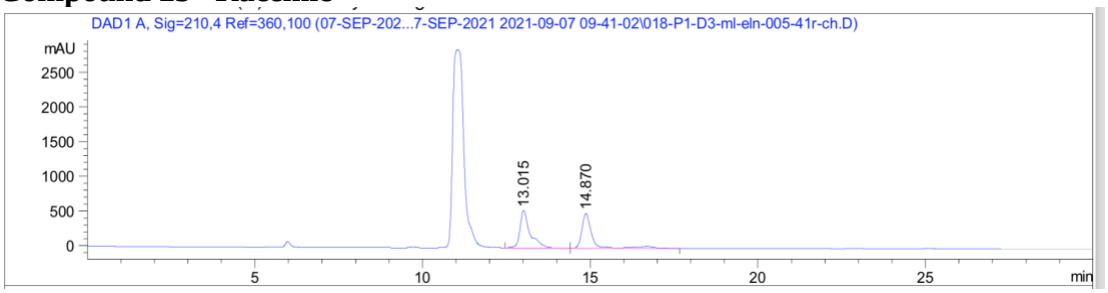

Signal 1: DAD1 A, Sig=210,4 Ref=360,100

Peak #	Ret Time [min]	Type	Width [min]	Area [mAU*s]	Height [mAU]	Area %
1	13.015	VB	0.3017	1.13815e4	540.45325	51.9915
2	14.870	BV R	0.2821	1.05096e4	500.89468	48.0085
Totals :				2.18910e4	1041.34793	

Compound 23 Rh_2(*S*-TPPTTL)$_4$:

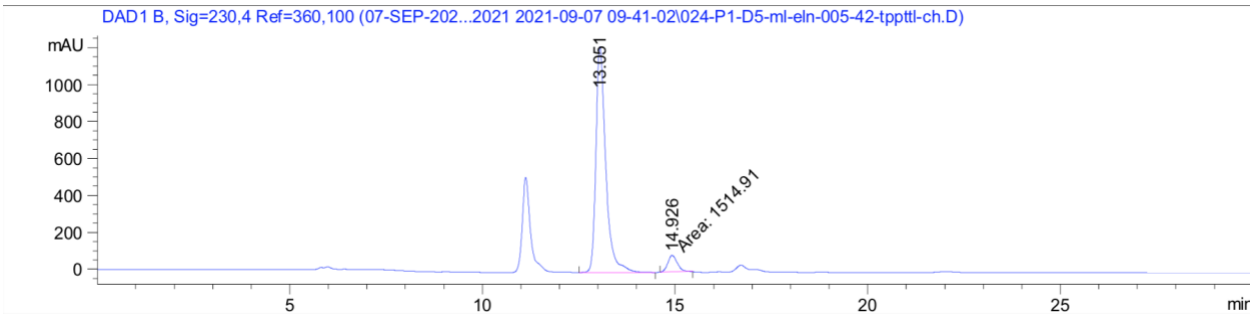

Signal 2: DAD1 B, Sig=230,4 Ref=360,100

Peak #	Ret Time [min]	Type	Width [min]	Area [mAU*s]	Height [mAU]	Area %
1	13.051	BB	0.2660	2.18171e4	1223.70215	93.5071
2	14.926	MM	0.2836	1514.91260	89.03326	6.4929
Totals :				2.33320e4	1312.73540	

HPLC (ADH column, 0.5 mL/min 0.5 % i-PrOH in n-hexane 30 min, UV 230 nm) retention times of 13.86 (major) and 14.90 min (minor) 87 % ee with Rh_2(S-TPPTTL)$_4$.

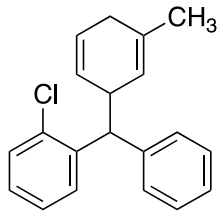

Compound 24 as C-H Insertion Intermediate –Racemic

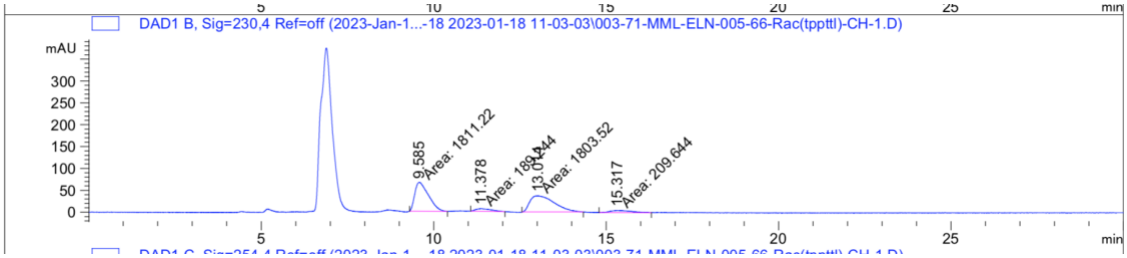

Signal 2: DAD1 B, Sig=230,4 Ref=off

Peak #	RetTime [min]	Type	Width [min]	Area [mAU*s]	Height [mAU]	Area %
1	9.585	MM	0.4569	1811.21509	66.06657	45.1267
2	11.378	MM	0.5046	189.24393	6.25117	4.7150
3	13.014	MM	0.8125	1803.51831	36.99650	44.9349
4	15.317	MM	0.6769	209.64355	5.16168	5.2233
Totals :				4013.62088	114.47591	

Compound 24 as C-H Insertion Intermediate Trace with Rh_2(*S*-TPPTTL)$_4$:

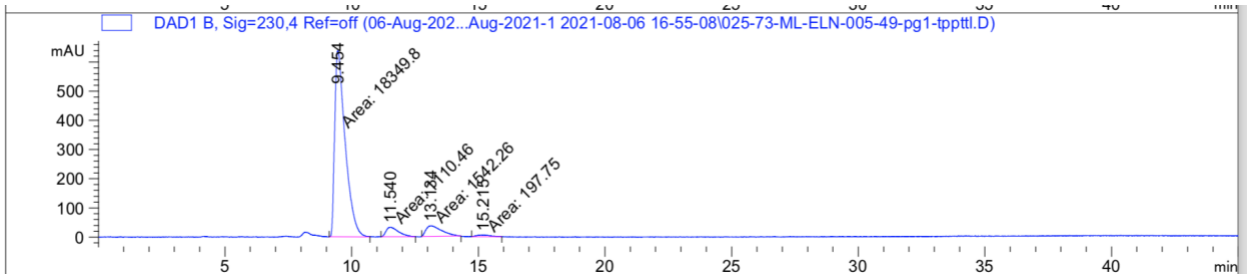

Signal 2: DAD1 B, Sig=230,4 Ref=off

Peak #	RetTime [min]	Type	Width [min]	Area [mAU*s]	Height [mAU]	Area %
1	9.454	MM	0.4790	1.83498e4	638.52008	86.5546
2	11.540	MM	0.5602	1110.45618	33.03613	5.2379
3	13.134	MM	0.7036	1542.26001	36.53149	7.2747
4	15.215	MM	0.5374	197.74982	6.13309	0.9328
Totals :				2.12003e4	714.22078	

HPLC (ODH column, 0.8 mL/min .1 % i-PrOH in n-hexane 45 min, UV 230 nm) retention times of 9.5 (major) and 13.1 min (minor) 85 % ee with Rh_2(S-TPPTTL)$_4$ for the major diastereomer; 11. .6 (major) and 15.2 min (minor) 70 % ee with Rh_2(S-TPPTTL)$_4$ for the minor diastereomers.

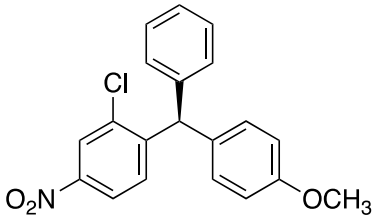

Compound 25 –Racemic

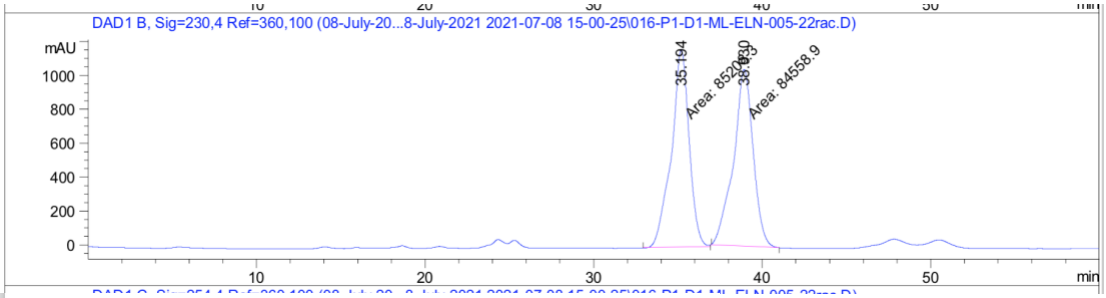

Signal 2: DAD1 B, Sig=230, 4 Ref=360, 100

Peak #	Ret Time [min]	Type	Width [min]	Area [mAU*s]	Height [mAU]	Area %
1	35.194	MM	1.2200	8.52083e4	1164.01221	50.1912
2	38.930	MM	1.3548	8.45589e4	1040.22314	49.8088
Totals :				1.69767e5	2204.23535	

Compound 25 Trace with Rh_2(*S*-TPPTTL)$_4$:

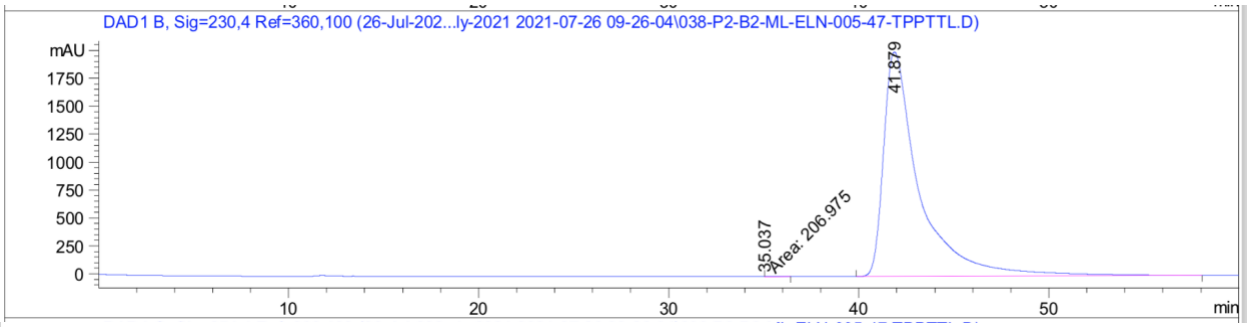

Signal 2: DAD1 B, Sig=230, 4 Ref=360, 100

Peak #	Ret Time [min]	Type	Width [min]	Area [mAU*s]	Height [mAU]	Area %
1	35.037	MM	0.4681	206.97479	5.24418	0.0786
2	41.879	BB	1.8818	2.63210e5	2009.94714	99.9214
Totals :				2.63417e5	2015.19132	

HPLC (ODH column, 0.25 mL/min 2.0 % i-PrOH in n-hexane 60 min, UV 230 nm) retention times of 35.04 (minor) and 41.88 min (major) 98 % ee with Rh_2(S-TPPTTL)$_4$.

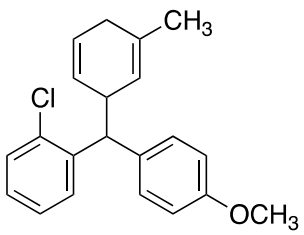

Compound 26 as C-H Insertion Intermediate –Racemic

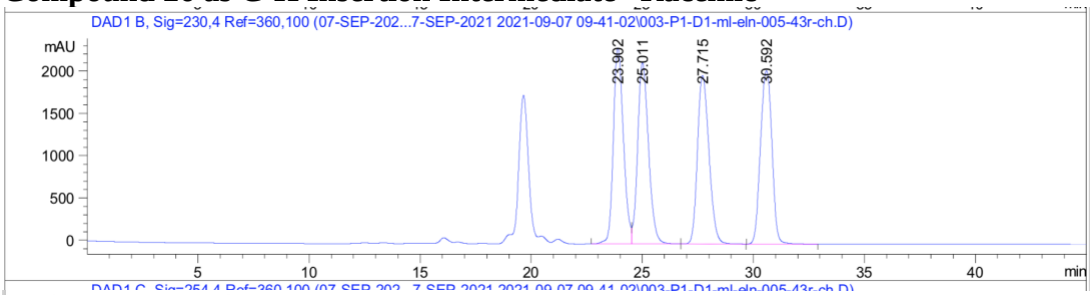

Signal 2: DAD1 B, Sig=230, 4 Ref=360, 100

Peak #	Ret Time [min]	Type	Width [min]	Area [mAU*s]	Height [mAU]	Area %
1	23.902	BV	0.4861	7.31142e4	2317.15845	25.0995
2	25.011	VB	0.5242	7.28261e4	2144.24634	25.0005
3	27.715	BB	0.5606	7.18309e4	1992.59241	24.6589
4	30.592	BB	0.5824	7.35267e4	2050.28882	25.2411
Totals :				2.91298e5	8504.28601	

In racemic reaction d.r. is 1:1; making it unclear which peak corresponds to which enantiomer.

Compound 26 as C-H Insertion Intermediate Trace with Rh_2(*S*-TPPTTL)$_4$:

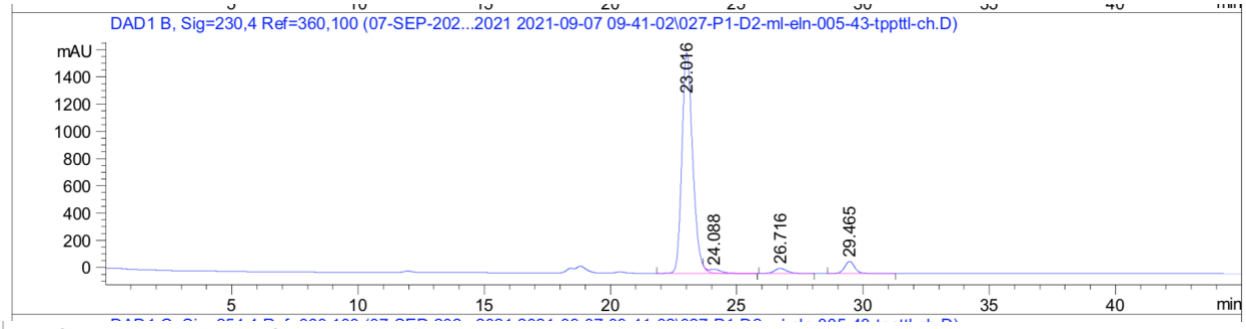

Signal 2: DAD1 B, Sig=230, 4 Ref=360, 100

Peak #	Ret Time [min]	Type	Width [min]	Area [mAU*s]	Height [mAU]	Area %
1	23.016	BV R	0.4585	4.83723e4	1619.46423	91.5082
2	24.088	VB E	0.4772	895.12067	27.39291	1.6933
3	26.716	BB	0.5045	1197.92212	36.53453	2.2662
4	29.465	BB	0.4188	2395.80298	88.21896	4.5323
Totals :				5.28611e4	1771.61064	

HPLC (ADH column, 0.25 mL/min 0.5 % i-PrOH in n-hexane 45 min, UV 230 nm) retention times of 23.02(major) and 29.47 min (minor) with Rh_2(S-TPPTTL)$_4$

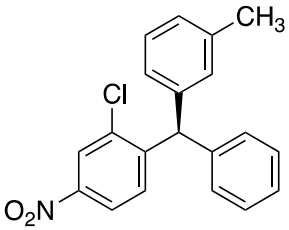

Compound 18 –Racemic

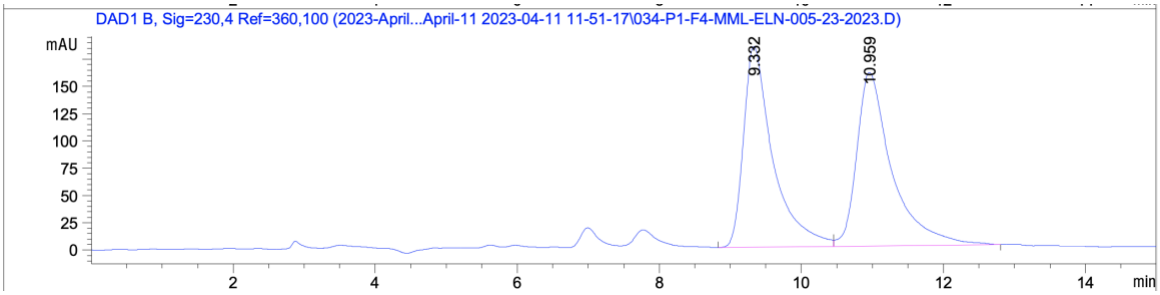

Signal 2: DAD1 B, Sig=230,4 Ref=360,100

Peak #	RetTime [min]	Type	Width [min]	Area [mAU*s]	Height [mAU]	Area %
1	9.332	BV	0.4152	5286.01904	183.98650	49.1916
2	10.959	VB	0.4965	5459.74756	159.04063	50.8084
Totals :				1.07458e4	343.02713	

Compound 18 Trace with Rh_2(*S*-TPPTTL)$_4$:

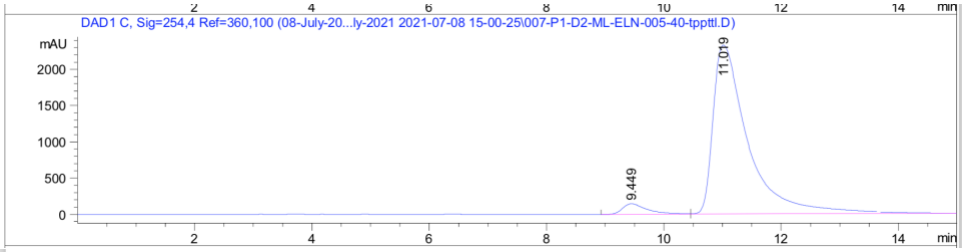

Signal 3: DAD1 C, Sig=254,4 Ref=360,100

Peak #	Ret Time [min]	Type	Width [min]	Area [mAU*s]	Height [mAU]	Area %
1	9.449	BV	0.4316	4328.86230	146.15254	4.2674
2	11.019	VBA	0.6084	9.71105e4	2329.03613	95.7326
Totals :				1.01439e5	2475.18867	

HPLC (ODH column, 1.0mL/min 1.0 % i-PrOH in n-hexane 15 min, UV 230 nm) retention times of 9.45 (minor) and 11.02 min (major) 91 % ee with Rh_2(S-TPPTTL)$_4$

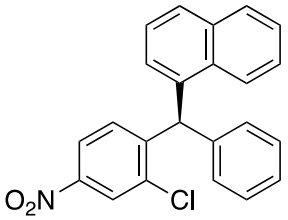

Compound 27 –Racemic

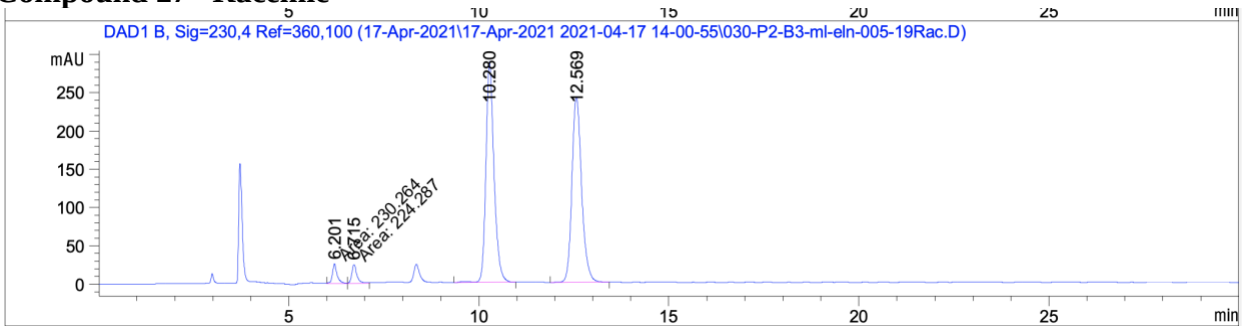

Signal 2: DAD1 B, Sig=230,4 Ref=360,100

Peak #	RetTime [min]	Type	Width [min]	Area [mAU*s]	Height [mAU]	Area %
1	6.201	MF	0.1490	230.26440	25.76005	2.5482
2	6.715	FM	0.1532	224.28708	24.39639	2.4821
3	10.280	VB R	0.2223	4286.21191	288.43939	47.4331
4	12.569	BB	0.2707	4295.56934	242.47028	47.5366

Compound 27 Trace with Rh_2(*S*-TPPTTL)$_4$:

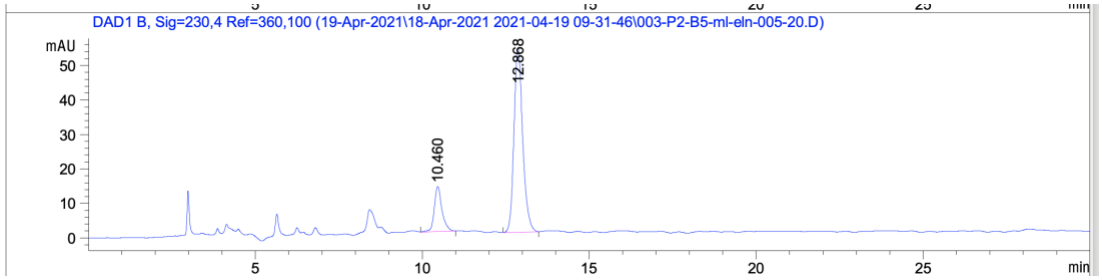

Signal 2: DAD1 B, Sig=230,4 Ref=360,100

Peak #	RetTime [min]	Type	Width [min]	Area [mAU*s]	Height [mAU]	Area %
1	10.460	BB	0.2359	208.43634	13.08079	17.6692
2	12.868	BB	0.2758	971.22510	53.50193	82.3308
Totals :				1179.66144	66.58272	

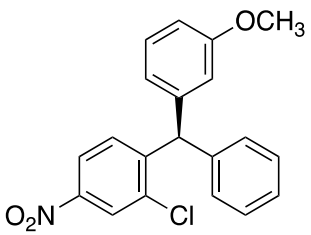

Compound 28 –Racemic

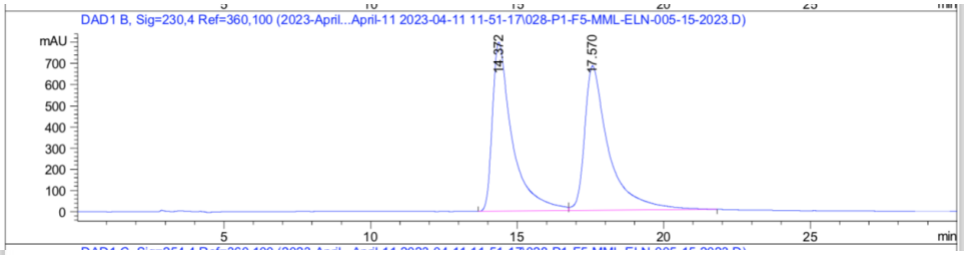

Signal 2: DAD1 B, Sig=230, 4 Ref=360, 100

Peak #	Ret Time [min]	Type	Width [min]	Area [mAU*s]	Height [mAU]	Area %
1	14.372	BV	0.6814	3.77297e4	798.30634	49.0370
2	17.570	VB	0.8222	3.92116e4	682.61328	50.9630
Totals :				7.69413e4	1480.91962	

Compound 28 Trace with Rh_2(*S*TPPTTL)$_4$:

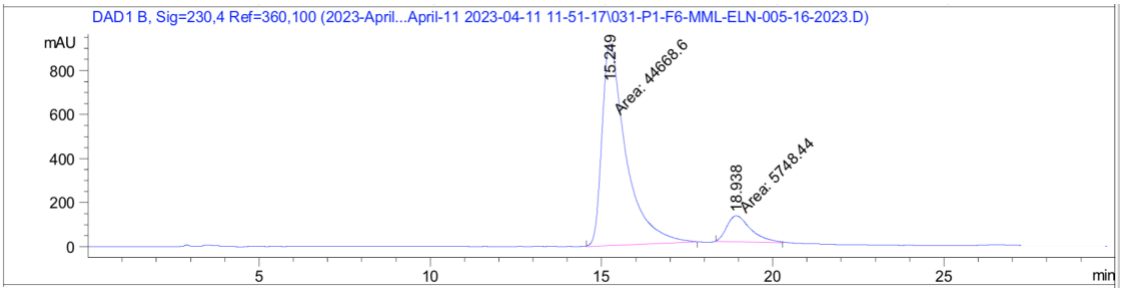

Signal 2: DAD1 B, Sig=230, 4 Ref=360, 100

Peak #	Ret Time [min]	Type	Width [min]	Area [mAU*s]	Height [mAU]	Area %
1	15.249	MM	0.8137	4.46686e4	914.94696	88.5982
2	18.938	MM	0.8110	5748.44043	118.13127	11.4018
Totals :				5.04170e4	1033.07823	

HPLC (ODH column, 1.0 mL/min 1% i-PrOH in n-hexane 30 min, UV 230 nm) retention times of 15.2 (major) and 19.0 min (minor) 75 % ee with Rh_2(*S*-TPPTTL)$_4$.

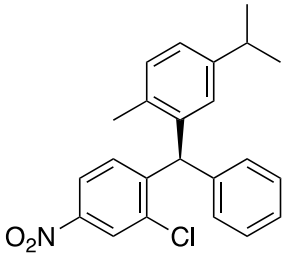

Compound 29 –Racemic

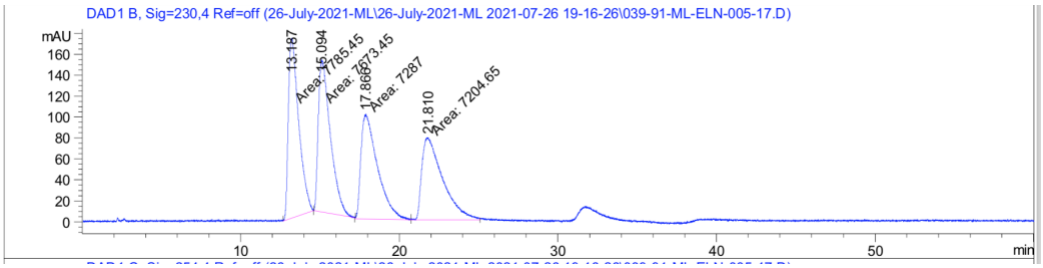

Signal 2: DAD1 B, Sig=230,4 Ref=off

Peak #	RetTime [min]	Type	Width [min]	Area [mAU*s]	Height [mAU]	Area %
1	13.187	MM T	0.7546	7785.45361	171.95609	25.9944
2	15.094	MM T	0.7704	7673.44727	145.45210	25.6204
3	17.866	MM	1.2102	7287.00342	100.35814	24.3301
4	21.810	MM	1.5218	7204.64697	78.90544	24.0551
Totals :				2.99506e4	496.67177	

Compound 29 Trace with Rh_2(*S*-TPPTTL)$_4$:

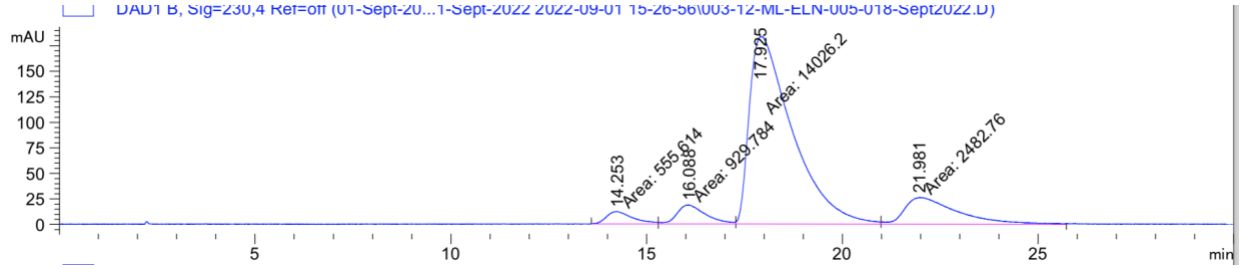

Signal 2: DAD1 B, Sig=230,4 Ref=off

Peak #	RetTime [min]	Type	Width [min]	Area [mAU*s]	Height [mAU]	Area %
1	14.253	MF	0.7573	555.61395	12.22836	3.0877
2	16.088	FM	0.8361	929.78375	18.53372	5.1671
3	17.925	MF	1.2735	1.40262e4	183.55954	77.9478
4	21.981	FM	1.5767	2482.75537	26.24434	13.7974
Totals :				1.79943e4	240.56597	

3.9 References

1. Lee, M.; Davies, H. M. L., Enantioselective Synthesis of Triarylmethanes via Intermolecular C–H Functionalization of Cyclohexadienes with Diaryldiazomethanes. *Org. Lett.* **2023,** *25* (22), 4000-4004.
2. Lee, M.; Ren, Z.; Musaev, D. G.; Davies, H. M. L., Rhodium-Stabilized Diarylcarbenes Behaving as Donor/Acceptor Carbenes. *ACS Catalysis* **2020,** *10* (11), 6240-6247.
3. Jagannathan, J. R.; Fettinger, J. C.; Shaw, J. T.; Franz, A. K., Enantioselective Si-H Insertion Reactions of Diarylcarbenes for the Synthesis of Silicon-Stereogenic Silanes. *J Am Chem Soc* **2020,** *142* (27), 11674-11679.
4. Yang, L. L.; Evans, D.; Xu, B.; Li, W. T.; Li, M. L.; Zhu, S. F.; Houk, K. N.; Zhou, Q. L., Enantioselective Diarylcarbene Insertion into Si-H Bonds Induced by Electronic Properties of the Carbenes. *J Am Chem Soc* **2020,** *142* (28), 12394-12399.
5. Diemoz, K. M.; Wilson, S. O.; Franz, A. K., Synthesis of Structurally Varied 1,3-Disiloxanediols and Their Activity as Anion-Binding Catalysts. *Chem.-Eur. J.* **2016,** *22* (51), 18349-18353.
6. Diemoz, K. M.; Hein, J. E.; Wilson, S. O.; Fettinger, J. C.; Franz, A. K., Reaction Progress Kinetics Analysis of 1,3-Disiloxanediols as Hydrogen-Bonding Catalysts. *J. Org. Chem.* **2017,** *82* (13), 6738-6747.
7. Davies, H. M. L.; Hansen, T.; Churchill, M. R., Catalytic asymmetric C-H activation of alkanes and tetrahydrofuran. *J. Am. Chem. Soc.* **2000,** *122* (13), 3063-3070.
8. Davies, H. M. L.; Stafford, D. G.; Hansen, T., Catalytic asymmetric synthesis of diarylacetates and 4,4-diarylbutanoates. A formal asymmetric synthesis of (+)-sertraline. *Org. Lett.* **1999,** *1* (2), 233-236.
9. Li, Z. X.; Wang, J. W.; Zhao, J. H.; Zhao, C. F.; Liu, X. P.; Yu, X. J., Advanced in the Synthesis of Triarylmethanes. *Chin. J. Org. Chem.* **2014,** *34* (3), 485-494.
10. Al-Qawasmeh, R. A.; Lee, Y.; Cao, M. Y.; Gu, X. P.; Vassilakos, A.; Wright, J. A.; Young, A., Triaryl methane derivatives as antiproliferative agents. *Bioorg. Med. Chem. Lett.* **2004,** *14* (2), 347-350.
11. Montagut, A. M.; Galvez, E.; Shafir, A.; Sebastian, R. M.; Vallribera, A., Triarylmethane Dyes for Artificial Repellent Cotton Fibers. *Chem.-Eur. J.* **2017,** *23* (16), 3810-3814.
12. Liu, X.; Wu, X. M.; Zhang, L.; Lin, X. Y.; Huang, D. Y., Recent Advances in Triarylmethane Synthesis. *Synthesis* **2020,** *52* (16), 2311-2329.
13. Johnson, A. G.; Tranquilli, M. M.; Harris, M. R.; Jarvo, E. R., Selective synthesis of either enantiomer of an anti-breast cancer agent via a common enantioenriched intermediate. *Tetrahedron Lett.* **2015,** *56* (23), 3486-3488.
14. Dardir, A. H.; Casademont-Reig, I.; Balcells, D.; Ellefsen, J. D.; Espinosa, M. R.; Hazari, N.; Smith, N. E., Synthesis of Triarylmethanes via Palladium-Catalyzed Suzuki-Miyaura Reactions of Diarylmethyl Esters. *Organometallics* **2021,** *40* (14), 2332-2344.
15. Zhao, Y. T.; Su, Y. X.; Li, X. Y.; Yang, L. L.; Huang, M. Y.; Zhu, S. F., Dirhodium-Catalyzed Enantioselective B-H Bond Insertion of gem-Diaryl Carbenes: Efficient Access to gem-Diarylmethine Boranes. *Angew Chem Int Ed Engl* **2021,** *60* (45), 24214-24219.
16. Huang, Y.; Hayashi, T., Asymmetric Synthesis of Triarylmethanes by Rhodium-Catalyzed Enantioselective Arylation of Diarylmethylamines with Arylboroxines. *J Am Chem Soc* **2015,** *137* (24), 7556-9.

17. Davies, H. M. L.; Hansen, T., Asymmetric intermolecular carbenoid C-H insertions catalyzed by rhodium(II) (S)-N-(p-dodecylphenyl)sulfonylprolinate. *J. Am. Chem. Soc.* **1997,** *119* (38), 9075-9076.
18. Hashimoto, S.; Watanabe, N.; Sato, T.; Shiro, M.; Ikegami, S., Enhancement Of Enantioselectivity in Intramolecular C-H Insertion Reactions of Alpha-Diazo Beta-Keto-Esters Catalyzed By Chiral Dirhodium(Ii) Carboxylates. *Tetrahedron Lett.* **1993,** *34* (32), 5109-5112.
19. Davies, H. M. L.; Liao, K. B., Dirhodium tetracarboxylates as catalysts for selective intermolecular C-H functionalization. *Nat. Rev. Chem.* **2019,** *3* (6), 347-360.
20. Davies, H. M. L.; Antoulinakis, E. G., Recent progress in asymmetric intermolecular C-H activation by rhodium carbenoid intermediates. *J. Organomet. Chem.* **2001,** *617* (1), 47-55.
21. Sharland, J. C.; Wei, B.; Hardee, D. J.; Hodges, T. R.; Gong, W.; Voight, E. A.; Davies, H. M. L., Asymmetric synthesis of pharmaceutically relevant 1-aryl-2-heteroaryl- and 1,2-diheteroarylcyclopropane-1-carboxylates. *Chem. Sci.* **2021,** *12* (33), 11181-11190.

Chapter 4. Oxidation of Hydrazones to Diazo Compounds- Strategies and Flow Conditions

A portion of the work has been published in the ACS Catalysis journal.[1] *Adapted with permission* from *ACS Catal.* **2021**, 11, 5, 2676–2683. *Copyright 2021 American Chemical Society.*

4.1 Introduction of Diazo Synthesis Strategies

Diazo compounds are useful synthetic reagents capable of a variety of transformations, most notably they are key precursors to carbene compounds discussed throughout this dissertation.[2-5] There are a variety of methods to access diazo compounds as shown in Scheme 1.[2] While these methods are all successful in the generation of diazo compounds, there are drawbacks and limitations to each approach. The first method employs a diazo transfer reagent, also known as Regitz diazo transfer agents, which utilizes sulfonyl azides and suitable bases, Scheme 1a.[6] The transformation proceeds through deprotonation to form an enolate that can react with the azide reagent. Tosyl azide (TsN_3) or mesyl (MsN_3) were the initially used diazo transfer reagents, but several other variants have been developed such as 4-acetamidobenzenesulfonyl azide, which has enhanced stability and *o*-nitrobenzenesulfonyl azide (*o*-NBSA), which is more reactive[7, 8] However, these reagents still require the use of potentially explosive azides and produce a one-to-one mol ratio of product to sulfonamide byproduct.[9] To avoid the use of azides, hydrazones as diazo compound precursors are a promising alternative. The Bamford-Stevens reaction converts a tosylhydrazone compound to the corresponding diazo compound under basic conditions and heat (Scheme 1b).[10] This method had been well utilized but has a disadvantage of generating toluenesulfinic acid byproduct.[11] Alternatively, hydrazone compounds can be oxidized to diazo compounds using a variety of stoichiometric metal oxidants or hypervalent iodine reagents (Scheme 1d).[12-17] Due to the widespread synthetic utility of diazo compounds, conditions that are

safe and avoid stoichiometric oxidants or byproducts would be highly valuable.

a.) Diazo Transfer Reagent

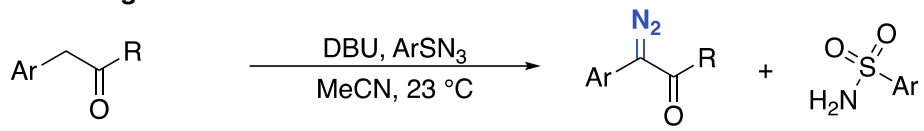

R = alkoxy, amino, aryl groups

b.) Bamford-Stevens Reaction

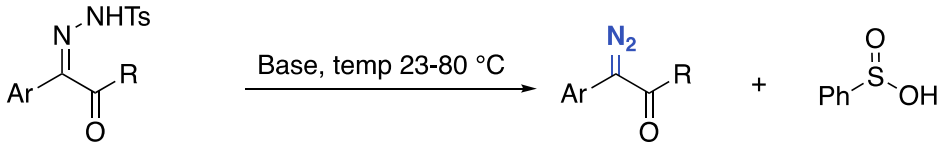

R = alkoxy, amino, aryl groups

c.) Hydrazone Oxidation

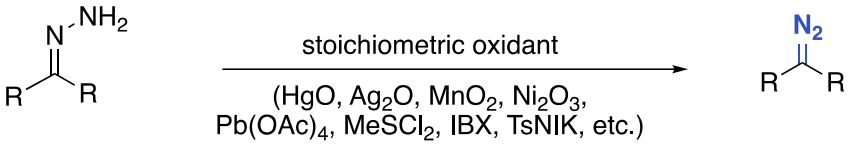

R = aryl,alkyl or alkoxy groups

Scheme 1. Common Strategies to Synthesize Diazo Compounds

4.2 Hydrazone Oxidation of Diazo Compounds: Initial Work by Davies and Stahl Labs

In collaboration with the Stahl Lab at the University of Wisconsin, Madison Dr. Wenbin Liu and Dr. Jack Twilton pioneered the aerobic oxidation of hydrazone compounds to diazo compounds using catalytic amounts of copper acetate (10 mol %) in the presence of a base, with oxygen as the terminal oxidant.[1] This work allowed for the generation of a variety of aryldiazoacetates to be formed in high yield, with water as the major byproduct (Scheme 2). This method converted hydrazone compounds with varying aryl substituents and ester groups including heterocycles. However, when this system was applied to diphenyl diazo hydrazone less than 5% of the desired product was observed. Diaryl diazo compounds are known to be less stable and readily decompose but the most common way to form them is through hydrazone oxidation. This method was believed to be incompatible with the diaryl system due to the use of silica gel, which

is slightly acidic and could lead to diazo degradation.

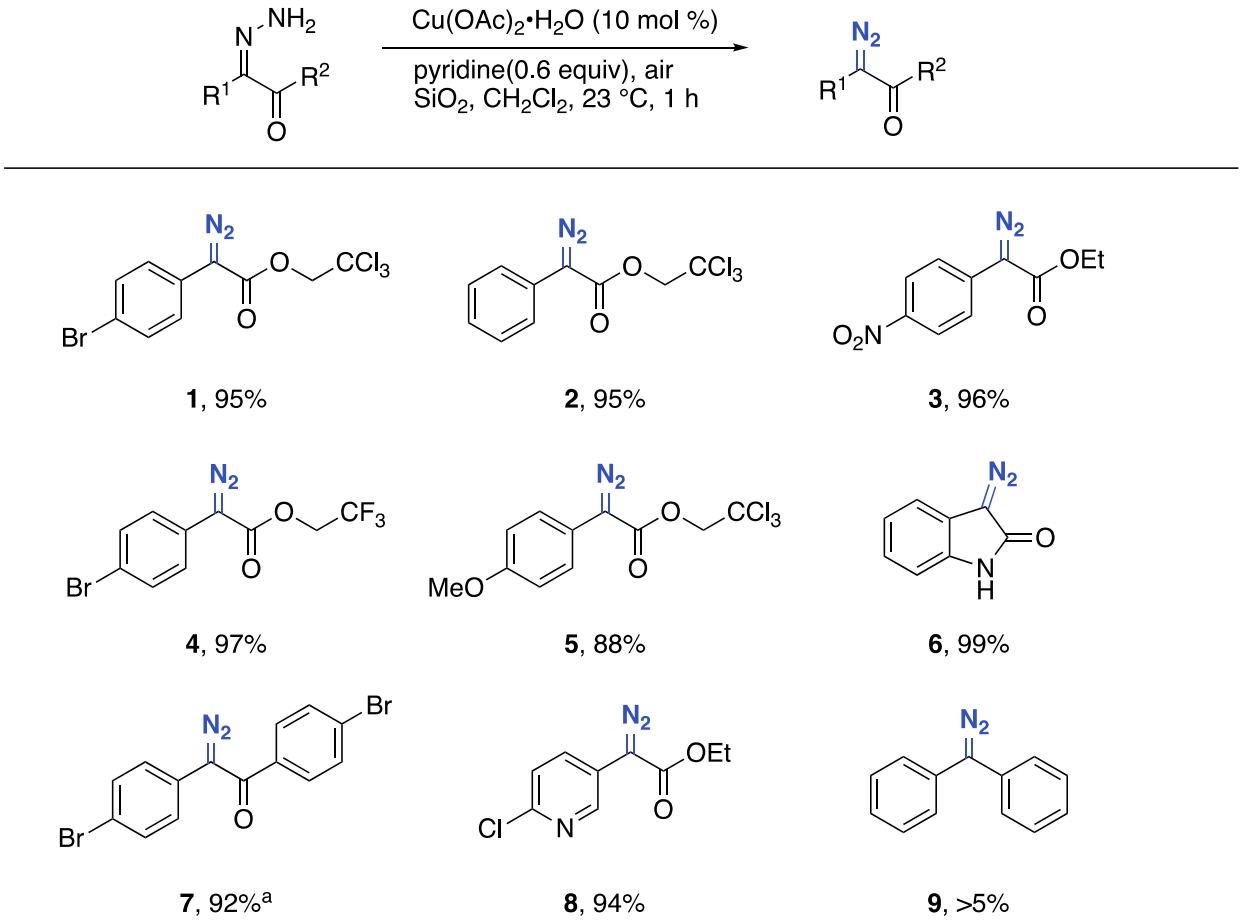

Reaction condition: a solution of hydrazone (0.5 mmol) in 1 mL of CH_2Cl_2 (0.5% pyridine) was added to a vial with $Cu(OAc)_2 \cdot H_2O$ (10 mol %) and SiO_2 (100 mg) in 4 mL of CH_2Cl_2 (0.5% pyridine) under ambient air (without cap) at 23 °C. The mixture was stirred vigorously for 1 h before silica plug.
[a]Reaction was conducted using 2.4 equiv of pyridine with O_2 balloon in dark (aluminum foil).

Scheme 2. Select Examples of Oxidation of Hydrazone to Diazo Compounds Using Cu

(Data from Dr. Wenbin Lui)

The method developed by Dr. Lui and Dr. Twilton demonstrated that catalytic oxidation of hydrazones could be achieved in high yield and minimal byproducts. At the time I was generating diaryl diazo compounds using hypervalent iodide TsNIK reagent discussed in Chapter 2 and had

a particular interest in expanding their method to achieve high conversion of diaryl hydrazone compounds.

4.3 Oxidation of Diaryl Hydrazone to Diazo Compounds Results and Discussion

Melissa Hall (Hopkins), a graduate student in the Stahl lab was able to join the project and work in collaboration with the Davies lab to develop conditions for the oxidation of diaryl hydrazones to diazo compounds. The initial screening, performed by Melissa, was on the biphenyl hydrazone compound **12**. It was found diaryl diazo **11** was relatively unstable and was converted *in situ* to acetate **11a** for analysis. Switching from pyridine as base to the stronger base, DMAP, increased yield from 7% to 17%, entry 3. Removal of silica from the reaction system lead to a yield of 34%, entry 4. Based on this trend, we sought to look at alternate electron-rich pyridine bases **P1**-**P4.** 9–Azajulolidine, **P4**, showed the best reactivity at 5 mol % $Cu(TFA)_2 \cdot H_2O$ resuling in 87% yield. 9–Azajulolidine has the amino group coplanar to the pyridine π-system which enhances the basicity relative to the other 4-aminopyridine derivatives.

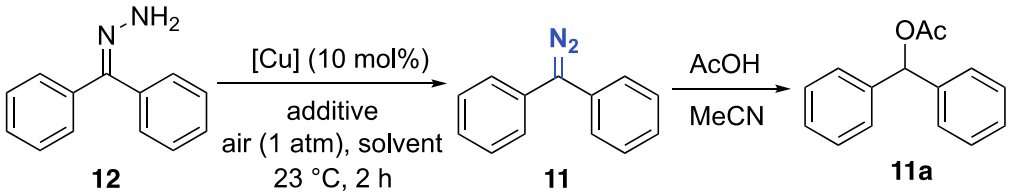

Entry	[Cu]	Solvent	Additive	Yield (**XX**), %
1	$Cu(OAc)_2•H_2O$	CH_2Cl_2	pyridine (0.5 equiv), silica	<5
2	$Cu(OAc)_2•H_2O$	DCE	pyridine (0.5 equiv), silica	7
3	$Cu(OAc)_2•H_2O$	DCE	DMAP (0.5 equiv), silica	17
4	$Cu(OAc)_2•H_2O$	DCE	DMAP (0.5 equiv)	34
5	$Cu(OAc)_2•H_2O$	DCE	P_1 (0.5 equiv)	38
6	$Cu(OAc)_2•H_2O$	DCE	P_2 (0.5 equiv)	34
7	$Cu(OAc)_2•H_2O$	DCE	P_3 (0.5 equiv)	24
8	$Cu(OAc)_2•H_2O$	DCE	P_4 (0.5 equiv)	59
9	5 mol% $Cu(OAc)_2•H_2O$	DCE	P_4 (0.25 equiv)	84
10	**5 mol% $Cu(TFA)_2•H_2O$**	**DCE**	**P_4 (0.25 equiv)**	**87**

[a]Reaction conditions: a solution of XX (0.01 mmol) in 0.05 mL of solvent was added in 1 to a vial with [Cu] and additive in 0.05 mL of solvent under air at 23 °C. The mixture was stirred vigorously for 2 hrs then cooled to 0ºC and quenched with AcOH (50 uL in 1mL MeCN). A stock solution of IS (1,3,5-triemthoxybenzene was added and assay yield was determined by calibrated UPLC analysis. DCE = 1,2-dichloroethane.

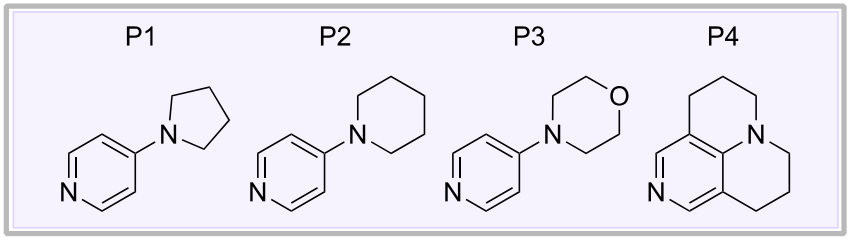

Table 1. Optimization of Diaryl hydrazone Oxidation *(Data from Melissa Hall)*

These optimized reaction conditions were then employed to a series of diaryl hydrazone derivatives (Scheme 3). The innate reactivity of the diaryl diazomethane derivatives can lead to large differences in NMR and isolated yields. For example, *p*-methoxy diazo **13** was converted in 89% yield, but the isolated amount was 62% yield. More stable diazo compounds have an electron-withdrawing group and little deviation from the NMR yield, as seen in **14** (92% vs. 90%), **16** (91%

vs. 86%,) and **17** (85% vs. 82%). These results are likely due to a combination of factors, including the more acidic nature of the N−H bonds of the hydrazone starting materials, which leads to enhanced reactivity and increased stability of the diazo products under the reaction conditions and during isolation.

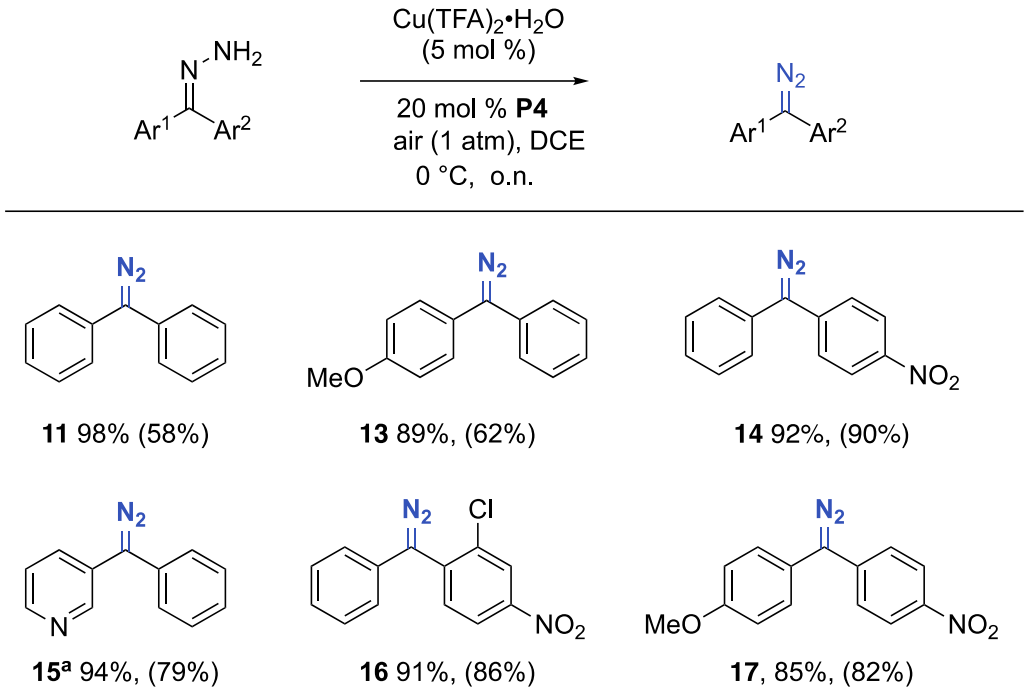

Reaction conditions: Hydrazone (0.20 mmol) was added to a vial with 5 mol % Cu(TFA)2·H2O and 20 mol % 9-azajulolidine (**P4**) in 2 mL of DCE under air at 0 °C. The mixture was stirred vigorously for 12 h. Yields shown reflect ^{1}H NMR analysis of the crude reaction with 1,3,5-trimethoxybenzene as the internal standard; yields shown in parenthesis are isolated. [a]Reaction run for 6 h.

Scheme 3. Scope of Diaryl Hydrazone Oxidation

To showcase the utility of this method a tandem one-pot oxidation then cyclopropanation was tested, Scheme 4. The crude diaryl diazomethane derivative **14**, obtained from aerobic dehydrogenation of the corresponding hydrazone **18** using a Cu(TFA)$_2$/ 9–Azajulolidine catalyst system, was used directly in the cyclopropanation of styrene with Rh_2(S-PTAD)$_4$ as the catalyst. The cyclopropane product **19** was obtained in moderate yield and good stereoselectivity (56% yield, 2:1 d.r., and 94% ee). This is advantageous, especially for less stable diaryl diazo compounds

where isolation of the diazo compound leads to diminished yields.

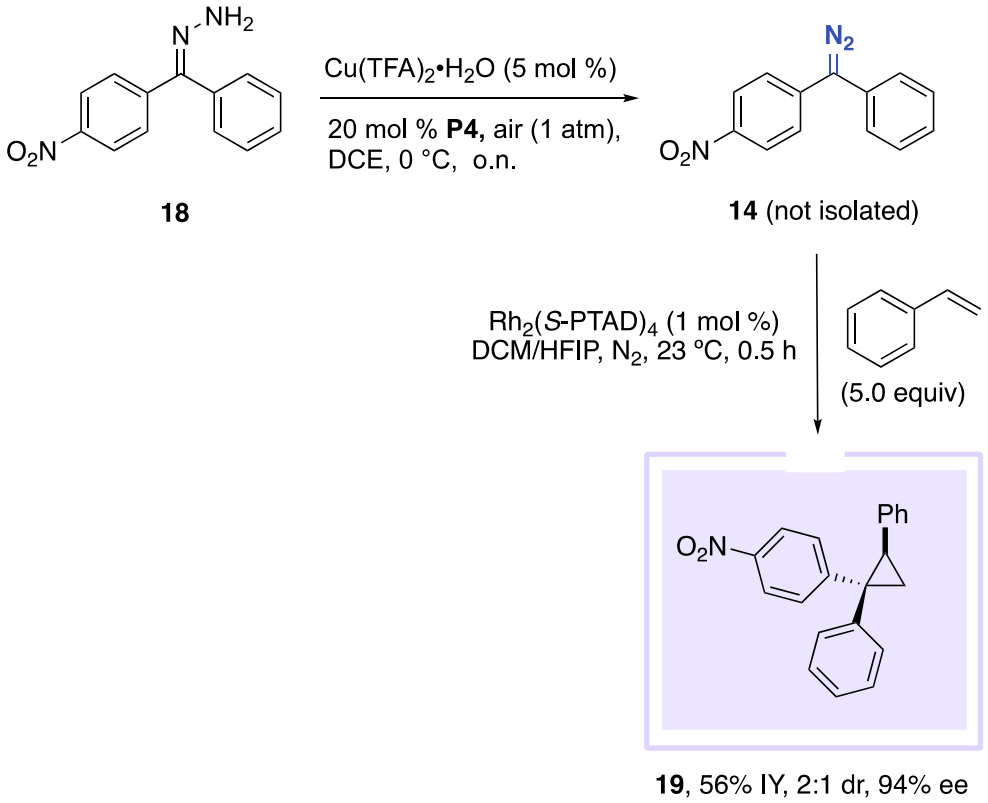

Scheme 4. Tandem Oxidation Cyclopropanation

This project details a new Cu-catalyzed method for the aerobic oxidation of hydrazone to diazo compounds using a low-cost catalyst, with ambient air as the oxidant. A diverse class of substrates can be accessed through minimal variation of base and reactions produce water as the sole byproduct. In addition, this method allows for subsequent C-H Functionalization reactions without the need for isolation or purification. This work has now been published online in the *ACS Catalysis* journal; figures and analyses from this paper have been adapted and incorporated into this chapter.[1]

4.4 Heterogeneous Metals on Nitrogen-Doped Carbon- Oxidation and Flow Applications

The conversion of hydrazones to diazo compounds in flow is highly advantageous to avoid handling large quantities of diazo compounds, especially for industrial processes. The Ley group in 2015 demonstrated a flow system using MnO_2 as an oxidant for the generation of unstable mono-substituted diazo intermediates which were then subjected to a downstream sp^2-sp^3 cross-coupling reaction.[18] Over the two-step process the desired product could be generated in up to 96% yield. The Charette group also developed a similar system, using Ag_2O and base in a packed column to generate diazoalkane compounds.[19, 20] Although these methods provided the desired diazo compounds, stoichiometric metal waste, especially on larger scales, is undesirable. Avoiding stoichiometric metals as oxidants and starting materials that produce byproducts makes the Cu system described previously an excellent alternative method for flow systems. To this end, Dr. Bo Wei from the Davies lab, in collaboration with Taylor Hatridge in Chris Jones' lab at Georgia Tech developed a three-phase packed bed reactor protocol that utilized the aerobic copper oxidation to generate diazo compounds in flow, Scheme 5.[21] The column is a mixture of $Cu(OAc)_2 \cdot H_2O$ and excess silica and the bottom has a silica plug to capture any solubilized Cu catalyst from the reaction stream. The desired hydrazone and DMAP were dissolved into dichloromethane and the liquid solution enters the glass column. Oxygen is added into the column by an ulta-zero air cylinder and controlled using a gas flow meter. This system allowed for the was able to oxidize hydrazone **20** to diazo **1**, which was subjected to a variety of rhodium-catalyzed C–H Functionalization reactions. The products were able to be formed in high yield and enantioselectivity. The reactor was able to maintain high conversion over 11 residence times, but product conversion did start to drop a bit at 4.5 residence times to 90%. The authors note a potential drawback to this system is the Cu catalyst leaching over time, which could have negative impacts

on downstream rhodium chemistry.

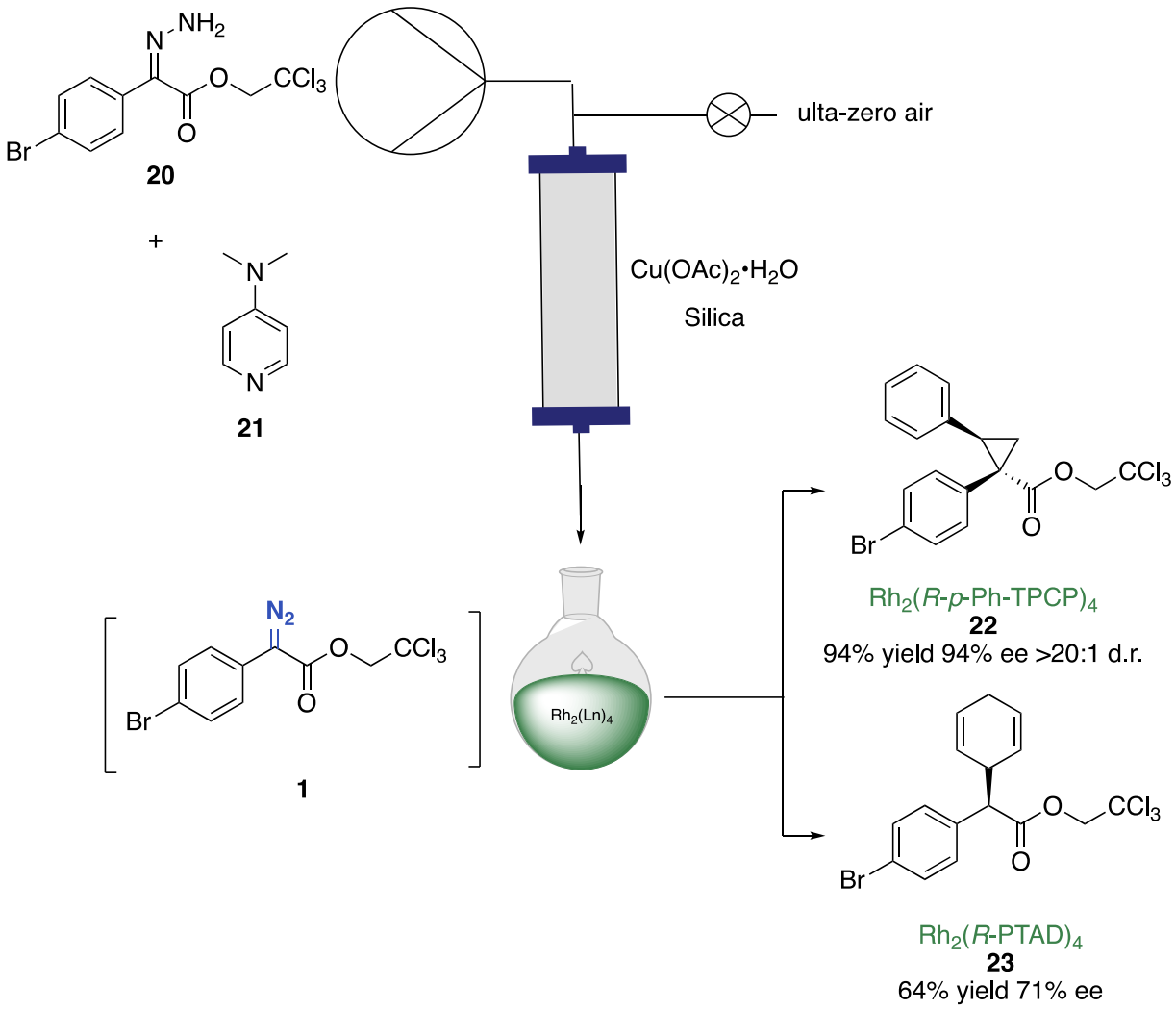

Scheme 5. Copper-Catalyzed, Aerobic Oxidation of Hydrazone in a Packed Bed Reactor

4.5 Heterogeneous MNC Results and Discussion

In collaboration with Melissa Hall at the University of Wisconsin, Madison we began investigating the use of metals on nitrogen-doped carbon (M-N-C) as heterogeneous catalysts for the formation of diazo compounds. Metals on nitrogen-doped carbon (M-N-C) materials have been used in electrochemical oxygen reduction towards platinum-group metal-free fuel cells wherein

oxygen (O_2) accepts electrochemically generated protons and electrons to generate water.[22] M-N-C materials are efficient at shuttling protons and electrons, making them ideal materials for aerobic oxidation.[23] Previous reports show M-N-C materials can be used in the aerobic oxidation of organic substrates with O_2 as the oxidant.[24, 25] Fe-N-C is a commercially available material known as Pajarito Powder™ (PAJ-Fe-N-C), and had been studied for fuel cell applications.[22, 23] We envisioned this material could be a competent heterogeneous catalyst to oxidize hydrazones to diazo compounds and would generate water as the sole byproduct. This would make isolation of the product simple, with only the removal of the heterogeneous catalyst needed, making the system amenable to flow conditions on a large scale. The initial screening of M-N-C materials was performed by Melissa Hall. This screen, revealed that M-N-C materials can catalyze hydrazone oxidation to diazo compounds under mild conditions, but also promote efficient catalysis in the absence of an added base (Table 2). Three hydrazones were tested in the initial screen because we have seen in our previous work the substituents of the hydrazone can affect the overall conversion. Ru/C and Pt/C, entries 1 and 2 respectively, gave a moderate yield of **1** and **3**, but for the diaryl hydrazone **17** almost no product was observed. Different cobalt on carbon catalysts were tested, but conversion was low in all cases, entries 3,4, and 6. Fe-Pc-C was able to convert the diaryl hydrazone to the corresponding diazo **17**, in a 21% yield, but only a 12% conversion to diazo **3** was observed. Switching to the Pajarito Powder, entry 8, gave a significant increase to the conversion across all 3 hydrazones. In the presence of 3 mol % PAJ-Fe-N-C and O_2, hydrazone **20** was converted to product **1** in 99% yield. In addition, diazo **17** was formed in 75% yield and diazo **3** in 76% yield, entry 8.

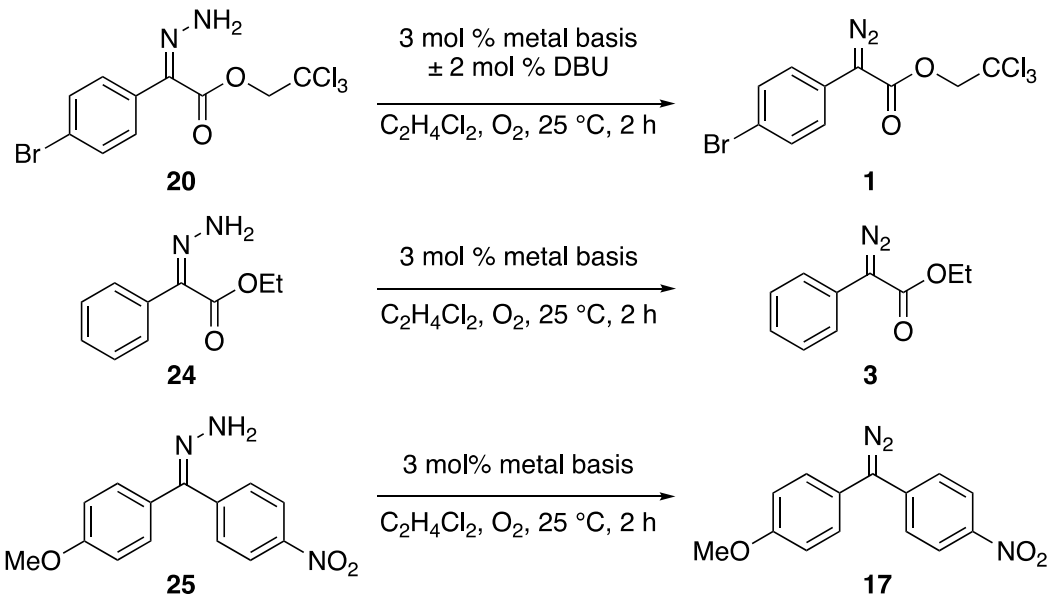

Entry	Catalyst	% Yield 1	% Yield 3	% Yield 17	% Yield 1 + 2 mol% DBU
1	Ru/C	25	27	5	7
2	Pt/C	32	29	1	26
3	Co-ZIF-8-C	3	2	1	7
4	Co-Phen-C	6	6	11	30
5	Fe-Phen-C	8	6	7	23
6	Co-Pc-C	10	9	4	13
7	Fe-Pc-C	25	12	21	21
8	**PAJ-Fe-N-C**	**99**	**76**	**75**	**71**

Reaction conditions: Hydrazone (0.01 mmol) in 0.5 mL of was added to a vial with Catalyst and additive in 1.5 mL of solvent under O_2 at 23 °C. The mixture was stirred vigorously for 2 hrs. A stock solution of IS (1,3,5-triemthoxybenzene) was added and assay yield was determined by calibrated UPLC analysis.

Table 2. Screening of Heterogeneous Catalyst for Hydrazone Oxidation *(Data collected by Melissa Hall)*

The optimized conditions were then employed to a variety of hydrazones. Donor/acceptor aryl diazoacetate compounds were able to be formed in high yields, with different phenyl and ester substituents. Diaryl diazo compounds were also formed in high yields with both electron-donating

and electron-withdrawing aryl rings. The diversity of the substituents highlights the utility of this method, without the need for further modification to accommodate different substrates as we saw in the previous Cu-catalyzed oxidation system. In only three cases, the addition of 2 mol % DBU was observed to increase yield for lower-performing substrates. The *ortho*-methoxy diazo **29** was formed in only 33% yield, but with the addition of 2 mol % DBU could be increased up to 90% yield.

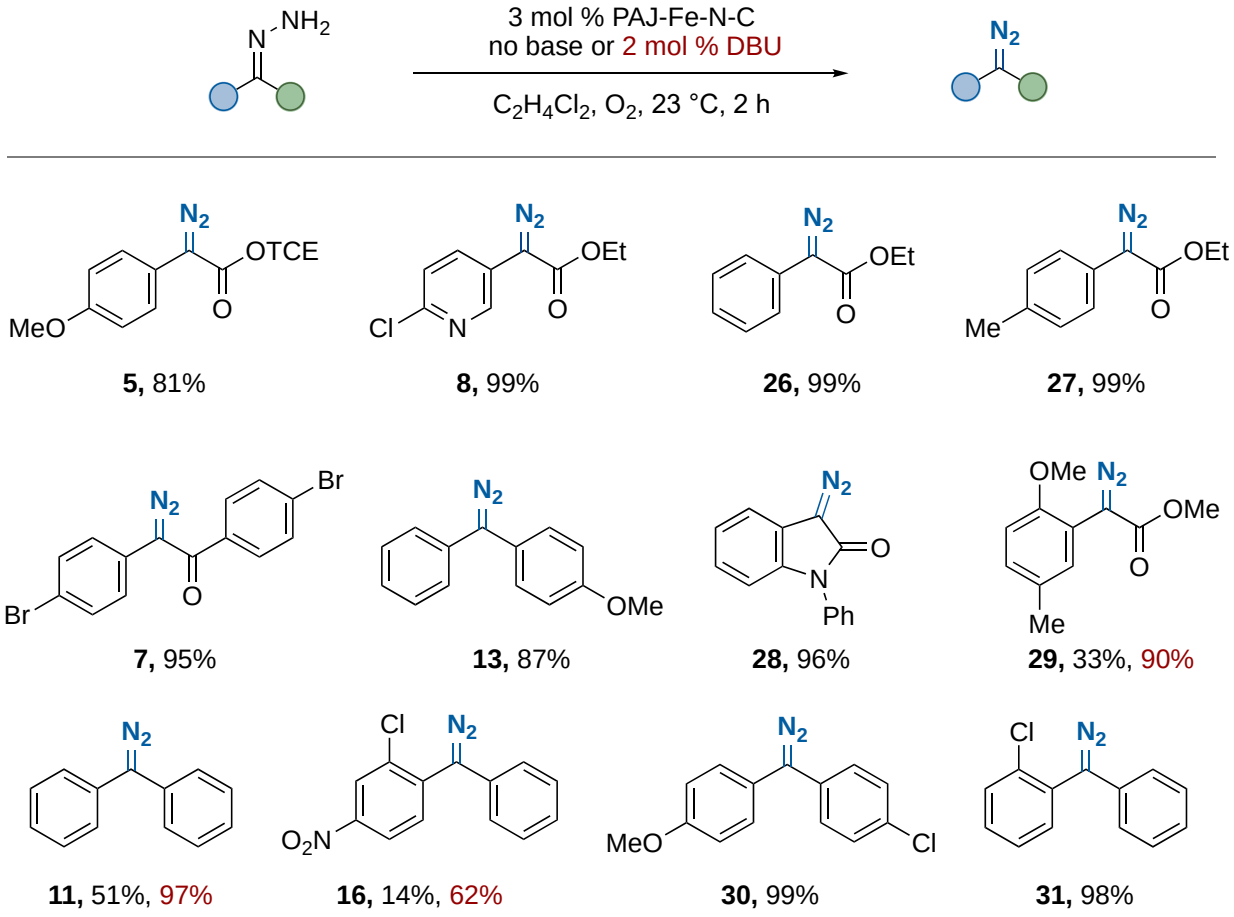

Reaction conditions: Hydrazone (0.01 mmol) in 0.5 mL of C_2H_4Cl was added to a vial with catalyst and additive in 1.5 mL of C_2H_4Cl under O_2 at 23 °C. The mixture was stirred vigorously for 2 hrs. A stock solution of IS (1,3,5-triemthoxybenzene) was added and assay yield was determined by calibrated UPLC analysis.

Scheme 6. Substrate scope of M-N-C-catalyzed oxidation of hydrazones. (*Data collected in collaboration with Melissa Hall)*

To test the utility of the current method, a one-pot oxidation then cyclopropanation of styrene with diaryl hydrazone **25** was tested. Firstly, control experiments outlined in Table 3 were screened based on the slight drop in ee from batch (87% ee) to one pot (83% ee). We believe the slight drop in enantioselectivity in this transformation is due to water formation during the oxidation. One method of water removal from the system is the use of molecular sieves, however, in the case of the diaryl system, these significantly diminish the level of asymmetric induction of the system. One hypothesis is due to the slightly acidic nature of mol. sieves.[26] Another method for the elimination of water in a system is the use of HFIP, due to its enhanced hydrogen bonding ability.[27, 28] Previous studies have shown that although in some cases HFIP can rescue the rhodium catalyst from poisons, water or nitrogen nucleophiles it can also greatly affect the asymmetric induction of a system; beneficially for some catalysts such as Rh_2(*S*-NTTL)$_4$ or harmful to others Rh_2(*S*-PTAD)$_4$.[29] To test if the M-N-C was causing the decrease in ee, the M-N-C catalyst was filtered through a large frit before addition to the rhodium reaction. This led to the desired cyclopropanation product in 78% yield, 50:1 d.r. and 83% ee, entry 1. The crude solution of the diazo mixture with the M-N-C catalyst led to very similar result of 75% yield, 50:1 d.r. and 83% ee. The slight drop in yield may be due to addition of the heterogeneous M-N-C catalyst which could interfere with stirring. We began to suspect the drop in ee could be a result of the amount of oxygen in the system. To test if air could be replaced as a terminal oxidant, the reaction was run without an oxygen balloon, Entry 3. Product was able to be formed, however, the yield was greatly diminished to 38%. Another possibility for the lowered ee was the use of oxygen in the first step. Entry 4, sparging the reaction with nitrogen for 15 mins, was able to recover the ee to 87%. Entry 5 confirmed that the M-N-C catalyst was necessary to oxidize the hydrazone to a diazo compound, and no product was formed without it. Without the rhodium catalyst, no desired cyclopropane

product was formed, this also indicated there is minimal to no iron leaching from the M-N-C catalyst, entry 6. This was an initial concern because iron in the presence of diazo compounds can form carbenes, but the cyclopropanation would not be asymmetric leading to a diminished overall ee of the system.[30]

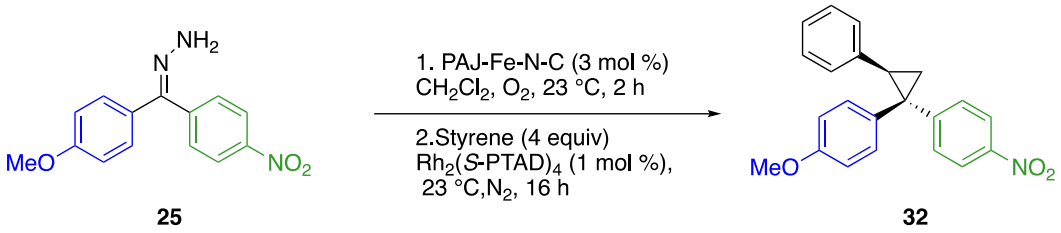

Entry	Conditions	ee, (%)	d.r.	Yield, %
1	Filter w/ large frit	83	50:1	78
2	No filter	83	50:1	75
3	No O_2	83	50:1	38
4	Sparge w/ N_2 15 min	87	50:1	75
5	No M-N-C	-	-	N.R.
6	No Rh	-	-	N.R.

Reaction conditions: Hydrazone **25** was added to a solution of PAJ-Fe-N-C (3 mol %) in 2 mL CH_2Cl_2 under an O_2 balloon. Reaction was stirred for 2 h. The reaction mixture was uptook in a syringe. To a flame dried vial with Rh_2(*S*-PTAD)$_4$ (1 mol %) and styrene (4 equiv) in 1 mL CH_2Cl_2 the reaction mixture was added over 1 h with a syringe pump.

Table 3. One Pot Oxidation– C-H Functionalization Conditions Control Experiments

With the necessary control experiments concluded, we tested the optimized tandem oxidation then C-H Functionalization on the *p*-NO2 *p*-OMe hydrazone, **25** with a variety of substrates, unsubstituted biphenyl hydrazone, and donor/acceptor p-Br TCE hydrazone (Scheme 5)**.** The diaryl hydrazone compound afforded the desired cyclopropanation product **33**, in 63% yield and 92% ee even with the presence of 10 equiv of water needed to get the full conversion to the diazo compound. C–H insertion reactions were also well tolerated in the system, with the C–

H insertion of 1,4-cyclohexadiene compound **34** in 72% yield and 99% ee. The C–H insertion of cyclohexane was also well tolerated affording the desired product, **36**, in 69% yield and 97% ee. The reaction was scaled up to a 1 mmol scale, to afford the cyclopropane compound **3** with a slight boost in yield to 83%, and maintained 87% ee.

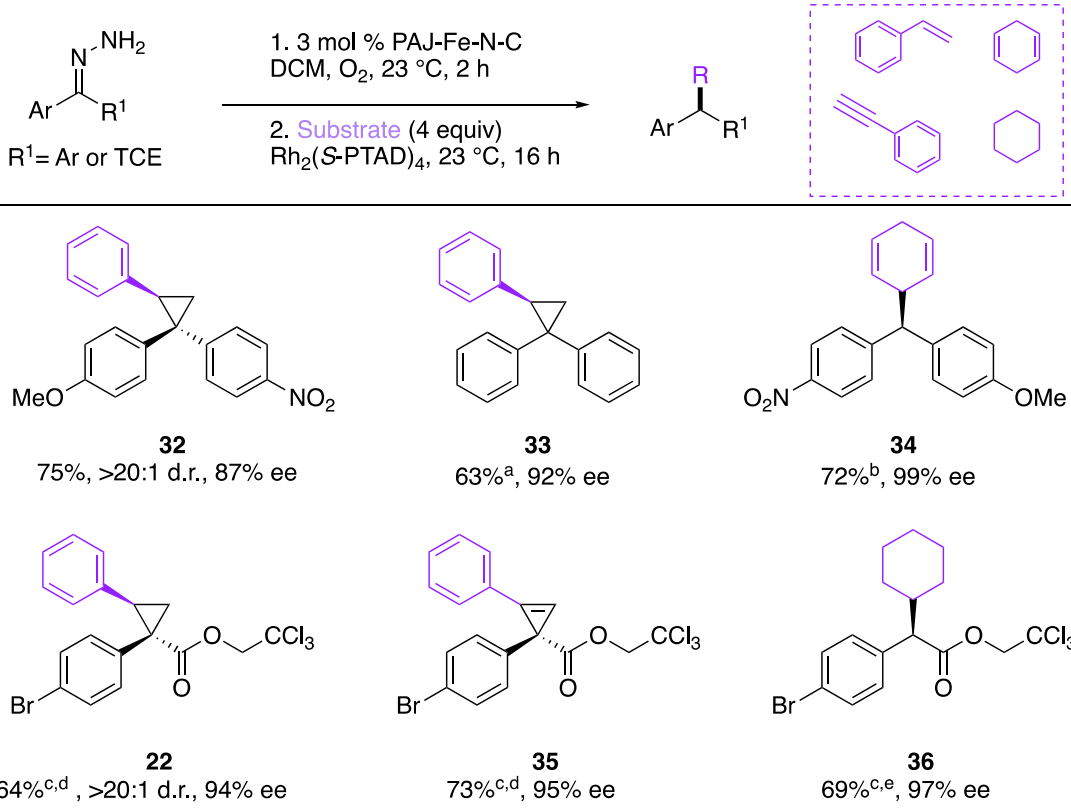

Reaction conditions: The desred hydrazone was added to a solution of PAJ-Fe-N-C (3 mol %) in 2 mL CH_2Cl_2 under an O_2 balloon. Reaction was stirred for 2 h. The reaction mixture was sparged for 15 min with N_2 and uptook in a syringe. To a flame dried vial with $Rh_2(Ln)_4$ (1 mol %) and subtrate (4 equiv) in 1 mL CH_2Cl_2 the reaction mixture was added over 1 h with a syringe pump.[a] 10 equiv of H_2O, and 20 equiv of HFIP were added.[b] Reaction was ran at –20 °C for C–H insertion.[c] 2 mol % equiv of DBU, and 20 equiv of HFIP were added. [d] Reaction was catalyzed by Rh_2(*S*-*p*-Ph-TPCP)$_4$. [e] Reaction was catalyzed by Rh_2(*S*-TPPTTL)$_4$.

Scheme 7. Scope of One Pot Oxidation– C-H Functionalization

As discussed at the beginning of this chapter, flow conditions to generate diazo compounds and perform downstream C-H Functionalization chemistry is highly desirable. By using a heterogeneous M-N-C catalyst where the only byproduct is water, our system is primed to be

adaptable to continuous flow conditions. Melissa Hall was able to build an initial flow-reactor system to showcase the potential of the current method in flow. An HPLC pump was fastened to a glass reaction tube to pump hydrazone substrate at a known rate with an additional gas inlet for the incorporation of oxygen. The hydrazone material flows through the reaction tube to be oxidized to the diazo compound, and is added dropwise to a flask containing the desired substrate and rhodium catalyst. This system is in the initial testing stages, however, is a good proof of concept. We envision this flow system would be an excellent way to make less stable compounds *in situ*, such as the diphenyl diazo compound.

4.6 Conclusions

Diazo compounds are useful synthetic intermediates used throughout the chemical literature but remain a safety concern.[11, 31, 32] Hydrazone oxidation is an alternate method to avoid the use of sodium azide, but stoichiometric byproducts or metals needed to generate the diazo compounds made these methods less attractive. In collaboration with the Stahl lab, the Davies lab has developed a Cu-catalyzed method for aerobic hydrogenation of hydrazones to the corresponding diazo compounds. The catalyst is low-cost and commercially available, the reaction is performed at ambient temperature and with air as the source of oxidant, making this method easily accessible. This method was also applied to the synthesis of cyclopropanes in a tandem hydrazone oxidation followed the rh-catalyzed cyclopropanation reaction and maintained high degrees of selectivity. Further studies conducted by the Jones and Davies lab, demonstrated these conditions could be applied to a flow system using a three-phase packed bed reactor. Inspired by these results a heterogenous catalytic-oxidation method was developed by the Stahl and Davies lab using commercially available Pajarito Powder™ (PAJ-Fe-N-C). This system was able to achieve high conversion of hydrazone to diazo compounds using 3 mol % metal loading, without

the use of base as an additive. The oxidation conditions were applied in tandem with Rh-catalyzed C-H Functionalization with a variety of substrates. The cyclopropanation and C-H insertions were accomplished in high yields and maintained high diastereo- and enantioselectivity. This method is currently being applied to flow conditions to study the scalability.

4.7 Experimental Data

4.7.1 General Considerations

All solvents for reactions were purified and dried by a *Glass Contour Solvent System* unless otherwise stated. ^{1}H and ^{13}C NMR spectra were recorded at 600 MHz (^{13}C at 151 MHz) on Bruker-600 spectrometer or IVONA-600 spectrometer or at 400 MHz (^{13}C at 101 MHz) on a Bruker Avance III 400 spectrometer at 25 °C or a at 500 MHz (13C at 125.7 MHz) on a Bruker Avance III 500 spectrometer at 25 °C. Unless otherwise stated, NMR spectra were run in solutions of deuterated chloroform ($CDCl_3$) with tetramethylsilane (TMS) as an internal standard (0 ppm for ^{1}H, and 0 ppm for ^{13}C), and were reported in parts per million (ppm). Abbreviations for signal multiplicity are as follow: s = singlet, d = doublet, t = triplet, q = quartet, m = multiplet, dd = doublet of doublet, etc. Coupling constants (*J* values) were calculated directly from the spectra. IR spectra were collected on a Nicolet iS10 FT-IR spectrometer and reported in unit of cm^{-1}. Mass spectra were taken on a Thermo Finnigan LTQ-FTMS spectrometer with APCI, ESI or NSI or a Thermo X Exactive Plus^{TM} Q-IT-MS with ESI.

Substrates and reagents were purchased from the following suppliers and used without further purification: Sigma-Aldrich, Alfa-Aesar, Oakwood Chemical America, and Fisher Scientific.

Racemic standards for enantiomeric determination were generated with reactions with $Rh_2(OAc)_4$ or from Rh_2((*R*) and (*S*)-DOSP)$_4$ which was generated by dissolving equimolar mixture of R and S catalyst in a minimal amount of benzene and lyophilizing. High performance liquid chromatography analysis (HPLC) was performed on Agilent 1100 Technologies HPLC instrument.

4.7.2 General Procedure for Diaryl Hydrazone Oxidation

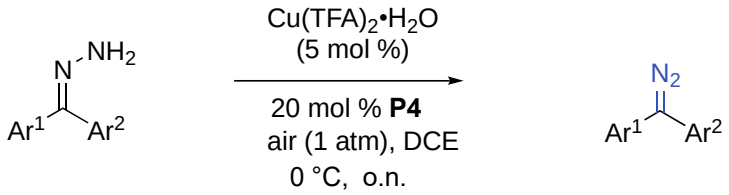

To an 8 mL vial fitted with a cross shaped stir bar, was added 0.20 mmol of diaryl hydrazone substrate. A solution of Cu(TFA)2•H2O (5 mol%, 3.1 mg, 0.01 mmol) and 9- azajulolidine (20 mol%, 7.0 mg, 0.04 mmol) in 1,2-Dichloroethane (2.0 mL) was added via an air displacement pipette and the vial was capped with septa fitted cap. A 16-gauge needle was inserted through the septa to facilitate movement of air and the reaction was stirred vigorously at 0 °C for 16 h. The reaction was stopped, concentrated and the crude material was purified using an alumina column under gradient of 0 to 5 % diethyl ether in hexanes to obtain purified diaryl diazo compounds.

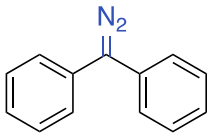

(diazomethylene)dibenzene (11)

Compound **11** was obtained as a purple solid in 58% yield (22 mg) following the general procedure above using (diphenylmethylene)hydrazine (0.20 mmol) as starting material. Spectroscopic data matched that previously reported.[33]

^{1}H NMR (500 MHz, CDCl3) δ 7.42 – 7.38 (m, 2H), 7.33 – 7.30 (m, 2H), 7.20 (ddt, J = 8.5, 7.3, 1.2 Hz, 1H).

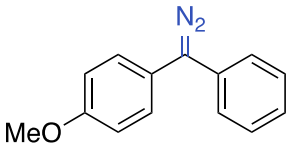

1-(diazo(phenyl)methyl)-4-methoxybenzene (13)

Compound **13** was obtained as a purple solid in 62 % yield (28 mg) following the general

procedure above using ((4-methoxyphenyl)(phenyl)methylene)hydrazine (0.20 mmol) as starting material. Spectroscopic data matched that previously reported.[34]

^{1}H NMR (500 MHz, CDCl3) δ 7.38 – 7.33 (m, 2H), 7.28 – 7.26 (m, 2H), 7.22 – 7.19 (m, 2H), 7.15 – 7.10 (m, 1H), 6.99 – 6.95 (m, 2H), 3.84 (s, 3H).

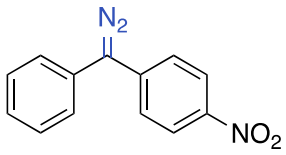

1-(diazo(phenyl)methyl)-4-nitrobenzene (14)

Compound **14** was obtained as an orange solid in 90% yield (43 mg) following the general procedure above using ((4-nitrophenyl)(phenyl)methylene)hydrazine (0.20 mmol) as starting material. Spectroscopic data matched that previously reported.[34]

^{1}H NMR (600 MHz, CDCl3)) δ 7.80 – 7.77 (m, 2H), 7.05 (dd, *J* = 8.3, 7.1 Hz, 2H), 6.97 – 6.93 (m, 1H), 6.89 (dd, *J* = 8.4, 1.2 Hz, 2H), 6.55 – 6.51 (m, 2H).

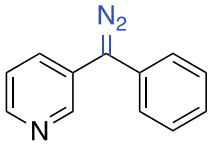

3-(diazo(phenyl)methyl)pyridine (15) Compound **15** was obtained as dark-pink oil in 79% yield (30 mg) following the general procedure above using 3-(hydrazineylidene(phenyl)methyl) pyridine (38.2 mg) as starting material.

^{1}H NMR (400 MHz, Acetone-*d*$_6$) δ 8.43 (d, *J* = 2.7 Hz, 1H), 8.28 (d, *J* = 3.2 Hz, 1H), 7.55 (dt, *J* = 8.2, 2.0 Hz, 1H), 7.34 (t, *J* = 7.8 Hz, 2H), 7.29 (dd, *J* = 8.1, 4.7 Hz, 1H), 7.20 (d, *J* = 8.0 Hz, 2H), 7.13 (t, *J* = 7.4 Hz, 1H).

^{13}C NMR (101 MHz, Acetone-*d*$_6$) δ 146.78, 146.23, 131.82, 129.46, 128.40, 126.17, 126.11, 124.96, 123.84. (The resonance resulting from the diazo carbon was not observed).

IR (neat): 3034, 2925, 2036, 1597, 1578, 1494, 1416, 1291, 1268, 1020, 931, 800, 752, 708, 694, 660 cm^{-1}.

HRMS (ESI-MS) calcd for $C_{12}H_{10}N_3$ [M+H] – 196.0869 found - 196.0870. calcd for $C_{12}H_{10}N$ [M- N_2+H] – 168.0808 found - 168.0809

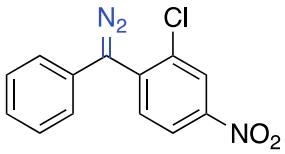

2-chloro-1-(diazo(phenyl)methyl)-4-nitrobenzene (16)

Compound **28** was obtained as a red/orange solid in 86% yield (47 mg) following the general procedure above using ((2-chloro-4-nitrophenyl)(phenyl)methylene)hydrazine (0.20 mmol) as starting material. Spectroscopic data matched that previously reported.[34]

^{1}H NMR (600 MHz, $CDCl_3$) δ 8.35 (d, *J* = 2.4 Hz, 1H), 8.10 (dd, *J* = 8.7, 2.4 Hz, 1H), 7.53 (d, *J* = 8.8 Hz, 1H), 7.40 (dd, *J* = 8.4, 7.5 Hz, 2H), 7.25 – 7.20 (m, 1H), 7.16 – 7.13 (m, 2H).

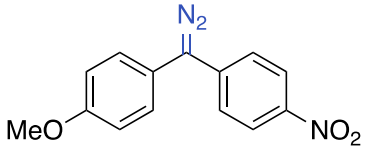

1-(Diazo(4-methoxyphenyl)methyl)-4-nitrobenzene (17)

Compound **17** was prepared using general procedure, ((4-methoxyphenyl)(4-nitrophenyl) methylene)hydrazone (54 mg, 0.20 mmol) was used to afford the titled diazo compound (82% yield). Spectroscopic data matched that previously reported.[34]

^{1}H NMR (600 MHz, $CDCl_3$) δ 7.94 (d, *J* = 8.99 Hz, 2H), 6.96 (d, *J* = 8.76 Hz, 2H), 6.80 (d, *J* = 8.76 Hz, 2H), 6.64 (d, *J* = 8.96 Hz, 2H), 3.37 (s, 3H).

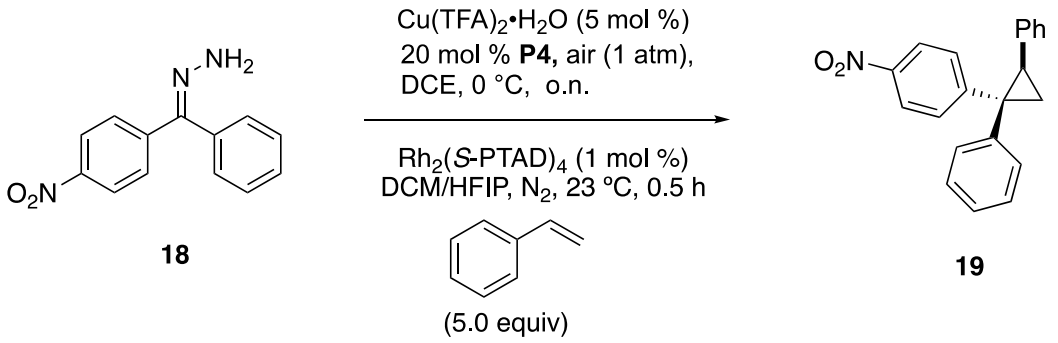

Tandem Sequence for Cyclopropane Synthesis with Diaryl Hydrazone

A 20 mL scintillation vial was charged with $Cu(TFA)_2•H_2O$ (2.8 mg 0.010 mmol, 5 mol%), 9-azajulolidine (7.0 mg, 0.040 mmol) and 1 mL DCE. The initial mixture was stirred vigorously with a stir bar (600 rpm) under air for 5 min before hydrazone was added. In a 4 mL scintillation vial, ((4-nitrophenyl)(phenyl)methylene)hydrazine (48 mg, 0.2 mmol, 1.0 equiv) was dissolved in 1.0 mL of DCE. The hydrazone/DCE solution was then transferred by syringe in one portion to the initial mixture of $Cu(TFA)_2•H_2O$/DCE solution. The reaction was stirred for 0.5 h before next step.

A 20 mL scintillation vial equipped with a stir bar was flame dried under vacuum. After cooling down, the vail was charged with $Rh_2(S\text{-PTAD})_4$ (2.8 mg, 1.0 mol%, 0.002 mmol), then flushed with nitrogen for 3 times and the nitrogen balloon was left on the septum. Then HFIP (0.42 mL, 20 equiv, 4.0 mmol), styrene (104.2 mg, 115 μL, 5.0 equiv, 1.0 mmol) and 2.0 mL sparged DCE (sparged with nitrogen for 2 h before use) were added sequentially via syringe, the mixture was stirred at 600 rpm for 10 min before crude diazo compound **23** injection. The crude diazo compound mixture from copper-catalyzed oxidation (~1.5 mL) was added by syringe to the styrene/$Rh_2(S\text{-PTAD})_4$/HFIP solution in one portion. The reaction was then stirred 1 h under nitrogen at 23 °C. After completion the solution was concentrated under rotovap and purified by flash column chromatography (0%, then 5%-15 % Et_2O in Hexanes). The product was obtained

as a mixture of diastereomers as a white solid (34 mg, 56 % yield, 2:1 dr, 94% ee).

Spectroscopic data matched that previously found in the literature.[34]

^{1}H NMR (600 MHz, $CDCl_3$) δ 8.13 – 8.09 (m, 2H), 7.36 – 7.32 (m, 2H), 7.25 – 7.01 (m, 8H), 6.86 – 6.83 (m, 2H), 2.89 (dd, *J* = 9.1, 6.8 Hz, 1H), 2.13 (dd, *J* = 6.8, 5.7 Hz, 1H), 1.90 (dd, *J* = 9.1, 5.7 Hz, 1H).

HPLC (ADH column, hexane, 1.0 mL min^{-1} 0.5 mg mL^{-1} 30 min, UV 230 nm) retention times of 12.65 min (major) and 13.55 min (minor) 94% ee with Rh_2(*S*-PTAD)$_4$.

General Conditions for C-H Insertion

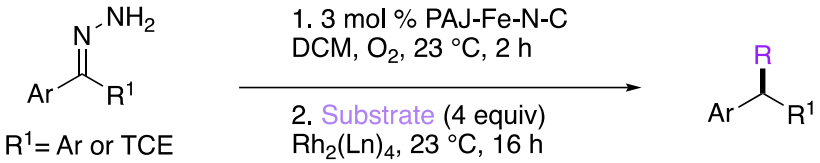

To a flame dried 8 mL dram vial charged with a stir bar, 3 mol % M–N–C (61mg) is added followed by 0.2 mmol of the desired hydrazone. If an additive is needed it is added to the material; H_2O (0.04 mL,10 equiv) or DBU (0.2 mol %), and 2 mL of DCM is added to solubilize the material, and an O_2 balloon is placed through the septa. The mixture is stirred at 700 rpm over 2 h. The solution is then sparged with Nitrogen for ~15 min without allowing the DCM to dry out.

A separate flame dried 8 mL dram vial is charged with a sir bar. The desired Rh catalyst (1 mol %) is added and the vial is purged with nitrogen 3x. 1 mL of DCM, substrate (4 equiv) and additive if noted (20 mol % HFIP or mol sieves) is added and the mixture and is stirred at 420 rpm. The purged MNC diazo mixture is added to the Rh solution via a syringe pump over the course of 1 h. The reaction was stopped filtered through celite and the crude NMR was analyzed. The reaction was purified via flash chromatography with a gradient of 1%-10% diethyl ether in Hexanes.

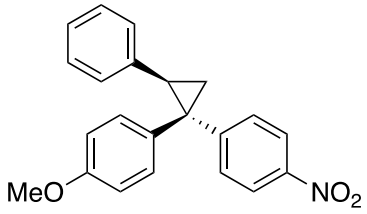

1-methoxy-4-((1*R*,2*R*)-1-(4-nitrophenyl)-2-phenylcyclopropyl)benzene (32)

Compound **32** was prepared from ((4-methoxyphenyl)(4-nitrophenyl)methylene)hydrazone (54mg, 0.20 mmol), Rh_2(*S*-PTAD)$_4$ (3.12 mg, 1 mol %), and styrene (0.12 mL, 4 equiv). The product was isolated as an off-white solid 51.6 mg, 75% yield. The NMR is consistent with literature reported values.[34]

^{1}H NMR (600 MHz, $CDCl_3$) δ 8.10 (d, *J* = 8.90 Hz, 2H), 7.30 (d, *J* = 8.96 Hz, 2H), 7.14 – 7.07 (m, 3H), 6.96 (d, *J* = 8.80 Hz, 2H), 6.89 – 6.80 (m, 2H), 6.70 (d, *J* = 8.77 Hz, 2H), 3.73 (s, 3H), 2.85 (dd, *J* = 9.1, 6.8 Hz, 1H), 2.08 (dd, *J* = 6.9, 5.6 Hz, 1H), 1.89 (dd, *J* = 9.1, 5.7 Hz, 1H).

HPLC conditions: HPLC (ADH column, 0.5 mL/min 3% *i*-PrOH in *n*-hexane 35 min, UV 230 nm) retention times of 20.7 (minor) and 28.0 min (major) 87 % ee with Rh_2(*S*-PTAD)$_4$.

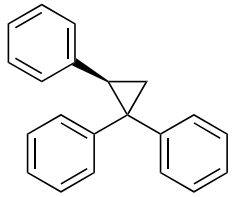

(*R*)-cyclopropane-1,1,2-triyltribenzene (33)

Compound **33** was prepared (diphenylmethylene)hydrazone (39 mg, 0.20 mmol), H_2O (0.04 mL, 10 equiv), Rh_2(*S*-PTAD)$_4$ (3.12 mg, 1 mol %), HFIP (0.42 mL, 4 equiv), and styrene (0.12 mL, 4 equiv). The product was isolated as an off-white solid 54 mg, 63% yield. The NMR is consistent with literature reported values.[13]

^{1}H NMR (600 MHz, $CDCl_3$) δ 7.27 (tdd, *J* = 10.0, 7.3, 1.8 Hz, 4H), 7.16 (td, *J* = 7.0, 1.9 Hz, 1H), 7.12 – 7.02 (m, 8H), 6.87 – 6.84 (m, 2H), 2.85 (ddd, *J* = 8.6, 6.5, 1.7 Hz, 1H), 1.99 – 1.96 (m, 1H), 1.80 (ddd, *J* = 9.4, 5.3, 1.7 Hz, 1H).

HPLC conditions: HPLC (ODH column, 1.0 mL/min 0.1% *i*-PrOH in *n*-hexane 30 min, UV 230 nm) retention times of 14.1 (major) and 22.1 min (minor) 92 % ee with Rh_2(*S*-PTAD)$_4$.

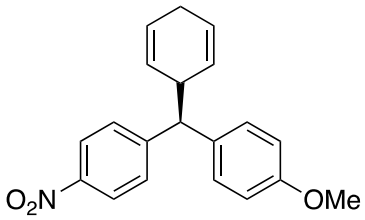

(*R*)-1-(cyclohexa-2,5-dien-1-yl(4-methoxyphenyl)methyl)-4-nitrobenzene (34)

Compound **34** was prepared from ((4-methoxyphenyl)(4-nitrophenyl)methylene)hydrazone (54 mg, 0.20 mmol), Rh_2(*S*-PTAD)$_4$ (3.12 mg, 1 mol %), and cyclohexadiene (0.14 mL, 4 equiv). The product was isolated as an off-white solid 48 mg, 72% yield. The NMR is consistent with literature reported values.[33]

^{1}H NMR (400 MHz, $CDCl_3$) δ 8.14 (d, *J* = 8.7 Hz, 3H), 7.45 (d, *J* = 8.8 Hz, 3H), 7.20 (d, *J* = 8.7 Hz, 3H), 6.85 (d, *J* = 8.7 Hz, 3H), 5.73 (dtd, *J* = 10.4, 3.3, 1.7 Hz, 4H), 5.53 (ddd, *J* = 10.8, 3.6, 2.0 Hz, 1H), 5.45 (ddd, *J* = 10.8, 3.7, 2.1 Hz, 1H), 3.91 (d, *J* = 9.7 Hz, 2H), 3.61 (ddt, *J* = 6.4, 3.3, 1.6 Hz, 1H), 2.63 (dtd, *J* = 8.3, 3.4, 1.7 Hz, 4H).

HPLC conditions: HPLC (ADH column, 1.0 mL/min 1% *i*-PrOH in *n*-hexane 30 min, UV 230 nm) retention times of 17.1 (minor) and 18.0 min (major) 99% ee with Rh_2(*S*-PTAD)$_4$.

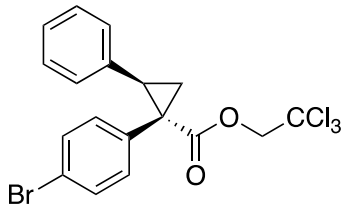

2,2,2-trichloroethyl (1*S*,2*R*)-1-(4-bromophenyl)-2-phenylcyclopropane-1-carboxylate (22)

Compound **22** was prepared by the general procedure from 2,2,2-trichloroethyl (*Z*)-2-(4-bromophenyl)-2-hydrazoneylideneacetate (75 mg, 0.20 mmol), DBU (0.60 μL, 2 mol %), Rh_2(*S*-p-PhTPCP)$_4$ (3.5 mg, 1 mol %), styrene (0.12 mL, 4 equiv), and HFIP (0.42 mL, 20 equiv) with 5-10 mol sieves. The product was isolated as an off-white solid 57.3 mg, 64% yield. The NMR is consistent with literature reported values.[35]

^{1}H NMR (400 MHz, $CDCl_3$) δ 7.27 – 7.26 (m, 2H), 7.15 – 7.04 (m, 3H), 6.97 – 6.89 (m, 2H), 6.80 (dd, *J* = 6.7, 2.9 Hz, 2H), 4.83 (d, *J* = 11.9, 1.1 Hz, 1H), 4.64 (d, *J* = 11.9, 1.1 Hz, 1H), 3.22 (dd, *J* = 9.5, 7.5 Hz, 1H), 2.28 (dd, *J* = 9.4, 5.2 Hz, 1H), 1.96 (dd, *J* = 7.5, 5.2 Hz, 1H).

HPLC conditions: HPLC (ADH column, 1.0 mL/min 1% *i*-PrOH in *n*-hexane 30 min, UV 230 nm) retention times of 6.2 (major) and 7.6 min (minor) 97% ee with Rh_2(*S*-p-PhTPCP)$_4$.

Batch to batch Scale up conditions: **HPLC conditions:** HPLC (ADH column, 1.0 mL/min 1% *i*-PrOH in *n*-hexane 30 min, UV 230 nm) retention times of 6.3 (major) and 7.8 min (minor) 97% ee with Rh_2(*S*-p-PhTPCP)$_4$.

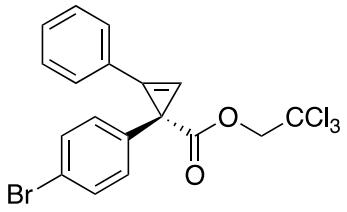

2,2,2-trichloroethyl (*R*)-1-(4-bromophenyl)-2-phenylcycloprop-2-ene-1-carboxylate (35)

Compound **35** was prepared from 2,2,2-trichloroethyl (*Z*)-2-(4-bromophenyl)-2-hydrazoneylideneacetate (54mgs, 0.20 mmol), DBU (0.60 μL, 2 mol %), Rh_2(*S*-p-PhTPCP)$_4$ (3.5 mgs, 1 mol %), phenylacetylene (0.09 mL, 4 equiv), and HFIP (0.42 mL, 20 equiv) with 5-10 mol sieves. The product was isolated as an off-white solid 65 mg, 73% yield. The NMR is consistent with literature reported values.[21]

^{1}H NMR: (400 MHz, Chloroform-d) δ 7.65 – 7.55 (m, 2H), 7.46 – 7.37 (m, 5H), 7.35 – 7.29 (m, 2H), 7.20 (s, 1H), 4.81 (d, J = 12.0 Hz, 1H), 4.76 (d, J = 12.0 Hz, 1H).

ADH_30min_1.0ML_1 .0%.M **HPLC conditions:** HPLC (ADH column, 1.0 mL/min 1% *i*-PrOH in *n*-hexane 30 min, UV 230 nm) retention times of 18.0 (minor) and 21.7 min (major) 97% ee with Rh_2(*S*-p-PhTPCP)$_4$.

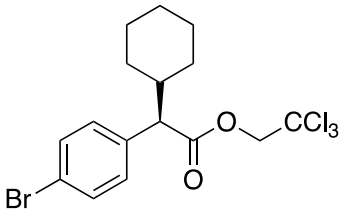

2,2,2-trichloroethyl (*R*)-2-(4-bromophenyl)-2-cyclohexylacetate (36)

Compound **36** was prepared from 2,2,2-trichloroethyl (*Z*)-2-(4-bromophenyl)-2-hydrazoneylideneacetate (54mgs, 0.20 mmol), DBU (0.60 μL, 2 mol %), Rh_2(*S*-TPPTTL)$_4$ (4.9 mgs, 1 mol %), cyclohexane (0.09 mL, 4 equiv) and HFIP (0.42 mL,20 equiv) with 5-10 mol sieves. The product was isolated as an off-white solid 59 mg, 69% yield. The NMR is consistent with literature reported values.[36]

^{1}H NMR: (400 MHz, Chloroform-d) δ 7.46 – 7.38 (m, 2H), 7.24 – 7.17 (m, 2H), 4.74 (d, J = 12.0 Hz, 1H), 4.61 (d, J = 12.1 Hz, 1H), 3.33 (d, J = 10.7 Hz, 1H), 2.03 (qt, J = 11.1, 3.4 Hz, 1H), 1.84 (dd, J = 11.8, 5.2 Hz, 1H), 1.78 – 1.69 (m, 1H), 1.69 – 1.57 (m, 2H), 1.38 – 1.21 (m, 2H), 1.19 – 1.01 (m, 3H), 0.75 (td, J = 15.4, 13.8, 10.3 Hz, 1H).

HPLC conditions: HPLC (ADH column, 1.0 mL/min 0.1% *i*-PrOH in *n*-hexane 30 min, UV 230 nm) retention times of 9.4 (minor) and 16.2 min (major) 97% ee with Rh_2(*S*-TPPTTL)$_4$.

4.8 HPLC Spectra for Enatnioselective Determination

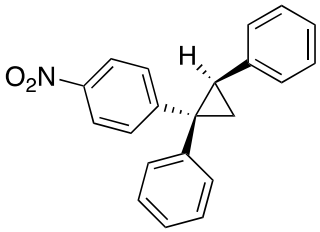

Compound 19 Racemic trace:

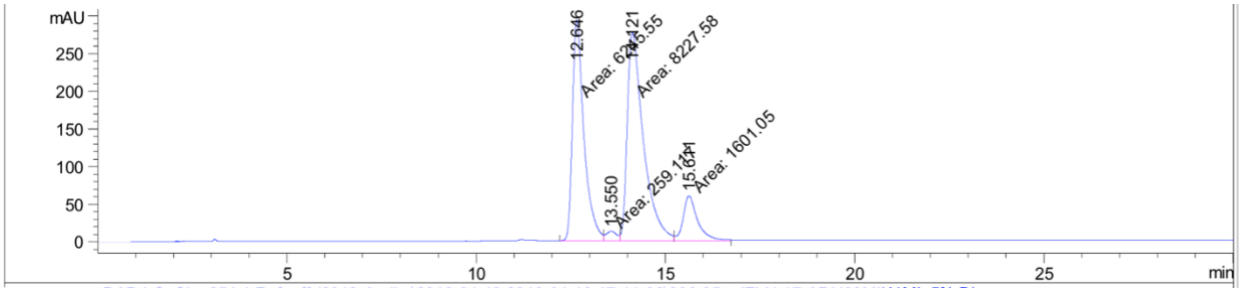

Peak #	RetTime [min]	Type	Width [min]	Area [mAU*s]	Height [mAU]	Area %
1	12.646	MF	0.3549	6245.55225	293.26422	38.2382
2	13.550	MF	0.3376	259.11688	12.79360	1.5864
3	14.121	MF	0.4968	8227.58008	276.01035	50.3730
4	15.611	FM	0.4466	1601.05176	59.75366	9.8024
Totals :				1.63333e4	641.82182	

Compound 19 trace with Rh_2(*S*-PTAD)$_4$:

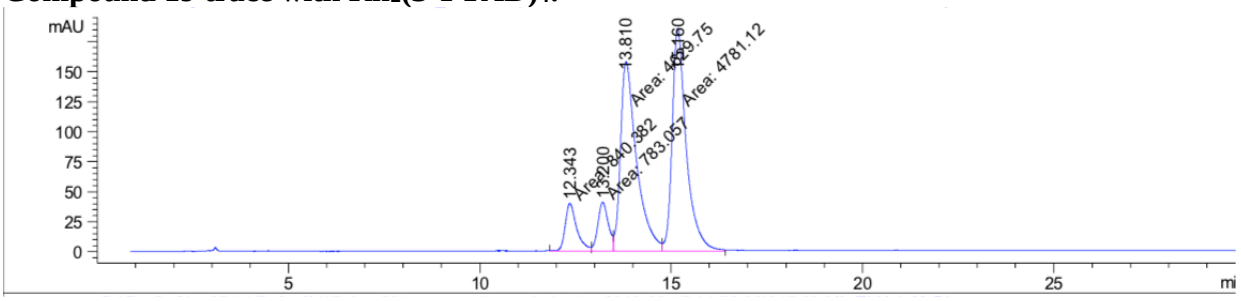

Signal 2: DAD1 B, Sig=230,4 Ref=off

Peak #	RetTime [min]	Type	Width [min]	Area [mAU*s]	Height [mAU]	Area %
1	12.343	MF	0.3525	840.38214	39.73832	7.6161
2	13.200	MF	0.3202	783.05688	40.76136	7.0966
3	13.810	MF	0.4890	4629.74609	157.79266	41.9578
4	15.160	FM	0.4287	4781.11523	185.89740	43.3296
Totals :				1.10343e4	424.18975	

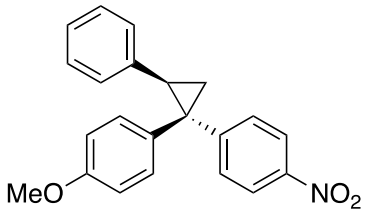

Compound 32 Racemic trace:

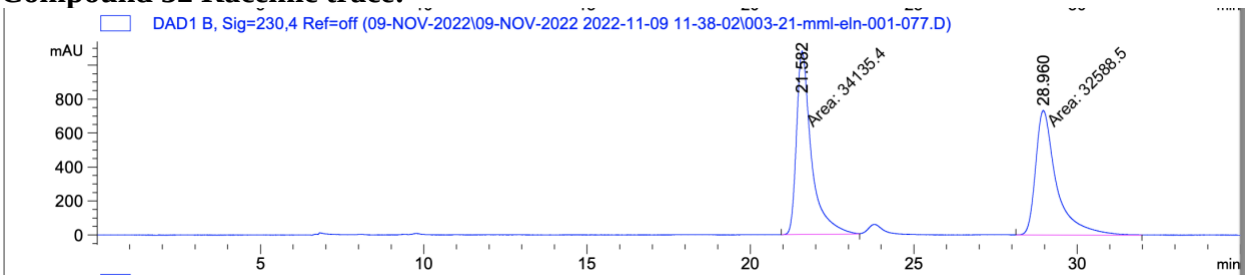

Signal 2: DAD1 B, Sig=230,4 Ref=off

Peak #	RetTime [min]	Type	Width [min]	Area [mAU*s]	Height [mAU]	Area %
1	21.582	MM	0.5263	3.41354e4	1080.96472	51.1591
2	28.960	MM	0.7398	3.25885e4	734.14130	48.8409
Totals :				6.67239e4	1815.10602	

Compound 32 trace with Rh_2(*S*-PTAD)$_4$:

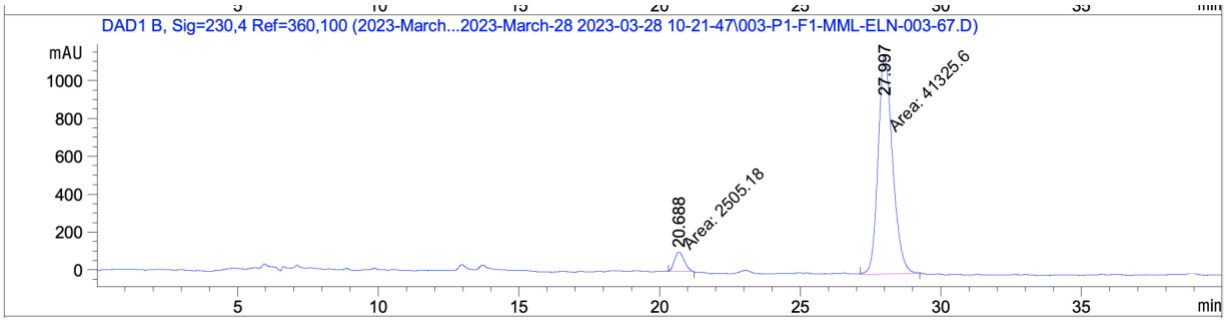

Signal 1: DAD1 A, Sig=210,4 Ref=360,100

Peak #	RetTime [min]	Type	Width [min]	Area [mAU*s]	Height [mAU]	Area %
1	20.690	MM	0.3974	3356.21045	140.75450	5.8053
2	27.997	MM	0.6135	5.44563e4	1479.44592	94.1947
Totals :				5.78125e4	1620.20042	

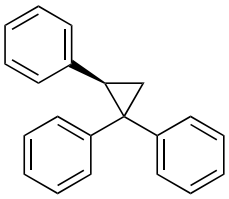

Compound 33 Racemic trace:

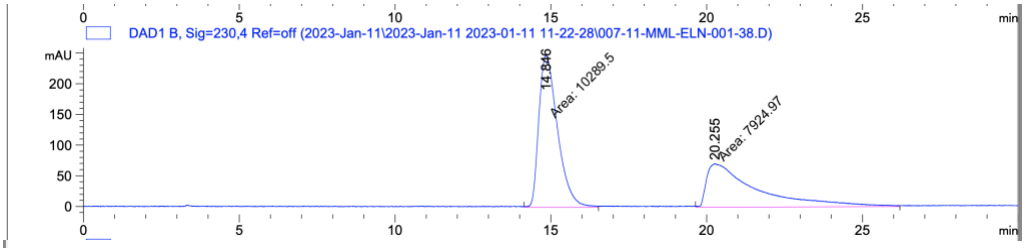

Signal 2: DAD1 B, Sig=230,4 Ref=off

Peak #	RetTime [min]	Type	Width [min]	Area [mAU*s]	Height [mAU]	Area %
1	14.846	MM	0.6936	1.02895e4	247.23250	56.4908
2	20.255	MM	1.8647	7924.97217	70.83245	43.5092
Totals :				1.82145e4	318.06495	

Compound 32 trace with Rh_2(*S*-PTAD)$_4$:

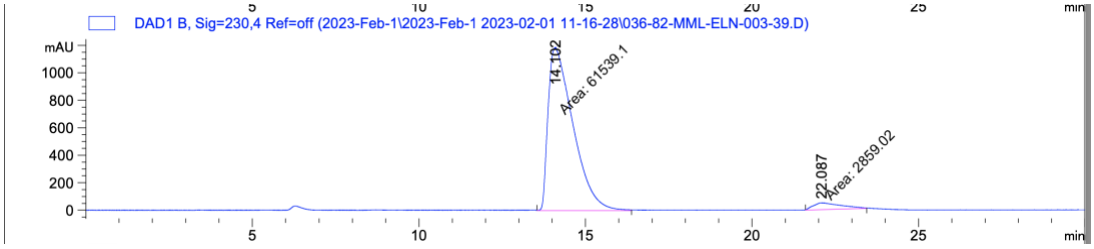

Signal 2: DAD1 B, Sig=230,4 Ref=off

Peak #	RetTime [min]	Type	Width [min]	Area [mAU*s]	Height [mAU]	Area %
1	14.102	MM	0.8633	6.15391e4	1188.08704	95.5604
2	22.087	MM	0.9514	2859.02148	50.08549	4.4396
Totals :				6.43981e4	1238.17253	

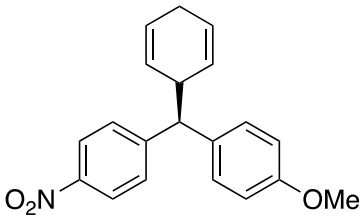

Compound 34 Racemic trace:

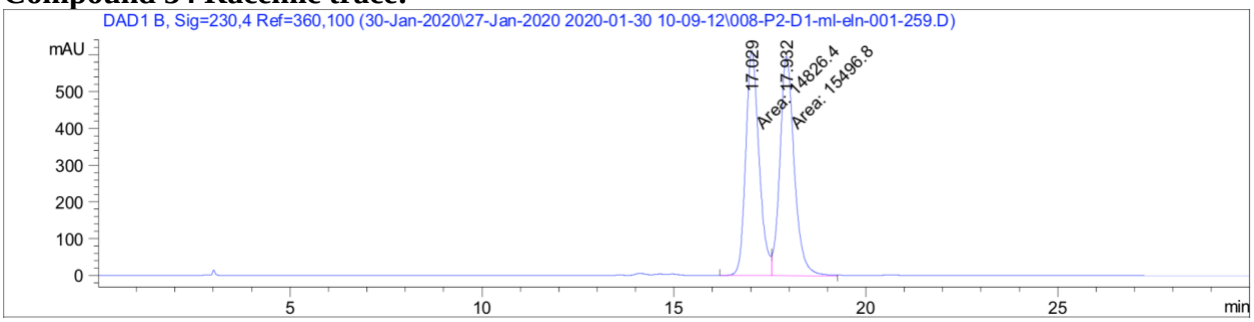

Signal 2: DAD1 B, Sig=230,4 Ref=360,100

Peak #	RetTime [min]	Type	Width [min]	Area [mAU*s]	Height [mAU]	Area %
1	17.029	MF	0.4038	1.48264e4	611.92981	48.8946
2	17.932	FM	0.4331	1.54968e4	596.41248	51.1054
Totals :				3.03232e4	1208.34229	

Compound 34 trace with Rh_2(*S*-PTAD)$_4$:

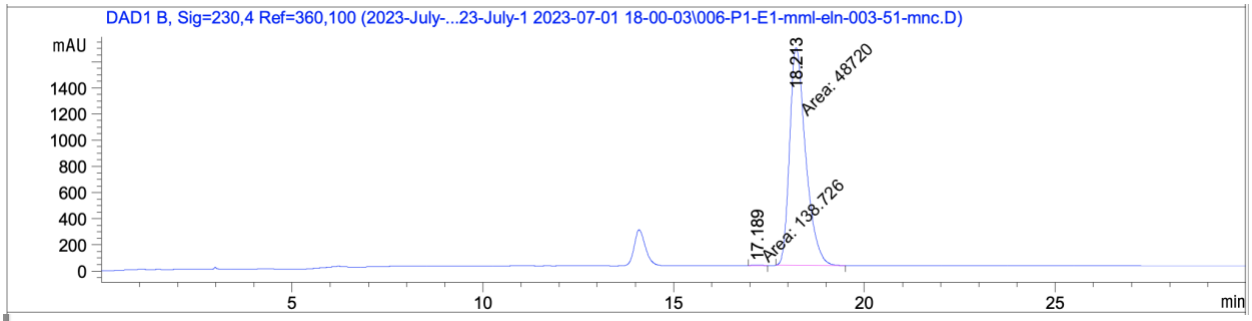

Signal 2: DAD1 B, Sig=230,4 Ref=360,100

Peak #	RetTime [min]	Type	Width [min]	Area [mAU*s]	Height [mAU]	Area %
1	17.189	MM	0.3646	138.72624	6.34152	0.2839
2	18.213	MM	0.4888	4.87200e4	1661.26282	99.7161
Totals :				4.88587e4	1667.60434	

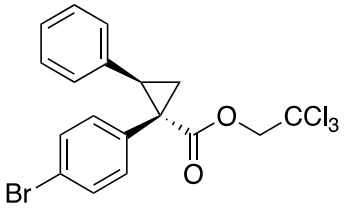

Compound 22 Racemic trace:

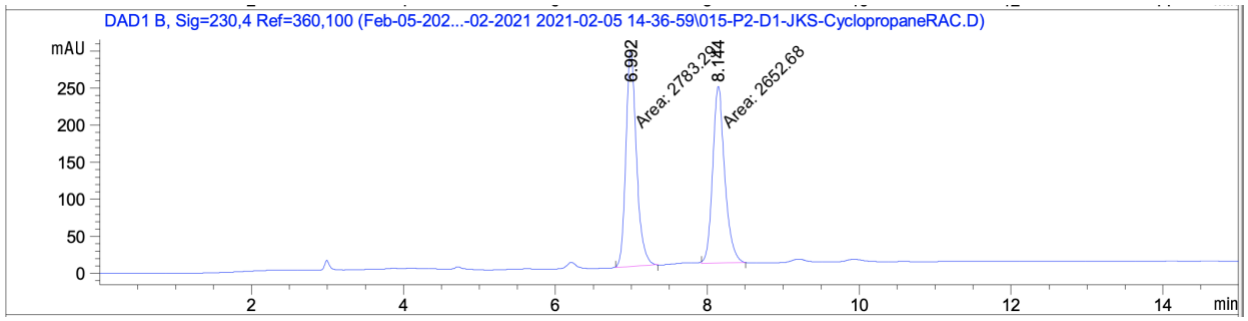

Signal 2: DAD1 B, Sig=230,4 Ref=360,100

Peak #	RetTime [min]	Type	Width [min]	Area [mAU*s]	Height [mAU]	Area %
1	6.992	MM	0.1590	2783.28638	291.76401	51.2013
2	8.144	MM	0.1852	2652.68018	238.66949	48.7987

Compound 22 trace with Rh_2(*S*-p-PhTPCP)$_4$:

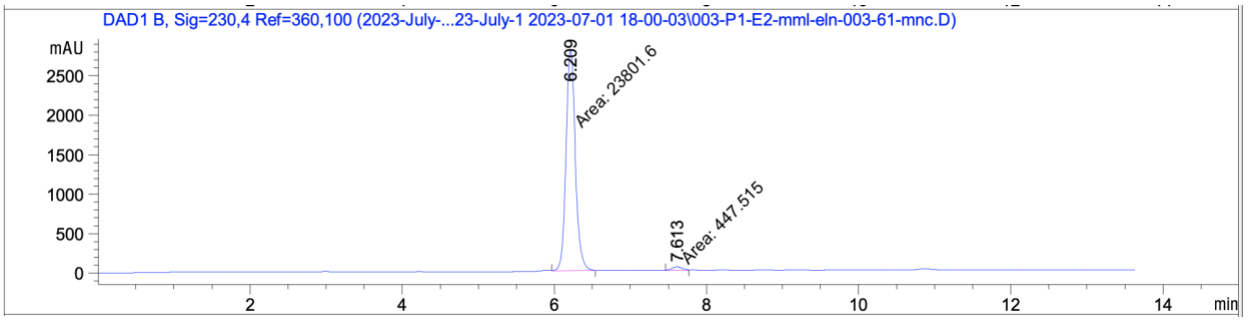

Peak #	RetTime [min]	Type	Width [min]	Area [mAU*s]	Height [mAU]	Area %
1	6.209	MM	0.1417	2.38016e4	2798.65820	98.1545
2	7.613	MM	0.1685	447.51471	44.25262	1.8455
Totals :				2.42491e4	2842.91082	

Compound 22 trace with Rh_2(*S*-p-PhTPCP)$_4$:
Batch to Batch 5 mmol scale:

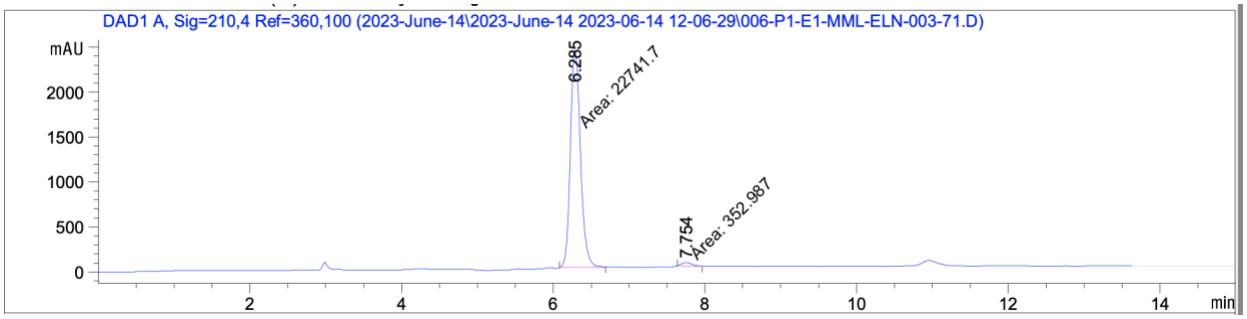

Peak #	RetTime [min]	Type	Width [min]	Area [mAU*s]	Height [mAU]	Area %
1	6.285	MM	0.1573	2.27417e4	2409.86938	98.4716
2	7.754	MM	0.1539	352.98654	38.22654	1.5284
Totals :				2.30947e4	2448.09593	

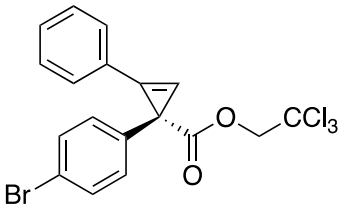

Compound 35 Racemic trace:

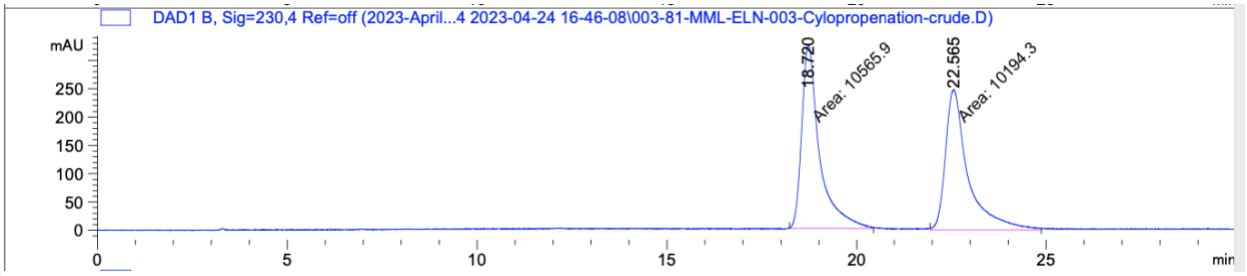

Signal 2: DAD1 B, Sig=230,4 Ref=off

Peak #	RetTime [min]	Type	Width [min]	Area [mAU*s]	Height [mAU]	Area %
1	18.720	MM	0.5442	1.05659e4	323.56647	50.8948
2	22.565	MM	0.6856	1.01943e4	247.81715	49.1052
Totals :				2.07602e4	571.38362	

Compound 35 trace with Rh_2(*S*-p-PhTPCP)$_4$:

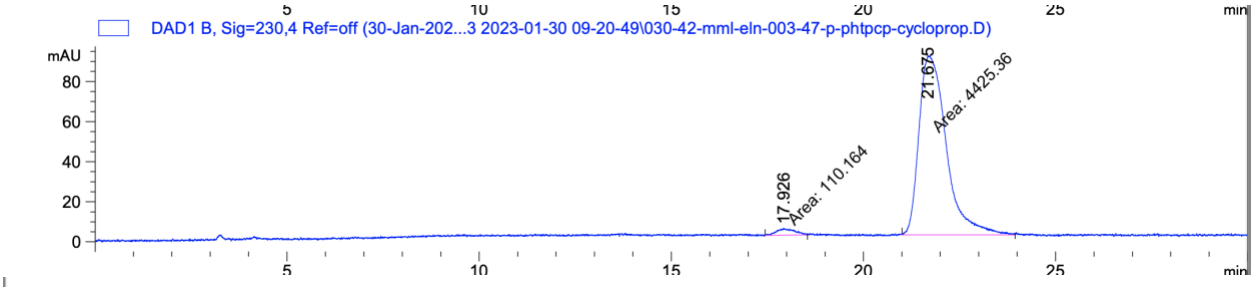

Signal 2: DAD1 B, Sig=230,4 Ref=off

Peak #	RetTime [min]	Type	Width [min]	Area [mAU*s]	Height [mAU]	Area %
1	17.926	MM	0.5194	110.16360	3.53496	2.4289
2	21.675	MM	0.8252	4425.35840	89.38105	97.5711
Totals :				4535.52200	92.91601	

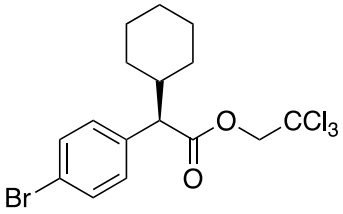

Compound 36 Racemic trace:

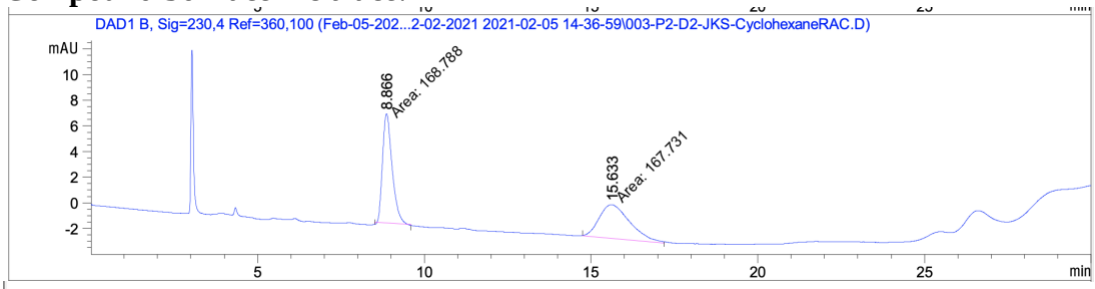

Signal 2: DAD1 B, Sig=230,4 Ref=360,100

Peak #	RetTime [min]	Type	Width [min]	Area [mAU*s]	Height [mAU]	Area %
1	8.866	MM	0.3314	168.78847	8.48839	50.1572
2	15.633	MM	1.0651	167.73071	2.62475	49.8428
Totals :				336.51918	11.11315	

Compound 35 trace with Rh_2(*S*-p-TPPTTL$_4$:

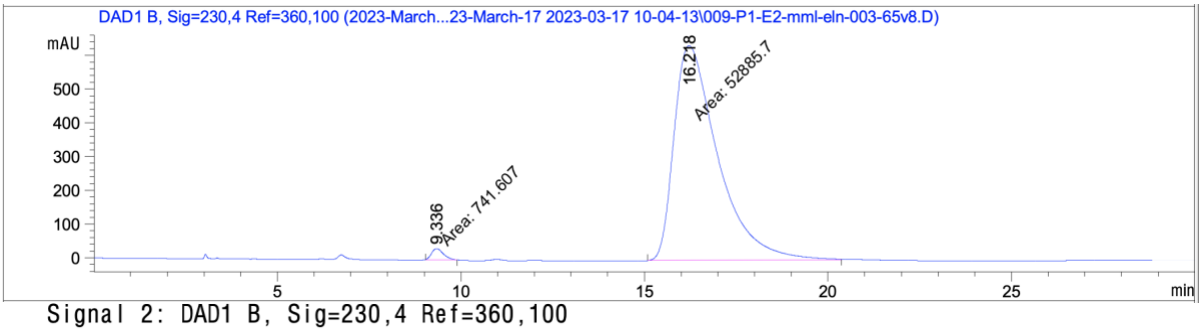

Signal 2: DAD1 B, Sig=230,4 Ref=360,100

Peak #	RetTime [min]	Type	Width [min]	Area [mAU*s]	Height [mAU]	Area %
1	9.336	MM	0.3714	741.60675	33.28219	1.3829
2	16.218	MM	1.3849	5.28857e4	636.47638	98.6171
Totals :				5.36273e4	669.75857	

4.9 References

1. Liu, W. B.; Twilton, J.; Wei, B.; Lee, M.; Hopkins, M. N.; Bacsa, J.; Stahl, S. S.; Davies, H. M. L., Copper-Catalyzed Oxidation of Hydrazones to Diazo Compounds Using Oxygen as the Terminal Oxidant. *Acs Catalysis* **2021,** *11* (5), 2676-2683.
2. Ford, A.; Miel, H.; Ring, A.; Slattery, C. N.; Maguire, A. R.; McKervey, M. A., Modern Organic Synthesis with alpha-Diazocarbonyl Compounds. *Chem. Rev.* **2015,** *115* (18), 9981-10080.
3. Ciszewski, L. W.; Rybicka-Jasinska, K.; Gryko, D., Recent developments in photochemical reactions of diazo compounds. *Org. Biomol. Chem.* **2019,** *17* (3), 432-448.
4. Davies, H. M. L.; Antoulinakis, E. G., Recent progress in asymmetric intermolecular C-H activation by rhodium carbenoid intermediates. *J. Organomet. Chem.* **2001,** *617* (1), 47-55.
5. Guptill, D. M.; Davies, H. M. L., 2,2,2-Trichloroethyl Aryldiazoacetates as Robust Reagents for the Enantioselective C-H Functionalization of Methyl Ethers. *J. Am. Chem. Soc.* **2014,** *136* (51), 17718-17721.
6. Reitz, J.; Antoni, P. W.; Holstein, J. J.; Hansmann, M. M., Room-Temperature-Stable Diazoalkenes by Diazo Transfer from Azides: Pyridine-Derived Diazoalkenes. *Angew. Chem.-Int. Edit.* **2023**, 6.
7. Baum, J. S.; Shook, D. A.; Davies, H. M. L.; Smith, H. D., Diazotransfer Reactions With Para-Acetamidobenzenesulfonyl Azide. *Synth. Commun.* **1987,** *17* (14), 1709-1716.
8. Bollinger, F. W.; Tuma, L. D., Diazotransfer reagents. *Synlett* **1996,** (5), 407-&.
9. Curphey, T. J., Preparation Of Para-Toluenesulfonyl Azide - A Cautionary Note. *Org. Prep. Proced. Int.* **1981,** *13* (2), 112-115.
10. Bamford, W. R.; Stevens, T. S., The Decomposition Of Toluene-Para-Sulphonylhydrazones By Alkali. *Journal of the Chemical Society* **1952,** (DEC), 4735-4740.
11. Fulton, J. R.; Aggarwal, V. K.; de Vicente, J., The use of tosylhydrazone salts as a safe alternative for handling diazo compounds and their applications in organic synthesis. *Eur. J. Org. Chem.* **2005,** *2005* (8), 1479-1492.
12. Nicolle, S. M.; Moody, C. J., Potassium N-Iodo p-Toluenesulfonamide (TsNIK, Iodamine-T): A New Reagent for the Oxidation of Hydrazones to Diazo Compounds. *Chem.-Eur. J.* **2014,** *20* (15), 4420-4425.
13. Liu, H. X.; Wei, Y. Y.; Cai, C., Hypervalent-iodine(III) oxidation of hydrazones to diazo compounds and one-pot nickel(II)-catalyzed cyclopropanation. *New J. Chem.* **2016,** *40* (1), 674-678.
14. Perusquia-Hernandez, C.; Lara-Issasi, G. R.; Frontana-Uribe, B. A.; Cuevas-Yanez, E., Synthesis and esterification reactions of aryl diazomethanes derived from hydrazone oxidations catalyzed by TEMPO. *Tetrahedron Lett.* **2013,** *54* (25), 3302-3305.
15. Holton, T. L.; Shechter, H., Advantageous Syntheses Of Diazo-Compounds By Oxidation Of Hydrazones With Lead-Tetraacetate In Basic Environments. *J. Org. Chem.* **1995,** *60* (15), 4725-4729.
16. Ibata, T.; Singh, G. S., Formation Of Diazoketones And Azines By Improved Oxidation Of Ketohydrazones Using Cu(Acac)(2) As A Catalyst. *Tetrahedron Lett.* **1994,** *35* (16), 2581-2584.
17. Nicolaou, K. C.; Mathison, C. J. N.; Montagnon, T., o-iodoxybenzoic acid (IBX) as a viable reagent in the manipulation of nitrogen- and sulfur-containing substrates: Scope, generality,

and mechanism of IBX-mediated amine oxidations and dithiane deprotections. *J. Am. Chem. Soc.* **2004,** *126* (16), 5192-5201.
18. Tran, D. N.; Battilocchio, C.; Lou, S. B.; Hawkins, J. M.; Ley, S. V., Flow chemistry as a discovery tool to access sp(2)-sp(3) cross-coupling reactions via diazo compounds. *Chem. Sci.* **2015,** *6* (2), 1120-1125.
19. Rulliere, P.; Benoit, G.; Allouche, E. M. D.; Charette, A. B., Safe and Facile Access to Nonstabilized Diazoalkanes Using Continuous Flow Technology. *Angew. Chem.-Int. Edit.* **2018,** *57* (20), 5777-5782.
20. Rullière, P.; Benoit, G.; Allouche, E. M. D.; Charette, A. B., Corrigendum: Safe and Facile Access to Nonstabilized Diazoalkanes Using Continuous Flow Technology. *Angew Chem Int Ed Engl* **2020,** *59* (8), 2936.
21. Hatridge, T. A.; Wei, B.; Davies, H. M. L.; Jones, C. W., Copper-Catalyzed, Aerobic Oxidation of Hydrazone in a Three-Phase Packed Bed Reactor. *Org. Process Res. Dev.* **2021,** *25* (8), 1911-1922.
22. Kumar, Y.; Kibena-Poldsepp, E.; Mooste, M.; Kozlova, J.; Kikas, A.; Aruvali, J.; Kaarik, M.; Kisand, V.; Leis, J.; Tamm, A.; Holdcroft, S.; Zagal, J. H.; Tammeveski, K., Iron and Nickel Phthalocyanine-Modified Nanocarbon Materials as Cathode Catalysts for Anion-Exchange Membrane Fuel Cells and Zinc-Air Batteries. *ChemElectroChem* **2022,** *9* (20), 13.
23. Lilloja, J.; Mooste, M.; Kibena-Poldsepp, E.; Sarapuu, A.; Zulevi, B.; Kikas, A.; Piirsoo, H. M.; Tamm, A.; Kisand, V.; Holdcroft, S.; Serov, A.; Tammeveski, K., Mesoporous iron-nitrogen co-doped carbon material as cathode catalyst for the anion exchange membrane fuel cell. *J. Power Sources Adv.* **2021,** *8*, 6.
24. Yang, X.; Yasukawa, T.; Maki, T.; Yamashita, Y.; Kobayashi, S., Well-Dispersed Trifluoromethanesulfonic Acid-Treated Metal Oxide Nanoparticles Immobilized on Nitrogen-Doped Carbon as Catalysts for Friedel-Crafts Acylation. *Chem.-Asian J.* **2021,** *16* (3), 232-236.
25. Shen, H.; He, J. Y.; He, F.; Xue, Y. R.; Li, Y. J.; Li, Y. L., Nitrogen-doped graphdiyne for effective metal deposition and heterogeneous Suzuki-Miyaura coupling catalysis. *Appl. Catal. A-Gen.* **2021,** *623*, 10.
26. Asakura, N.; Hirokane, T.; Hoshida, H.; Yamada, H., Molecular sieves 5A as an acidic reagent: the discovery and applications. *Tetrahedron Lett.* **2011,** *52* (4), 534-537.
27. Motiwala, H. F.; Armaly, A. M.; Cacioppo, J. G.; Coombs, T. C.; Koehn, K. R. K.; Iv, V. M. N.; Aube, J., HFIP in Organic Synthesis. *Chem. Rev.* **2022,** *122* (15), 12544-12747.
28. Pozhydaiev, V.; Power, M.; Gandon, V.; Moran, J.; Leboeuf, D., Exploiting hexafluoroisopropanol (HFIP) in Lewis and Bronsted acid-catalyzed reactions. *Chem. Commun.* **2020,** *56* (78), 11548-11564.
29. Sharland, J. C.; Dunstan, D.; Majumdar, D.; Gao, J. H.; Tan, K.; Malik, H. A.; Davies, H. M. L., Hexafluoroisopropanol for the Selective Deactivation of Poisonous Nucleophiles Enabling Catalytic Asymmetric Cyclopropanation of Complex Molecules. *ACS Catal.* **2022,** *12* (20), 12530-12542.
30. Batista, V. F.; Pinto, D.; Silva, A. M. S., Iron: A Worthy Contender in Metal Carbene Chemistry. *ACS Catal.* **2020,** *10* (17), 10096-10116.
31. Davies, H. M. L.; Morton, D., Guiding principles for site selective and stereoselective intermolecular C-H functionalization by donor/acceptor rhodium carbenes. *Chem. Soc. Rev.* **2011,** *40* (4), 1857-1869.

32. Clark, J. D.; Shah, A. S.; Peterson, J. C.; Patelis, L.; Kersten, R. J. A.; Heemskerk, A. H.; Grogan, M.; Camden, S., The thermal stability of ethyl diazoacetate. *Thermochim. Acta* **2002,** *386* (1), 65-72.
33. Lee, M.; Davies, H. M. L., Enantioselective Synthesis of Triarylmethanes via Intermolecular C–H Functionalization of Cyclohexadienes with Diaryldiazomethanes. *Org. Lett.* **2023,** *25* (22), 4000-4004.
34. Lee, M.; Ren, Z.; Musaev, D. G.; Davies, H. M. L., Rhodium-Stabilized Diarylcarbenes Behaving as Donor/Acceptor Carbenes. *ACS Catal* **2020,** *10* (11), 6240-6247.
35. Hirayama, T.; Ueda, S.; Okada, T.; Tsurue, N.; Okuda, K.; Nagasawa, H., Facile One-Pot Synthesis of 1,2,3 Triazolo 1, 5-a Pyridines from 2Acylpyridines by Copper(II)-Catalyzed Oxidative N-N Bond Formation. *Chem.-Eur. J.* **2014,** *20* (14), 4156-4162.
36. Fu, J. T.; Ren, Z.; Bacsa, J.; Musaev, D. G.; Davies, H. M. L., Desymmetrization of cyclohexanes by site- and stereoselective C-H functionalization. *Nature* **2018,** *564* (7736), 395-+.